APPLICATION OF ORGANIC PHOTOREDOX CATALYSIS IN NEW REACTION METHODOLOGY: SYNTHESIS OF BUTYROLACTONES VIA POLAR RADICAL CROSSOVER CYCLOADDITION AND HYDRODECARBOXYLATION OF CARBOXYLIC ACIDS

Mary A. Zeller

A dissertation submitted to the faculty at the University of North Carolina at Chapel Hill in partial fulfillment of the requirements for the degree of Doctor of Philosophy in the Department of Chemistry.

Chapel Hill
2016

Approved by:

David A. Nicewicz

Simon J. Meek

Jeffrey S. Johnson

Maurice S. Brookhart

Jillian L. Dempsey

© 2016
Mary A. Zeller
ALL RIGHTS RESERVED

ABSTRACT

Mary A. Zeller: Application of Organic Photoredox Catalysis in new Reaction Methodology:
Synthesis of Butyrolactones via Polar Radical Crossover Cycloaddition and
Hydrodecarboxylation of Carboxylic Acids
(Under the direction of David A. Nicewicz)

Synthesis of Butyrolactones via Polar Radical Crossover Cycloaddition

A direct catalytic synthesis of γ-butyrolactones from simple alkene and unsaturated acid starting materials is reported. The catalytic system consists of the Fukuzumi acridinium photooxidant and substoichiometric quantities of a redox-active cocatalyst. Oxidizable alkenes such as styrenes and trisubstituted aliphatic alkenes are cyclized with unsaturated acids via polar radical crossover cycloaddition (PRCC) reactions. Using this method, α-alkylidine butyrolactones can be synthesized. This method has been applied to the diastereoselective total synthesis of methylenolactocin and protolichesterinic acid.

Hydrodecarboxylation of Carboxylic and Malonic Acid Derivatives

A direct catalytic hydrodecarboxylation of primary, secondary, and tertiary carboxylic acids is reported. The catalytic system consists of a Fukuzumi acridinium photooxidant with phenyldisulfide acting as a redox-active cocatalyst. Substoichiometric quantities of Hünig's base are used to reveal the carboxylate. Use of trifluoroethanol as a solvent allowed for significant improvements in substrate compatibilities, as the method reported is not limited to carboxylic acids bearing α-heteroatom or –phenyl substitution. This method has been applied to the direct

double decarboxylation of malonic acid derivatives, which allows for the convenient use of dimethyl malonate as a methylene synthon.

To my family, and especially, my father

ACKNOWLEDGMENTS

When I started the graduate school journey five years ago, I did not know anyone at UNC and I was already tired, determined to make a fresh start. I would like very much to thank Dave, and the early members of the Nicewicz lab, for welcoming me from the start. I did not expect to be part of a family, but Perkowski, Tien, Michelle, Hami, Jean-Marc, Nate, and Pete (for Pete's sake!) wrapped me up in their humor and support, and let me be myself. These members, and the many who came after, all helped shape my experience here in numerous positive ways.

I would like to thank Jeremy, Cole, and Cortney for their endless banter. I will miss it when I'm gone. I'll always have fond memories of the trips to student stores, and Buns.

I would like to thank my parents for their unconditional support as I've tried to meet the world as honestly as I know how. Over the course of my time in graduate school I've evolved and changed and grown in numerous ways, sometimes seemingly backwards, and they have been with me every step of the way. I would like to thank my brothers for always striving to grow, learn, and explore. It makes it easier for me to do the same, in my own way.

I would like to thank Michelle and Jeremy for collaborating with me on my projects. I learned so much from having a second perspective, and from being part of a team.

I would like to thank Dave for his unique mentoring style of combining support and space. I strongly believe that this quality has been instrumental in helping me turn the challenging experience of graduate school into an experience that will have a very positive impact on the rest of my life, in whichever direction I chose to go.

Lastly (but not least), I would like to thank those who have served on my committees. Jeff Johnson and Maurice Brookhart have served on both my orals and my defense committees, and I appreciate the willingness of everyone to engage with me on this journey.

PREFACE

The results and supporting information disclosed regarding the butyrolactone project have been published in Organic Letters in 2014 (*Org, Lett.* 2014, 16, 4810-4813), and those regarding the hydrodecarboxylation project have been published in the Journal of the American Chemical Society in 2015 (*J. Am. Chem. Soc.* 2015, 137, 11340).

TABLE OF CONTENTS

LIST OF TABLES…………………………………………………………………..….xiii

LIST OF FIGURES…………………………………………………………...……xiv

LIST OF ABBREVIATIONS AND SYMBOLS……………..…………………………...xix

CHAPTER ONE: INTRODUCTION TO PHOTOREDOX CATALYSIS…………...……….1

1.1 Introduction………………………………………………………………………1

1.2 Thermodynamics of photoinduced electron transfer…………………………………4

1.3 Recent advances in photoredox catalysis……………………………………...8

1.4 The Fukuzumi acridinium catalyst………………………………………………...12

1.5 Development of the hydrofunctionalization catalyst system……………………...15

1.6 Other uses of the Fukuzumi acridinium…………………………………………...19

References……………………………………………………………………..22

CHAPTER TWO: SYNTHESIS OF BUTYROLACTONES ……………………………..25

2.1 Introduction……………………………………………………………………..25

2.1.1 Importance of the butyrolactone moiety…………………………………...25

2.1.2 Importance of the paraconic acids………………………………………....26

2.1.3 Intramolecular strategies for the synthesis of butyrolactones……………...27

2.1.4 Intermolecular strategies for the synthesis of butyrolactones……………...28

2.1.5 Strategies for α-methylene and α-alkylidine butyrolactone synthesis……..29

2.1.6 Initial idea for our method…………………………………………………32

2.1.7 Previous syntheses of paraconic acids……………………………………..34

2.1.8 Initial strategy for the synthesis of paraconic acids………………………..35

2.2 Background…………………………………………………………………………..36

2.2.1 Anti-Markovnikov hydroacetoxylation of alkenes………………………...36

2.2.2 Synthesis of tetrahydrofurans via polar radical crossover cycloaddition….38

2.2.3 5-exo-trig radical cyclizations to form butyrolactones……………………41

2.2.4 The arene oxidation………………………………………………………...43

2.3 Results and Discussion………………………………………………………………44

2.3.1 Initial results with acrylic and crotonic acid……………………………….44

2.3.2 Adaptation to monoester fumarates………………………………………..46

2.3.3 Adaptation to cinnamic acid derivatives…………………………………...48

2.3.4 Adaptation to alkynoic acids……………………………………………….49

2.3.5 Determination of relative stereochemistry…………………………………51

2.3.6 Insights into the irreversibility of the radical cyclization…………………52

2.3.7 Application to the synthesis of methylenolactocin and protolichesterinic acid…………………...............……………………………………………………….53

2.4 Conclusion………………………………………………………………………...57

2.5 Further developments of this Strategy…………………………………………….57

2.6 Experimental Details………………………………………………………………58

References……………………………………………………………………………..74

CHAPTER THREE: HYDRODECARBOXYLATION………………………………...77

3.1 Introduction…………………………………………………………………………..77

3.1.1 Importance of carboxylic acids and esters in synthesis……………………77

3.1.2 Barton decarboxylation…………………………………………………….79

3.1.3 Kolbe electrolysis………………………………………………………..80

3.1.4 Ground state oxidation methods…………………………………………...81

3.1.5 Photoredox catalysis……………………………………………………….82

3.1.6 The proposed method……………………………………………………….85

3.2 Background…………………………………………………………………………..85

3.2.1 Reduction potentials of carboxylates……………………………………85

3.2.2 The Acyloxyl radical……………………………………………………….86

3.2.3 Hydrodecarboxylation using Mes-Acr-Me in Dichloroethane…………….87

3.3 Results and Discussion……………………………………………………………88

3.3.1 Development with phenyl acetic acid derivatives…………………………89

3.3.2 Issues in applying towards less functionalized carboxylic acids…………..89

3.3.3 Unsuccessful substrates……………………………………………………93

3.3.4 Insights into the role of trifluoroethanol…………………………………...95

3.3.5 Application towards malonic acid derivatives……………………………100

3.4 Conclusion and Outlook………………………………………………………103

3.5 Experimental Details…………………………………………………………..105

References………………………………………………………………………118

APPENDIX ONE: NMR SPECTRA FOR CHAPTER TWO………………………………….121

APPENDIX TWO: NMR SPECTRA FOR CHAPTER THREE..……………………………..143

LIST OF TABLES

Table 2.1: Optimization of the hydroacetoxylation reaction…………………………………….37

Table 2.2: Initial consideration of crotonic anc acrylic acid……………………………………..45

Table 2.3: Optimization with mono-*t*-butylfumarate…………………………………………….47

Table 3.1: Optimization of conditions for monoacid substrates…………………………………91

Table 3.2: Optimization of malonic acid double decarboxylation……………………………...102

LIST OF FIGURES

Figure 1.1: Photoinduced electron transfer promoting single-electron oxidation……………….1

Figure 1.2: Photoinduced electron transfer promoting single-electron reduction……………….1

Figure 1.3: Photoredox mediated anti-Markovnikov transformations…………………………….2

Figure 1.4: Typical mechanism of photo-NOCAS reactivity……………………………………..3

Figure 1.5: Trends in ground state reduction potential based on functional group……………….5

Figure 1.6: Reduction potentials of representative alkenes……………………………………….6

Figure 1.7: Reduction potentials of some Ground-state and Excited-state oxidants……………...8

Figure 1.8: Proposed mechanism for α-functionalization of amines……………………………...9

Figure 1.9: [2+2] cycloaddition after access to Ru(bpy)$_3^{3+}$……………………………………...10

Figure 1.10: [2+2] Heterodymerization…………………………………………………………….11

Figure 1.11: Access to more challenging alkenes using an organic photooxidant………………12

Figure 1.12: Summary of excited states from Fukuzumi and Verhoeven……………………….13

Figure 1.13: Aryl bromination catalyzed by **Mes-Acr-Me**……………………………………...14

Figure 1.14: Hamilton's initial strategy for the hydroetherification reaction……………………15

Figure 1.15: Initial results in the hydroetherification reaction…………………………………..16

Figure 1.16: Addition of 2-phenylmalononitrile as hydrogen atom donor………………………17

Figure 1.17: Trifold requirements of a quality additive……………………………………………17

Figure 1.18: Proposed mechanism for the hydrotrifluoromethylation reaction…………………19

Figure 1.19: Amination of arenes……………………………………………………………..20

Figure 2.1: Examples of bioactive α-methylene and α-alkylidine natural products……...……...25

Figure 2.2: Examples of paraconic acids…………………………………………………...27

Figure 2.3: Butyrolactones via dynamic kinetic resolution of α-ketoesters……………………..28

Figure 2.4: The homoenolate approach to butyrolactone synthesis……………………………..28

Figure 2.5: Synthesis of butyrolactones via photoreduction……………………………………29

Figure 2.6: Aldol-elimination strategy for α-methylene synthesis………………………………30

Figure 2.7: The Dreiding-Schmidt reaction…………………………………………………...30

Figure 2.8: Butyrolactones from allylboronic esters and aldehydes……………………………..31

Figure 2.9: Butyrolactone formation via transfer hydrogenation………………………………..32

Figure 2.10: Horner-Wadsworth-Emmons strategy for α-alkylidine butyrolactone synthesis…..32

Figure 2.11: Proposed disconnection for our strategy…………………………………………...33

Figure 2.12 PRCC strategy for butyrolactone synthesis…………………………………………34

Figure 2.13: Diasteroselective control from Meepowpan………………………………………..34

Figure 2.14: Synthesis of (-)-Methylenolactocin by Zhu and Lu………………………………..34

Figure 2.15: Retrosynthetic analysis of the proposed method to synthesize Methylenolactocin..35

Figure 2.16: Proposed mechanism for the hydroacetoxylation reaction…………………………38

Figure 2.17: Proposed method for the PRCC synthesis of tetrahydrofurans………………….…39

Figure 2.18: Diastereoselectivty in the PRCC reaction…………………………………………40

Figure 2.19: Rationalization of the diastereoselectivity…………………………………………40

Figure 2.20: PRCC with propargyl alcohol……………………………………………………...40

Figure 2.21: Radical cyclization of phenylselenocrotonates……………………………………41

Figure 2.22: Comparison of phenylselenocrotonates to phenylselenoacrylates…………………42

Figure 2.23: Diastereoselectivity from different starting materials……………………………...42

Figure 2.24: Oxidation of electron deficient alkenes with RuO_4………………………………...44

Figure 2.25: Polymerization of polymethylmethyacrylate………………………………………46

Figure 2.26: Alkene scope with mono-*t*-butyl fumarate…………………………………………48

Figure 2.27: Alkene scope with cinnamic acid derivatives……………………………………...49

Figure 2.28: Alkynoic acids in the PRCC……………………………………………………….50

Figure 2.29: Diastereoselectivities of the PRCC products……………………………………….51

Figure 2.30: Epimeriztion of butyrolactone products…………………………………………...52

Figure 2.31: Radical dehalogenation of minor diastereomer…………………………………….53

Figure 2.32: Synthesis of the chloro-butyrolactone……………………………………………...54

Figure 2.33: Rationalization of the inconsequential low diastereoselectivity…………………...54

Figure 2.34: Arene oxidation and the bicyclic byproduct……………………………………..55

Figure 2.35: Theory on how to limit byproduct formation………………………………………55

Figure 2.36: Formation of desired products from both diastereomers…………………………..55

Figure 2.37: Elimination conditions and re-emergence of the byproduct……………………….56

Figure 2.38: Total diastereoselective synthesis of methylenolactocin and protolichesterinic acid……………………………...…………………………………………………………..56

Figure 2.39: Further developments in PRCC methodology……………………………………...58

Figure 3.1: Some ways in which carboxylic esters favor bond formation……………………….77

Figure 3.2: Use and removal of malonic esters…………………………………………………..78

Figure 3.3: The Barton decarboxylation…………………………………………………………79

Figure 3.4: The Kolbe electrolysis……………………………………………………………….80

Figure 3.5: The Minisci Reaction………………………………………………………………..82

Figure 3.6: Hydrodecarboxylation via photosensitizer…………………………………………..83

Figure 3.7: Hydrodecarboxylation from Yoshimi et. al………………………………………….83

Figure 3.8: Photoredox decarboxylative coupling……………………………………………….84

Figure 3.9: Proposed mechanism for this strategy……………………………………………….84

Figure 3.10: Proposed method for hydrodecarboxylation……………………………………….85

Figure 3.11: Reduction potentials of carboxylates with different substitution patterns…………86

Figure 3.12: Rate constants of representative aliphatic acyloxyl radical decomposition………..87

Figure 3.13: Decarboxylation of α-heteroatom carboxylates……………………………………87

Figure 3.14: Unsubstituted carboxylic acids are unreactive……………………………………..88

Figure 3.15: Initial results with phenylacetic acid derivatives…………………………………..89

Figure 3.16: Scope of monoacid hydrodecarboxylation…………………………………………92

Figure 3.17: Less successful and unsuccessful substrates for mondecarboxylation……………94

Figure 3.18: Proposed mechanism of hydrodecarboxylation……………………………………96

Figure 3.19: Competition experiment in two solvent systems…………………………………...98

Figure 3.20: Rate constants of oxidation………………………………………………………...99

Figure 3.21: Comparison of malonates and mono-ester malonates…………………………….101

Figure 3.22: Substrate scope of the Malonic acid hydrodecarboxylation………………………103

Figure 3.23: Possible application of hydrodecarboxylation methodology to the hydrofunctionalization of alkenes………………………………………………………………104

LIST OF ABBREVIATIONS AND SYMBOLS

A	Acceptor
Ac	Acetate
AIBN	Azobisisobutyronitrile
Ar	Aryl
aq	Aqueous
atm	Atmosphere
BET	Back electron transfer
Bn	Benzyl
br	Broad
br s	Broad singlet
n-Bu	*normal*-Butyl
t-Bu	*tert*-Butyl
bpm	bipyrimidine
bpy	bipyridine
bpz	bipyrazine
Bz	Benzoyl

^{13}C NMR	Carbon nuclear magnetic resonance spectroscopy
cat	Catalytic quantities or catalyst
Cbz	Carboxy benzoyl
conv	Conversion
Cy	Cyclohexyl
C-C	Carbon carbon single bond
CT	Charge transfer state
δ	Chemical shift
ΔG	Change in Gibbs free energy
d	Doublet or days
DBU	1,8-diazabicyclo[5.4.0]undec-7-ene
DCB	1.4-dicyanobenzene
DCC	*N,N'*-Dicyclohexylcarbodiimide
DCE	1,2-dichloroethane
DCM	Dichloromethane
dd	Doublet of doublets
ddt	Doublet of doublet of triplets
DEAD	Diethyl azodicarboxylate

DMAP	4-dimethylaminopyridine
DMF	*N*,*N*-dimethylformamide
DMSO	Dimethylsulfoxide
dq	Doublet of quartets
d.r.	Diastereomeric ratio
dt	Doublet of triplets
E^+ or El	Electrophile
EDG	Electron donating group
ent	Enantiomeric
eq	Equation
equiv.	Equivalents
e.r.	Enantiomeric ration
Et	Ethyl
EtOH	Ethanol
Et_3N	Trimethylamine
Et_2O	Diethyl ether
EtOAc	Ethyl acetate
EWG	Electron withdrawing group

^{19}F NMR	Fluorine nuclear magnetic resonance spectroscopy
fac	Facial
F	Faraday’s constant
FVP	Flash vacuum pyrolysis
GC	Gass chromatography
^{1}H NMR	Proton nuclear magnetic resonance spectroscopy
HAT	Hydrogen atom transfer
HOAc	Acetic acid
HOMO	Highest occupied molecular orbital
HMDS	1,1,1,3,3,3-hexamethyldisiloxane
HRMS	High resonance mass spectrometry
Hz	Hertz
I	Intermediate
IR	Infrared spectroscopy
J	Coupling constant
k	Rate constant
kcal	Kilocalorie
KIE	Kinetic isotope effect

λ	wavelength
L	liter
LA	lewis acid
LDA	lithiumdiisopropylamide
LEDs	light emitting diodes
LUMO	lowest unoccupied molecular orbital
μL	microliter
M	metal or molarity
m	multiplet
m	meta
*m*CPBA	meta-chlroperoxybenzoic acid
Me	methyl
MeCN	acetonitrile
MeOH	methanol
Mes-Acr-Me	9-mesityl-10-methylacridinium
Mes-Acr-Ph	9-mesityl-10-phenylacridinium
mg	Milligrams
MHz	Megahertz

min	minutes
MS	Mass spectrometry or molecular sieves
ms	Millisecond
MsCl	Methylsulfonyl chloride
MTBE	Methyl tert-butyl ether
n	Number of moles of electrons
nm	Nanometers
NMA	9-mesityl-10-methylacridinium
NHE	Normal hydrogen electrode
ns	Nanoseconds
Nu	Nucleophile
o	Ortho
ox	Oxidant or oxidation
p	Para
PDC	Pyridinium dichromate
PET	Photoinduced electron transfer
PG	Protecting group
Ph	Phenyl

PhCN	cyanobenzene
Phen	Phenanthrene
Phth	Phthalimidyl
PMP	*para*-methoxyphenyl
PMN	2-phenylmalononitrile
ppm	Parts per million
PRCC	Polar radical crossover cycloaddition
PTSA	*p*-toluenesulfonic acid
i-Pr	*iso*-Propyl
q	quartet
R_f	retention factor
RCHO	aldehyde
red	reduction
r.t.	room temperature
S	singlet or second (lower case)
SCE	standard calomel electrode
SET	single-electron transfer
S_N1	unimolecular nucleophilic substitution

S_N2	Bimolecular nucleophilic substitution
T	Triplet
TEA	Trimethylamine
TEMPO	(2,2,6,6-Tetramethylpiperidin-1-yl)oxyl
Tf	Trifluoromethanesulfonyl
TFA	Trifluoroacetic acid
TFE	Trifluoroethanol
THF	Tetrahydrofuran
TLC	Thin-layer chromatography
TMS	Tirmethylsilyl
Ts	*para*-toluenesulfonyl
uv	ultraviolet
X	anionic ligand, halide, substituent, or number
V	volt
9-CNF	9-cyanofluorene

CHAPTER ONE

INTRODUCTION TO PHOTOREDOX CATALYSIS

1.1 Introduction

Photoredox catalysis is a form of catalysis whereby the catalyst is excited by light, thus becoming either a strong oxidant or a strong reductant, allowing it to promote single-electron transfer (SET) processes from the excited state. In considering a simple diagram, one can see that excitation of a particular acceptor molecule (A) by light can elevate an electron, leaving a hole in what had been the HOMO (Figure 1.1). This produces a strong single electron oxidant, which can oxidize the donor molecule if energetically favorable. Depending on the relative energy levels of the relevant molecular orbitals, one could envision the promotion of single-electron reduction via light excitation as well (Figure 1.2). Although photoredox catalysis via single-electron reduction of a substrate is an important field, and valuable contributions have been made[1,2], the focus of this work will be on single-electron oxidation.

Figure 1.1: Photoinduced electron transfer promoting single-electron oxidation

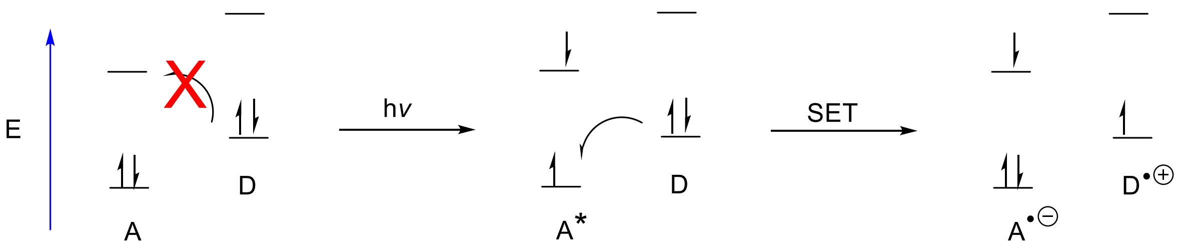

Figure 1.2: Photoinduced electron transfer promoting single-electron reduction

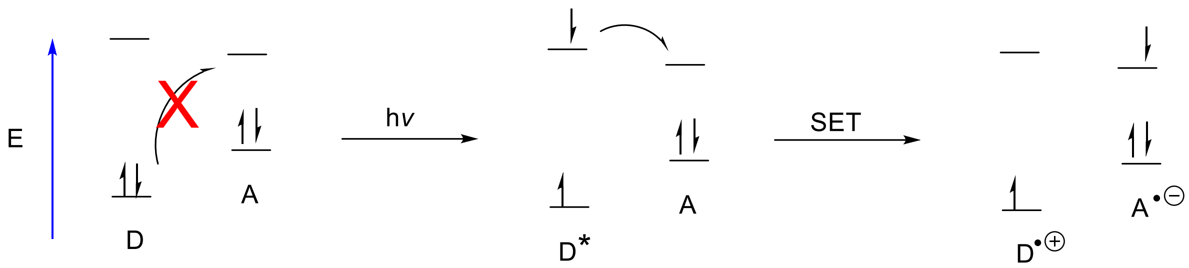
E
D
A
hv
D*
A
SET
D•⊕
A•⊖

As can be seen in figure 1.1 and 1.2, single-electron transfer via photoinduced electron transfer (PET) could be a powerful tool for chemical catalysis, as it has the ability to form a strong single electron oxidant (or reductant) relative to the ground state, as well as the ability to drastically change the polarity of the substrate by removal (or addition) of one electron. Early reactions employing this type of activation strategy, such as that developed by Gassman[3], employed the use of cyanoarenes under ultraviolet irradiation with biphenyl as a cosensitizer, in stoichiometric quantities (Figure 1.3). Nevertheless, Gassman was able to demonstrate key photoredox mediated transformations in the anti-Markovnikov addition of water, methanol, and acetate to olefins.

Figure 1.3: Photoredox mediated anti-Markovnikov transformations

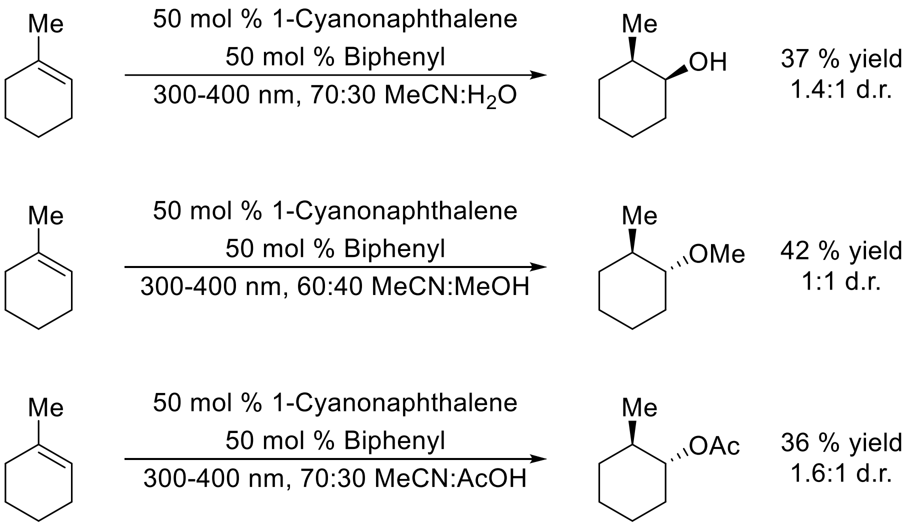
Me
50 mol % 1-Cyanonaphthalene
50 mol % Biphenyl
300-400 nm, 70:30 MeCN:H$_2$O
Me
OH
37 % yield
1.4:1 d.r.
Me
50 mol % 1-Cyanonaphthalene
50 mol % Biphenyl
300-400 nm, 60:40 MeCN:MeOH
Me
OMe
42 % yield
1:1 d.r.
Me
50 mol % 1-Cyanonaphthalene
50 mol % Biphenyl
300-400 nm, 70:30 MeCN:AcOH
Me
OAc
36 % yield
1.6:1 d.r.

The transformations rely on the single-electron oxidation of the alkene to the alkene radical cation by the excited cyanoarene. The major byproduct of these transformations comes from the photo-NOCAS[4-6] (Photochemical Nucleophile-Olefin Combination, Aromatic Substitution), whereby the cyanoarene incorporates into the final product (Figure 1.4). Notice the determination of regiochemistry. The nucleophile, methanol, adds to the radical cation such that the more stable radical intermediate is formed. This radical then recombines with the aryl radical anion, and loss of cyanide gives the product. This arylation side reaction contributes to the need for high loadings, and complicates their ability to be used catalytically.

Figure 1.4: Typical mechanism of photo-NOCAS reactivity

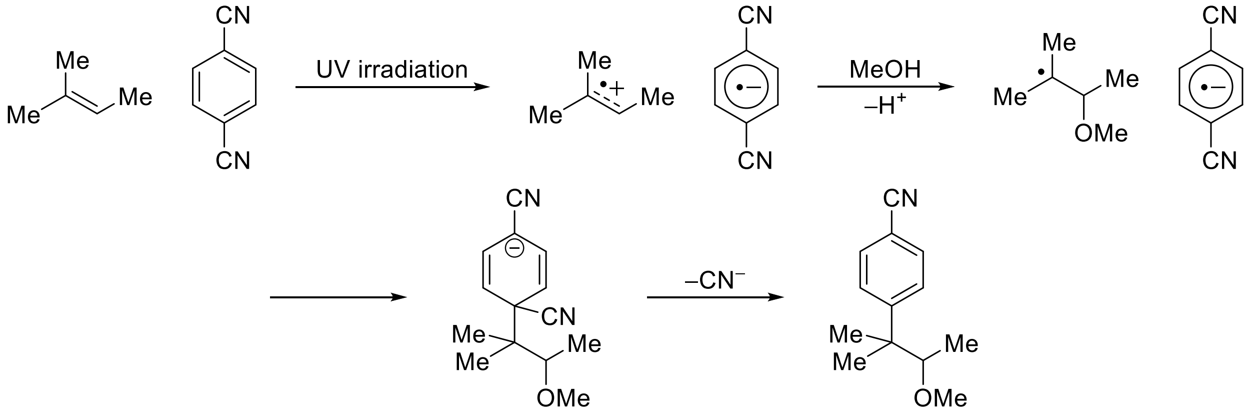

Another issue that complicates the catalytic use of cyanoarenes is their relatively short-lived excited states (~1 ns[7]) and their participation in back electron transfer (BET). Back electron transfer is the reverse of the initial single electron transfer, in which the reduced photosensitizer donates the electron back to the oxidized substrate. In the case of Gassman’s work, the alkene radical cation oxidizes the cyanoarene radical anion, forming again the alkene and cyanoarene starting materials. This type of process is more likely to occur with neutral photooxidants, as the products of the initial single-electron transfer are charged and often form strong ionic interactions, especially in less polar solvents, which facilitates back electron transfer instead of the dissociation of the ion pair. Another issue with using cyanoarenes in synthesis is that, with the exception of 9,10-dicyanoanthracene, they all absorb in the uv spectrum, which requires the use of specialized glassware. The high energy light also poses a risk for byproduct formation, and limits the use to substrates that do not also absorb in the uv.

Nevertheless, these early transformations demonstrate the utility of photoredox catalysis to undergo anti-Markovnikov hydrofunctionalization reactions via oxidation of olefins to a key radical cation intermediate. In recent years, attention has returned to this type of reactivity, with the aim of developing truly catalytic transformations.[8] This new generation of interest in photoredox catalysis started with reports in 2008 from Yoon[9] and MacMillan[10] and their use of ruthenium polypyridyl complexes to undergo photoredox processes. Ruthenium polypyridyl complexes have had decades of widespread study in inorganic chemistry, and were studied for potential synthetic use because of a few key factors.[11] They could be excited by lower energy visible light, they had long lived excited states, and in the excited state the complex can undergo single electron transfer via both oxidation and reduction, depending on the nature of the quencher. These advances will be discussed in more detail in section 1.3.

1.2 Thermodynamics of photoinduced electron transfer

When considering whether an electron transfer event is thermodynamically favorable, between ground state reagents, one can estimate the feasibility of transfer by comparing the standard reduction potentials of the reductant and oxidant. These standard reduction potentials can be related to the standard change in Gibbs free energy of the reaction by the following equation (equation 1.1), where n is the moles of electrons exchanged and F is Faraday's constant.

In this case, only reduction potentials are used. Ground state oxidation potentials are identical to reduction potentials and as such standard potentials are reduction potentials.

$$\Delta G^o = -nF(E^o_{(A/A^-)} - E^o_{(D^+/D)}) \quad (1.1)$$

Ground state reduction potentials for a variety of organic substrates have been calculated by many researchers before[12], however more recently an extensive study of the ground state reduction potentials of organic compounds has been undertaken by Hudson Roth and Nathan Romero, of the Nicewicz lab.[13] A general summary of the findings is shown in Figure 1.5.

Figure 1.5: Trends in ground state reduction potential based on functional group

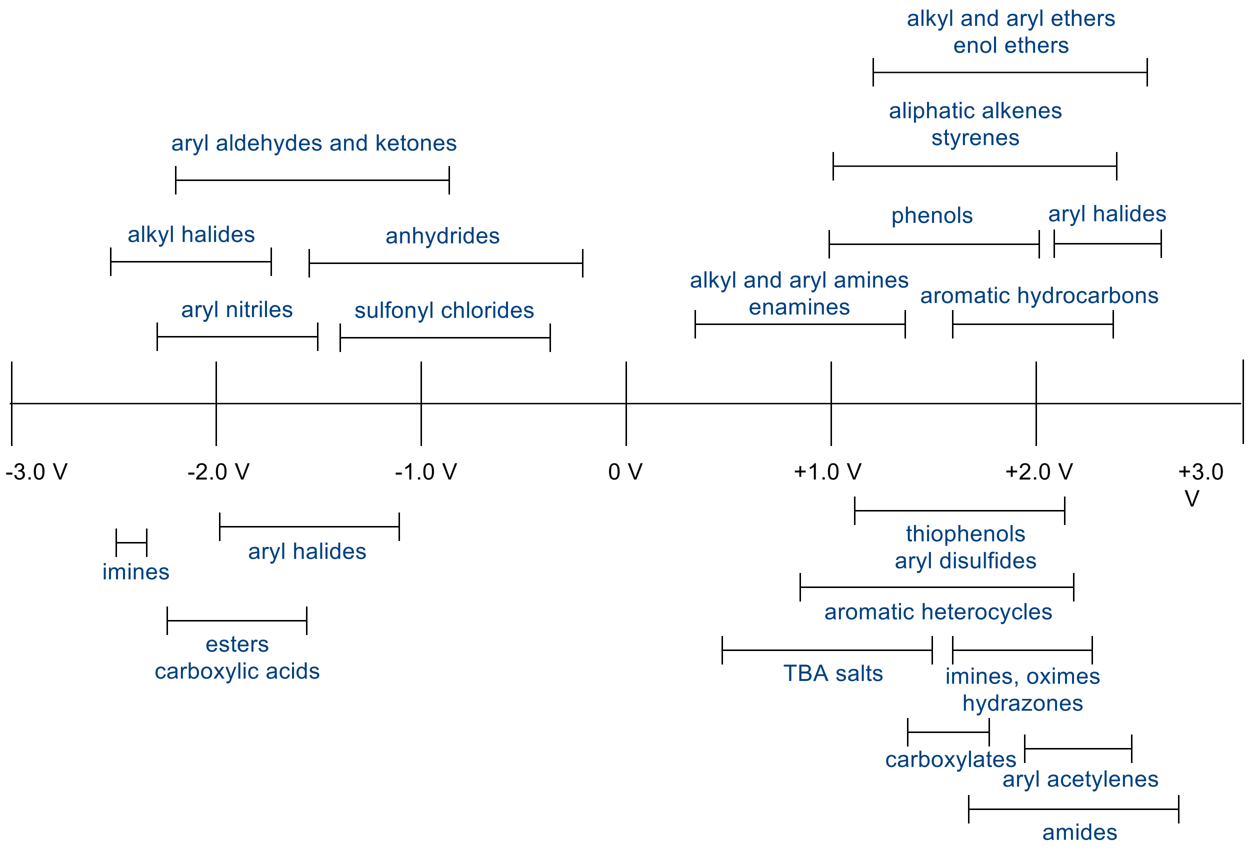

alkyl and aryl ethers
enol ethers
aliphatic alkenes
styrenes
aryl aldehydes and ketones
phenols
aryl halides
alkyl halides
anhydrides
alkyl and aryl amines
enamines
aromatic hydrocarbons
aryl nitriles
sulfonyl chlorides
-3.0 V
-2.0 V
-1.0 V
0 V
+1.0 V
+2.0 V
+3.0 V
thiophenols
aryl disulfides
imines
aryl halides
aromatic heterocycles
esters
carboxylic acids
TBA salts
imines, oximes
hydrazones
carboxylates
aryl acetylenes
amides

Of particular importance to understanding reactivity developed in the Nicewicz lab, in particular the project that will be discussed in Chapter 2, are the aliphatic alkenes and styrenes

(Figure 1.6). In the shown representative alkenes, one can see how factors such as substitution pattern, ring strain, and the presence of electron donating or withdrawing substituents can affect the reduction potential of the alkene. For example, the di-substituted alkene 2-methylpent-1-ene, at +2.5 V, is much harder to oxidize than the di-substituted alkenes in rings (norbornene at +2.22 V and cyclopentene at 2.32 V). The tri-substituted alkene 2-methyl-2-butene, at 1.98 V, is easier still. Phenyl substitution decreases the reduction potential even further, and increased substitution and the presence of electron donating substituents decreases the reduction potential further still. Again, a lower reduction potential of $E^{o}_{(D+/D)}$ indicates that the substrate is easier to oxidize.

Figure 1.6: Reduction potentials of representative alkenes

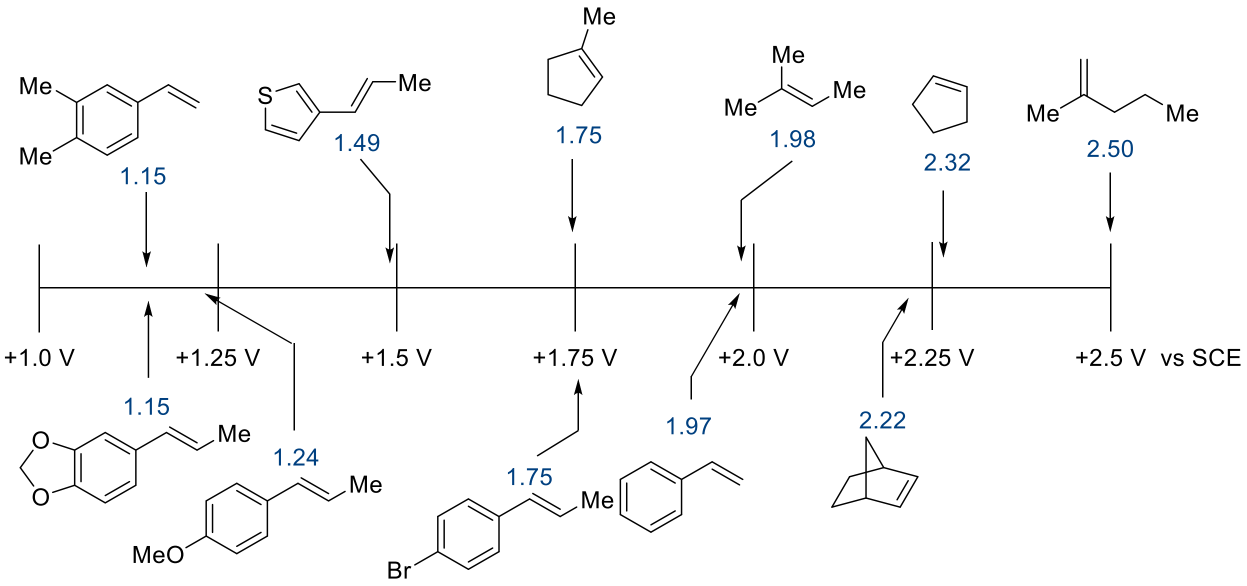

Although the feasibility of ground state electron transfer processes can be estimated using equation 1.1, the feasibility of photoinduced electron transfer processes is not quite so simple. This is because the excited state reduction potential must be used instead of the ground state reduction potential. Excited state reduction potentials are not measured directly, but are instead calculated by the relationship between measurable quantities. Unlike in ground state reduction potentials, the potential at which the excited catalyst is oxidized is different than the potential at which the excited catalyst is reduced.[14] The excited state oxidation potential of a catalyst which undergoes oxidation (equation 1.2) is equal to the ground state reduction potential of the catalyst, minus the one-electron potential corresponding to the zero-zero spectroscopic energy ($E_{0,0}$ in eV). The excited state reduction potential of a catalyst which undergoes reduction (equation 1.3) is equal to the ground state reduction potential of the catalyst plus the $E_{0,0}$. Thus, it is important to note that excited state species are both stronger oxidants and stronger reductants than their ground state counterparts, and how the catalyst behaves depends on its nature and the potential of the substrate.

$$E^{o}_{(A^{+}/*A)} = E^{o}_{(A^{+}/A)} - E_{0,0} \quad (1.2)$$

$$E^{o}_{(*A/A^{-})} = E^{O}_{(A/A^{-})} + E_{0,0} \quad (1.3)$$

Photoinduced electron transfer, in the case shown using a catalyst that is behaving as an oxidant, is favorable when the excited state reduction potential of the acceptor (i.e. the catalyst) is larger than the ground state reduction potential of the donor (i.e. the substrate), as can be seen in equation 1.4.

$$\Delta G^{o} = -nF(E^{o}_{(*A/A^{-})} - E^{o}_{(D^{\cdot +}/D)}) \quad (1.4)$$

Both ground state and excited state compounds can behave as single electron oxidants (Figure 1.7). However, in general excited state compounds are much stronger oxidants than ground state oxidants, due to the increase in reduction potential from the zero,zero spectroscopic energy from excitation. Ground-state single-electron oxidants which have found use in organic chemistry include ferrocene ($E_{p/2}$ = 0.47 V vs. SCE[15]), iron tris-phenanthroline ($E_{p/2}$ = 1.17 V vs.

SCE[16]) and tris-(4-bromophenyl)aminium hexachloroantimonate ($E_{p/2}$ = 1.47 V vs. SCE[17]). In considering Figure 1.6, one can see that many of these photooxidants would be able to oxidize a variety of synthetically useful substrates, such as aliphatic alkenes and styrenes, which most ground state oxidants could not. The reason for this is the added bonus that $E_{0,0}$ gives to photooxidants (equation 1.3).

Figure 1.7: Reduction potentials of some Ground-state and Excited-state oxidants

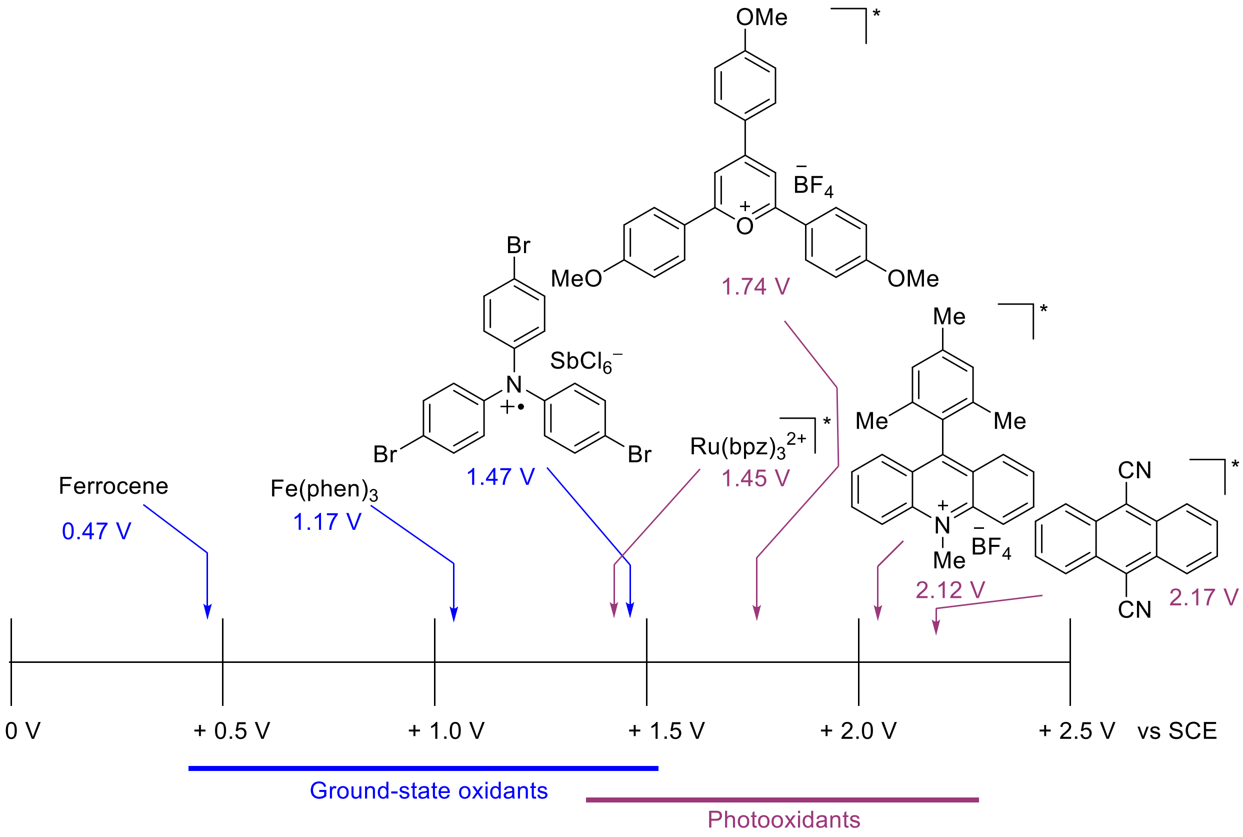
OMe
BF_4^-
MeO
OMe
1.74 V
Br
$SbCl_6^-$
Br
Br
Ferrocene
0.47 V
$Fe(phen)_3$
1.17 V
1.47 V
$Ru(bpz)_3^{2+}$
1.45 V
Me
Me
Me
Me
BF_4^-
2.12 V
CN
CN
2.17 V
0 V
+ 0.5 V
+ 1.0 V
+ 1.5 V
+ 2.0 V
+ 2.5 V
vs SCE
Ground-state oxidants
Photooxidants

Another advantage that photooxidants have is that these excited-state reduction potentials are not obtained without irradiation, and as such the photooxidants are both bench-top stable and can be chemoselective.

1.3 Recent advances in photoredox catalysis

As previously mentioned in section 1.1, photoredox mediated reactions have been known for many decades. However, these early reactions were generally not catalytic. More recently, attention has been given to inorganic photoredox catalysts to generate new reaction methodologies. However, many but the most electron rich olefins have remained beyond the oxidative ability of these photooxidants, as inorganic photoredox catalysts generally have lower excited-state reduction potentials than the organic photoredox agents, as seen by the comparison of $Ru(bpz)_3^{2+}$ (E^*_{red} = +1.47 V vs. SCE) and 9,10-dicyanoanthracene (E^*_{red} = +2.17 V vs. SCE) in Figure 1.7.

Amines, however, have much lower reduction potentials than olefins ($E_{p/2}$ = +0.7 V vs. SCE for N,N-dimethylaniline[18]). When an amine is oxidized by one electron, the bond dissociation of a C-H bond α to the nitrogen radical cation (aminium) is greatly reduced. This has allowed for the development of reactions in which the α hydrogen atom can be abstracted, furnishing an iminium ion, which can then act as an electrophile to a wide variety of nucleophiles, forming α-functionalized amines. The Stephenson group, for example, published an aza-Henry reaction between nitromethane and a catalytically generated iminium ion.[19] The photoredox catalyst used was $Ir(ppy)_2(dtbbpy)PF_6$ (E^*_{red} = 0.66 V vs. SCE[20]), and molecular oxygen was used to turn over the catalyst via oxidation (Figure 1.8). The product of this oxidation, superoxide, could then abstract the α-hydrogen atom of the aminium ion, thus generating the key iminium ion intermediate. Nitromethane anion then added to this electrophile, generating the aza-Henry products.

Figure 1.8: Proposed mechanism for α-functionalization of amines

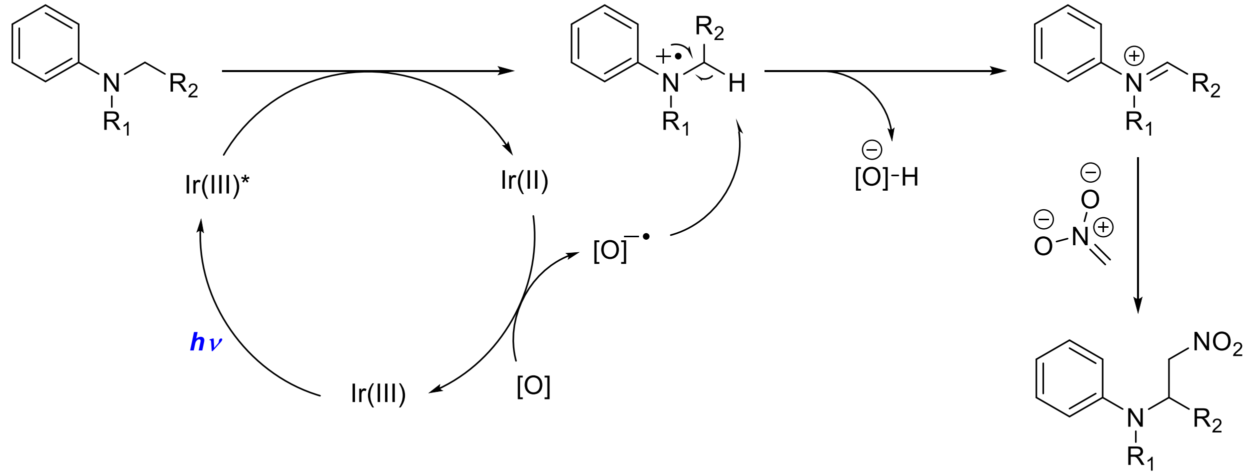

The Yoon group was able to utilize $Ru(bpy)_3Cl_2$ as a photooxidant to access alkene cation radicals by using methyl viologen as an oxidative quencher to access the ground state $Ru(bpy)_3^{3+}$, in order to conduct [2+2] cycloadditions.[21] $Ru(bpy)_3^{2+}$ (E^*_{red} = 0.77 V vs SCE[22]) would not on its own be strong enough, however $Ru(bpy)_3^{3+}$ ($E_{p/2}$ = 1.29 V vs. SCE) was a strong enough single-electron oxidant to generate alkene radical-cations. However, it was only strong enough to oxidize electron rich olefins such as *p*-methoxy and *o*-methoxy styrenyl derivatives (Figure 1.9). Unsubstituted styrenyl substrates and *m*-methoxy substituted styrenyl substrates had reduction potentials outside of the range of the catalytic system, and as such were unreactive.

Figure 1.9: [2+2] cycloaddition after access to $Ru(bpy)_3^{3+}$

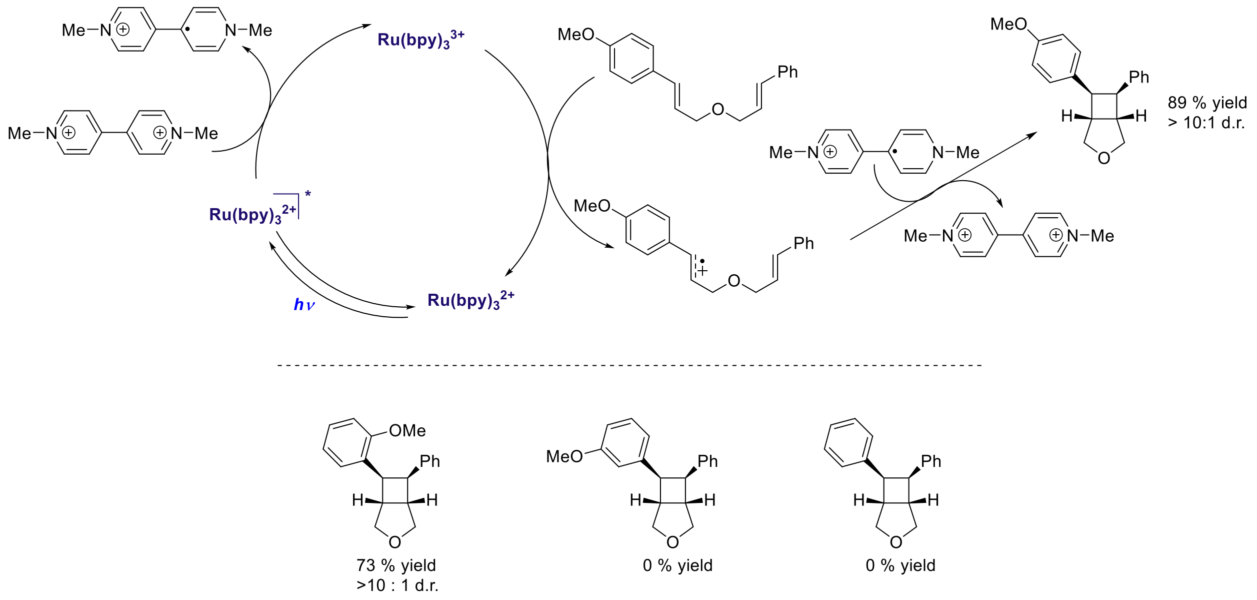
Ru(bpy)$_3^{3+}$
Ru(bpy)$_3^{2+}$*
Ru(bpy)$_3^{2+}$
hν
MeO
Ph
Me−N
N−Me
H
O
89 % yield
> 10:1 d.r.
OMe
73 % yield
>10 : 1 d.r.
0 % yield
0 % yield

A few years later, Yoon developed a method for intermolecular [2+2] heterodimerization[23] which used a different ligand system on the Ruthenium, Ru(bpm)$_3^{2+}$ (E^*_{red} = 1.2 V vs SCE[24]), allowing for a greater excited state reduction potential (Figure 1.10). However, the method still relied on the oxidation of the electron rich olefin anethole ($E_{p/2}$ = 1.24 V vs. SCE, Figure 1.6), prior to undergoing [2+2] cycloaddition with less oxidizable alkenes.

Figure 1.10: [2+2] Heterodimerization

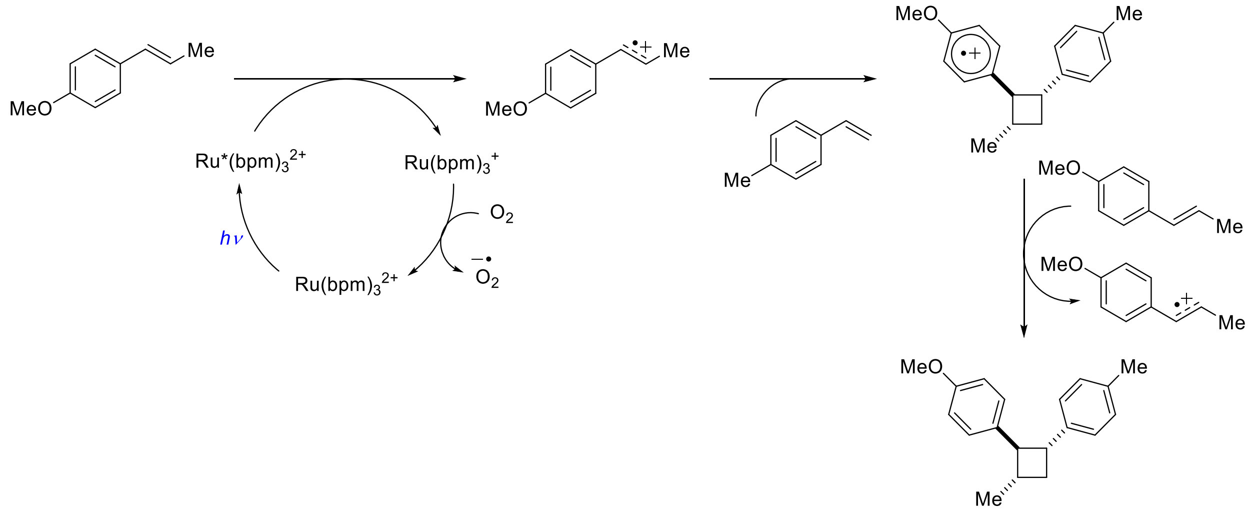
MeO
Me
Ru*(bpm)$_3^{2+}$
Ru(bpm)$_3^{+}$
Ru(bpm)$_3^{2+}$
hν
O$_2$
O$_2^{\bullet -}$

Michelle Riener, of the Nicewicz lab, was able to demonstrate the utility of 2,4,6-tris(4-methoxyphenyl)pyrylium as a photooxidant in a [2+2] homodimerization reaction method.[25] This method gave access to a broader range of alkenes for [2+2] reactivity, as the photooxidant has a high excited state reduction potential (E^*_{red} = +1.74 V vs. SCE[26], corrected as the reported literature value is +1.98 V vs. NHE). The use of triarylpyryriliums as photooxidants have been the subject of reviews.[27]

Figure 1.11: Access to more challenging alkenes using an organic photooxidant

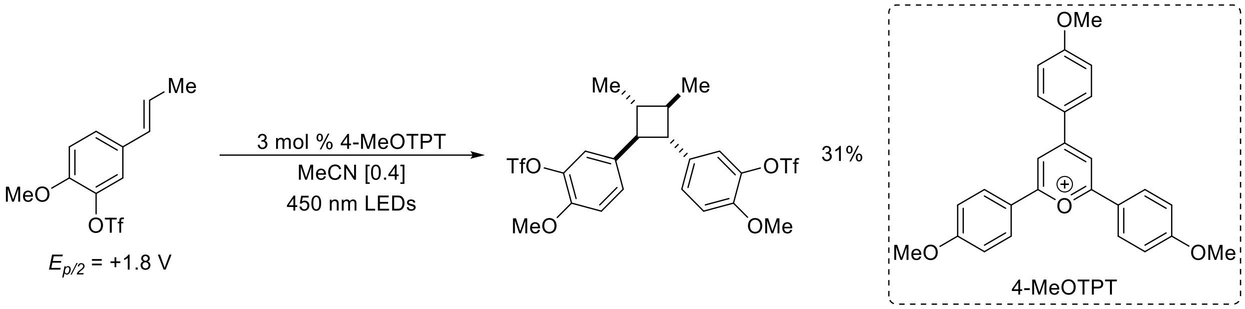

The elevated excited state reduction potential of the triarylpyrilium allows access to a broader range of alkene substrates, however the susceptibility of these highly electrophilic species to nucleophilic attack limits their use in a broader range of transformations. These developments, a brief summary, demonstrate the need for the development of stronger, and more stable and robust, photooxidants to be able to catalytically generate radical cation intermediates from alkenes, and other substrates, that are more challenging to access.

1.4 The Fukuzumi acridinium catalyst

In 2004, Fukuzumi reported the synthesis and characterization of 9-mesityl-10-methylacridinium.[28] The 9-mesityl-10-methylacridinium absorbs blue light. According to the crystal structure, the bulky mesityl substituent is nearly perpendicular with the acridinium core.

In this initial report, Fukuzumi made an argument for a long lived charge-transfer state (CT) with a reduction potential of 1.88 V vs SCE, whereby after excitation of the acridinium, charge separation could occur with a radical cation on the nearly perpendicular mesityl substituent, and a radical on the acridine core. A year later, however, Verhoeven[29] and co-workers reported a singlet excited-state localized on the acridinium chromophore (LE^S) with a reduction potential of 2.18 V vs. SCE, a singlet CT state with a reduction potential of 2.06 V vs. SCE, and a triplet excited-state localized on the acridinium chromophore (LE^T) with a reduction potential of 1.45 V vs. SCE.[30] The information from these reports is summarized in Figure 1.12.[31]

Figure 1.12: Summary of excited states from Fukuzumi and Verhoeven

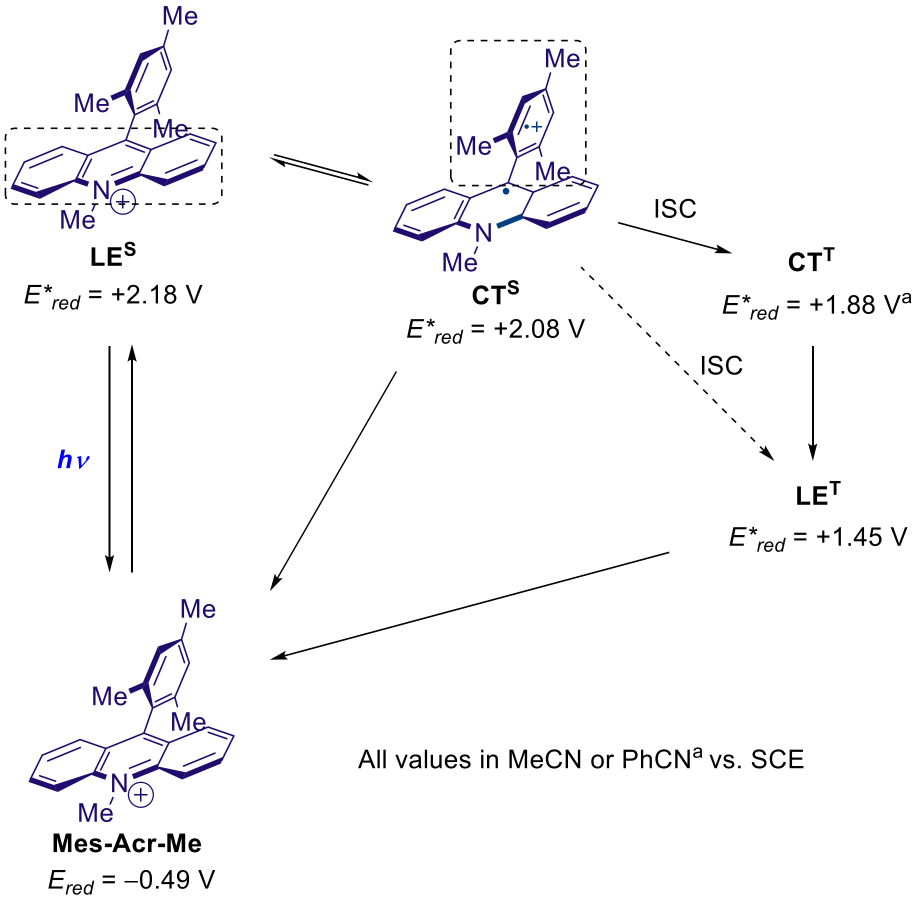
Me
Me
Me
N
Me
LE^S
E^*_{red} = +2.18 V
Me
Me
Me
N
Me
CT^S
E^*_{red} = +2.08 V
ISC
CT^T
E^*_{red} = +1.88 V^a
ISC
LE^T
E^*_{red} = +1.45 V
$h\nu$
Me
Me
Me
N
Me
Mes-Acr-Me
E_{red} = –0.49 V

All values in MeCN or PhCN^a vs. SCE

In 2011, Fukuzumi reported that 9-mesityl-10-methylacridinium (**Mes-Acr-Me**) could catalyze the bromination of electron rich arenes.[32] The transformation occurred upon visible light irradiation of an oxygen saturated solution containing the oxidizable aryl substrate, catalytic amounts of **Mes-Acr-Me**, and 50% aqueous hydrogen bromide (Figure 1.13). Such strong conditions of aqueous hydrogen bromide demonstrate the broader range of conditions this catalyst can tolerate, in comparison with the triarylpyryliums. Electron rich arenes, such as methoxy substituted arenes and some heteroaromatic compounds gave brominated products in good regioselectivity and in good yields. For reference, 1,3-dimethoxybenzene has a reduction potential of +1.50 V vs. SCE.[13] The reaction was shown to proceed via the formation of aryl radical cations, and dissolved molecular oxygen could turn over the catalyst.

Figure 1.13: Aryl bromination catalyzed by **Mes-Acr-Me**

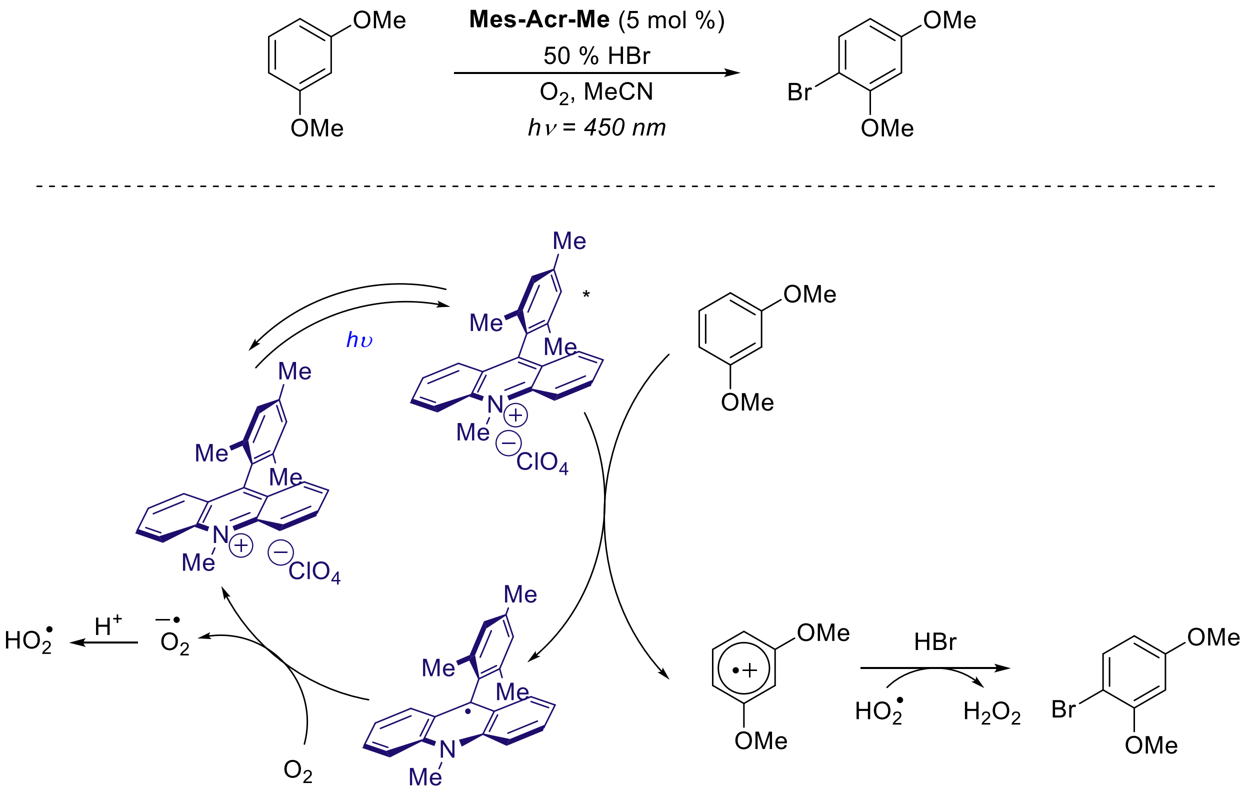
OMe
OMe
Mes-Acr-Me (5 mol %)
50 % HBr
O2, MeCN
hν = 450 nm
OMe
Br
OMe
Me
Me
Me
*
hυ
N
Me
ClO4
Me
Me
Me
N
Me
ClO4
OMe
OMe
HO2•
H+
O2•−
O2
Me
Me
Me
N
Me
•+
OMe
OMe
HBr
HO2•
H2O2
Br
OMe
OMe

This important report demonstrates the ability of **Mes-Acr-Me** to catalyze reactions via oxidizing substrates to their radical cation intermediates. The presence of multiple excited states, some with high reduction potentials of > +2.0 V vs. SCE, begged the question of whether this photocatalyst could be used to access radical cation intermediates from alkenes or other substrates with higher reduction potentials.

1.5 Development of the hydrofunctionalization catalyst system

David Hamilton, of the Nicewicz lab, was instrumental in developing a broader synthetic use for the **Mes-Acr-Me** catalyst. He developed a catalytic system that formed the basis for a number of advances in the Nicewicz lab over the subsequent few years, including the advances that will be discussed in chapters 2 and 3. Inspired by Gassman's work in the anti-Markovnikov addition of water, methanol, and acetic acid to methylcyclohexene[3], Hamilton considered whether the Fukuzumi acridinium catalyst might be used in a similar type of transformation, instead of stoichiometric quantities of a cyanoarene (Figure 1.14). In order to explore this possibility, Hamilton considered using the acridinium in an intramolecular hydroetherification reaction.[33] With mechanistic insight on nucleophilic additions to radical cation intermediates from Arnold,[34] Hamilton believed that a catalytically generated radical cation could form a basis for anti-Markovnikov hydrofunctionalization methodology. He reasoned that a nucleophile would add to the radical cation with regiochemical control such that the more stable radical would be formed.

Figure 1.14: Hamilton's initial strategy for the hydroetherification reaction

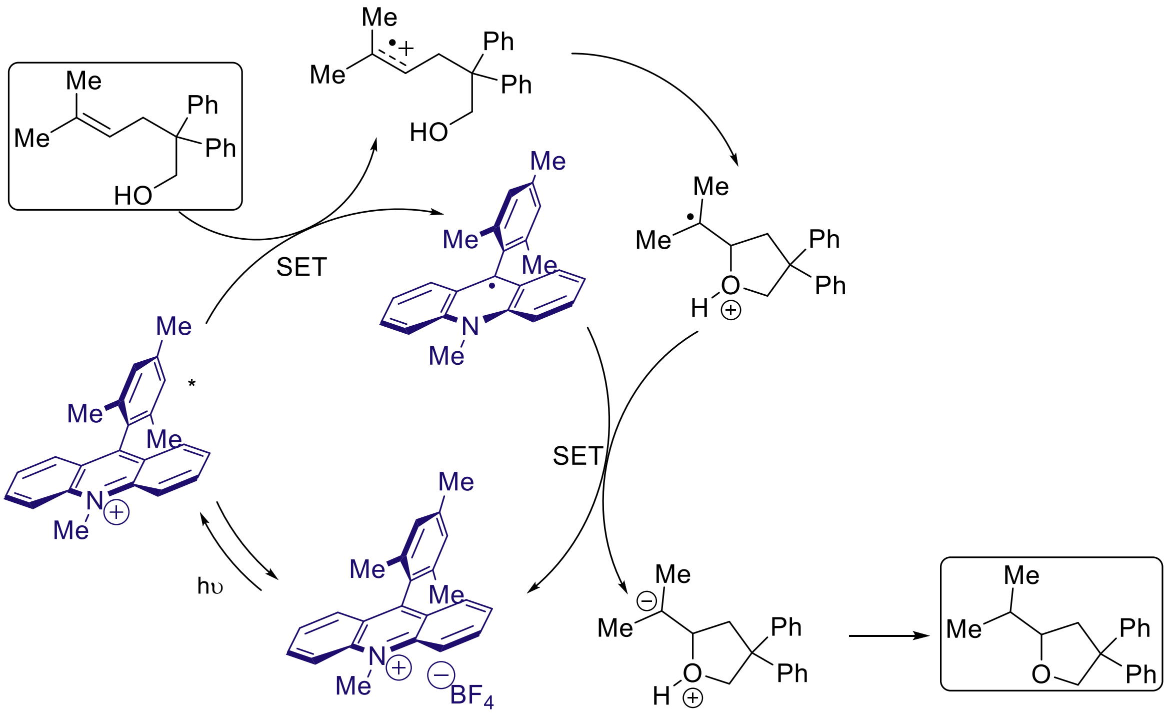
Me
Me
Ph
Ph
HO
SET
SET
hυ
N
BF4

In his initial exploration, Hamilton proposed that the radical intermediate of the substrate would turn over the catalyst by oxidizing the acridine radical to the ground state **Mes-Acr-Me**. However, despite the high conversion, low yields of the desired product were observed even after extended 96 hours of irradiation (Figure 1.15).[35]

Figure 1.15: Initial results in the hydroetherification reaction

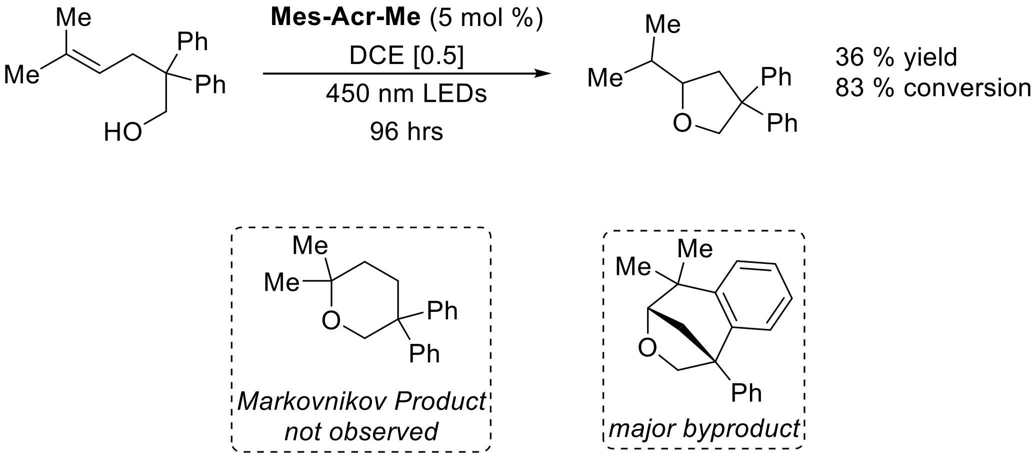
Mes-Acr-Me (5 mol %)
DCE [0.5]
450 nm LEDs
96 hrs
36 % yield
83 % conversion
Markovnikov Product not observed
major byproduct

While the conditions gave the desired product in good anti-Markovnikov selectivity, the major byproduct arose from intramolecular aryl trapping of the radical intermediate. The appearance of this byproduct prompted Hamilton to consider additives that might improve the turnover of the catalyst. Under this strategy, instead of having the substrate radical intermediate turn over the catalyst forming an anion which would subsequently undergo proton transfer, the substrate radical intermediate would instead form the product directly via hydrogen atom transfer (Figure 1.16). In trying a number of different additives, Hamilton found success with substoichiometric quantities of 2-phenylmalononitrile (PMN).

Figure 1.16: Addition of 2-phenylmalononitrile as hydrogen atom donor

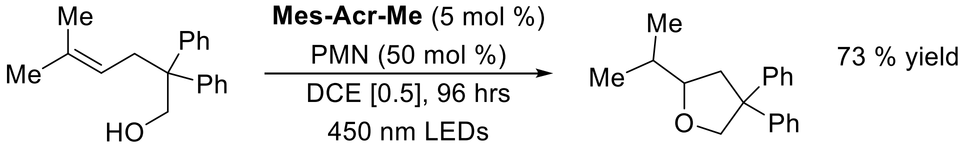

The success of 2-phenylmalononitrile in this reaction is attributed to its ability to facilitate multiple key steps in the mechanism. It can behave as a hydrogen atom donor, the resultant radical can oxidize the acridine radical and turn over the acridinium catalyst, and the subsequent anion can act as a base to quench the oxonium ion intermediate (Figure 1.17).

Figure 1.17: Trifold requirements of a quality additive

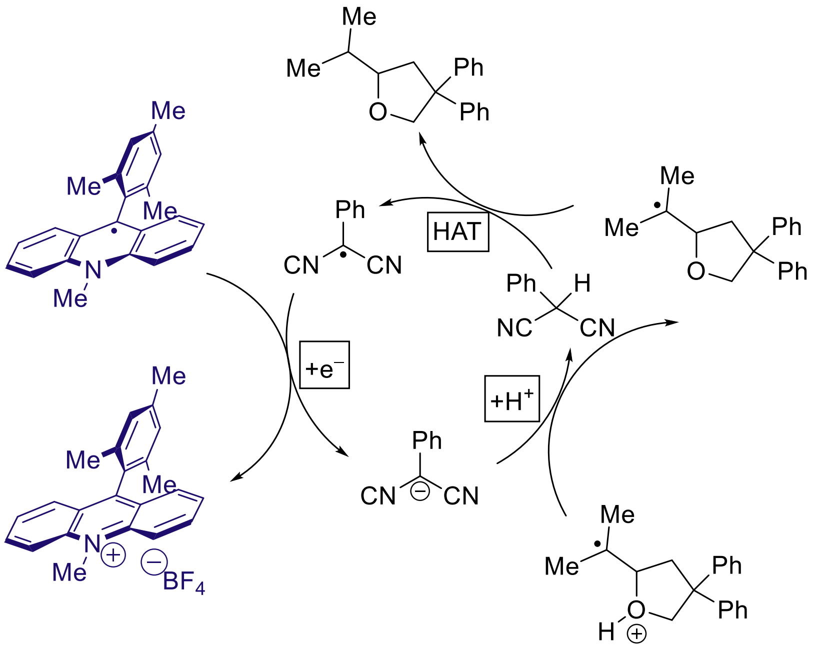

HAT = Hydrogen Atom Transfer

BDE = 77 kcal/mol
Thermodynamically Favorable
HAT (~18 kcal/mol)

$+e^-$ = Electron Transfer

E^{red} = 0.19 V
E^{red}*(catalyst)* = -0.55 V
Favorable by 0.74 V

$+H^+$ = Proton Transfer

pK_a = 4.2
Weak Base Protonated by
Strong Oxonium (pK_a ~ -2.0)

The framework of this catalyst system, of the Fukuzumi acridinium working in concert with a redox active hydrogen atom donor, became the basis of many transformations developed subsequently in the Nicewicz lab. Using this system, many nucleophiles have been added to oxidizable olefins, including carboxylic acids[36], allyl alcohols[37], amines[38,39], allyl amines and unsaturated amides[40], mineral acids[41], as well as the work that will be discussed in chapter 2.[42]

Most of these elaborations of this methodology utilized either thiophenol or phenyl disulfide derivatives as the redox active hydrogen atom donor instead of 2-phenylmalononitrile. Thiophenol or disulfides were found to drastically decrease reaction times. The BDE of the thiol S-H bond is similar to the C-H bond in 2-phenylmalononitrile (79 kcal/mol vs 77 kcal/mol respectively), so this improvement in reactivity is deemed to be kinetic. The resultant thiyl radical has a reduction potential of +0.16 V vs. SCE, and as such can oxidize the acridine radical and turn over the catalyst. The thiolate anion can be protonated, thus turning over the redox active hydrogen atom donor. Nathan Romero has studied the mechanism of the hydrofunctionalization methodology.[31] He computed the transition structures of hydrogen atom transfer between both 2-phenylmalononitrile and thiophenol and a standard intermediate for the intramolecular hydroetherification, and found that hydrogen atom transfer with thiophenol had a significantly decreased activation barrier relative to 2-phenylmalononirile, resulting in a calculated 4-fold rate enhancement for that key step. In addition, Romero demonstrated that disulfides behaved comparably to thiophenols in these reactions, because they could be homolytically cleaved by the 450 nm LEDs and enter the catalytic cycle as the thiyl radical.

1.6 Other uses of the Fukuzumi acridinium

Photoredox catalysis does not inherently need to be used to promote nucleophilic attack of olefins. The Nicewicz lab has pursued other synthetic uses of the Fukuzumi acridinium, including what will be discussed in chapter 3.[43] For example, Dale Wilger and Nathan Gesmundo developed an anti-Markovnikov hydrotrifluoromethylation reaction which proceeds through a different mechanism than the other hydrofunctionalization reactions.[44] In this transformation, Langlois reagent (CF_3SO_2Na) is oxidized by the photocatalyst, losing SO_2 and forming a trifluoromethyl radical. This radical then adds into the olefin, and then undergoes a hydrogen atom transfer process similar to the other systems. A variety of olefins were found to be successful, even those which would not otherwise be oxidized by the **Mes-Acr-Me**, a result of the mechanistic difference. They also find improved yields with trifluoroethanol as an additive, and they propose that this aids in the hydrogen atom transfer step(s). They propose that the acridine radical can be oxidized by either the TFE radical or the thiyl radical.

Figure 1.18: Proposed mechanism for the hydrotrifluoromethylation reaction

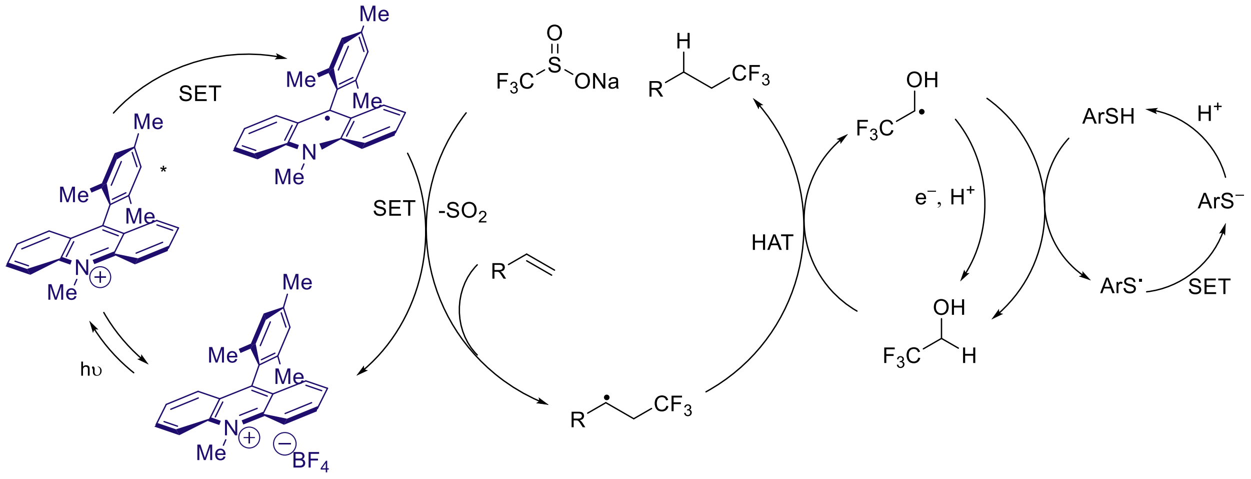
SET
Me
Me
Me
Me
Me
Me
N
Me
*
N
Me
SET
-SO2
hυ
Me
Me
Me
N
Me
BF4
O
S
F3C
ONa
H
R
CF3
R
R
CF3
HAT
OH
F3C
e⁻, H⁺
OH
F3C
H
ArSH
H⁺
ArS⁻
ArS·
SET

Nathan Romero, Kaila Margrey, and Nick Tay, of the Nicewicz lab, developed a site-selective arene C-H amination reaction using an acridinium catalyst.[45] This reaction relies on the oxidation of electron rich arenes to the corresponding radical cation, followed by nucleophilic addition. TEMPO, in the presence of air, is the terminal oxidant and allows for turn-over of the catalyst as well as aromatization of the aminated arene. This transformation required that something other than thiophenol be used to turn over the catalyst, as the desired transformation was a net oxidative transformation instead of redox neutral, and greatly expanded the toolbox of reactivity being developed in the Nicewicz laboratory.

Figure 1.19: Amination of arenes

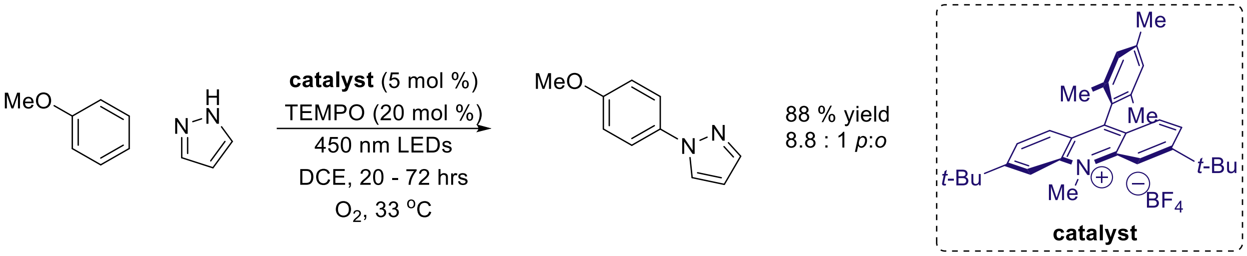
MeO
H
N
N
catalyst (5 mol %)
TEMPO (20 mol %)
450 nm LEDs
DCE, 20 - 72 hrs
O2, 33 °C
MeO
N
N
88 % yield
8.8 : 1 p:o
Me
Me
Me
t-Bu
N
Me
BF4
t-Bu
catalyst

The advances in our understanding of the mesityl acridinium as a photoredox catalyst were the basis for the advances that will be discussed in Chapters 2 and 3.

REFERENCES

(1) Prier, C.K.; Rankic, D. A.; MacMillan, D. W. C. *Chem. Rev.* **2013**, *113*, 5322.

(2) Meyer, A. U.; Slanina, T.; Yao, C. J.; König, B. *ACS Catal.* **2016**, *6*, 369.

(3) Gassman, P. G.; Bottorff, K. J. *Tetrahedron Lett.* **1987**, *28,* 5449.

(4) Arnold, D. R.; Chan, M. S. W.; McManus, K. A. *Can. J. Chem.* **1996**, *74*, 2143.

(5) McManus, K. A.; Arnold, D. R. *Can. J. Chem.* **1995**, *73*, 2158.

(6) Mangion D.; Arnold, D. R. *Acc. Chem. Res.* **2002**, *35*, 297.

(7) Kavarnos, G.; Turro, N. *Chem. Rev.* **1986**, *86*, 401.

(8) Narayanam, J. M. R.; Stephenson, C. R. J. *Chem. Soc. Rev.* **2011**, *40*, 102.

(9) Ischay, M. A.; Anzovino, M. E.; Du, J.; Yoon, T. P. *J. Am. Chem. Soc.* **2008**, *130*, 12886.

(10) Nicewicz, D. A.; MacMillan, D. W. C. *Science* **2008**, *32*2, 77.

(11) Kalyanasundaram, K. *Coordination Chemistry Reviews*, **1982**, *46*, 159.

(12) Connelly, N. G.; Geiger, W. E. *Chem. Rev.* **1996**, *96*, 877.

(13) Roth, H. G.; Romero, N. A.; Nicewicz, D. A. *Synlett*, **2016**, *27,* 714.

(14) Ceroni, P.; Balzani, V. Photoinduced Energy and Electron Transfer Processes. In The Exploration of Supramolecular Systems and Nanostructures by Photochemical Techniques, Lecture Notes in Chemistry 78; Ceroni, P., Ed; Springer Science+Business Media B., 2012; pp.21-23

(15) Batterjee, S. M.; Marzouk, M. I.; Aazab, M. E.; El-Hashash, M. A. *Appl. Organomet. Chem.* **2003**, *17*, 291.

(16) Schmittel, M.; Ammon, H.; Wöhrle, C. *Chem. Ber.* **1995**, *128*, 845.

(17) Bauld, N. L.; Stufflebeme, G. W.; Lorenz, K. T. *J. Phys. Org. Chem.* **1989**, *2*, 585.

(18) Seo, E. T.; Nelson, R. F.; Fritsch, J. M.; Marcoux, L. S.; Leedy, D. W.; Adams, R. N. *J. Am. Chem. Soc.* **1966**, *178*, 3498.

(19) Condie, A. G.; González-Gómez, J. C.; Stephenson, C. R. J. *J. Am. Chem. Soc.* **2010,** *132*, 1464.

(20) Slinker, J. D.; Gorodetsky, A. A.; Lowry, M. S.; Wang, J.; Parker, S.; Rohl, R.; Bernhard, S.; Malliaras, G. G. *J. Am. Chem. Soc.* **2004**, *126*, 2763.

(21) Ischay, M.; Lu, Z.; Yoon, T. *J. Am. Chem. Soc.* **2010**, *132*, 8572.

(22) Juris, A.; Balzani, V. *Helv. Chim. Acta* **1981**, *64*, 2175.

(23) Ischay, M. A.; Ament, M. S.; Yoon, T. P. *Chem. Sci.* **2012**, *3*, 2807

(24) Kawanishi, Y.; Kitamura, N.; Kim, Y.; Tazuke, S. *Sci. Pap. Inst. Phys. Chem. Res. (Jpn.)*, **1984**, *78*, 212.

(25) Riener, M.; Nicewicz, D. A. *Chem. Sci.* **2013**, *4*, 2625

(26) Martiny, M. A.; Steckhan, E.; Esch, T. *Chem. Ber.* **1993**, *126*, 1671

(27) Miranda, M.; Garcia, H. *Chem. Rev.* **1994**, *94*, 1063.

(28) Fukuzumi, S.; Kotani, H.; Ohkubo, K.; Ogo, S.; Tkachenko, N. V.; Lemmetyinen, H. *J. Am. Chem. Soc.* **2004**, *126*, 1600.

(29) Verhoeven, J. W.; van Ramesdonk, H. J.; Zhang, H.; Groeneveld, M. M.; Benniston, A. C.; Harrimar, A. *Int. J. Photoenergy* **2005**, *07*, 103.

(30) Benniston, A. C.; Harriman, A.; Li, P.; Rostron, J. P.; van Ramesdonk, H. J.; Groeneveld, M. M.; Zhang, H.; Verhoeven, J. W. *J. Am. Chem. Soc.* **2005**, *127*, 16054.

(31) Romero, N.; Nicewicz, D. A. *J. Am. Chem. Soc.* **2014**, *136*, 17024.

(32) Ohkubo, K.; Mizushima, K.; Iwata, R.; Fukuzumi, S. *Chem. Sci* **2013**, *135*, 10334.

(33) Hamilton, D.; Nicewicz, D. A. *J. Am. Chem. Soc.* **2012**, *134*, 18577.Oh

(34) Arnold, D. R.; Chan, M. S. W.; McManus, K. A. *Can. J. Chem.* **1996**, *74*, 2143

(35) Hamilton, D. S. PhD. Dissertation, UNC Chapel Hill, 2014.

(36) Perkowski, A. J.; Nicewicz, D. A. *J. Am. Chem. Soc.* **2013**, *135*, 10334

(37) Grandjean, J. M.; Nicewicz, D. A. *Angew. Chem. Int. Ed.* **2013**, *52*, 3967.

(38) Nguyen, T. M.; Nicewicz, D. A. *J. Am. Chem. Soc.* **2013**, *134*, 9588.

(39) Nguyen, T. M.; Monohar, N.; Nicewicz, D. A. *Angew. Chem. Int. Ed.* **2014**, *53*, 6198.

(40) Gesmundo, N. J.; Grandjean, J. M.; Nicewicz, D. A. *Org. Lett.* **2015**, *17*, 1316.

(41) Wilger, D. J.; Grandjean, J. M.; Nicewicz, D. A. *Nature Chem*. **2014**, *6*, 720.

(42) Zeller, M. A.; Riener, M.; Nicewicz, D. A. *Org. Lett.* **2014**, *16*, 4810.

(43) Griffin, J. D.; Zeller, M. A.; Nicewicz, D. A. *J. Am. Chem. Soc.* **2015**, *137*, 11340.

(44) Wilger, D. J.; Gesmundo, N. J.; Nicewicz, D. A. *Chem. Sci.* **2013**, *4*, 3160.

(45) Romero, N. A.; Margrey, K. A.; Tay, N. E.; Nicewicz, D. A. *Science* **2015**, *349*, 1326.

CHAPTER TWO

SYNTHESIS OF BUTYROLACTONES

2.1 Introduction

2.1.1 Importance of the butyrolactone moiety

γ-Butyrolactones are highly prevalent moieties in natural products. It is estimated that α-methylene and α-alkylidine γ-butyrolactones alone make up 3% of known natural products, and many of these compounds exhibit high levels of biological activity.[1] Butyrolactones with any substitution pattern in the α position make up an estimated 10% of known natural products.[2] Of these bioactive natural products, the α-unsaturation, if present, is often implicated as the active pharmacophore.[2] Butyrolactone natural products can exist as monocyclic, bicyclic, and tricyclic compounds. Due to the prevalence of the butyrolactone core in natural products, many strategies exist for their synthesis.[3] However, these strategies generally use prefunctionalized starting materials in order to synthesize a single desired product. Convergent methods that can be used to synthesize a variety of butyrolactones from simple starting materials are much rarer in the literature. In Figure 2.1, some representative multicyclic bioactive α-methylene and α-alkylidine natural products are shown. Andrographolide was the first isolated α-alkylidine natural product, first isolated in 1911.

Figure 2.1: Examples of bioactive α-methylene and α-alkylidine natural products

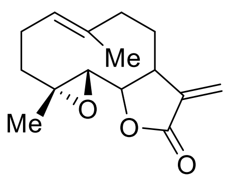

Parthenolide (Feverfew)
Anti-inflammatory
Anticancer
Antiviral

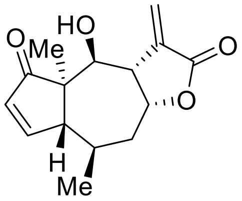

Helenalin (Arnica)
Anti-inflammatory

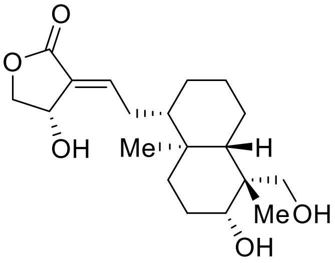

Andrographolide (1911)
α-Glucosidase inhibitor

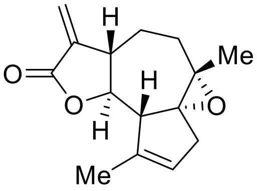

Arglabin
Tumor Inhibitor

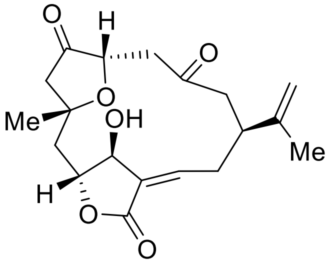

Scabrolide E
Cytotoxic

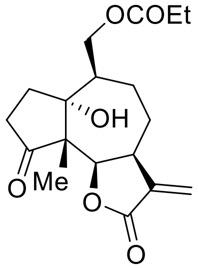

Hispitolide A
Antiviral

2.1.2 Importance of the paraconic acids

Paraconic acids are a class of butyrolactone natural products found most often in lichen, characterized by a carboxylic acid in the β position, a long greasy chain in the γ position, and generally either a methyl or methylene at the α position.[4] A representaitive sample of paraconic acids are shown in Figure 2.2. Many paraconic acids show biological activity, and this activity is greatly enhanced by the presence of the α-methylene moiety. In our investigations into the synthesis of butyrolactones generally, we sought to apply our method to the synthesis of two representative α-methylene paraconic acids: Methylenolactocin and protolichesterinic acid. Methylenolactocin, isolated by Park and co-workers, was found to possess unique antibacterial activity.[5] Protolichesterinic acid exhibits antifungal activity and inhibitory activity toward colon carcinoma.[6-8]

Figure 2.2: Examples of paraconic acids

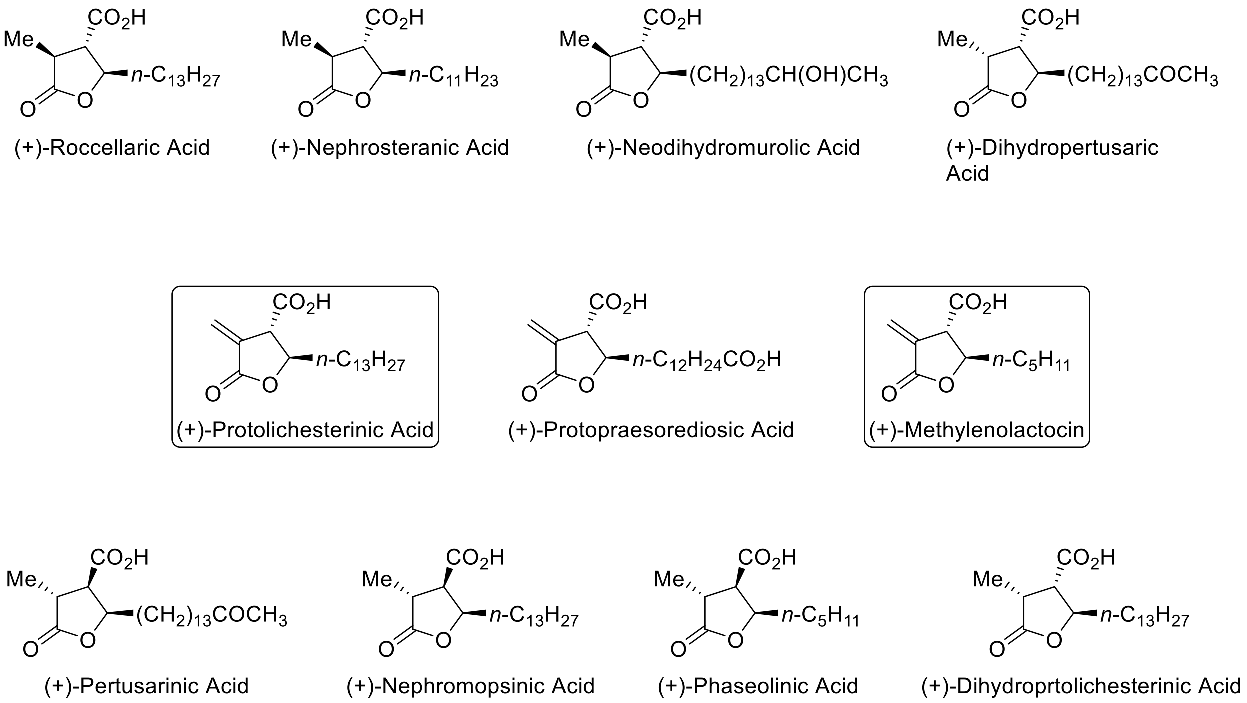

(+)-Roccellaric Acid
(+)-Nephrosteranic Acid
(+)-Neodihydromurolic Acid
(+)-Dihydropertusaric Acid
(+)-Protolichesterinic Acid
(+)-Protopraesorediosic Acid
(+)-Methylenolactocin
(+)-Pertusarinic Acid
(+)-Nephromopsinic Acid
(+)-Phaseolinic Acid
(+)-Dihydroprtolichesterinic Acid

2.1.3 Intramolecular strategies for the synthesis of butyrolactones

One of the more widely used intramolecular methods for the synthesis of γ-butyrolactones is halocyclization, whereby a halide (often iodide) activates an alkene for intramolecular carboxylic acid nucleophilic attack through a three membered halonium ion intermediate. Recently, advances have been made in asymmetric iodolactonization methodology.[9] The Johnson lab has developed an asymmetric method for the synthesis of butyrolactones from α-ketoesters.[10] This method relies on the dynamic kinetic resolution of α-ketoesters, producing the desired enantiomer of the key intermediate via an asymmetric transfer hydrogenation from both diastereomers of the α-ketoester. This key intermediate then undergoes a diastereoselective lactonization spontaneously in solution to produce the lactone products in high enantioselectivities (Figure 2.3).

Figure 2.3: Butyrolactones via dynamic kinetic resolution of α-ketoesters

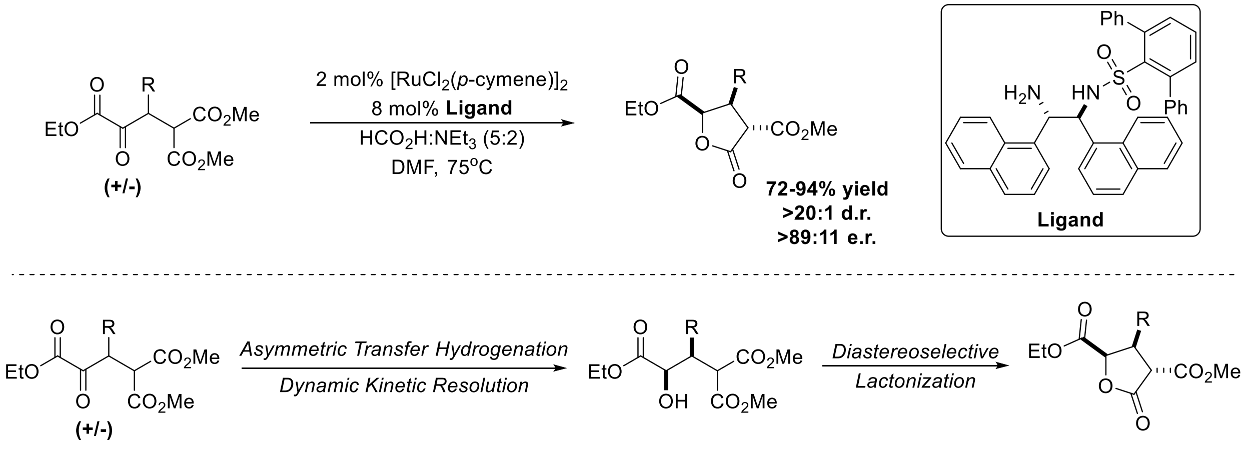

(+/-)
2 mol% [RuCl2(p-cymene)]2
8 mol% Ligand
HCO2H:NEt3 (5:2)
DMF, 75°C
72-94% yield
>20:1 d.r.
>89:11 e.r.
Ligand
Asymmetric Transfer Hydrogenation
Dynamic Kinetic Resolution
Diastereoselective
Lactonization

Pd catalyzed en-yne cyclizations have been developed, such as the method employed by Zhu and coworkers in the synthesis of (-)-Methylenolactocin[11] (Section 2.1.7, Figure 2.14).

2.1.4 Intermolecular strategies for the synthesis of butyrolactones

Bode[12] and Glorius[13] have demonstrated the synthesis of butyrolactones through an enal-aldehyde annulation. The key homoenolate intermediate is catalytically generated via N-heterocyclic carbene catalysis (Figure 2.4).

Figure 2.4: The homoenolate approach to butyrolactone synthesis

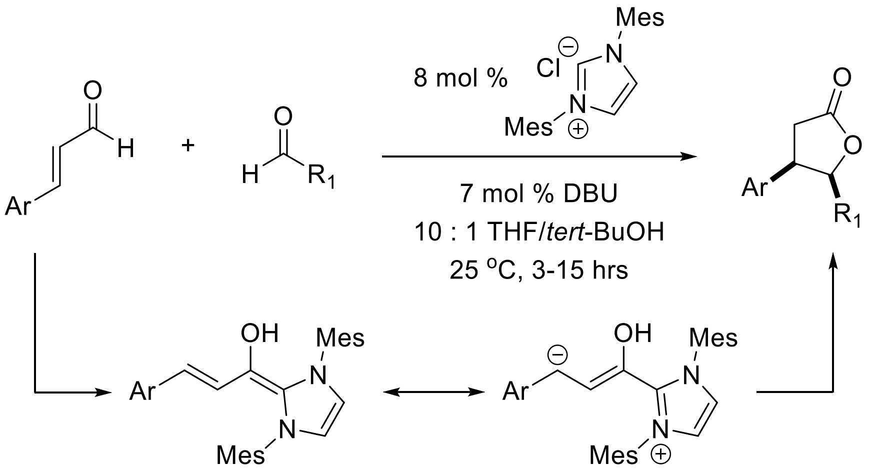

8 mol %
7 mol % DBU
10 : 1 THF/tert-BuOH
25 °C, 3-15 hrs

In 2013, Wu reported an Ir(III/IV) catalyzed photoredox method for the synthesis of butyrolactones from α-Bromo esters and activated alkenes.[14] The proposed mechanism for this methodology involves the single electron reduction of the carbon-bromine bond by the excited Ir(III) species, followed by radical addition to the alkene, followed by single electron oxidation of that resultant stabilized carbocation. Nucleophilic addition of water to that carbocation and subsequent lactonization gives the product (Figure 2.5).

Figure 2.5: Synthesis of butyrolactones via photoreduction

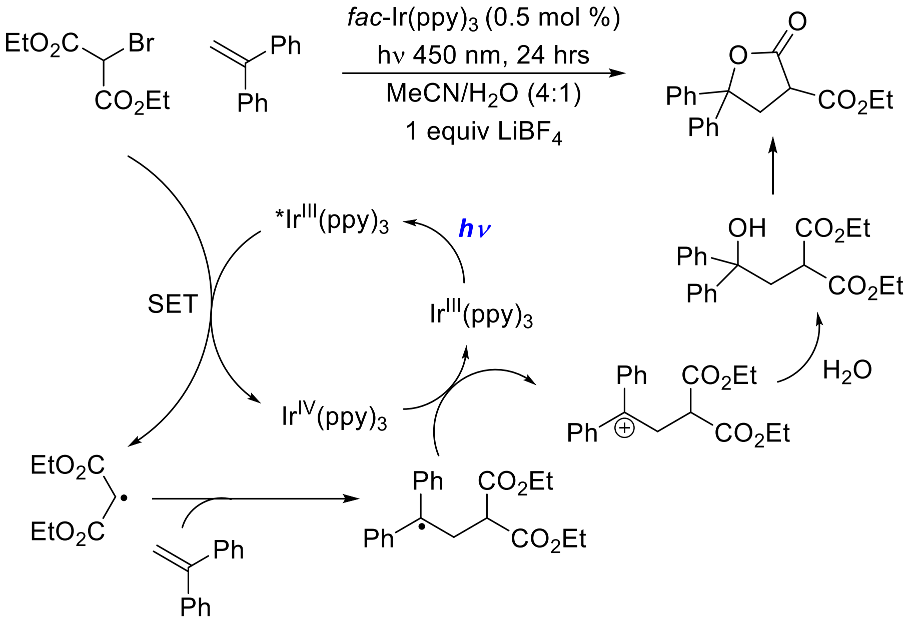

EtO2C
Br
CO2Et
Ph
Ph
fac-Ir(ppy)3 (0.5 mol %)
hν 450 nm, 24 hrs
MeCN/H2O (4:1)
1 equiv LiBF4
O
O
Ph
Ph
CO2Et
*IrIII(ppy)3
hν
SET
IrIII(ppy)3
IrIV(ppy)3
OH
CO2Et
Ph
Ph
CO2Et
H2O
Ph
CO2Et
Ph
CO2Et
EtO2C
EtO2C
Ph
Ph
Ph
CO2Et
Ph
CO2Et

A Pd (II) carbonylation-lactonization reaction, such as that utilized by Tamaru in 1991, forms γ-butyrolactones and α-alkylidine butyrolactones from homoallylic and homopropargylic alcohols with carbon monoxide.[15]

2.1.5 Strategies for α-methylene and α-alkylidine butyrolactone synthesis

One of the most widely used methods to obtain the α-methylene functionality is to append it to an already existing lactone via an aldol/elimination sequence or similar method (Figure 2.6). Danishefsky employed this method in the total synthesis of Spirotenuipesines A and B, whereby the α-methylene unit is later employed in a Diels-Alder reaction with Danishefsky's diene.[16] Although this method is convenient as it can be appended to a large variety of lactone substrates, it also has the limitation of being highly linear.

Figure 2.6: Aldol-elimination strategy for α-methylene installation

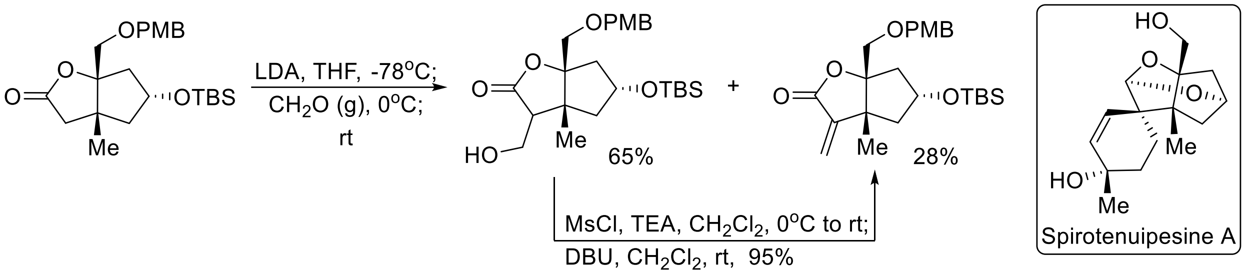

One of the most convergent, commonly used methods is the Dreiding-Schmidt reaction, and variations thereof, independently developed by Schmidt[17] and Dreiding[18] in 1970 (Figure 2.7). Although the initial scope was limited, the reaction has been used on numerous occasions and has also been reported using chromium[19], tin[20], indium[21], and Cu/Zn[22].

Figure 2.7: The Dreiding-Schmidt reaction

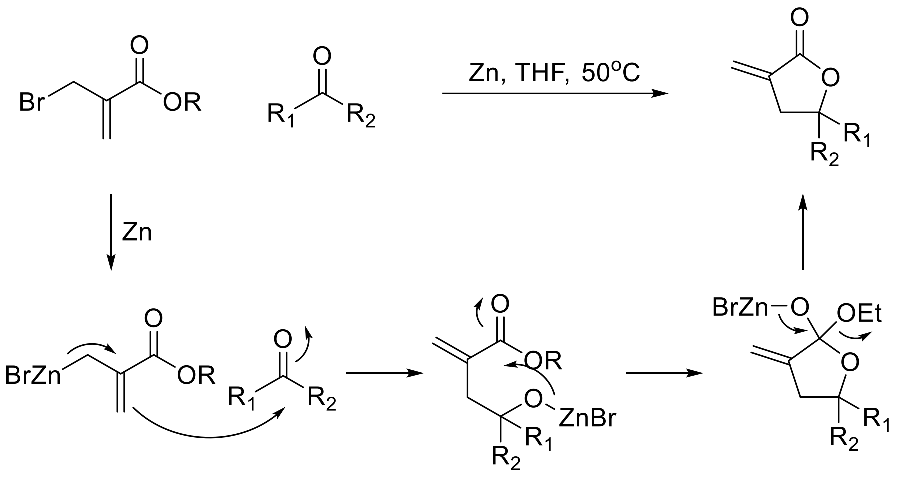

Modification of the starting material allyl bromide to an allylboronic ester with addition of catalytic Lewis acids allows for enhanced substrate tolerance and enhanced reactivity. Hall first discovered that the addition of Lewis acid could be used to dramatically increase the rate of this reaction.[23] The addition of 10 mol% scandium triflate, or a different effective Lewis acid, greatly increased the rate of the reaction. A standard reaction would take 14 days at room temperature or 24 hours at 110 °C without a Lewis acid additive, however the addition of scandium triflate allowed the same reaction to complete at room temperature in 6 hours. Hall proposes that the Lewis acid coordinates with the pinacol oxygen and the ester, increasing the Lewis acidity of the boron (Figure 2.8). He proposes a closed transition state, as he observes a high diastereoselectivity for the transformation. He also finds that when the ester group on the allylboronic ester is removed, a dramatic rate enhancement is not observed.

Figure 2.8: Butyrolactones from allylbornic esters and aldehydes

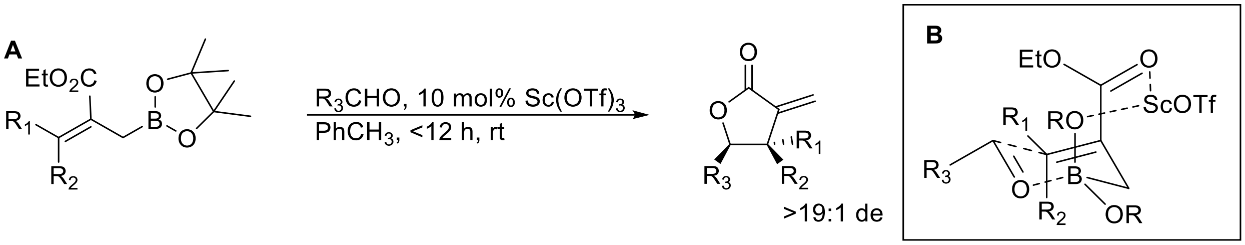
A
EtO2C
R1
R2
O
B
O
R3CHO, 10 mol% Sc(OTf)3
PhCH3, <12 h, rt
O
O
R1
R3
R2
>19:1 de
B
EtO
O
ScOTf
R1
RO
R3
O
B
R2
OR

In 2012, Krische extended this type of reactivity to an enantioselective catalytic version involving carbon-carbon bond formation through a transfer hydrogenation (Figure 2.9).[24]

Figure 2.9: Butyrolactone formation via transfer hydrogenation

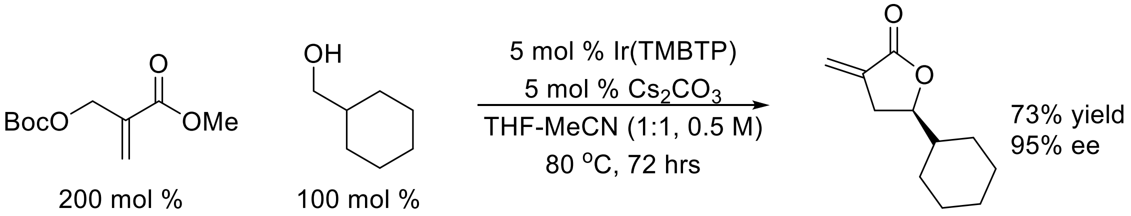
BocO
O
OMe
200 mol %
OH
100 mol %
5 mol % Ir(TMBTP)
5 mol % Cs2CO3
THF-MeCN (1:1, 0.5 M)
80 °C, 72 hrs
O
O
73% yield
95% ee

α-Alkylidine moieties are often installed through a Horner-Wadsorth-Emmons reaction. This technique involves synthesis of the desired lactone and alkylidine R group separately, and subsequent modification to add the α-alkylidine functionality, and as such is a highly linear methodology. For example, (+)-Pacovatinin A was synthesized by Akita and co-workers using this strategy (Figure 2.10).[25]

Figure 2.10: Horner-Wadsworth-Emmons strategy for α-alkylidine butyrolactone synthesis

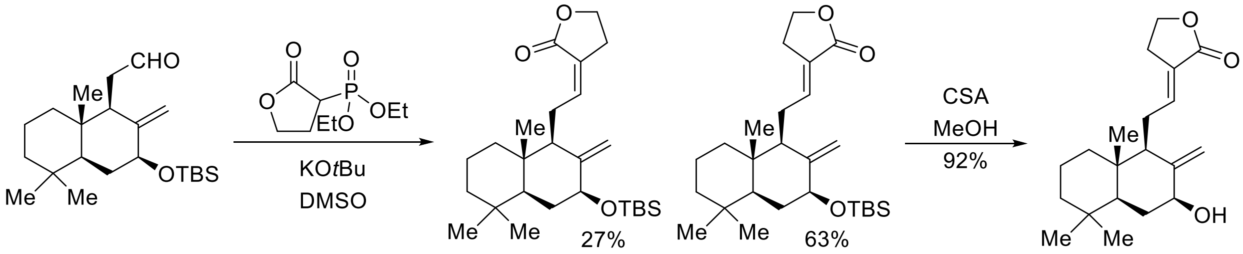
CHO
Me
OTBS
Me
Me
O
O
O
P
OEt
EtO
KOtBu
DMSO
O
O
Me
OTBS
Me
Me
27%
O
O
Me
OTBS
Me
Me
63%
CSA
MeOH
92%
O
O
Me
OH
Me
Me

2.1.6 Initial idea for our method

Due to how common butyrolactones are, there are many methods to generate them. Many of these more common methods, especially those mentioned in sections 2.1.3 through 2.1.5, rely on reactivity with the carbonyl functionality from previously functionalized starting materials. Our method sought to synthesize butyrolactones through a different strategy of bond formation. Instead of synthesizing complicated prefunctionalized starting materials, we wanted to synthesize butyrolactones from simple, often commercially available, alkene and unsaturated acid starting materials (Figure 2.11), greatly increasing the complexity in a single synthetic step. Additionally, we wanted to develop a method that was applicable to a wide variety of alkenes and unsaturated acids, so that α-methylene and α-alkylidine functionality would not have to be appended in a later step. We foresaw synthesizing α-unsaturated butyrolactones from alkynoic acids and alkenes.

Figure 2.11: Proposed disconnection for our strategy

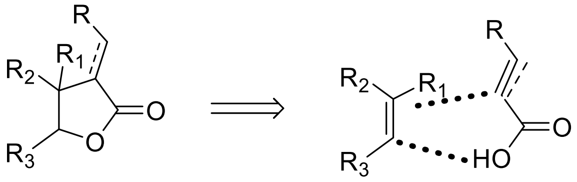

This goal had a number of inherent challenges. The first challenge would be to reverse the inherent nucleophile/electrophile behavior of the starting materials, requiring electron rich alkenes to act as electrophiles and the electrophilic α, β-unsaturated acids to act as nucleophiles at the oxygen. The second challenge would be the requirement of radical addition at the α position of the unsaturated acid, forming a radical intermediate at the unstabilized β-position instead of the stabilized α-position. This strategy is an example of Polar Radical Crossover Cycloaddition[26] (PRCC), whereby the polar step (addition of the nucleophile to the radical cation) is followed by the radical step (cycloaddition via a 5-exo-trig radical cyclization) (Figure 2.12).

Figure 2.12: PRCC strategy for butyrolactone synthesis

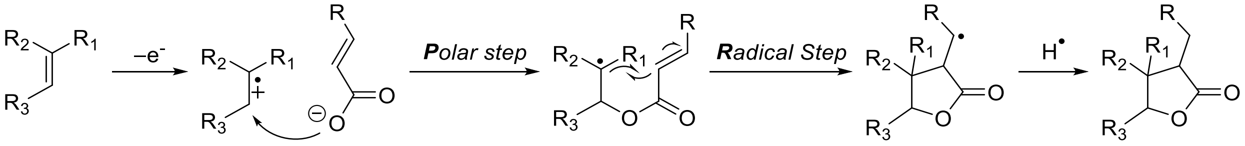

−e⁻
Polar step
Radical Step
H•

2.1.7 Previous syntheses of paraconic acids

Methylenolactocin was first synthesized by Greene in 1992.[27] Meepowpan reported a partial diastereoselective synthesis of methylenolactocin in 2009, where diastereoselectivity was controlled by the use of a dimethyl itaconate-anthracene aduct as its base (Figure 2.13).[28] Zhu and Lu reported an enantioselective synthesis in 1995, where they utilized a Pd(II) catalyzed ene-yne cyclization to form the butyrolactone core (Figure 2.14).[11] The key butyrolactone forming step, the Pd catalyzed ene-yne cyclization, was mentioned in section 2.1.3. Methylenolactocin has been synthesized in an enantioselective manner many times, including by Hajra[29], Ghosh[30], and Fernandes.[31] Many groups have also reported the enantioselective synthesis of both methylenolactocin and protolichesterinic acid, including Brückner[32], Phansavath[33], and Roy.[34]

Figure 2.13: Diastereoselective control from Meepowpan

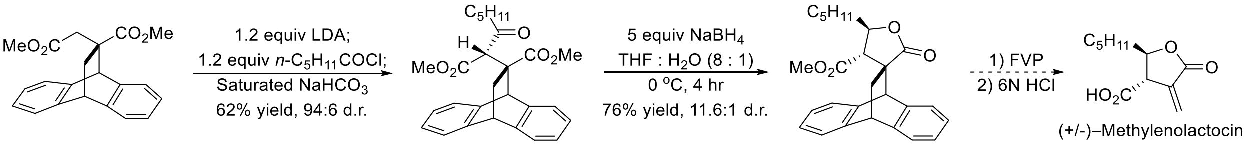

1.2 equiv LDA;
1.2 equiv n-C5H11COCl;
Saturated NaHCO3
62% yield, 94:6 d.r.
5 equiv NaBH4
THF : H2O (8 : 1)
0 °C, 4 hr
76% yield, 11.6:1 d.r.
1) FVP
2) 6N HCl
(+/-)–Methylenolactocin

Figure 2.14: Synthesis of (-)-Methylenolactocin by Zhu and Lu

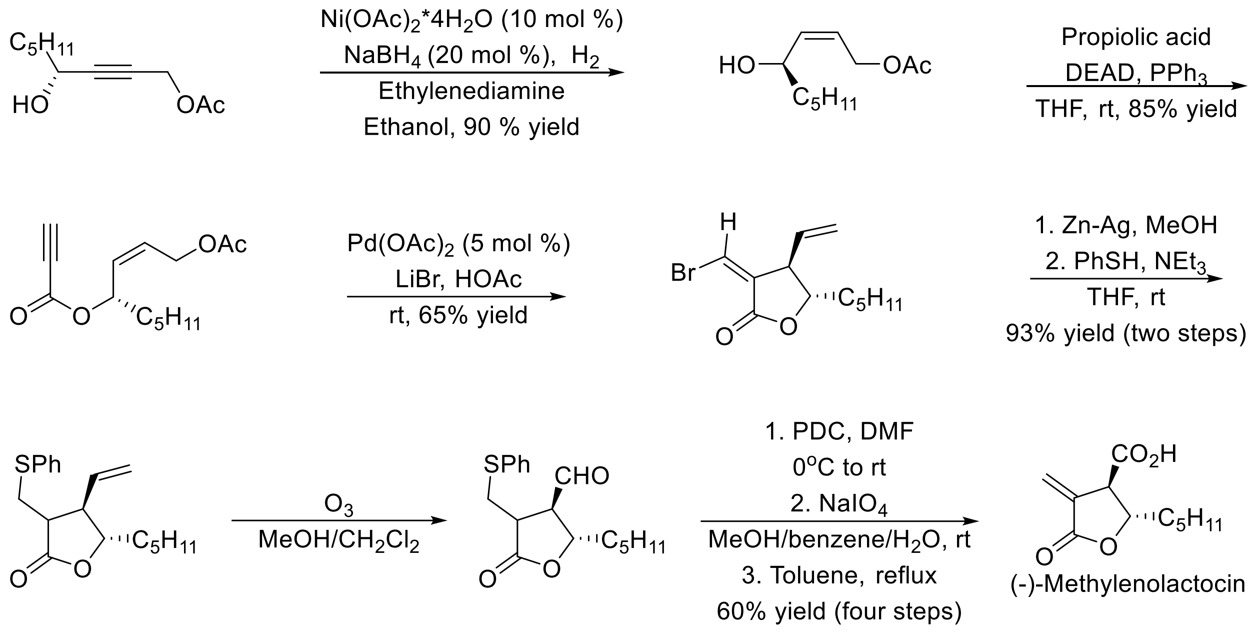
C5H11
HO
OAc
Ni(OAc)2*4H2O (10 mol %)
NaBH4 (20 mol %), H2
Ethylenediamine
Ethanol, 90 % yield
HO
OAc
C5H11
Propiolic acid
DEAD, PPh3
THF, rt, 85% yield
OAc
O
O
C5H11
Pd(OAc)2 (5 mol %)
LiBr, HOAc
rt, 65% yield
H
Br
C5H11
O
O
1. Zn-Ag, MeOH
2. PhSH, NEt3
THF, rt
93% yield (two steps)
SPh
C5H11
O
O
O3
MeOH/CH2Cl2
SPh
CHO
C5H11
O
O
1. PDC, DMF
0°C to rt
2. NaIO4
MeOH/benzene/H2O, rt
3. Toluene, reflux
60% yield (four steps)
CO2H
C5H11
O
O
(-)-Methylenolactocin

2.1.8 Initial strategy for the synthesis of paraconic acids

Initially, we proposed synthesizing the paraconic acids methylenolactocin and protolichesterinic acid in three steps. We would synthesize the desired styrene with the aliphatic chain via an olefination reaction such as the Wittig olefination, and would react it with propiolic acid to form the aryl substituted α-methylene butyrolactone. This would then undergo an oxidative aryl degradation to the desired β-carboxylic acid. The diastereoselectivity for the process would be determined by the diastereoselectivity of the initial polar-radical crossover cycloaddition reaction.

Figure 2.15: Retrosynthetic analysis of the proposed method to synthesize Methylenolactocin

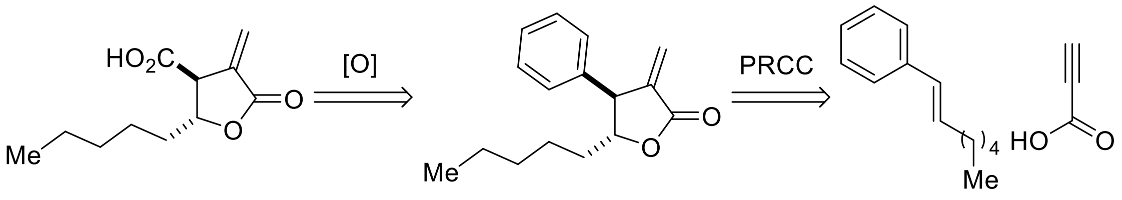
HO2C
O
O
Me
[O]
O
O
Me
PRCC
4
Me
HO
O

2.2 Background

2.2.1 Anti-Markovnikov hydroacetoxylation of alkenes

The proposed strategy of butyrolactone synthesis relies on the ability of carboxylic acids to add to alkenes. However, the addition of carboxylic acids to alkenes is not a trivial matter. Historically, strong acids can add to alkenes. For example, in the industrial synthesis of 2-propanol in concentrated H_2SO_4, this acid adds to propene and is later hydrolyzed. However Hammett acidity function of 18.4 M sulfuric acid is -12.[35] However, carboxylic acids are much stronger, and require a catalyst to add to alkenes. Andrew Perkowski, of the Nicewicz lab, developed a method for the direct, anti-Markovnikov hydroacetoxylation of alkenes.[36] This system provides direct precedent for the addition of carboxylic acids to cation radical intermediates. The catalytic system consists of the Fukuzumi acridinium as photo-oxidant, and either thiophenol or sulfinic acid sodium salt as hydrogen atom donor in substoichiometric quantities. A variety of styrenyl alkenes and tri-substituted alkenes were able to work for this chemistry. Two conditions were developed, one which used benzene sulfinic acid sodium salt in a dual role of base and hydrogen atom donor, and one which used 2,6-lutidine as base and thiophenol as hydrogen atom donor. In addition, a number of hydrogen atom donors were considered (Table 2.1). Hydrogen atom donors where the bond that undergoes homolytic cleavage is a Carbon-Hydrogen bond were moderately successful in the formation of hydroacetoxylation product (entries 2 through 5). Gains were not seen with an increase in catalyst loading (entries 8 and 9), or more dilute solvent conditions (entries 10 and 11). Benzene sulfinic acid, with the addition of 25 mol % sodium acetate as base, gave equivalent results to the standard benzene sulfinic acid sodium salt conditions (entry 6), although it was found that substoichiometric quantities of base were necessary for reactivity (entry 7). In addition to hydroacetoxylation reactions, Perkowski also extended this reactivity to include propiolic acid, *n*-butyric acid, *iso*-butyric acid, pivolic acid, and benzoic acid. He found, however, that the bulkier acids required extended reaction times. Pivolic acid, for example, only achieved a 30% yield after 96 hours of reaction time.

Table 2.1: Optimization of the hydroacetoxylation reaction

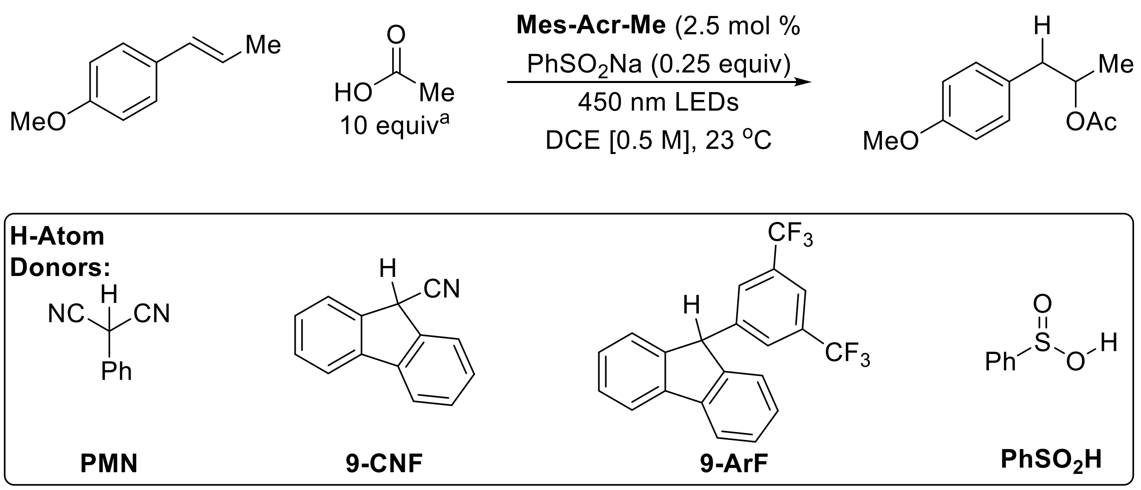
Me
MeO
O
HO
Me
10 equiv[a]
Mes-Acr-Me (2.5 mol %
PhSO$_2$Na (0.25 equiv)
450 nm LEDs
DCE [0.5 M], 23 °C
H
Me
OAc
MeO
H-Atom Donors:
H
NC
CN
Ph
PMN
H
CN
9-CNF
CF$_3$
H
CF$_3$
9-ArF
O
S
Ph
O
H
PhSO$_2$H

Entry	conditions	conversion	yield
1	standard	100%	70%
2[c]	no H-Atom donor	22%	6%
3[c]	with 0.25 equiv PMN instead of PhSO$_2$Na	34%	30%
4[c]	with 0.25 equiv 9-CNF instead of PhSO$_2$Na	44%	26%
5[c]	with 0.25 equiv 9-ArF instead of PhSO$_2$Na	24%	10%
6[c]	with 0.25 equiv PhSO$_2$H instead of PhSO$_2$Na	100%	70%
7[d]	with 0.25 equiv PhSO$_2$H instead of PhSO$_2$Na	40%	0%
8	5 mol % **Mes-Acr-Me**	100%	70%
9	10 mol % **Mes-Acr-Me**	100%	64%
10	DCE [0.25 M]	100%	58%
11	DCE [0.1 M]	100%	54%

In the proposed mechanism (Figure 2.16), the acridinium is excited by blue light, and becomes a strong oxidant in its excited state. This excited state species then oxidizes the alkene substrate by one electron to its corresponding cation radical intermediate, forming the ground state acridine radical. This high energy intermediate reacts with the acetate anion nucleophile, forming the resultant radical species. Hydrogen atom transfer from the redox active hydrogen atom donor forms the product, and the resultant radical turns over the catalyst and regenerates the base.

Figure 2.16: Proposed mechanism for the hydroacetoxylation reaction

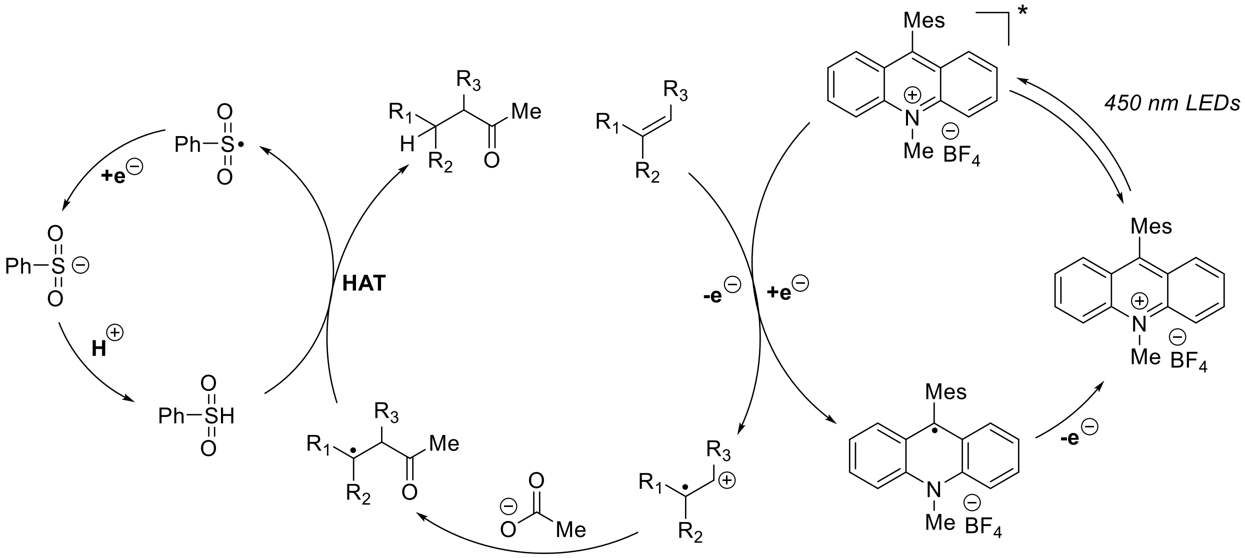

Andrew Perkowski's work on the hydroacetoxylation reaction utilizing the acridinium photocatalyst and acetic acid indicated the possibility that other types of acids could be added in a similar manner to radical cation intermediates. It indicated that the polar step in our proposed polar radical crossover cycloaddition (PRCC) reaction was well precedented.

2.2.2 Synthesis of tetrahydrofurans via polar radical crossover cycloaddition

The next key part of the proposed transformation is the radical cyclization. We wanted the key radical intermediate, formed following nucleophilic attack of the radical cation intermediate, to be intercepted by a pendent alkene prior to hydrogen atom transfer. Jean-Marc Grandjean demonstrated in 2013 that a radical cyclization could occur subsequent to nucleophilic addition but prior to hydrogen atom transfer.[37] He was able to demonstrate this polar radical crossover cycloaddition with the use of allyl alcohols as nucleophiles to alkene radical cation intermediates. In this case, instead of the reaction undergoing a hydroetherification to form an uncyclized product, the benzylic radical intermediate undergoes a 5-exo-trig radical cyclization following nucleophilic addition but prior to hydrogen atom transfer (Figure 2.17). Grandjean finds optimum reactivity with a full equivalent of 2-phenylmalononitrile (PMN) as hydrogen atom donor. PMN was also tested by Andrew Perkowski in the hydroacetoxylation, and was found to demonstrate suboptimal reactivity (Table 2.1 entry 3)

Figure 2.17: Proposed method for the PRCC synthesis of tetrahydrofurans

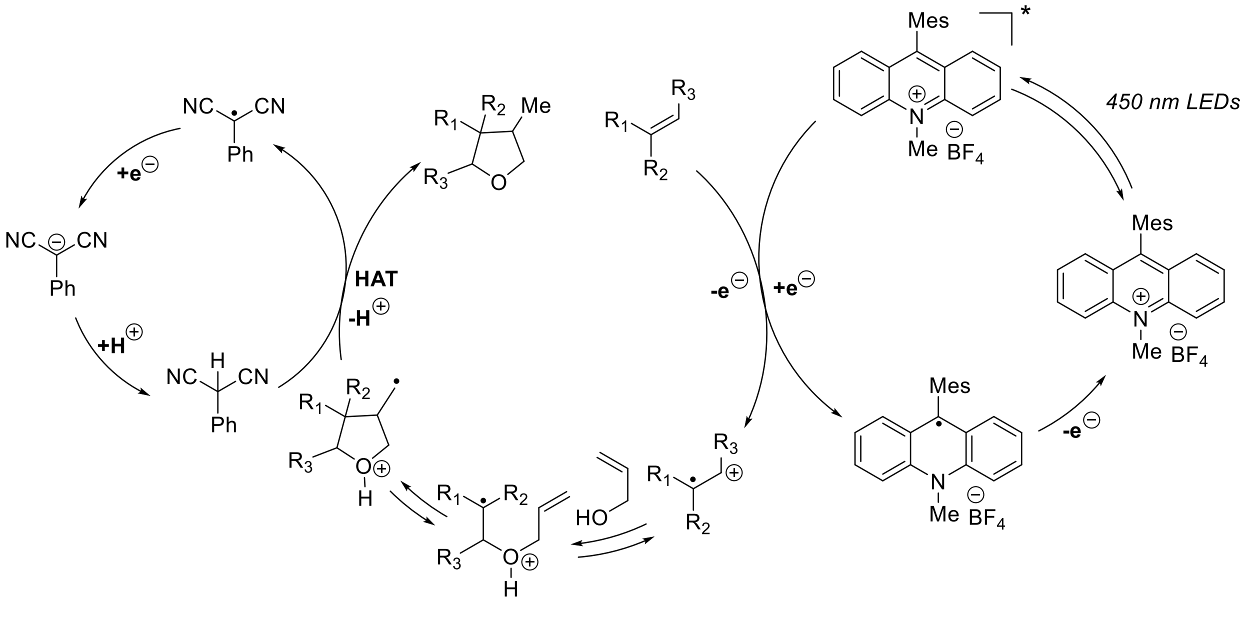

Grandjean found that the diastereoselectivity is determined by the radical cyclization step, as evidenced by the greater than 20:1 selectivity for stereocenters determined during the polar step (Figure 2.18), while the selectivities for the radical cyclization were generally around 1.5:1 d. r.

Figure 2.18: Diastereoselectivity in the PRCC reaction

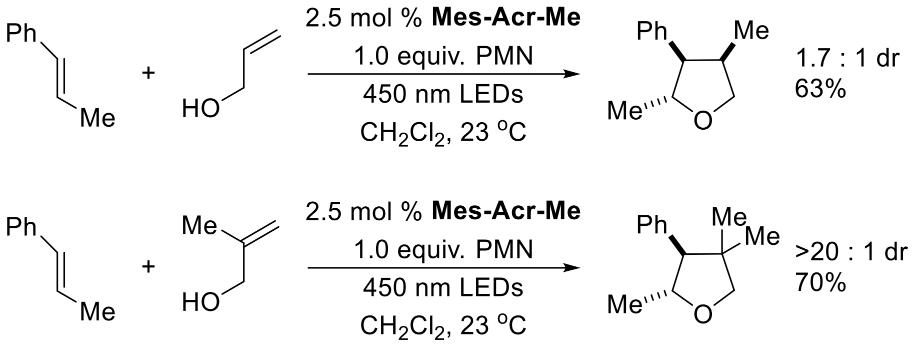

Ph
Me
+
HO
2.5 mol % **Mes-Acr-Me**
1.0 equiv. PMN
450 nm LEDs
CH2Cl2, 23 °C
Ph
Me
Me
O
1.7 : 1 dr
63%
Ph
Me
+
Me
HO
2.5 mol % **Mes-Acr-Me**
1.0 equiv. PMN
450 nm LEDs
CH2Cl2, 23 °C
Ph
Me
Me
Me
O
>20 : 1 dr
70%

The slight preference for the *trans-cis* diastereomer over the *all trans* was rationalized through the use of a Beckwith model of the more stable transition state (Figure 2.19).[38]

Figure 2.19: Rationalization of the diastereoselectivity

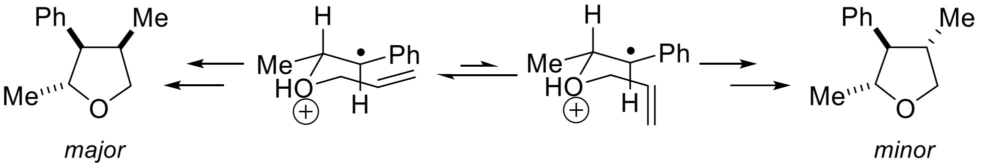

Ph
Me
Me
O
major
H
Me
Ph
HO
H
H
Me
Ph
HO
H
Ph
Me
Me
O
minor

In addition to allyl alcohols, Grandjean was able to demonstrate that propargyl alcohol was also a competent nucleophile (Figure 2.20). This result indicated the possibility that propiolic acid, as a carboxylic acid analog to the alcohol, could be used to acquire α-methylene butyrolactone products, or that a substituted propiolic acid derivative could provide α-alkylidine butyrolactone products.

Figure 2.20: PRCC with propargyl alcohol

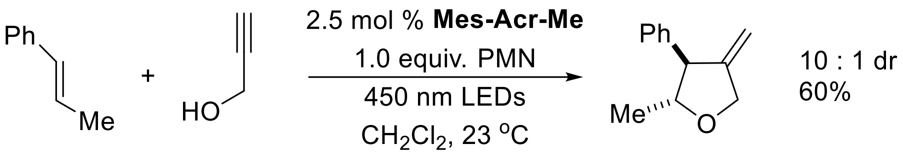
Ph
Me
+
HO
2.5 mol % Mes-Acr-Me
1.0 equiv. PMN
450 nm LEDs
CH2Cl2, 23 °C
Ph
Me
O
10 : 1 dr
60%

2.2.3 5-exo-trig radical cyclizations to form butyrolactones

Although Grandjean demonstrated that a 5-exo-trig radical cyclization could occur with allyl ethers, the analogous cyclization onto α,β-unsaturated esters would be electronically very different. Clive demonstrated this radical cyclization in a similar system, in the radical ring closure of β-phenylselenocrotonates (Figure 2.21).[39] The ring closure step had to be carried out under very dilute, slow addition conditions. Clive specifies that individual benzene solutions of Ph_3SnH (1.7-2.2 mmol, 0.17-0.22 M) and AIBN (0.03-0.06 mmol, 0.003-0.006 M) were injected over a 10 hour period to a refluxing solution of the phenylselenocrotonate in benzene (1.5-2.0 mmol, 0.015-0.02 M). Although an explanation is not discussed, it is probable that these conditions are important to favor the lactone product over an uncyclized byproduct arising from premature hydrogen atom transfer.

Figure 2.21: Radical cyclization of phenylselenocrotonates

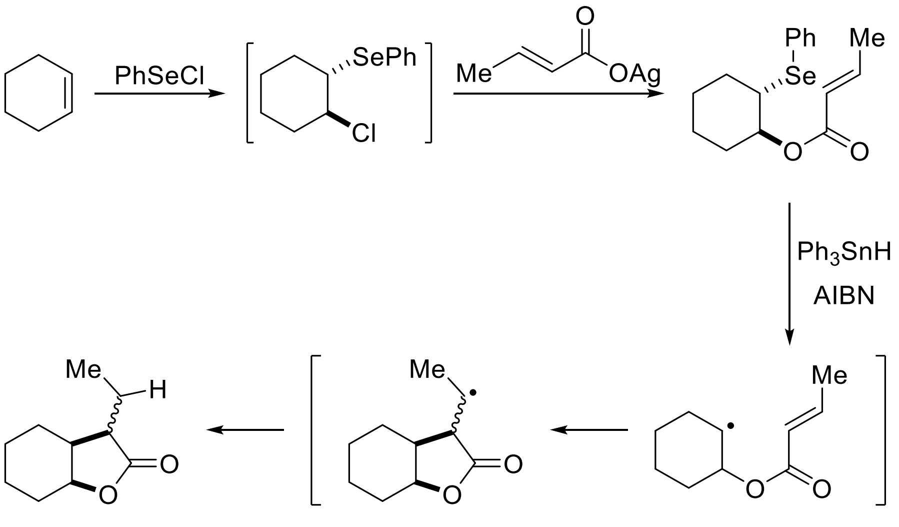
PhSeCl
SePh
Cl
O
Me
OAg
Ph
Se
Me
O
O
Ph3SnH
AIBN
Me
O
O
Me
O
O
Me
H
O
O

Clive found that crotonates gave much better yields than acrylates (Figure 2.22), perhaps due to increased byproduct formation when the post cyclization radical intermediate is a primary radical vs. a secondary radical.

Figure 2.22: Comparison of phenylselenocrotonates to phenylselenoacryaltes

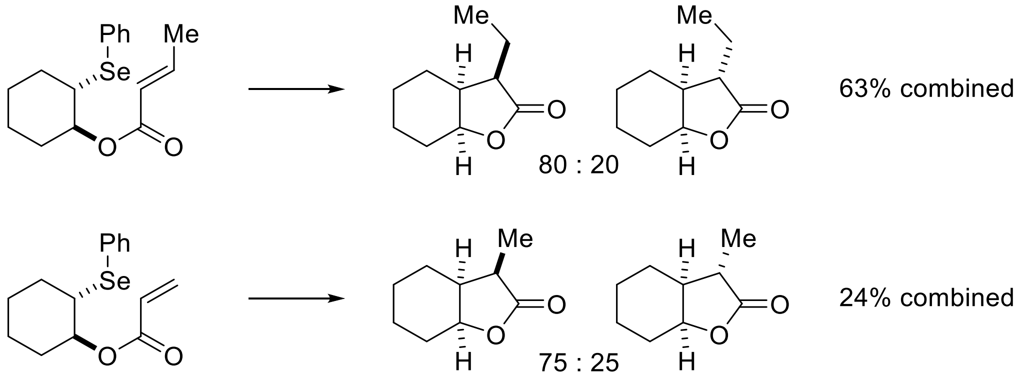

He also found that phenylselenocrotanates arising from both cis and trans alkenes gave nearly identical diastereoselectivities (Figure 2.23). The *all trans* diastereomer of the lactone product was generally the slight favorite of the four possible diastereomers, although the selectivity was not very high. This is in contrast to the slight preference for the *trans-cis* diastereomer Grandjean observed in the synthesis of tetrahydrofurans (Section 2.2.2).

Figure 2.23: Diastereoselectivity from different starting materials

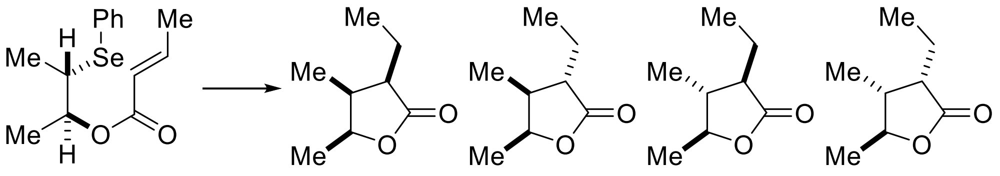

34 : 5 : 39 : 22

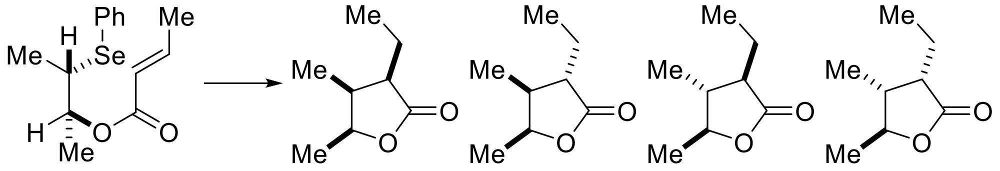

31 : 5.5 : 41 : 22

With precedent from Perkowski, Grandjean, and Clive, we were confident that a method could be developed to produce butyrolactones from oxidizable alkenes and unsaturated acids, with the mesityl acridinium as catalyst and a redox active hydrogen atom donor.

2.2.4 The arene oxidation

The proposed synthesis of paraconic acids relies on a late stage arene degradation to form the β-carboxylic acid from the arene that had initially been present in the styrene. Arene degredations have been utilized already in the synthesis of paraconic acids.[27] Arene degredation to carboxylic acids via oxidation are typically performed using ozonolysis or a ruthenium tetraoxide/sodium periodate system.[40] Typically, ruthenium tetraoxide oxidations are carried out with significant (~10 mol %) loadings of Ruthenium trichloride as catalyst and a large excess (>10 equivalents) of sodium periodate as terminal oxidant in a biphasic solution of water and an organic solvent of choice. Electron rich arenes are oxidized more easily. For example, furans can be oxidized in the presence of other more electron poor arenes, by using lower catalyst loadings and lower terminal oxidant loadings.[41] Our initial proposal for using an arene degredation to reveal the carboxylic acid of methylenolactocin or protolichesterinic acid, however, did not rely on selectivity of oxidation for one arene in the presence of another, but rather on the selectivity of one arene in the presence of an electron deficient olefin. Initially, we proposed performing the arene oxidation as the final step in paraconic acid synthesis, on an α-methylene-β-aryl-butyrolactone. In 2003, Plietker showed that electron deficient olefins could be selectively oxidized in the presence of arenes, under conditions nearly identical to typical arene oxidation conditions (Figure 2.24).[42] This electron deficient olefin could be oxidized under significantly lower loadings of catalyst and sodium periodate than would be required to sufficiently oxidize the phenyl ring, as well as drastically reduced times, and highlights a significant challenge in our strategy. The added sulfuric acid was used only to favor the dihydroxylation products over oxidative cleavage products.

Figure 2.24: Oxidation of electron deficient alkenes with RuO_4

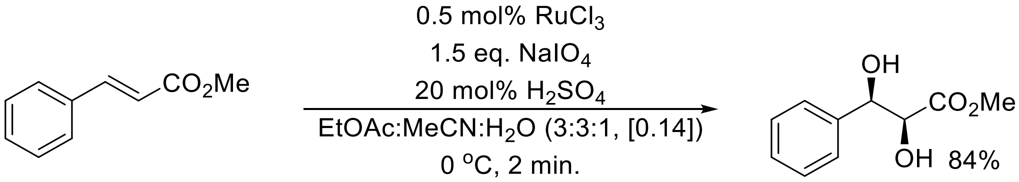

2.3 Results and Discussion

2.3.1 Initial results with acrylic and crotonic acid

Initially, we considered some of the cheapest and simplest unsaturated acids for cyclization. We first considered acrylic and crotonic acids in a polar radical crossover cycloaddition with β-methyl styrene as the oxidizable alkene (Table 2.2). We started with loadings of **Mes-Acr-Me** at 2.5 mol %, as this was the loading used both by Perkowski and Grandjean in the hydroacetoxylation reaction and in the synthesis of tetrahydrofurans. We also considered dichloromethane as solvent. Both the hydroacetoxylation reaction and the tetrahydrofuran PRCC worked well in chlorinated solvents. The hydroacetoxylation reaction was developed in dichloroethane, while the tetrahydrofuran used dichloromethane. When 2-phenylmalononitrile (PMN) or 9-cyanofluorene (9-CNF) were used, the lactone product could be produced along with a significant amount of an uncyclized byproduct (Table 2.2, entries 1 and 2). When thiophenol was used, the lactone product was suppressed in favor of the uncyclized byproduct (entries 3 and 4). This has to do with the relative rates of cyclization compared to hydrogen atom transfer. As mentioned in section 1.5, Romero calculated the rates of hydrogen atom transfer from 2-phenylmalononitrile and thiophenol to a representative alkyl radical, and found that thiophenol should have a 4 fold rate enhancement (Chapter 1, Section 1.5).

Table 2.2: Initial consideration of crotonic and acrylic acid

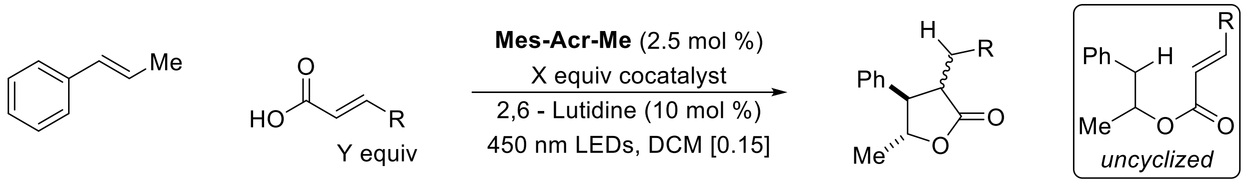

entry	R	Y	X equiv cocatalyst	conversion (%)	yield (%)	uncyclized (%)
1	Me	5	1 equiv PMN	96	20	34
2	Me	5	1 equiv 9-CNF	88	18	20
3	Me	1.1	20 mol % PhSH	63	2	44
4	H	1.1	20 mol % PhSH	50	2	44

Although solvent concentration was found to have a moderate impact on product distribution when PMN or 9-CNF were used, with more dilute concentrations tending to favor the lactone product relative to more concentrated conditions, the uncyclized byproduct was consistently produced in large quantities. When thiophenol was used, the uncyclized product was always the predominant product, as the faster hydrogen atom donor could donate a hydrogen to the radical intermediate prior to the radical cyclization step. As the desired reactivity required radical addition to the unsaturated ester intermediate with regiochemical control contrary to the polarization of that electron deficient alkene, these results do not come as a complete surprise. Without the constraint of a ring, free radical additions to unsaturated esters occur at the β-position, subsequently forming a stabilized α-radical (Figure 2.25). This is the case in the polymerization of methyl methacrylate to form polymethylmethacrylate (PMMA) or plexiglas.[43]

Figure 2.25: Polymerization of polymethylmethacrylate

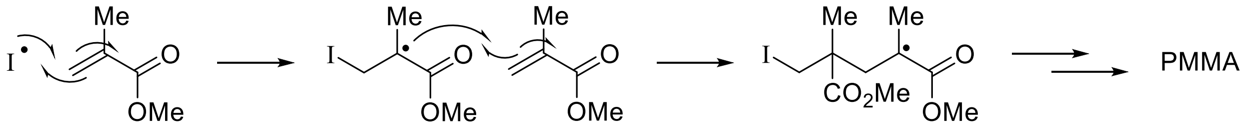

Although we were pleased to see that a lactone product could be formed under the described conditions, it appeared that true gains in product distribution would not be had unless there were fundamental electronic modifications made to the nature of the unsaturated acid. If the unsaturated acid could be changed such that the alkene was not so polarized, then perhaps the necessary radical addition at the α-position could occur at a more reasonable rate.

2.3.2 Adaption to monoester fumarates

We first considered fumaric acid, as its symmetrically substituted alkene could offer the electronic properties we believed our reaction required to suppress the undesired uncyclized byproduct. Unfortunately, fumaric acid is not efficiently soluble in dichloromethane, and no lactone product was observed. Monoester fumarates, on the other hand, were highly soluble in DCM and also proved to be effective coupling partners (Table 2.3). In considering hydrogen atom donors, phenyl disulfide was found to be the most effective (entry 3). It had already been demonstrated that phenyl disulfide could be an effective hydrogen atom donor, as the S-S bond homolyzes under our light conditions to the thiyl radical, which can then enter the catalytic cycle.[44] Furthermore, it was found that removing base resulted in a small reduction in yield (entry 5).

Table 2.3: Optimization with mono-*t*-butylfumarate

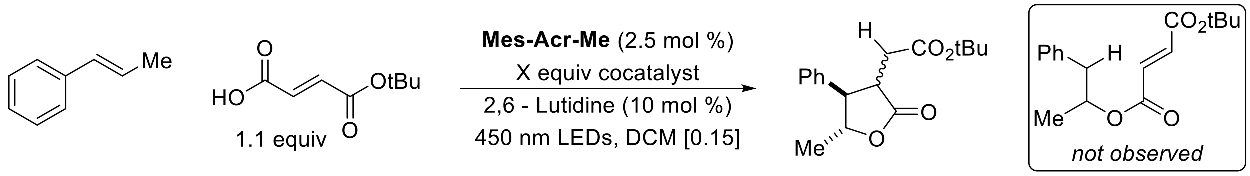

entry	conditions	conversion (%)	yield (%)
1	20 mol % PhSH	80	62
2	20 mol % *p*-NO_2PhSH	100	64
3	10 mol % Ph_2S_2	99	79
4	10 mol % (*p*-NO_2Ph)$_2S_2$	100	64
5	10 mol % Ph_2S_2, no base	100	64

With these optimized conditions in hand, we turned our attention to substrate scope (Figure 2.26). It was found that *m*-methyoxy β-methylstyrene was a good substrate, although the *para* equivalent was not. *p*-Chloro β-methylstyrene and isosafrole were also viable alkenes for this transformation. Commercially available mono-ethylfumarate was a viable acid. The *tert*-butyl derivative was chosen for the simplicity of the NMR characterization in demonstrating the scope of reactivity. The trisubstituted alkene 1-phenylcyclohexene was also a viable substrate. Relative stereochemistry of the product was determined by considering the anisotropic effect in the proton NMR. 2-methyl-2-butene was also a viable alkene substrate, however the conditions had to be modified for optimum yield. An excess of alkene (3 equivalents) was used. The low boiling point of the alkene meant that an excess was important to maintain adequate amounts of alkene in solution. Additionally, it was found that the use of *p*-nitrothiophenol (5 mol %) instead of phenyl disulfide gave optimum results for this particular substrate.

Figure 2.26: Alkene scope with mono-*t*-butyl fumarate

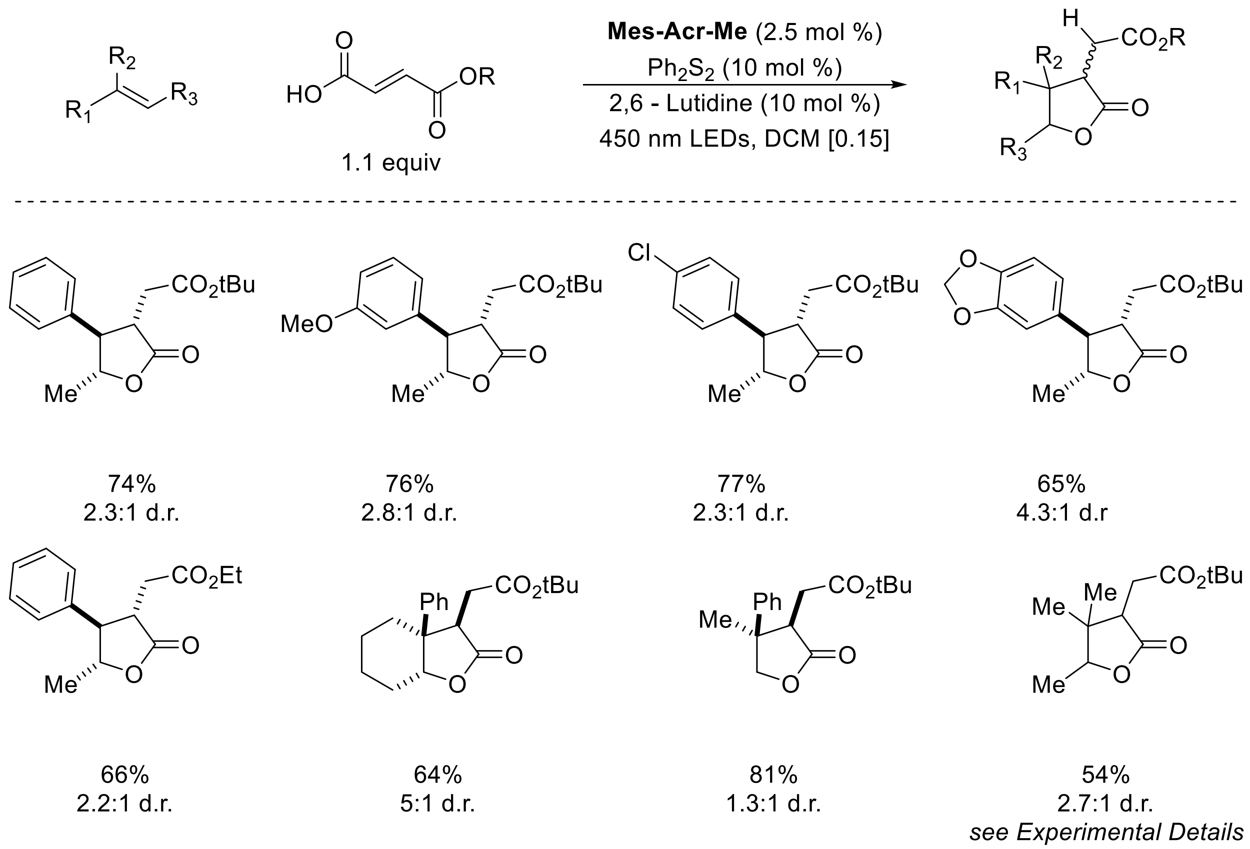
R2
R1
R3
HO
O
OR
O
1.1 equiv
Mes-Acr-Me (2.5 mol %)
Ph2S2 (10 mol %)
2,6 - Lutidine (10 mol %)
450 nm LEDs, DCM [0.15]
H
CO2R
CO2tBu
MeO
Cl
CO2Et
Ph
Me
O
74%
2.3:1 d.r.
76%
2.8:1 d.r.
77%
2.3:1 d.r.
65%
4.3:1 d.r
66%
2.2:1 d.r.
64%
5:1 d.r.
81%
1.3:1 d.r.
54%
2.7:1 d.r.
see Experimental Details

2.3.3 Adaption to cinnamic acid derivatives

Michelle Riener adopted this methodology to cinnamic acid derivatives (Figure 2.27). In the course of her optimization, she found that the addition of 2,6-Lutidine did not give as substantial improvement in yield as was the case with monoester fumarates. She thus excluded base from her reactions. She found that cinnamic acid, 4-chlorocinnamic acid, and the 2-thiophenyl derivative were each satisfactory coupling partners. She also found that, in general, the diastereoselectivity was improved with cinnamic acid derivatives vs. the monoester fumarate derivatives.

Figure 2.27: Alkene scope with cinnamic acid derivatives

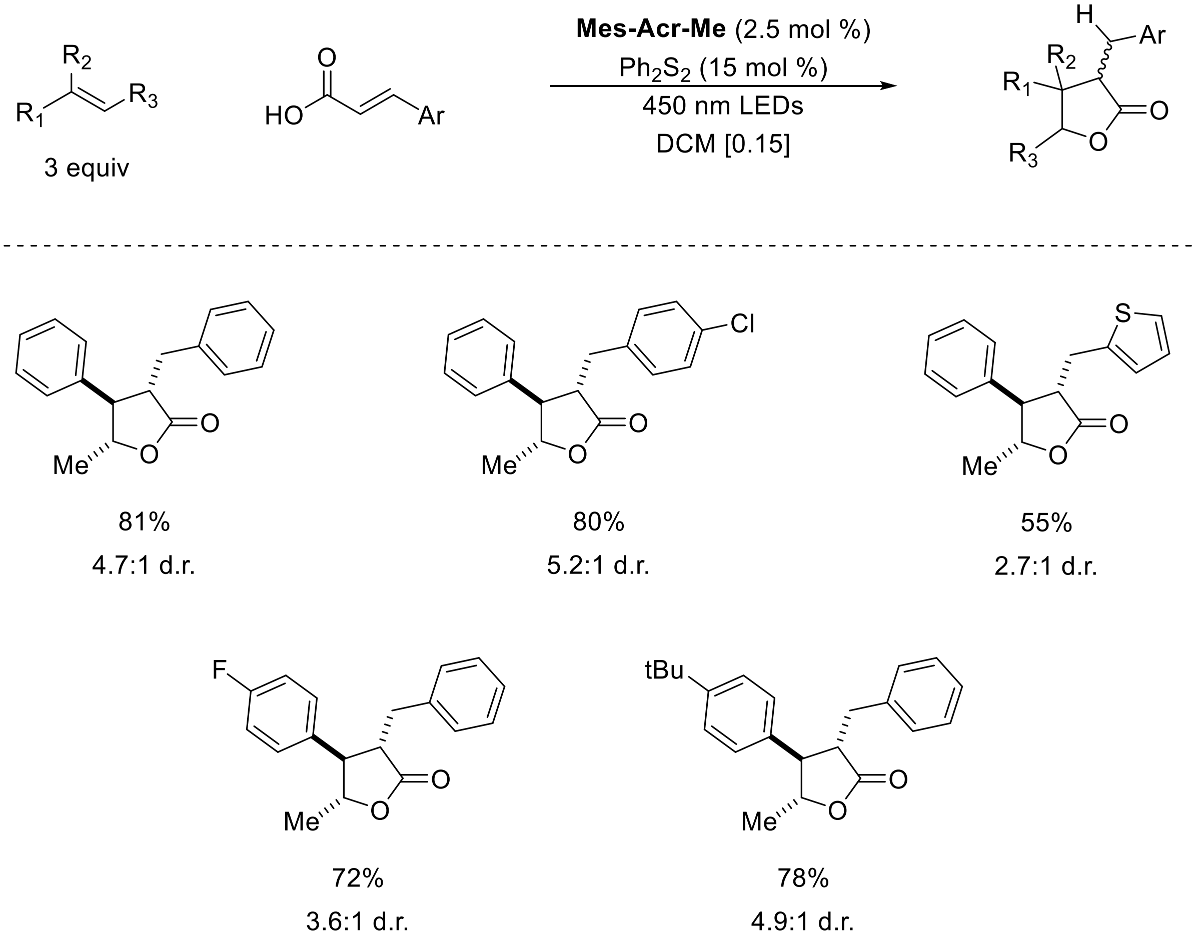
R2
R1
R3
3 equiv
O
HO
Ar
Mes-Acr-Me (2.5 mol %)
Ph2S2 (15 mol %)
450 nm LEDs
DCM [0.15]
H
Ar
R2
R1
O
R3
O
Cl
S
Me
O
O
F
tBu
81%
4.7:1 d.r.
80%
5.2:1 d.r.
55%
2.7:1 d.r.
72%
3.6:1 d.r.
78%
4.9:1 d.r.

2.3.4 Adaption to alkynoic acids

When applying this methodology to the synthesis of α-alkylidine butyrolactones, it was found that the many different alkynoic acids benefited from minor variations in methodology, such as the ratio of alkene to acid or the presence or absence of base (Figure 2.28). For example, it was found that aryl substituted alkynoic acids, such as 3-phenylpropiolic acid and 3-

(thiophene-3-yl)propiolic acid, as well as 3-cyclohexylpropiolic acid, benefited in reactivity by the addition of 10 mol % 2,6-lutidine. However, 3-(trimethylsilyl)propiolic acid obtained similar reactivity without the addition of base. Interestingly, similar yields could be optained using a lower ratio of alkene:acid when *m*-methoxy-β-methylstyrene was used as alkene with 3-(trimethylsilyl)propiolic acid, which would prove a useful find in our initial route towards paraconic acid synthesis. With 3-(trimethylsilyl)propiolic acid as an example of a standard alkynoic acid, we considered the varieties of alkenes that could be viable reaction partners. 2-propenethiophene and indene reacted in good yield. 2-methyl-2-butene was a viable alkene substrate, and interestingly only the (*Z*)-isomer was observed. It is possible that the fleeting vinyl radical intermediate equilibrates to relieve nonbonding interactions between the neighboring *gem*-dimethyl group and the bulky trimethylsilyl group.[45]

Figure 2.28: Alkynoic acids in the PRCC

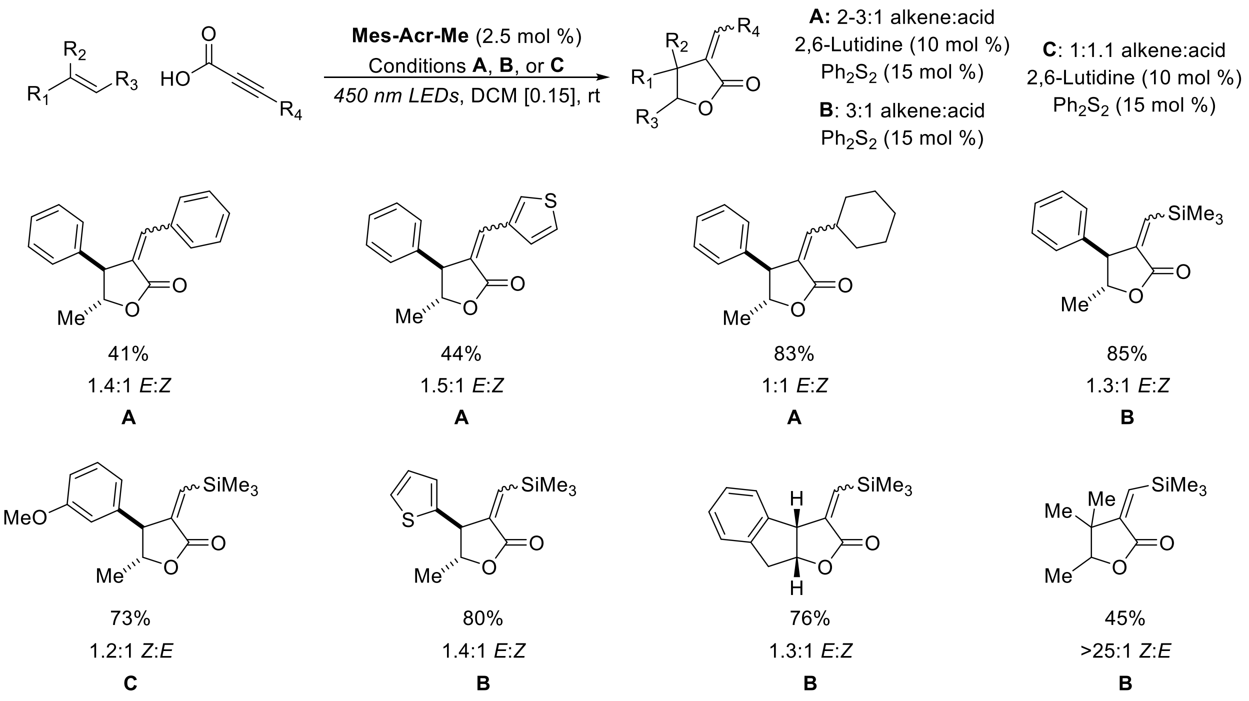

R2
R1
R3
HO
O
R4
Mes-Acr-Me (2.5 mol %)
Conditions **A**, **B**, or **C**
450 nm LEDs, DCM [0.15], rt
R2
R4
R1
R3
O
O
A: 2-3:1 alkene:acid
2,6-Lutidine (10 mol %)
Ph2S2 (15 mol %)
B: 3:1 alkene:acid
Ph2S2 (15 mol %)
C: 1:1.1 alkene:acid
2,6-Lutidine (10 mol %)
Ph2S2 (15 mol %)
Me
O
O
41%
1.4:1 E:Z
A
S
Me
44%
1.5:1 E:Z
A
Me
83%
1:1 E:Z
A
SiMe3
Me
85%
1.3:1 E:Z
B
MeO
SiMe3
Me
73%
1.2:1 Z:E
C
S
SiMe3
Me
80%
1.4:1 E:Z
B
H
SiMe3
H
76%
1.3:1 E:Z
B
Me
Me
SiMe3
Me
45%
>25:1 Z:E
B

2.3.5 Determination of relative stereochemistry

The described methodology results in substantial amounts of two diastereomers, with diastereoselectivities ranging from 1.3:1 to 4.9:1 d.r. Of the four possible diastereomers, the 3rd and 4th are sometimes observable via NMR, however are never found in substantial amounts. The two most common diastereomers are generally favored by >20:1 d.r. over the two least common diastereomers (Figure 2.29). The high relative selectivities for these centers is rationalized by low barrier to inversion of the benzylic radical intermediate. For this reason, and the loss of geometrical control in the alkene radical cation intermediate, both the *cis* and *trans* alkene starting materials give identical product distributions.

Figure 2.29: Diastereoselectivities of the PRCC products

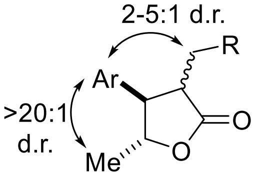

This is similar to the selectivities observed for the tetrahydrofuran methodology developed by Jean-Marc Grandjean and discussed in Section 2.2.2. In the tetrahydrofuran case, the *trans-cis* diastereomer was found to be major, albeit with generally low selectivities. This was attributed to the Beckwith model of radical cyclization. However, in the Clive case which utilized a radical cyclization onto an unsaturated ester instead of an allylic ether (Section 2.2.3), there was a slight preference for the *all trans* diastereomer when acyclic alkenes were used. In order to discern the relative stereochemistry of the major diastereomer, we conducted an epimerization study (Figure 2.30). It has been documented that the *all trans* diastereomer of butyrolactones is the more thermodynamically stable conformer.[47]

Figure 2.30: Epimeriztion of butyrolactone products

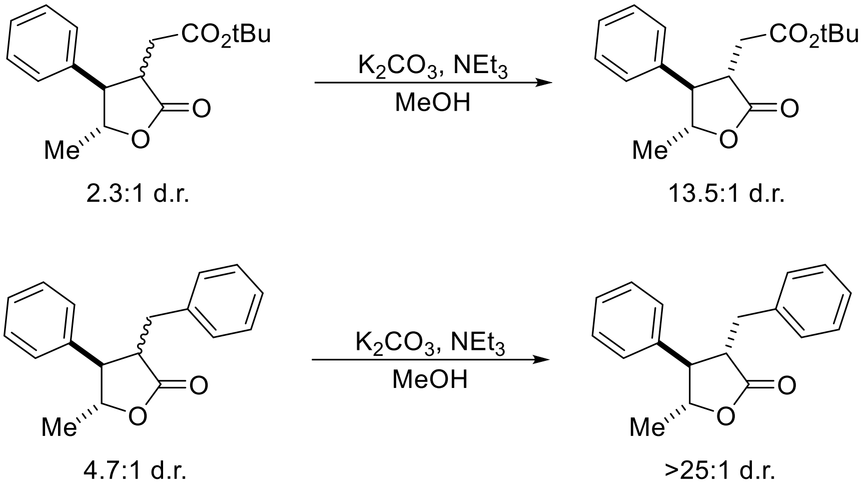

The epimerization study revealed that the major product continued to be the major product, however in much higher ratios. This indicates that the major product of the polar radical crossover cycloaddition reaction is the *all trans* diastereomer.

2.3.6 Insights into the irreversibility of the radical cyclization

In an effort to understand the potential reversibility of the putative radical cyclization step, we synthesized the *trans-cis* β-bromobutyrolactone from β-bromoacrylic acid and β-methylstyrene using our typical reaction protocol. Interestingly, the desired minor diastereomer could be isolated cleanly, and was actually the only diastereomer that could be isolated easily. The major *all trans* diastereomer eliminated under all attempted column conditions to the α-methylene butyrolactone. With the desired minor diastereomer in hand as a single diastereomer, we subjected it to radical dehalogenation conditions (Figure 2.31). If the radical cyclization were reversible, variable quantities of either the *all trans* dehalogenated product or the uncyclized product would be expected. However, we observed only clean hydrodebromination, and isolated the product as a single diastereomer in a 73% yield. This result suggests that the radical cyclization step of the PRCC is irreversible and that the observed predominance of the uncyclized adduct, particularly in the reaction of acrylic acid with β-methylstyrene (Table 2.2 entry 4), is likely the result of a slow radical cyclization relative to hydrogen atom abstraction when thiophenol is used and not due to a thermodynamic property.

Figure 2.31: Radical dehalogenation of minor diastereomer

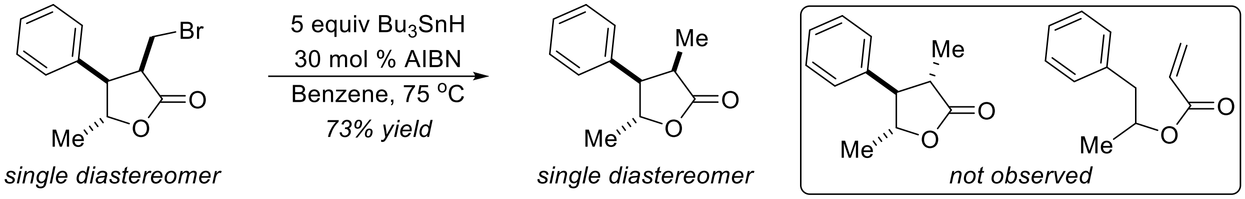

2.3.7 Application to the synthesis of methylenolactocin and protolichesterinic acid

Some of the potential complications have been discussed (Section 2.2.4). In fact, these complications did prove to impact the direction of our strategy. Initially, we considered directly the reaction between propiolic acid and the corresponding alkene, however this strategy did not result in significant yields of α-methylene butyrolactone product despite extensive consideration of hydrogen atom donor, solvent, starting material ratios, concentration, and even extended addition times. From this, we turned our attention to 3-(trimethylsilyl)propiolic acid as a propiolic acid surrogate. Although the desired lactone with an electron rich arene could be synthesized in good yield between 3-(trimethylsilyl)propiolic acid and 1-methoxy-3-(prop-1-en-1-yl)benzene (Figure 2.28), the arene oxidation proved a challenge. Subjection to the oxidation conditions resulted in decomposition of starting material, although the arene remained in-tact in the uncharacterized products. Even use of a furan as the arene[41], which has been oxidized using much lower equivalents of terminal oxidant and lower $RuCl_3$ loadings, resulted in undesired reactivity.

We then considered masking α-unsaturation. We considered circumventing this selectivity issue by using a β-halogen acrylic acid, which could form a butyrolactone with protected, pre-α-methylene functionality. We were pleased to see that (*Z*)-β-chloroacrylic acid could give the desired lactone in a 64% combined yield as a mixture of diastereomers (Figure 2.32).

Figure 2.32: Synthesis of the chloro-butyrolactone

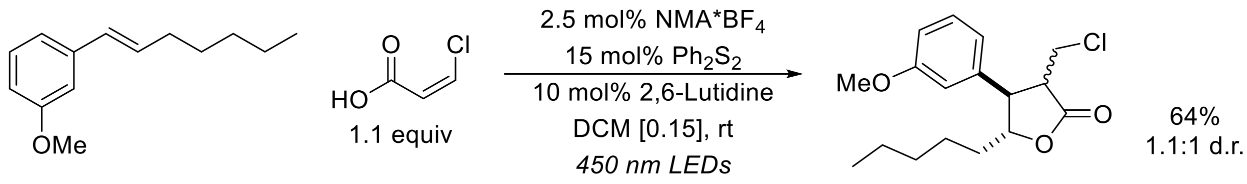
OMe
HO
O
Cl
1.1 equiv
2.5 mol% NMA*BF$_4$
15 mol% Ph$_2$S$_2$
10 mol% 2,6-Lutidine
DCM [0.15], rt
450 nm LEDs
MeO
Cl
O
O
64%
1.1:1 d.r.

We reasoned that the low diastereoselectivity of this reaction would not be a negative to the strategy as a whole, because the suspect stereocenter would not be present in the final product. High diastereoselectivity, of greater than 20:1, was observed for the other two stereocenters.

Figure 2.33: Rationalization for the inconsequential low diastereoselectivity

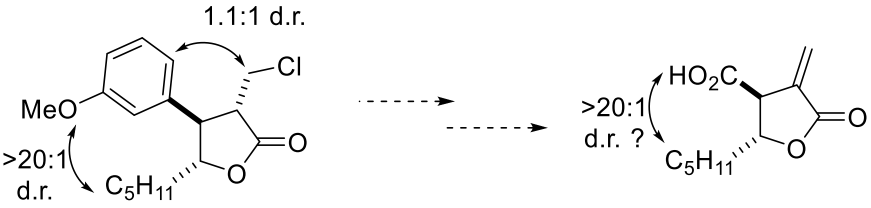
1.1:1 d.r.
Cl
MeO
>20:1
d.r.
C$_5$H$_{11}$
O
O
HO$_2$C
>20:1
d.r. ?
C$_5$H$_{11}$
O
O

However, when this lactone was subjected to oxidation conditions the desired product was only obtained for one diastereomer. The minor diastereomer formed entirely a bicyclic byproduct. The combined yield was 80% for the oxidation, with the bybroduct formed in a 1:1 ratio by NMR.

Figure 2.34: Arene oxidation and the bicyclic byproduct

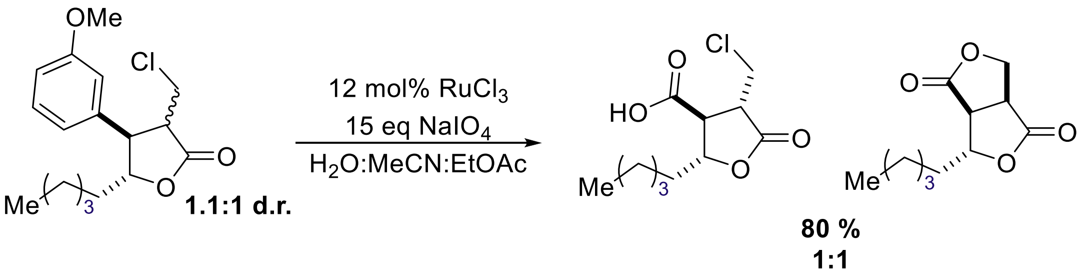
OMe
Cl
O
Me
3
O
1.1:1 d.r.
12 mol% RuCl3
15 eq NaIO4
H2O:MeCN:EtOAc
Cl
O
HO
O
Me
3
O
O
O
O
Me
3
O
80 %
1:1

We theorized that the pathway that lead to the undesired bicyclic byproduct proceeded through an intramolecular 5-exo-tet S_N2 reaction between a bare carboxylate and the halide. We hypothesized that this pathway could be shut down if the carboxylic acid would remain protonated throughout the reaction (Figure 2.35).

Figure 2.35: Theory on how to limit byproduct production

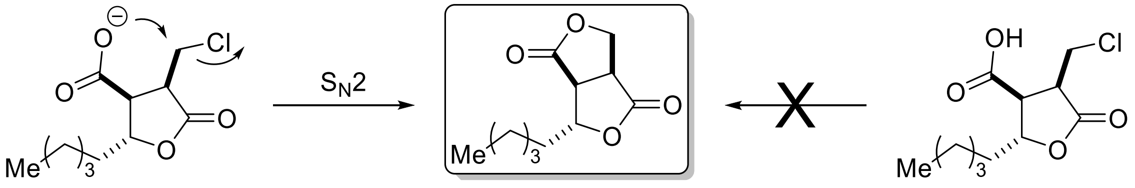
O
Cl
O
O
Me
3
O
SN2
O
O
O
O
Me
3
OH
Cl
O
O
Me
3
O

This proved to be the case, as the addition of 5 mol% acetic acid to the oxidation reaction resulted in the formation of the desired product of both diastereomers (Figure 2.36).

Figure 2.36: Formation of desired products from both diastereomers

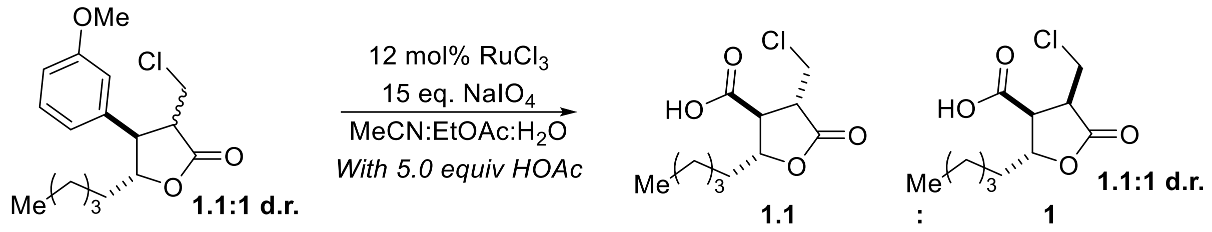
OMe
Cl
Me
3
1.1:1 d.r.
12 mol% RuCl3
15 eq. NaIO4
MeCN:EtOAc:H2O
With 5.0 equiv HOAc
HO
O
Cl
1.1
:
1
1.1:1 d.r.

However, this discovery was not fruitful for our desired strategy, as the elimination conditions to form the α-methylene functionality were incompatible with preventing this pathway, and the bicyclic byproduct was formed regardless in the subsequent step (Figure 2.37).

Figure 2.37: Elimination conditions and the re-emergence of the byproduct

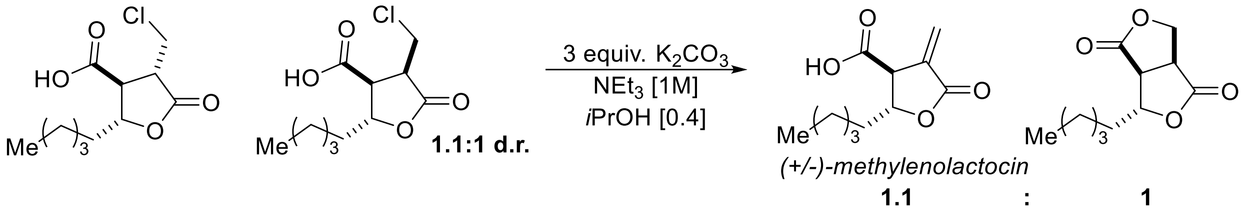
HO
O
Cl
Me
3
1.1:1 d.r.
3 equiv. K2CO3
NEt3 [1M]
iPrOH [0.4]
(+/-)-methylenolactocin
1.1
:
1

The key drawback of this strategy is the diastereoselectivity of our photoredox catalyzed polar radical crossover cyclization methodology. If the desired chloro-lactone intermediate could be formed in either high *all trans* selectivity, or easily and effectively epimerized to the all trans, the bicyclic byproduct could be minimized and the paraconic acids could be synthesized in much higher yields. As is, the bicyclic byproduct accounts for a significant amount of the mass balance. Nevertheless, the paraconic acids methylenolactocin and protolichesterinic acid (synthesized by Michelle Riener), could be obtained in high diastereoselectivity (>20:1) in three synthetic steps from simple alkene and unsaturated acid starting materials.

Figure 2.38: Total diastereoselective synthesis of methylenolactocin and protolichesterinic acid

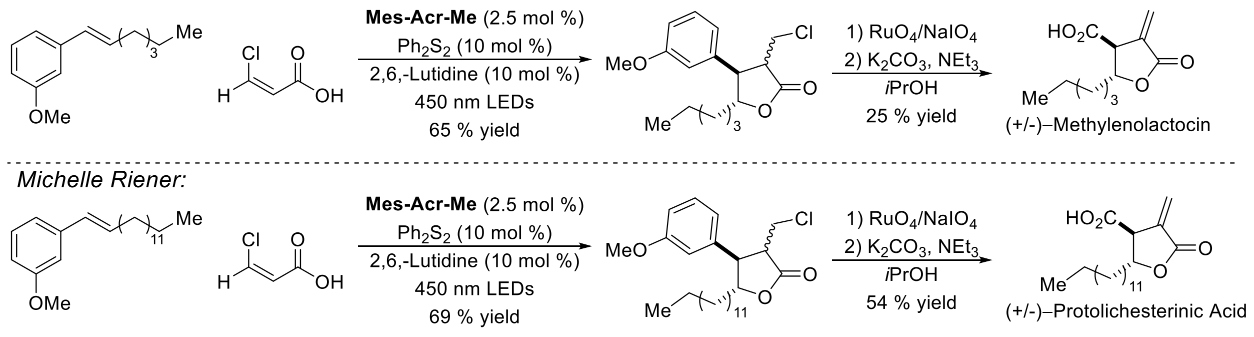
Me
3
OMe
Cl
O
H
OH
Mes-Acr-Me (2.5 mol %)
Ph2S2 (10 mol %)
2,6,-Lutidine (10 mol %)
450 nm LEDs
65 % yield
MeO
Cl
O
Me
3
O
1) RuO4/NaIO4
2) K2CO3, NEt3
iPrOH
25 % yield
HO2C
O
Me
3
O
(+/-)–Methylenolactocin
Michelle Riener:
Me
11
OMe
Cl
O
H
OH
Mes-Acr-Me (2.5 mol %)
Ph2S2 (10 mol %)
2,6,-Lutidine (10 mol %)
450 nm LEDs
69 % yield
MeO
Cl
O
Me
11
O
1) RuO4/NaIO4
2) K2CO3, NEt3
iPrOH
54 % yield
HO2C
O
Me
11
O
(+/-)–Protolichesterinic Acid

2.4 Conclusion

Using knowledge gained from precedented reactions developed in the Nicewicz lab, we were able to develop a method for the synthesis of γ-butyrolactones from simple, often commercially available, alkene and unsaturated acid starting materials. The catalytic system consists of the Fukuzumi acridinium photooxidant and a redox active hydrogen atom donor. The methodology relies on the single electron oxidation of oxidizable olefins, which makes them competent electrophiles for the nucleophilic addition of unsaturated carboxylic acids. Radical cyclization onto the unsaturated acid can be made more favorable by appropriate substitution. Monoesterfumarates and cinnamic acid derivatives, as well as a variety of substituted propiolic acid derivatives and β-haloacrylic acids, allow for adequate rates of radical cyclization, while unactivated acrylic and crotonic acids have a much slower rate of radical cyclization and as such the uncyclized product predominates. In all, 23 examples of this reactivity have been demonstrated using a variety of alkenes and unsaturated acids, in yields ranging from 41 to 85%, and diastereoselectivities as high as 5:1. This method has been applied to a highly diastereoselective synthesis of two paraconic acid natural products, methylenolactocin and protolichesterinic acid, in three steps from the relevant alkene and unsaturated acid starting materials. The route to these particular natural products would be made more effective if the

PRCC methodology developed could give the *all trans* diastereomer of the chloro-lactone intermediate in much higher diastereoselectivity, as this would limit the formation of the major byproduct following the arene oxidation. However, the described route to the paraconic acids still represents a very concise synthesis of these important natural products.

2.5 Further Developments of this Strategy

Other members of the Nicewicz lab have further explored the scope of nucleophiles that can add to alkenes under PRCC methodology. In 2014, Nate Gesmundo reported the synthesis of butyrolactams from alkene and unsaturated amide nucleophiles.[47] A few months later, Cortney Cavanaugh reported the synthesis of substituted α-benzyloxyamino-γ-butyrolactones from alkenes and substituted *O*-benzyloxime acids.[48] A summary of these projects is shown in Figure 2.39.

Figure 2.39: Further developments in PRCC methodology

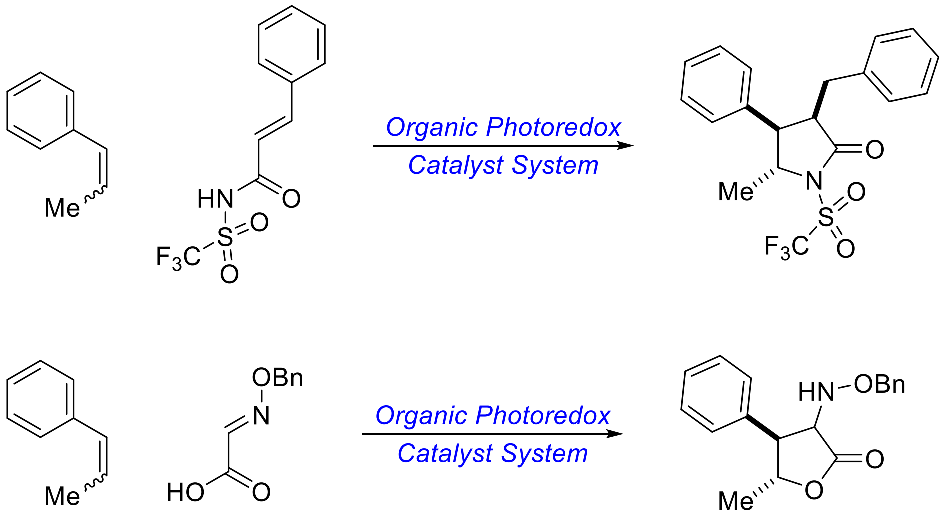
Me
HN
O
F_3C
S
O
O
Organic Photoredox
Catalyst System
O
Me
N
S
O
O
F_3C
OBn
N
HO
O
Me
Organic Photoredox
Catalyst System
HN
OBn
O
O
Me

2.6 Experimental Details

General Methods and Materials

Infrared (IR) spectra were obtained using a Jasco 260 Plus Fourier transform infrared spectrometer. Proton and carbon magnetic resonance spectra (1H NMR and 13C NMR) were recorded on a Bruker model DRX 400, DRX 500, or a Bruker AVANCE III 600 CryoProbe (1H NMR at 400 MHz, 500 MHz or 600 MHz and 13C NMR at 101, 126, or 151 MHz) spectrometer with solvent resonance as the internal standard (^{1}H NMR: $CDCl_3$ at 7.26 ppm; ^{13}C NMR: $CDCl_3$ at 77.0 ppm). ^{1}H NMR data are reported as follows: chemical shift, multiplicity (s = singlet, d = doublet, t = triplet, dd = doublet of doublets, ddt = doublet of doublet of triplets, ddd = doublet of doublet of doublets, dddd = doublet of doublet of doublet of doublets m = multiplet, brs = broad singlet), coupling constants (Hz), and integration. Mass spectra were obtained using a Micromass (now Waters Corporation, 34 Maple Street, Milford, MA 01757) Quattro-II, Triple Quadrupole Mass Spectrometer, with a Z-spray nano-Electrospray source design, in combination with a NanoMate (Advion 19 Brown Road, Ithaca, NY 14850) chip based electrospray sample introduction system and nozzle. Thin layer chromatography (TLC) was performed on SiliaPlate 250 μm thick silica gel plates provided by Silicycle. Visualization was accomplished with short wave UV light (254 nm), aqueous basic potassium permanganate solution, or cerium ammonium molybdate solution followed by heating. Flash chromatography was performed using SiliaFlash P60 silica gel (40-63 μm) purchased from Silicycle. Tetrahydrofuran, diethyl ether, dichloromethane, and toluene were dried by passage through a column of neutral alumina under nitrogen prior to use. Irradiation of photochemical reactions was carried out using a 15W PAR38 blue LED floodlamp purchased from EagleLight (Carlsbad, CA), with borosilicate glass vials purchased from Fisher Scientific. All other reagents were obtained from commercial sources and used without further purification, or made according to published procedures the references of which can be found in the published report, unless otherwise noted.

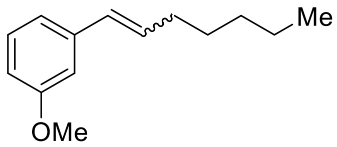

1-(hept-1-en-1-yl)-3-methoxybenzene: To a flame dried 250 mL round bottom flask equipped with a stir bar was added hexyltriphenylphosphonium bromide (11.32 g, 26.5 mmol, 1.05 equiv) and 65 mL dry THF. The solution was cooled to 0 °C, and potassium *tert*-butoxide (3.6 g, 26.5 mmol, 1.05 equiv) was added. The reaction turned bright orange, and was allowed to stir under N_2 for 45 minutes. *m*-anisaldehyde (3.07 mL, 25.2 mmol, 1.0 equiv) was dissolved in 16 mL THF, and the resulting solution was added dropwise to the reaction at 0 °C. By the end of the addition, the reaction had lost its orange color. The mixture was allowed to react at room temperature overnight, at which point the solvent was evaporated. The product was purified via column chromatography, resulting in a clear, colorless oil (3.7 g, 72%). **^{1}H NMR** (400 MHz, $CDCl_3$) δ 7.26 (t, J = 7.9 Hz, 1H), 6.93-6.88(m, 1H), 6.84 (t, *J* = 2.0 Hz, 1H), 6.79 (ddd, *J* = 8.2, 2.7, 0.9 Hz, 1H), 6.40 (dt, *J* = 11.7, 1.9 Hz, 1H), 5.69 (dt, *J* = 11.6, 7.3 Hz, 1H), 3.83 (s, 3H), 2.35 (dq, *J* = 7.4, 1.9 Hz, 2H), 1.57-1.40 (m, 2H), 1.41-1.22 (m, 4H), 0.97-0.80 (m, 3H). **^{13} C NMR** (101 MHz, $CDCl_3$) δ 159.36, 139.20, 133.54, 129.01, 128.55, 121.31, 114.29, 111.92, 55.13, 31.59, 31.57, 29.66, 28.69, 22.65, 22.56, 14.11, 14.03. Spectral data were in agreement with literature values.[49]

General Procedures for the PRCC reaction methodology:

General Procedure A (For monoester-fumarates). To a flame-dried two dram vial equipped with a magnetic stir bar was added the alkene (1 equiv.), α,β-unsaturated acid (1.1 equiv.), **Mes-Acr-Me** (2.5 mol%), phenyl disulfide (10 mol%), and 2,6-lutidine (10 mol%). The vial was purged with N_2 and sparged dichloromethane was added to achieve a concentration of 0.15 M with respect to substrate, and sealed with a septum screwcap. The reaction was irradiated with a 450 nm lamp and stirred at room temperature for 24 hours. Upon completion, the reaction was passed through a silica plug to remove the catalyst and eluted with dichloromethane. The product was further purified by flash chromatography with acetone/hexanes as the eluent.

General Procedure B (For cinnamic acid derivatives). This method was undertaken by Michelle Riener. Details of this method can be found in the supplementary information of the published report.

General Procedure C (For alkynoic acids). This method was undertaken by Michelle Riener. Details of this method can be found in the supplementary information of the published report. One transformation for butyrolactone formation using 3-(trimethylsilyl)propiolic acid and 1-methoxy-3-(prop-1-en-1-yl)benzene utilized a different method than the general method. This can be found here, under the characterization for that product. The method used for this particular example is most similar to General Procedure A.

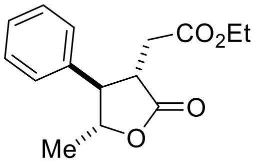

Ethyl 2-(5-methyl-2-oxo-4-phenyltetrahydrofuran-3-yl)acetate The lactone was prepared according to General procedure A using 65 μL of β-methylstyrene, 79.3 mg of mono-ethylfumarate, 10.9 mg phenyl disulfide, 5.2 mg **Mes-Acr-Me**, and 6 μL of 2,6-lutidine. Yield was 66% (2.2:1 dr). The major and minor diastereomers could be separated via column chromatography (3% acetone in hexanes). ^{1}**H NMR** (400 MHz, $CDCl_3$) δ major: 7.39-7.23 (m, 5H), 4.50 (dq, J = 6.1, 9.9 Hz, 1H), 3.95 (m, 2H), 3.25 (dt, J = 6.0, 12.0 Hz, 1H), 3.08 (dd, J =

9.8, 12.3 Hz, 1H), 2.70 (dd, J = 5.2, 16.5 Hz, 1H), 2.56 (dd, J = 6.4, 16.5 Hz, 1H), 1.39 (d, J = 6.1 Hz, 3H), 1.13 (t, J = 7.2 Hz, 3H). δ minor: 7.33-7.06 (m, 5H), 4.90 (dq, J = 6.4, 1.1 Hz, 1H), 4.08 (dq, J = 7.2, 1.8 Hz, 2H), 3.55 (m, 2H), 2.63 (dd, J = 2.9, 17.2 Hz, 1H), 1.92 (dd, J = 9.9, 17.8 Hz, 1H), 1.53 (d, J = 6.5 Hz, 3H), 1.17 (t, J = 7.1 Hz, 3H). **^{13}C NMR** (101 MHz, $CDCl_3$) δ major: 175.95, 170.61, 136.26, 129.10, 128.12, 127.80, 81.03, 60.84, 55.58, 45.13, 32.84, 18.56, 13.95. δ minor: 177.08, 171.45, 138.45, 129.08, 127.79, 127.54, 81.55, 60.79, 50.01, 40.01, 31.14, 20.67, 14.06. **MS** (+ESI) Calculated *m/z* for $[M+H]^{+}$ = 263.12. Experimental *m/z* for $[M+H]^{+}$ = 263.16. **IR** (Thin Film, cm^{-1}) 3056, 2983, 1772, 1733, 1540, 1266.

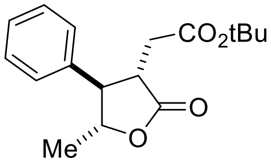

***tert*-Butyl 2-(5-methyl-2-oxo-4-phenyltetrahydrofuran-3-yl)acetate** The lactone was prepared according to General Procedure A using 65 μL of β-methylstyrene, 94.7 mg of mono-*tert*-butylfumarate, 10.9 mg phenyl disulfide, 5.2 mg **Mes-Acr-Me**, and 6 μL 2,6-lutidine. Yield was 74% (2.3:1 dr). The major and minor diastereomers could be separated via column chromatography (3% acetone in hexanes). **^{1}H NMR** (500 MHz, $CDCl_3$) δ major: 7.24-7.38 (m, 5H), 4.49 (m, 1H), 3.22 (m, 1H), 3.05 (dd, J = 9.9, 12.3 Hz, 1H), 2.62 (dd, J = 5, 16.5 Hz, 1H), 2.50 (dd, J = 6.4, 16.5 Hz, 1H) 1.38 (d, J = 6.1 Hz, 3H), 1.31 (s, 9H). δ minor: 7.33-7.08 (m, 5H), 4.87 (dq, J = 1.4, 6.5 Hz, 1H), 3.50 (m, 2H), 2.57 (dd, J = 3.8, 17.9 Hz, 1H), 1.83 (dd, J = 10.2, 18 Hz, 1H), 1.51 (d, J = 6.5 Hz, 3H), 1.37 (s, 9H). **^{13}C NMR** (126 MHz, $CDCl_3$) δ major: 176.13, 169.71, 136.37, 129.11, 128.05, 127.84, 81.28, 80.94, 55.70, 45.28, 34.12, 27.79, 18.53. δ minor: 177.26, 170.74, 138.62, 129.02, 127.69, 127.57, 81.49, 80.96, 49.97, 40.01, 32.12, 27.89, 20.65. **MS** (+ESI) Calculated *m/z* for $[M+H]^+$ = 291.15. Experimental *m/z* for $[M+H]^+$ = 291.19. **IR** (Thin Film, cm^{-1}) 3055, 2982, 2933, 2306, 1770, 1724, 1368, 1266.

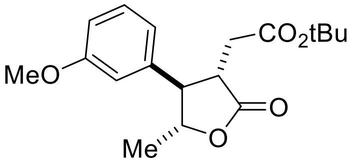

***tert*-Butyl 2-(4-(3-methoxyphenyl)-5-methyl-2-oxotetrahydrofuran-3-yl)acetate** The lactone was prepared according to General Procedure A using 77 μL 1-methoxy-3-(prop-1-en-1-yl)benzene, 94.7 mg mono-*tert*-butylfumarate, 10.9 mg phenyl disulfide, 5.2 mg **Mes-Acr-Me**, and 6 μL 2,6-lutidine. Yield was 76% (2.8:1 dr). The major and minor diastereomers could be separated via column chromatography (3% acetone in hexanes). **^{1}H NMR** (500 MHz, $CDCl_3$) δ major: 7.28 (t, J = 7.9 Hz, 1H), 6.84 (m, 2H), 6.77 (t, J = 1.9 Hz, 1H), 4.48 (m, 1H), 3.81 (s, 3H), 3.19 (m, 1H), 3.03 (dd, J = 9.9, 12.3 Hz, 1H), 2.60 (dd, J = 5.1, 16.5 Hz), 2.51 (dd, J = 6.2, 16.6 Hz, 1H) 1.38 (s, 9H). δ minor: (400 MHz, CDCl3) 7.23 (t, J = 8 Hz, 1H), 6.81 (dd, J = 2.1, 8.3 Hz, 1H), 6.66 (d, J = 7.6 Hz, 1H), 6.62 (t, J = 2.2 Hz, 1H), 4.85 (dq, J = 1, 6.6 Hz, 1H), 3.77 (s, 3H), 3.48 (m, 2H), 2.58 (dd, J = 3.5, 18.4 Hz, 1H), 1.87 (dd, J = 9.5, 17.6 Hz, 1H), 1.51 (d, J = 6.6 Hz, 3H), 1.37 (s, 9H). **^{13}C NMR** (126 MHz, $CDCl_3$). δ major: 176.05, 169.70, 160.04, 138.05, 130.17, 119.98, 114.00, 112.88, 81.28, 80.77, 55.58, 55.24, 45.31, 34.02, 27.83, 18.62. δ minor: (101 MHz, CDCl3) 177.19, 170.79, 159.98, 140.16, 130.10, 119.73, 113.56, 112.78, 81.32, 80.98, 55.14, 55.01, 39.97, 32.10, 27.90, 20.63. **MS** (+ESI) Calculated *m/z* for $[M+H]^+$ = 221.16. Experimental *m/z* for $[M+H]^+$ = 221.19. **IR** (Thin Film, cm^{-1}) 2976, 2932, 2837, 1775, 1728, 1601, 1586, 1489, 1456, 1367, 1266.

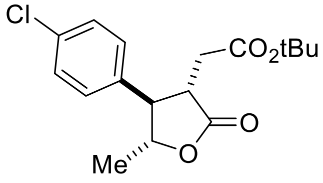

***tert*-Butyl 2-(4-(4-chlorophenyl)-5-methyl-2-oxotetrahydrofuran-3-yl)acetate** The lactone was prepared according to General Procedure A using 72 µL *p*-Cl-β-methylstyrene, 94.7 mg mono-*tert*-butylfumarate, 10.9 mg phenyl disulfide, 5.2 mg **Mes-Acr-Me**, and 6 µL 2,6-lutidine. Yield was 77% (2.3:1 dr). The major and minor diastereomers could be separated via column chromatography (3% acetone in hexanes). **^{1}H NMR** (400 MHz, $CDCl_3$) δ major: 7.33 (d, J = 8.4 Hz, 2H), 7.19 (d, J = 8.4 Hz, 2H), 4.43 (m, 1H), 3.17 (m, 1H), 3.03 (dd, J = 9.8, 12.2 Hz, 1H), 2.60 (dd, J = 4.8, 16.5 Hz, 1H), 2.47 (dd, J = 6.3, 16.5 Hz, 1H), 1.36 (d, J = 6.1 Hz, 3H), 1.31 (s, 9H). δ minor: 7.28 (d, J = 8.4 Hz, 2H), 7.03 (d, J = 8.4 Hz, 2H), 4.81 (dq, J = 1.6, 6.5 Hz, 1H), 3.55-3.44 (m, 2H), 2.60 (dd, J = 3.7, 18 Hz, 1H), 1.82 (dd, J = 10.3, 18, 1H), 1.51 (d, J = 6.6 Hz, 3H), 1.38 (s, 9H). **^{13}C NMR** (101 MHz, $CDCl_3$) δ major: 175.69, 169.59, 134.92, 133.88, 129.24, 129.16, 81.36, 80.61, 55.06, 45.19, 33.97, 27.76, 18.42. δ minor: (125 MHz, CDCl3) 176.88, 170.61, 137.11, 133.61, 129.18, 128.97, 81.30, 81.20, 49.42, 39.89, 32.03, 27.90, 20.59. **MS** (+ESI) Calculated *m/z* for $[M+H]^+$ = 325.11. Experimental *m/z* for [M+H]+ = 325.09. **IR** (Thin Film, cm^{-1}) 3057, 2979, 2931, 1776, 1726, 1494, 1368, 1266.

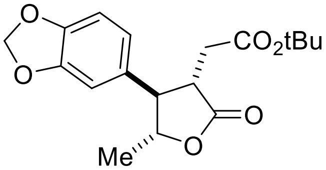

***tert*-Butyl 2-(4-(benzo[d][1,3]dioxol-5-yl)-5-methyl-2-oxotetrahydrofuran-3-yl)acetate** The lactone was prepared according to General Procedure A using 72.5 µL isosafrole, 94.7 mg mono-

tert-butylfumarate, 10.9 mg phenyl disulfide, 5.2 mg **Mes-Acr-Me**, and 6 µL 2,6-lutidine. Yield was 65% (4.3:1 dr). The major and minor diastereomers could be separated via column chromatography (5% acetone in hexanes). **^{1}H NMR** (400 MHz, $CDCl_3$) δ major: 6.79 (d, J = 7.9 Hz, 1H), 6.70 (m, 2H), 5.97 (s, 2H), 4.41 (m, 1H), 3.11 (m, 1H), 2.98 (dd, J = 9.8, 12.3, 1H), 2.90 (dd, J = 5, 16.5 Hz, 1H), 2.49 (dd, J = 6.1, 16.5 Hz, 1H), 1.37 (d, J = 6.1 Hz, 1.36 (s, 9H). δ minor: 6.73 (d, J = 7.9 Hz, 1H), 6.54 (m, 2H), 5.96 (s, 2H), 4.81 (q, J = 6.3 Hz, 1H), 3.43 (m, 2H), 2.59 (dd, J = 3.4, 18 Hz, 1H), 1.89 (dd, J = 10.2, 17.9 Hz, 1H), 1.50 (d, J = 6.5 Hz, 3H), 1.39 (s, 9H). **^{13}C NMR** (101 MHz, $CDCl_3$) δ major: 175.96, 169.71, 148.25, 147.38, 129.99, 121.43, 108.68, 107.55, 101.24, 81.28, 80.84, 55.37, 45.33, 33.88, 27.84, 18.44. δ minor: 177.18, 170.85, 148.24, 147.02, 132.34, 120.87, 108.55, 107.73, 101.19, 81.55, 81.07, 49.73, 40.09, 32.08, 27.95, 20.61. **MS** (+ESI) Calculated *m/z* for $[M+H]^+$ = 335.14. Experimental *m/z* for $[M+H]^+$ = 335.17. **IR** (Thin Film, cm^{-1}) 3056, 2980, 2932, 2307, 1773, 1726, 1506, 1489, 1446, 1368, 1266.

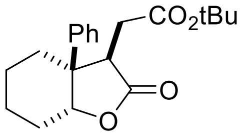

***tert*-Butyl 2-(2-oxo-3a-phenyloctahydrobenzovuran-3-yl)acetate** The lactone was prepared according to General Procedure A using 80 µL 1-phenylcyclohexene, 94.7 mg mono-*tert*-butylfumarate, 10.9 mg phenyl disulfide, 5.2 mg **Mes-Acr-Me**, and 6 µL 2,6-lutidine. The mixture was allowed to react for 30 hours instead of the typical 24. Yield was 64% (5:1 dr). The major and minor diastereomers could not be separated, and the product was isolated as a mixture of isomers following column chromatography (2% acetone in hexanes). **^{1}H NMR** (400 MHz, $CDCl_3$) δ major: 7.42-7.33 (m, 5H), 4.95 (bs, 1H), 3.38 (t, J = 7 Hz, 1H), 2.57 (dd, J = 7.4, 16.2

Hz, 1H), 2.28 (d, J = 13.2 Hz, 1H) 2.20 (dd, J = 6.2, 16.2 Hz, 1H), 2.10 (d, J = 13.6 Hz, 1H), 1.70-1.37 (m, 6H), 1.26 (s, 9H). δ minor: 7.29-7.22 (m, 5H), 5.01 (t, J = 4.4 Hz, 1H), 3.17 (t, J = 6.8 Hz, 1H), 2.17 (dd, J = 6.8, 16.3 Hz, 1H), 2.1-1.9 (m, 3H), 1.7-1.4 (m, 6H), 1.33 (s, 9H). **^{13}C NMR** (101 MHz, $CDCl_3$) δ major: 176.37, 170.09, 138.34, 128.94, 127.22, 126.62, 81.79, 80.92, 53.37, 47.64, 29.86, 27.74, 26.42, 24.63, 21.04, 19.36. minor: 177.46, 169.96, 139.65, 128.78, 127.13, 127.06, 81.11, 79.46, 48.67, 48.29, 34.91, 32.98, 31.52, 27.85, 26.61, 22.59, 20.34, 14.06. **MS** (+ESI) Calculated *m/z* for $[M+H]^+$ = 331.18. Experimental *m/z* for $[M+H]^+$ = 331.15. **IR** (Thin Film, cm^{-1}) 3054, 2360, 2341, 1771, 1507, 1266.

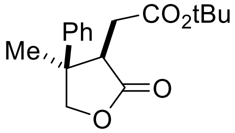

***tert*-Butyl 2-(4-methyl-2-oxo-4-phenyltetrahydrofuran-3-yl)acetate** The lactone was prepared using General Prodedure A, however a 3:1 ratio of alkene:acid was employed, and the mixture was allowed to react for 48 hours instead of the typical 24. The lactone was prepared using 195 μL α-methylstyrene, 86.1 mg mono-*tert*-butylfumarate, 10.9 mg phenyl disulfide, 5.2 mg **Mes-Acr-Me**, and 6 μL 2,6-lutidine. The major and minor diastereomers could not be separated, and the product was isolated in an 81% yield (1.3:1 dr) following column chromatography (3% acetone in hexanes). **^{1}H NMR** (400 MHz, $CDCl_3$) δ major: 7.43-7.22 (m, 5H), 4.28 (d, J = 8.9 Hz, 1H), 4.21 (d, J = 8.9 Hz, 1H), 3.61 (dd, J = 5.1, 8.4 Hz, 1H), 2.61 (dd, J = 8.4, 16.1 Hz, 1H), 2.38 (dd, J = 5.2, 16.2 Hz, 1H), 1.43 (s, 3H), 1.38 (s, 9H). δ minor: 7.43-7.22 (m, 5H), 4.71 (d, J = 9.3 Hz, 1H), 4.28 (d, J = 9.3 Hz, 1H), 3.19 (dd, J = 6, 7.4 Hz, 1H), 2.30 (dd, J = 6, 17 Hz, 1H), 1.89 (dd, J = 7.4, 17 Hz, 1H), 1.64 (s, 3H), 1.42 (s,9H). **^{13}C NMR** (101 MHz, $CDCl_3$) δ major: 177.05, 170.26, 141.45, 129.02, 127.52, 125.64, 81.35, 78.17, 46.48, 46.22, 31.43, 27.87, 20.82.

δ minor: 177.58, 170.58, 141.16, 128.95, 127.52, 126.04, 81.13, 78.31, 48.18, 46.41, 32.71, 27.94, 24.59. **MS** (+ESI) Calculated *m/z* for $[M+H]^+$ = 291.15. Experimental *m/z* for $[M+H]^+$ = 291.19. **IR** (Thin Film, cm^{-1}) 3058, 2979, 2932, 2306, 1775, 1728, 1498, 1455, 1368, 1266.

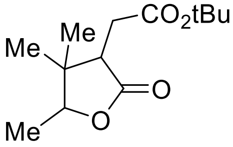

***tert*-Butyl 2-(4,4,5-trimethyl-2-oxotetrahydrofuran-3-yl)acetate** The lactone was prepared according to a modified General Procedure B. The lactone was prepared using 159 μL of 2-methyl-2-butene (3 equiv.), 86.1 mg of mono-*tert*-butylfumarate (1 equiv.), 5.2 mg **Mes-Acr-Me**, 3.8 mg *p*-nitrothiophenol (5 mol%), and 6 μL 2,6-lutidine. The major and minor diastereomers could not be separated, and relative stereochemistry could not be determined. The yield was 55% (2.7:1 d.r.) following column chromatography (5% acetone in hexanes). ^{1}**H NMR** (500 MHz, $CDCl_3$) δ major: 4.18 (q, J = 6.5 Hz, 1H), 2.90 (t, J = 6.9 Hz, 1H), 2.58 (dd, J = 6.8, 16.3 Hz, 1H), 2.23 (dd, J = 7.1, 16.4 Hz, 1H), 1.45 (s, 9H), 1.25 (d, J = 6.5 Hz, 3H), 1.06 (s, 3H), 0.79 (s, 3H). δ minor: 4.21 (q, J = 6.7 Hz, 1H), 2.91 (t, J overlap, 1H), 2.55 (dd, J = 6.3, 16.3 Hz, 1H), 2.29 (dd, J = 7.8, 16.4 Hz, 1H), 1.44 (s, 9H), 1.26 (d, J = 6.6 Hz, 3H), 1.04 (s, 3H), 0.98 (s, 3H). ^{13}**C NMR** (126 MHz, $CDCl_3$) δ major: 176.93, 170.74, 83.20, 81.14, 48.87, 42.43, 30.85, 27.96, 23.18, 15.81, 13.00. δ minor: 177.31, 170.73, 84.03, 81.23, 45.31, 40.74, 31.20, 27.94, 22.86, 22.11, 15.56. **MS** (+ESI) Calculated *m/z* for $[M+H]^+$ = 243.15. Experimental *m/z* for $[M+H]^+$ = 243.18. **IR** (Thin Film, cm^{-1}) 3056, 2980, 2360, 1771, 1731, 1497, 1266.

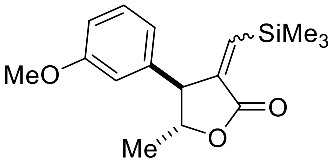

(*E/Z*)-4-(3-methoxyphenyl)-5-methyl-3-((trimethylsilyl)methylene)dihydrufran-2-(3H)-one The lactone was prepared using General Procedure A using 77 µL *m*-methoxy-β-methylstyrene, 76 µL 3-(trimethylsilyl)propiolic acid, 10.9 mg phenyl disulfide, 5.2 mg **Mes-Acr-Me**, and 6 µL 2,6-lutidine. Yield was 73% (0.8:1 *E*:*Z*). The *E*- and *Z*- isomers could be separated via column chromatography (3% acetone in hexanes). **^{1}H NMR** (400 MHz, CDCl$_3$) δ *E*: 7.24 (t, J = 7.9 Hz, 1H), 7.19 (d, J = 2,6 Hz, 1H), 6.80 (dd, J = 2.4, 8.2 Hz, 1H), 6.72 (d, J = 7.6 Hz, 1H), 6.65 (t, J = 2 Hz, 1H), 4.40 (m, 1H), 3.77 (s, 3H), 3.74 (dd, J = 2.6, 4.4 Hz, 1H), 1.46 (d, J = 6.3 Hz, 3H), -0.11 (s, 9H). δ *Z*: 7.30 (t, J = 8 Hz, 1H), 6.85 (m, 1H), 6.75 (d, J = 7.6 Hz, 1H), 6.69 (t, J = 1.8 Hz, 1H), 6.15 (d, J = 2.9 Hz, 1H), 4.49 (m, 1H), 3.81 (s, 3H), 3.64 (dd, J = 2.9, 8 Hz, 1H), 1.44 (d, J = 6.2 Hz, 3H), 0.19 (s, 9H). **^{13}C NMR** (101 MHz, CDCl$_3$) δ *E*: 169.93, 160.01, 143.85, 143.64, 143.12, 130.06, 120.16, 113.57, 112.71, 82.08, 55.23, 52.59, 21.44, -1.49. δ *Z*: 169.29, 159.97, 145.95, 145.37, 140.47, 130.09, 120.89, 114.60, 112.63, 81.27, 57.25, 55.23, 20.04, -0.79. **MS** (+ESI) Calculated *m/z* for $[M+H]^+$ = 291.13. Experimental *m/z* for $[M+H]^+$ = 291.12. **IR** (Thin Film, cm^{-1}) 3055, 2956, 2837, 2306, 1757, 1600, 1585, 1490, 1455, 1266.

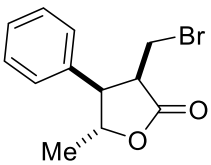

3-(bromomethyl)-5-methyl-4-phenyldihydrofuran-2(3*H*)-one: The lactone was prepared according to a modified General Procedure A, using 130 µL of β-methylstyrene (2 equiv), 75.5

mg (*Z*)-3-bromoacrylic acid (1 equiv), 10.9 mg phenyldisulfide, 5.2 mg **Mes-Acr-Me**, and 6 μL 2,6-Lutidine. The reaction was carried out at room temperature over 4 days. Due to degradation issues on silica chromatography, only one diastereomer could be isolated. The other major product observed was the elimination to the α-methylene-γ-butyrolactone. The indicated diastereomer was isolated in a 14% yield (19 mg) via silica chromatography (2% acetone in hexanes). **^{1}H NMR** (400 MHz, $CDCl_3$) δ 7.39-7.24 (m, 5H), 4.91 (dq, J = 1.8, 6.5 Hz, 1H), 3.58-3.45 (m, 3H), 2.76 (t, J = 10.12 Hz, 1H), 1.53 (d, J = 6.6 Hz, 3H). **^{13}C NMR** (101 MHz, $CDCl_3$) δ 174.26, 136.97, 129.07, 128.06, 127.91, 81.37, 50.03, 46.85, 26.77, 20.40. **MS** (+ESI) Calculated *m/z* for $[M+H]^+ = 271.01$. Experimental *m/z* for $[M+H]^+ = 271.02$. **IR** (Thin Film, cm^{-1}) 3063, 3032, 2979, 2931, 2254, 1772, 1603, 1498, 1455, 1357.

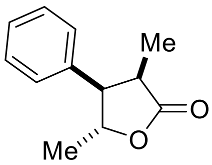

3,5-dimethyl-4-phenyldihydrofuran-2(3*H*)-one: The lactone was prepared by dehalogenation of 3-(bromomethyl)-5-methyl-4-phenyldihydrofuran-2(3*H*)-one (16 mg), using tributyltin hydride (80 μL, 5 equiv) and AIBN (3 mg, 0.3 equiv) in [0.2] benzene (0.3 mL). A 1-dram vial equipped with a stir bar and a Teflon septum screw cap was charged with the lactone, AIBN, tributyltin hydride, and benzene. The reaction mixture was capped and sparged with N_2 for 5 minutes, and then the vial was sealed with Teflon tape prior to heating at 65 ºC for 2 hours. At this point, the solvent was evaporated under reduced pressure, and a crude ^{1}H NMR was taken to determine if any ring opening or isomerization products could be observed. The only observed product was the dehalogenated product 3,5-dimethyl-4-phenyldihydrofuran-2(3*H*)-one. The reaction was purified via silica chromatography, flushing with hexanes to remove the tributyltin hydride, followed by dichloromethane to isolate 8.2 mg (73%) of lactone Y. **^{1}H NMR** (400 MHz, CDCl$_3$) δ 7.37-7.26 (m, 3H), 7.13 (dd, J = 1.4, 7.8 Hz, 2H), 4.87 (m, 1H), 3.34 (dd, J = 4.8, 8.7 Hz, 1H), 3.04 (m, 1H), 1.48 (d, J = 6.4 Hz, 3H), 0.89 (d, J = 7.5 Hz, 3H). **^{13}C NMR** (101 MHz, CDCl$_3$) δ 178.96, 137.65, 128.87, 127.84, 127.50, 79.75, 52.07, 38.95, 20.12, 11.40. **MS** (+ESI) Calculated *m/z* for [M+H]$^+$ = 191.10. Experimental [M+H]$^+$ = 191.15. **IR** (Thin Film, cm^{-1}) 3031, 2978, 2935, 1771, 1456, 1206.

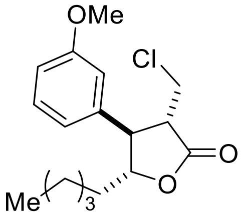

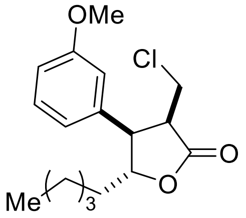

3-(chloromethyl)-4-(3-methoxyphenyl)-5-pentyldihydrofuran-2(3*H*)-one: The lactone was prepared according to modified General Procedure C using 58.5 mg (*Z*)-3-chloroacrylic acid, 108 µL 1-(hept-1-en-1-yl)-3-methoxybenzene, 5.2 mg **Mes-Acr-Me**, 16.3 mg phenyldisulfide, and 6 µL 2,6-lutidine. The diastereomers could be separated via column chromatography if using a gradient eluent. 2% acetone in hexanes was used until the minor diastereomer was observed, followed by 5% acetone in hexanes to isolate the all trans diastereomer. The all trans would eliminate on the column to the α-methylene if a less polar solvent was used. Using these conditions, elimination was minimized. Yield was 100.7 mg (65%), with a 1.1:1 d.r. **^{1}H NMR** (400 MHz, CDCl$_3$) δ major: 7.31 (t, J = 7.9 Hz, 1H), 6.85 (m, 2H), 6.80 (t, J = 1.9 Hz, 1H), 4.46 (ddd, J = 6.1, 9.8, 11.9 Hz, 1H), 4.00 (dd, J = 3.4, 11.6 Hz, 1H), 3.83 (s, 3H), 3.55 (dd, J = 3.4, 11.6 Hz, 1H), 3.43 (dd, J = 9.9, 11.7 Hz, 1H), 3.17 (dt, J = 3.4, 11.7 Hz, 1H), 1.68 (m, 2H), 1.51

(m, 1H), 1.35 (m, 1H), 1.25 (m, 4H), 0.84 (t, J = 6.9 Hz, 3H). δ minor: 7.29 (d, J = 7.9 Hz, 1H), 6.85 (m, 3H), 4.73 (ddd, J = 2.4, 5.5, 8.1 Hz, 1H), 3.80 (s, 3H), 3.70 (dd, J = 3.5, 11.4 Hz, 1H), 3.54 (dd, J = 2.4, 8.7 Hz, 1H), 3.36 (dt, J = 3.6, 9.8 Hz, 1H), 3.05 (dd, J = 9.9, 11.3 Hz, 1H), 1.85-1.25 (m, 8H), 0.88 (t, J = 6.9 Hz, 3H). **^{13}C NMR** (101 MHz, $CDCl_3$) δ major: 173.71, 160.14, 138.41, 130.36, 119.91, 114.04, 112.83, 84.30, 55.27, 50.83, 49.99, 40.64, 33.58, 31.41, 25.26, 22.36, 13.89. δ minor: 174.42, 159.91, 138.66, 130.17, 119.91, 114.01, 113.07, 85.33, 55.22, 48.43, 47.12, 39.88, 34.62, 31.35, 25.27, 22.45, 13.92. **MS** (+ESI) calculated *m/z* for $[M+H]^+$ = 311.13. Experimental *m/z* for $[M+H]^+$ = 311.11. **IR** (Thin Film, cm^{-1}) 3055, 2957, 2932, 2859, 1773, 1601,1585, 1489, 1456, 1266.

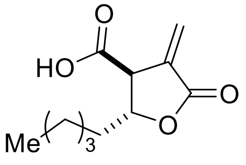

(+/-)-methylenolactocin

Methylenolactocin: 155 mg of 3-(chloromethyl-4-(3-methyphenyl)-5-pentyldihydrofuran-2(3*H*)-one were stirred in 7.5 mL EtOAc and 7.5 mL MeCN. To this was added, fast dropwise, a solution of 13.1 mg $RuCl_3*3H_2O$ (10 mol%) and 1.6 g $NaIO_4$ (15 equiv) in 15 mL H_2O. The reaction was allowed to stir for 3 hours, after which the white precipitate was filtered over celite. The filtrate was diluted with EtOAc, and washed with sat. $NaHSO_3$. The aqueous solution was extracted with EtOAc and the combined organics were washed with H_2O and Brine, dried over $MgSO_4$, and evaporated under reduced pressure. The resulting product mixture was used in the next step without further purification. The lactone was dissolved in 2-propanol (12.5 mL, [0.04]) and 207 mg of K_2CO_3 (3 equiv) was added, followed by 0.5 mL NEt_3 (1M). The reaction was allowed to stir overnight, following which it was diluted with EtOAc and quenched with 3M

HCl. The product was extracted with EtOAc, and washed with brine, and dried over Na_2SO_4. The product was purified on silica chromatography. The bicycle byproduct could be separated using dichloromethane as eluent, and the desired methylenolactocin could be isolated cleanly using 1% acetic acid in dichloromethane. The desired paraconic acid methylenolactocin was isolated in a 25% yield (27 mg) over these two steps. **^{1}H NMR** (400 MHz, $CDCl_3$) δ 8.64 (bs, 1H), 6.46 (d, J = 2.3 Hz, 1H), 6.03 (d, J = 2.3 Hz, 1H), 4.81 (q, J = 5.8 Hz), 3.63 (m, 1H), 1.73 (m, 2H), 1.50-1.25 (m, 6H), 0.89 (t, J = 6.8 Hz, 3H). **^{13}C NMR** (101 MHz, $CDCl_3$) δ 174.58, 168.26, 132.34, 125.98, 78.87, 49.47, 35.66, 31.29, 24.40, 22.40, 13.90.

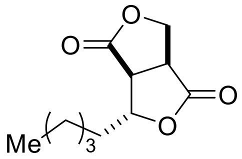

3-pentyltetrahydrofuro[3,4-*c*]furan-1,4-dione: White solid. **^{1}H NMR** (400 MHz, $CDCl_3$) δ 4.81 (dt, J = 1.2, 7.2 Hz, 1H), 4.69 (dd, J = 1.5, 9.7 Hz, 1H), 4.53 (dd, J = 7.7, 9.7 Hz, 1H), 3.52 (dt, J = 1.5, 9.7 Hz, 1H), 3.20 (dd, J = 1.4, 9.5 Hz, 1H), 1.75 (m, 2H), 1.46 (m, 2H), 1.34 (m, 4H), 0.90 (t, J = 6.9 Hz, 3H). **^{13}C NMR** (101 MHz, $CDCl_3$) δ 175.51, 175.33, 81.85, 68.99, 45.38, 40.68, 36.26, 31.15, 24.29, 22.40, 13.88. **MS** (+ESI) calculated *m/z* for $[M+H]^+$ = 213.10. Experimental *m/z* for $[M+H]^+$ = 213.10. **IR** (Thin Film, cm^{-1}) 2953, 2924, 2857, 1771, 1456, 1340.

General Procedure for Improving Lactone Diastereomeric Ratio:

A 25 mL round bottom flask equipped with a stir bar was charged with **12a** (108 mg, 0.4 mmol, 1 equiv), MeOH (10 mL, 0.04 M), triethylamine (1 ml, 0.4 M), and Potassium Carbonate (276 mg, 5 equiv). The mixture was allowed to react for 3 hours, at which point the reaction was diluted with Et_2O, and washed with H_2O and Brine, dried over $MgSO_4$, and the solvent was evaporated. Michelle Riener carried out the epimerization for the lactone derived from cinnamic acid. The starting diastereomeric ratio for this lactone was 4.6:1 and the final ratio was >25:1 as determined by ^1H NMR. The lactone from *t*-butylfumarate was subjected to the same conditions. The starting diastereomeric ratio was 2.3:1, and the final ratio was 13.5:1, as determined by ^1H NMR.

REFERENCES

(1) Kitson, R. R. A.; Millemaggi, A.; Taylor, R. J. K. *Angew. Chem. Int. Ed.* **2009**, *48*, 9426.

(2) Hoffmann, H. M. R.; Rabe, J. *Angew. Chem. Int. Ed., Engl.* **1985**, *24*, 94.

(3) Seitz, M.; Reiser, O. *Curr. Opin. Chem. Bio.* **2005**, *9*, 285.

(4) Bandichhor, R.; Nosse, B.; Reiser, O. *Top Curr Chem.* **2005**, *243*, 43.

(5) Park, B. K.; Nakagawa, M.; Hirota, A.; Nakayama, M. *J. Antibiot.* **1988**, *41*, 751.

(6) Brisdelli, F.; Perilli, M.; Sellitri, D.; Piovano, M.; Garbarino, J. A.; Nicoletti, M.; Bozzi, A.; Amicosante, G.; Celenza, G. *Phytother. Res.* **2012**, *27*, 431.

(7) Goel, M.; Dureja, P.; Rani, A.; Uniyal, P. L. Laatsch, H. *J. Agric. Food Chem.* **2011**, *59*, 2299.

(8) Kumar, KC. S.; Müller, K. *J. Nat. Prod.* **1999**, *62*, 817.

(9) Nolsoe, J. M. J.; Hansen, T. V. *Eur. J. Org. Chem.***2014**, 3051.

(10) Steward, K. M.; Gentry, E. C.; Johnson, J. S. *J. Am. Chem. Soc.* **2012**, *134*, 7329.

(11) Zhu, G.; Lu, X. *J. Org. Chem.* **1995**, *60*, 1087.

(12) Sohn, S. S.; Rosen, E. L.; Bode, J. W. *J. Am. Chem. Soc.* **2004**, *126*, 14370.

(13) Burstein, C.; Tschan, S.; Xie, X.; Glorius, F. *Synthesis* **2006**, 2418.

(14) Wei, X.-J.; Yang, D.-T.; Wang, L.; Song, T.; Wu, L.-Z.; Liu, Q. *Org. Lett.* **2013**, *15*, 6054.

(15) Tamaru, Y. *J. Org. Chem.* **1991**, *56*, 1099.

(16) Dai, M.; Danishefsky, S. J. *J. Am. Chem. Soc.* **2007**, *129*, 3498.

(17) Ohler, E.; Reininger, K.; Schmidt, U.; *Angew. Chem. Int. Ed. Engl.* **1970**, *9*, 457.

(18) Dreiding, A. S. *Helv. Chim. Acta.* **1970**, *53*, 383.

(19) Okuda, Y.; Nakatsukasa, S.; Oshima, K.; Nozaki, H. *Chem. Lett.* **1985**, 481.

(20) Uneyama, K.; Ueda, K.; Torii, S. *Chem. Lett.* **1986**, 1201.

(21) Bryan, V. J.; Chan, T.-H. *Tetrahedron Lett.* **1996**, *37*, 5341.

(22) Sidduri, A. R.; Knochel, P. *J. Am. Chem. Soc.* **1992**, *114*, 7579.

(23) Kennedy, J. W.; Hall, D. G. *J. Am. Chem. Soc.* **2002**, *124*, 11586.

(24) Montgomery, T. P.; Hassan, A.; Park, B. Y.; Krische, M. J. *J. Am. Chem. Soc.* **2012**, *134*, 11100.

(25) Miyake, T.; Uda, K.; Kinoshita, M.; Fujii, M.; Akita, H. *Chem. Pharm. Bull.* **2008**, *56*, 398.

(26) Murphy, J. A. The Radical-Polar Crossover Reaction. In *Radicals in Organic Chemistry*; Renaud, P., Sibi, M. P., Eds.; Wiley-VCH: Weinheim, 2001; Vol. 1; pp 298-315

(27) de Azevedo, M. B. M.; Murta, M. M.; Greene, A. E. *J. Org. Chem.* **1992**, *57*, 4567.

(28) Jongkoi, R.; Choommongkol, R.; Tarnchompoo, B.; Nimmanpipug, P.; Meepowpan, P. *Tetrahedron Lett.* **2009**, *65*, 6382.

(29) Hajra, S.; Karmakar, A.; Giri, A.; Hazra, S. *Tetrahedron Lett.* **2008**, *49*, 3625.

(30) Ghosh, M.; Bose, S.; Maity, S.; Ghosh, S. *Tetrahedron Lett.* **2009**, *50*, 7102.

(31) Fernandes, R. A.; Chowdhury, A. K. *Tetrahedron: Asymmetry* **2011**, *22*, 1114.

(32) Braukmüller, S.; Brückner, R. *Eur. J. Org. Chem.* **2006**, 2110.

(33) Blanc, D.; Madec, J.; Popowyck, F.; Ayad, T.; Phansavath, P.; Ratovelomanana-Vidal, V.; Genêt, J.-P. *Adv. Synth. Catal.* **2007**, *349*, 943.

(34) Saha, S.; Roy, S. C. *Tetrahderon*, **2010**, *66*, 4278.

(35) Gillespie, R. J.; Peel, T. E. *J. Am. Chem. Soc.* **1973**, *95*, 5173.

(36) Perkowski, A. J.; Nicewicz, D. A. *J. Am. Chem. Soc.* **2013**, *135*, 10334.

(37) Grandjean, J. Nicewicz, D. A. *Angew. Chem., Int. Ed.* **2013**, *52*, 3967.

(38) Beckwith, A.; Christopher, J.; Lawrence, T.; Serelis, A. *Aust. J. Chem.* **1983**, *36*, 545.

(39) Clive, D. L. J.; Beaulieu, P. L. *J. Chem. Soc., Chem. Commun.* **1983**, 307.

(40) Mander, L. N.; Williams, C. M. *Tetrahedron*, **2003**, *59*, 1105.

(41) Noji, M.; Sunahara, H.; Tsuchiya, K.; Mukai, T.; Komasaka, A.; Ishii, K. *Synthesis*. **2008**, 3835.

(42) Plietker, B.; Niggermann, M. *Org. Lett.* **2003**, *5*, 3353.

(43) Otto, R. *Chemische Fabrik* **1936**, 529.

(44) Nguyen, T. M.; Nicewicz, D. A. *J. Am. Chem. Soc.* **2013**, *135*, 9588.

(45) Singer, L. A.; Kong, N. P. *Tetrahedron Lett.* **1966**, *19*, 2089.

(46) Shimada, S.; Hashimoto, Y.; Saigo, K. *J. Org. Chem.* **1993**, *58*, 5226.

(47) Gesmundo, N. J.; Grandjean, J-M. M.; Nicewicz, D. A. *Org. Lett.* **2015**, *17*, 1316.

(48) Cavanaugh, C. L.; Nicewicz, D. A. *Org. Lett.* **2015**, *17*, 6082

(49) Denmark, S. E.; Sweis, R. F. *J. Am. Chem. Soc.* **2001**, *123*, 6439-6440.

CHAPTER THREE

HYDRODECARBOXYLATION

3.1 Introduction

3.1.1 Importance of carboxylic acids and esters in synthesis

Alkyl carboxylic acids and esters are important functional handles and activating groups to enhance reactivity and selectivity in classical carbon-carbon bond forming reactions via enolate and Michael reactivity.[1,2] Carboxylic acids and esters are also commonly used to activate dienophiles for Diels-Alder cycloadditions, a highly important reaction in complex molecule synthesis (Figure 3.1).[3] Although carbonyls are valuable for their ability to facilitate carbon-carbon bond formation, the carboxylic acid functionality is not always desired in the final product. Removing alkyl carboxylic acid functionality can be a challenge, however accomplishing this via a hydrodecarboxylation strategy would allow for the use of carbonyls as traceless functional handles for the formation of carbon-carbon bonds and the generation of molecular complexity.

Figure 3.1: Some ways in which carboxylic esters favor bond formation

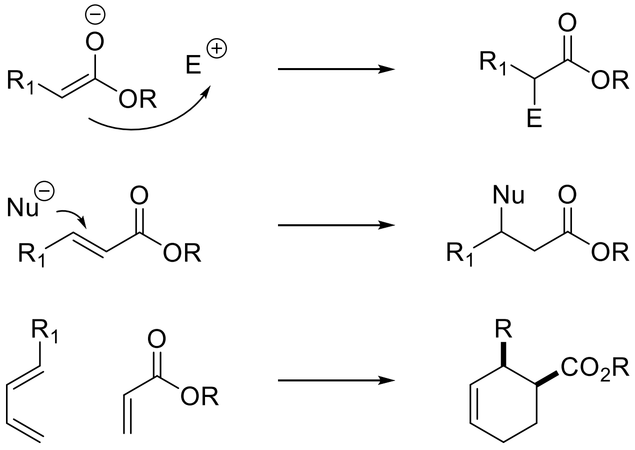

Malonic acids and esters are also useful handles for synthesis. There are numerous examples of reactions that rely on malonates to increase the rate of intramolecular reactions such as intramolecular Diels-Alder reactions or olefin metathesis.[4] Although malonates are useful for facilitating Thorpe-Ingold effects, and as functional handles for the coupling of two electrophiles via alkylation of malonic esters, they are not often desired in the final product. Malonates are generally removed in multiple steps, with an initial removal of one of the carboxylic acids via thermal decomposition in the presence of acid, followed by removal of the second carboxylic acid through formation of a Barton ester and radical decomposition (Section 3.1.2). A direct catalytic hydrodecarboxylation, possibly using organic photoredox catalysis, of malonic acid derivatives would allow for the sue of malonates as a traceless (–)CH_2(−) synthon with much more ease than current methodology allows (Figure 3.2).

Figure 3.2: Use and removal of malonic esters

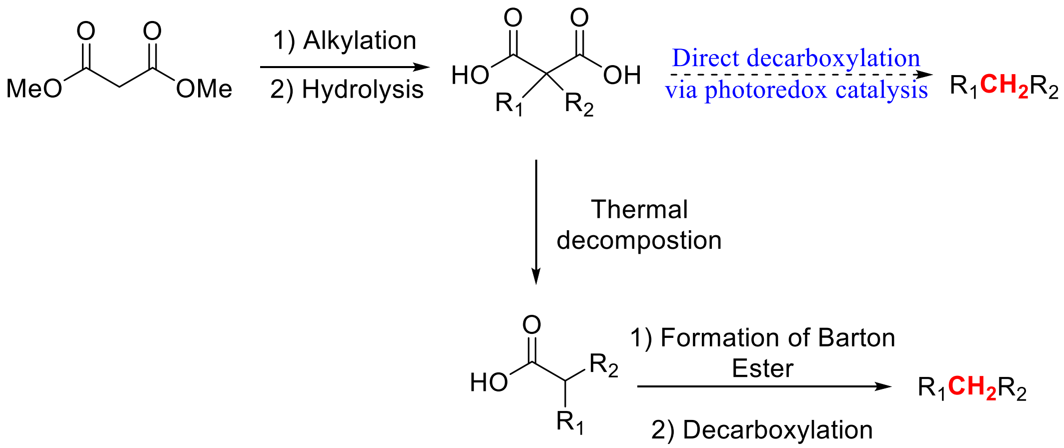
MeO
OMe
1) Alkylation
2) Hydrolysis
HO
OH
R1
R2
Direct decarboxylation
via photoredox catalysis
R1CH2R2
Thermal
decompostion
HO
R2
R1
1) Formation of Barton
Ester
2) Decarboxylation
R1CH2R2

3.1.2 Barton decarboxylation

One of the most reliable methods for the removal of carboxylic acids is the Barton decarboxylation (Figure 3.3). The Barton decarboxylation involves the formation of an activated thiohydroxamate ester, which has a weak Oxygen-Nitrogen bond prone to radical homolytic cleavage.[5] The Barton decarboxylation has seen a lot of use in natural products synthesis, however produces significant quantities of byproducts. Originally, tributyltin hydride was used stoichiometrically both as a hydrogen atom donor and to carry on the radical chain, however some advances have been made to use thiols,[6,7] silanes,[8] chloroform[9] and other hydrogen atom donors as a replacement for this toxic metal. In addition to a hydrodecarboxylation, the Barton thiohydroxamate ester can decompose in the presence of a radical acceptor to form new carbon-carbon bonds.[10] Many more recent catalytic methods for decarboxylation have expanded on this strategy to form carbon-carbon and carbon-heteroatom bonds (section 3.1.4 and 3.1.5).

Figure 3.3: The Barton decarboxylation

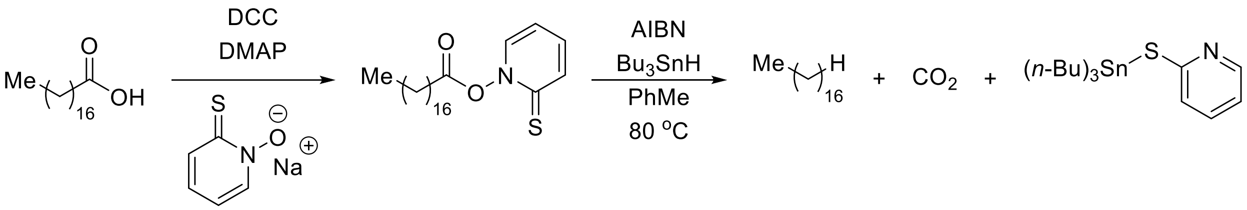

Despite its utility, the Barton decarboxylation has the significant disadvantage of waste generation. Multiple stoichiometric reagents are required, both in the activation of the carboxylic acid and in the radical decomposition process.

3.1.3 Kolbe electrolysis

The Barton decarboxylation has the disadvantage of requiring use of significant amounts of stoichiometric reagents, and highly prefunctionalized starting materials. Interestingly, carboxylic acids can be decarboxylated through electrochemical methods, directly from the carboxylic acid or carboxylate, although this strategy has not found widespread synthetic utility. The Kolbe electrolysis, or the Kolbe reaction, is an old transformation first discovered by Hermann Kolbe in 1849.[11] The Kolbe electrolysis involves the decarboxylation of a carboxylic acids in an electrochemical cell (Figure 3.4). This strategy allows for the decarboxylation of carboxylic acids without the use of prior functionalization or catalyst, however strong issues with selectivity are found due to rapid reactivity.[12]

Figure 3.4: The Kolbe electrolysis

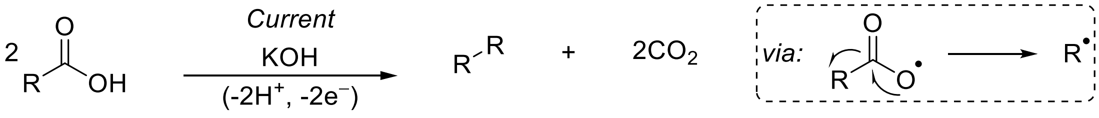

The electrochemical cell oxidizes the carboxylate to the corresponding acyloxyl radical. These acyloxyl radicals are intermediates known to rapidly rearrange and expel CO_2, forming carbon centered radicals.[13,14] In the Kolbe electrolysis, these carbon centered radicals then undergo homo- or hetero- dimerization processes. On the surface of the electrode, these radicals can be successively oxidized to the corresponding cation, a process which is known as the non-Kolbe pathway.[15] Although the Kolbe electrolysis provides proof of concept that carboxylates can be directly decarboxylated via oxidation, inherent challenges such as controlling dimerization, other pathways, and other radical processes, as well as the strongly basic conditions of the electrochemical cell, have limited the synthetic utility of the Kolbe pathway to very specific applications.

3.1.4 Ground state oxidation methods

The main drawback of using an electrochemical cell to generate acyloxyl radicals, is that they are all generated for the most part at once. To avoid the rather unselective dimerization of radicals and successive radical oxidation, some catalytic methods for oxidation and subsequent hydrodecarboxylation methods have been developed using ground state oxidants. For example, Anderson et al. has developed a method using the readily available peroxydisulfate ion ($S_2O_8^{2-}$, $E_{p/2}$ = 2.01 V) with catalytic silver to hydrodecarboxylate carboxylic acids.[16] The silver acts as a catalyst to accelerate the rate of the decomposition of the peroxydisulfate to sulfate, thus increasing the rate of oxidation. Using these conditions, Anderson studied the product distribution of acids such as acetic acid, isobutyric acid, and *n*-butyric acid. Anderson found that the alkane products arising from hydrodecarboxylation were favored when there was a large excess of carboxylic acid in aqueous solution. When the concentration of acid decreased, other products of oxidation such as alkenes, alcohols, ketones, aldehydes, and esters started to predominate. The use of trace amounts of Cu(II) as a co-catalyst produced predominantly alkene products under all conditions tried.

A year later, Minisci et al. developed this strategy further, developing a reaction that allowed for the selective coupling of alkyl radicals, formed via oxidation of carboxylic acids, with heteraromatic bases (Figure 3.5).[17] Using the Ag/$S_2O_8^{2-}$ system, Minisci coupled a variety of simple alkyl carboxylic acids (such as acetic, propionic, isobutyric, pivalic acids) with a variety of heteraromatic bases (quinolone, 2-methylquinoline, isoquinoline, pyridine, 4-cyanopyridine, and acridine) arriving at selectively alkylated bases in excellent yield and modest regioselectivity.

Figure 3.5: The Minisci Reaction

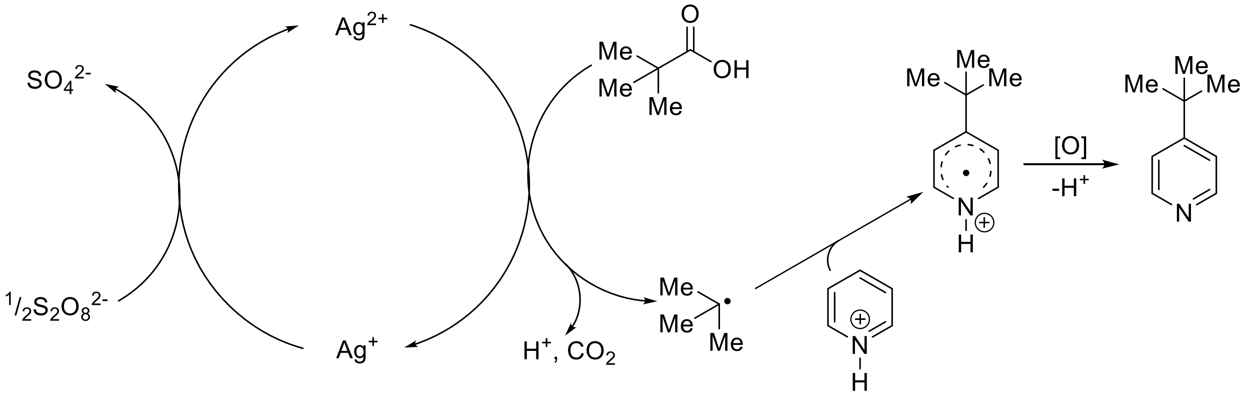

3.1.5 Photoredox catalysis

Hydrodecarboxylation strategies have been developed using stoichiometric quanitites of photosensitizer. For example, phenylacetic acid derivatives can be decarboxylated with stoichiometric quantities of benzophenone or quinone derivatives under UV irradiation.[18] Benzophenone, when excited by light, abstracts the hydrogen atom from the carboxylic acid. The addition of thiophenol required an increase in irradiation time, but provided a better selectivity for the desired hydrocarbon product (Figure 3.6).

Figure 3.6: Hydrodecarboxylation via photosensitizer

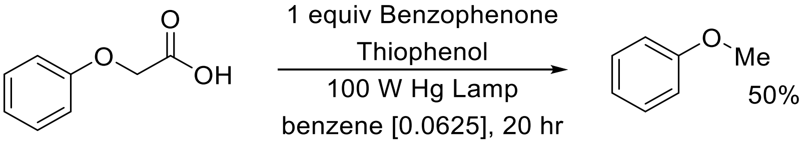
O
OH
O
1 equiv Benzophenone
Thiophenol
100 W Hg Lamp
benzene [0.0625], 20 hr
O
Me
50%

In 2007, Yoshimi et al. demonstrated that *N*-Boc amino acids could be hydrodecarboxylated via oxidation with the photogenerated phenanthrene cation radical (Figure 3.7.[19] Their system involved the use of stoichiometric quantities of phenanthrene (Phen) and 1.4-dicyanobenezene (DCB), as well as two equivalents of *t*-dodecanethiol under irradiation from a 400 Watt mercury lamp with special glassware to ensure UV penetration.

Figure 3.7: Hydrodecarboxylation from Yoshimi et al.

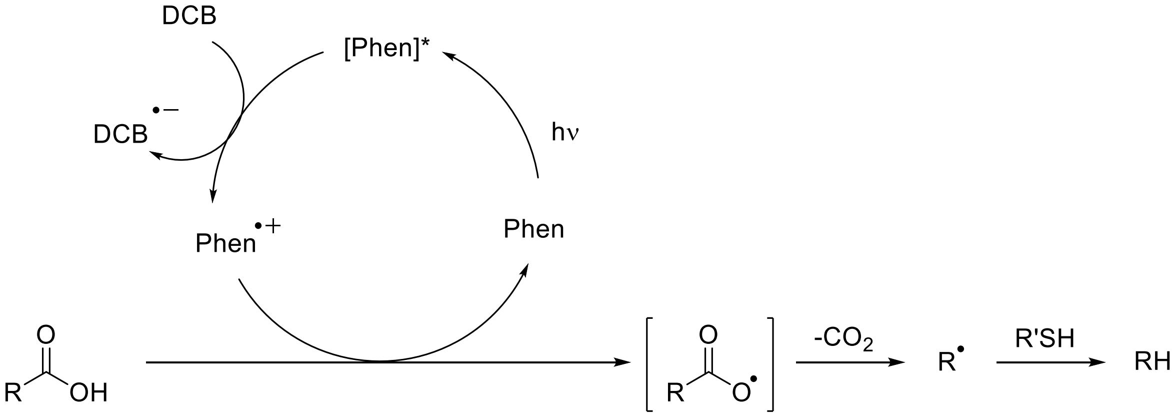
DCB
[Phen]*
DCB•−
hν
Phen•+
Phen
O
R
OH
O
R
O•
-CO2
R•
R'SH
RH

Although catalytic hydrodecarboxylations using organic photoredox catalysts had remained out of reach at the start of our own investigations, inorganic photoredox catalysts and methods for the purposes of decarboxylative coupling have been explored. Macmillan has developed a substantial repertoire of photoredox decarboxylative coupling reactions utilizing an Ir(ppy)$_3$ or similar photo-catalyst (Figure 3.8). The system works well for aliphatic α-heteroatom carboxylic acids, as well as some secondary carboxylic acids, and has been applied to decarboxylative couplings to arenes,[20] alkenes,[21] and decarboxylative fluorinations.[22] Due to the requirements on catalyst turnover, this strategy has not been applied to a hydrodecarboxylation (Figure 3.9). The coupling partner in this transformation is formed by performing the key step of oxidizing the catalyst to a species strong enough to oxidize the carboxylate.

Figure 3.8: Photoredox decarboxylative coupling

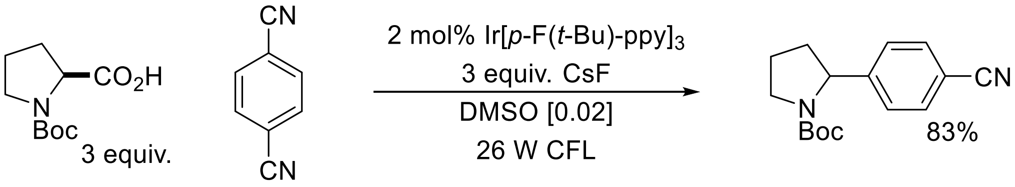
CO2H
N
Boc
3 equiv.
CN
CN
2 mol% Ir[p-F(t-Bu)-ppy]3
3 equiv. CsF
DMSO [0.02]
26 W CFL
N
Boc
CN
83%

Figure 3.9: Proposed mechanism for this strategy

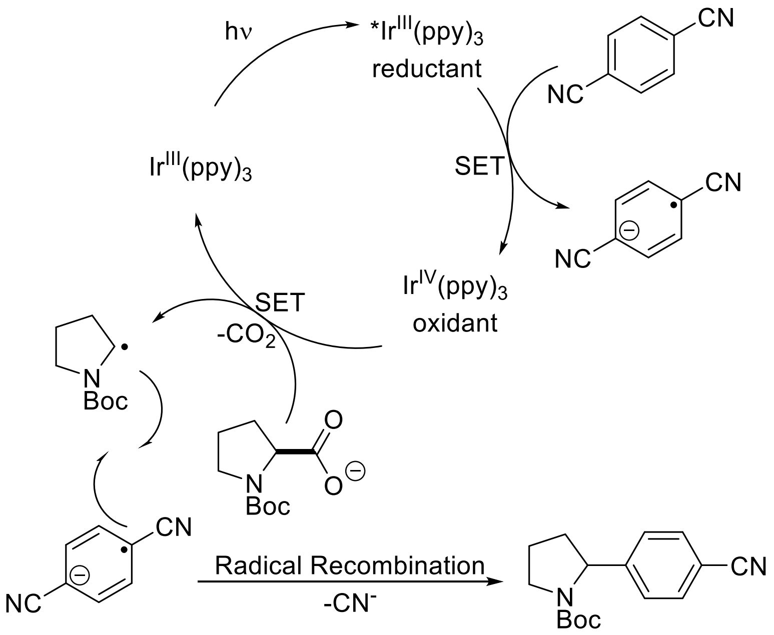
hν
*Ir^III(ppy)3
reductant
Ir^III(ppy)3
SET
CN
NC
CN
NC
Ir^IV(ppy)3
oxidant
SET
-CO2
N
Boc
O
O
N
Boc
CN
NC
Radical Recombination
-CN-
N
Boc
CN

Later in 2014, MacMillan and Doyle collaborated to develop a decarboxylative aryl coupling reaction that merged photoredox catalysis with nickel cross coupling catalysis.[23] However, despite advances in photoredox catalytic decarboxylative Carbon-Carbon and Carbon-Heteroatom bond forming reactivity, a catalytic version of hydrodecarboxylation had not been developed at the time of our initial investigations.

3.1.6 The proposed method

In our initial approach, we sought to use the mesityl acridinium photoredox catalyst with a redox active hydrogen atom donor co-catalyst to conduct hydrodecarboxylation of aliphatic carboxylic acids. It was our intention to develop a method that could effectively hydrodecarboxylate carboxylic acids of a variety of substitution patterns, including activated α-heteroatom and α-aryl carboxylic acids, as well as primary, secondary, and tertiary aliphatic carboxylic acids.

Figure 3.10: Proposed method for hydrodecarboxylation

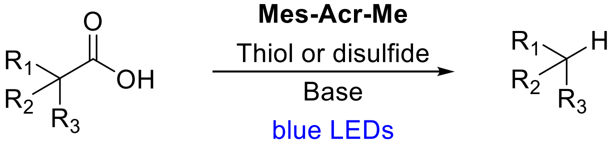

3.2 Backgound

3.2.1 Reduction potentials of carboxylates

Deprotonation of carboxylic acids dramatically decreases their reduction potential. Roth et al. have placed the range for carboxylate reduction potentials from +1.2 to +1.6 V vs. SCE, well within the range of what the mesityl acridinium can oxidize (Figure 1.5). There does not seem to be much impact of substitution pattern on the reduction potential of alkyl carboxylates. For example, Jeremy Griffin measured the reduction potentials of a representative primary, secondary, and tertiary carboxylate and found that each were similar, and within error (Figure 3.11). This information can be found in the published report.[24]

Figure 3.11: Reduction potentials of carboxylates with different substitution patterns

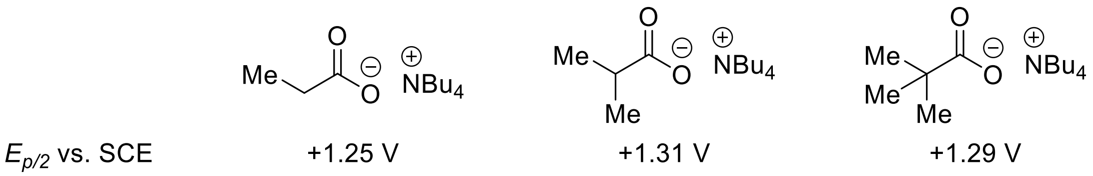

With this information in hand, we believed that our proposed method was sound. The mesityl acridinium should, at least according to thermodynamic arguments, be able to effectively oxidize a variety of aliphatic carboxylates regardless of substitution pattern.

3.2.2 The Acyloxyl radical

As has been alluded to in section 3.1.3, the rate of rearrangement of the acyloxyl radical to expel carbon dioxide and form the carbon centered radical is generally recognized as fast. Rates of loss of CO_2 have been estimated at ~10^9 s^{-1} for CH_3CO_2•.[25] The weaker the carbon-carbon bond, generally the faster the rate. For example the 9-methyl-9-carboxyfluorene acyloxyl radical expels carbon dioxide at a measured rate of 1.8 x 10^{10} s^{-1}.[26] The sp^2 hybridized $PhCO_2$• has a much stronger carbon-carbon bond, and the measured rate of decarboxylation is much slower at 2 x 10^6 s^{-1}.[27] Pincock et al. estimated the rates of decarboxylation of a variety of acyloxyl radicals through the photolysis of 1-Naphthylmethyl esters in methanol, and considering the product distributions.[28] He reported the k_{CO2} for a variety of substrates (Figure

3.12). The rate of expulsion of CO_2 increases with steric bulk, however in each case with aliphatic acyloxyl radicals, the expulsion of CO_2 is quite rapid.

Figure 3.12: Rate constants of representative aliphatic acyloxyl radical decomposition

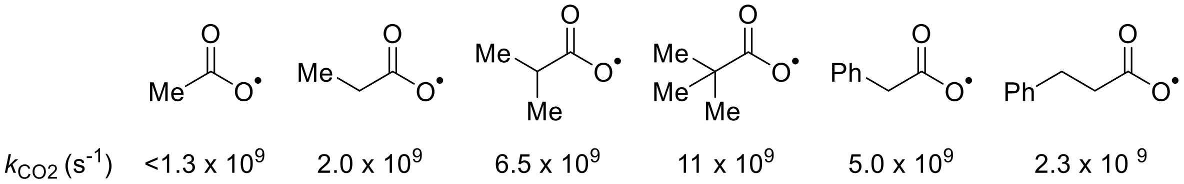

The rate of expulsion of CO_2 gave us hope as we started our investigations that if oxidation would occur, so would the expulsion of CO_2 to form carbon centered radicals. These carbon centered radicals would easily undergo hydrogen atom transfer with thiophenol, a process that was well precedented through all of the prior hydrofunctionalization reactions developed in the Nicewicz lab.

3.2.3 Hydrodecarboxylation using Mes-Acr-Me in Dichloroethane

During the course of the development of our method, a report came out from the Wallentin group which conducted a hydrodecarboxylation using a **Mes-Acr-Me** and disulfide system[29]. With the use of a chlorinated solvent, and *p*-Chlorophenyl disulfide as hydrogen atom donor, they were able to successfully perform hydrodecarboxylation transformations. However, they were limited to the decarboxylation of acids with α-heteroatom (protected N or O) or α-phenyl substituents, a brief summary of their substrate scope shown in Figure 3.13. Carboxylic acids without this substitution pattern were unreactive under these conditions (Figure 3.14).

Figure 3.13: Decarboxylation of α-heteroatom carboxylates

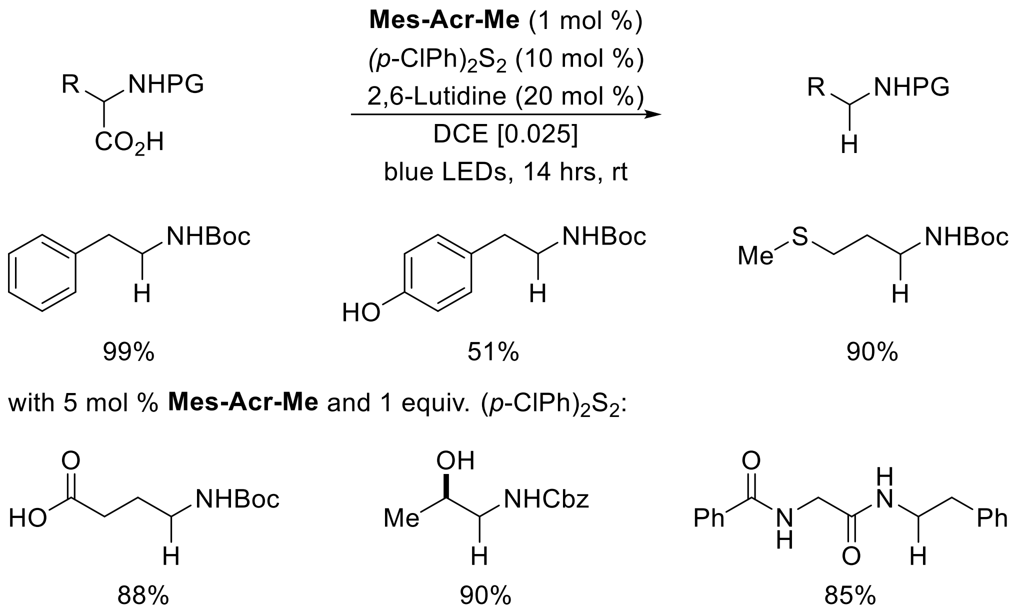
Mes-Acr-Me (1 mol %)
(p-ClPh)2S2 (10 mol %)
2,6-Lutidine (20 mol %)
DCE [0.025]
blue LEDs, 14 hrs, rt
99%
51%
90%
with 5 mol % **Mes-Acr-Me** and 1 equiv. (p-ClPh)2S2:
88%
90%
85%

Figure 3.14: Unfunctionalized carboxylic acids are unreactive

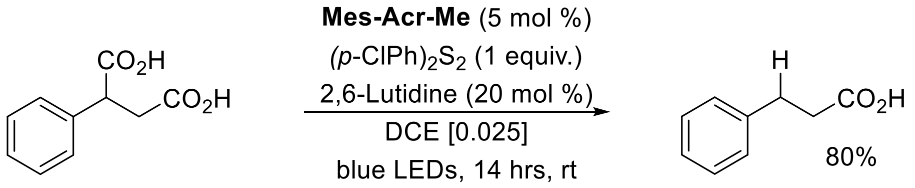
Mes-Acr-Me (5 mol %)
(p-ClPh)2S2 (1 equiv.)
2,6-Lutidine (20 mol %)
DCE [0.025]
blue LEDs, 14 hrs, rt
80%

Because of the arguments described in sections 3.2.1 and 3.2.2, we were puzzled that this methodology had the limitations that it did. Merely considering the low reduction potential of the carboxylates relative to the much higher excited state reduction potential of **Mes-Acr-Me**, as well as the fast rates of decomposition once oxidation occurs, indicated to us that a broader scope for this transformation was theoretically possible. When this report came out, we refocused our attention on the decomposition of aliphatic carboxylates without α-heteroatom or α-phenyl substitution.

3.3 Results and Discussion

3.3.1 Development with phenyl acetic acid derivatives

In the course of developing the hydrodecarboxylation reaction, and significantly prior to the Wallentin report, Jeremy Griffin quickly discovered that carboxylic acids exhibiting specific functionality could be readily decarboxylated on some of the earliest conditions tried. In this case, the diphenyl substituted carboxylic acid could be hydrodecarboxylated. Although this reaction was discovered prior to the Wallentin report (section 3.2.3), similarities can be found in the conditions. For example, substoichiometric quantities of 2,6-Lutidine and a thiol based hydrogen atom donor could be used in chlorinated solvent, and the product could be obtained in quantitative yield by NMR (Figure 3.15). However, applying these conditions, specifically with this choice of solvent and base, to substrates without this phenyl substitution pattern proved unsuccessful. It would take substantial optimization to develop conditions with a broader substrate applicability than that reported from Wallentin.

Figure 3.15: Initial results with phenylacetic acid derivatives

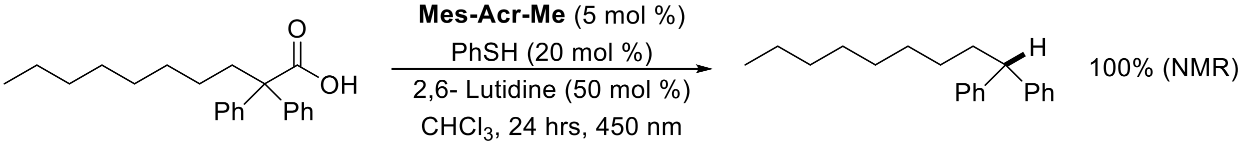

3.3.2 Issues in applying towards less functionalized carboxylic acids

Despite the easy reactivity of benzylic or doubly benzylic phenylacetic acid derivatives, this success did not translate for unactivated tertiary carboxylic acids. For example, 2,2-dimethyl-3-phenylpropanoic acid did not show desired reactivity with chloroform as solvent and 2,6-lutidine as base (Table 3.1, entry 1). We hypothesized that this lack of reactivity could be due to the polarity of the solvent, as a carboxylate ion has a significantly decreased oxidation potential relative to the protonated carboxylic acid, and the availability of the free carboxylate increases with solvent polarity. Acetonitrile and methanol showed no improvements in yield (entries 2 and 3), however we were pleased to see a 21% yield of the desired hydrodecarboxylated product, isobutylbenzene, in a 9:1 Methanol:Water system (entry 4). This success indicates that increasing the equilibrium concentration of the carboxylate relative to the carboxylic acid is important. The pK_a of carboxylic acids can be up to five units greater in methanol than in water, while the pK_a of protonated amines are similar in both solvents. For example, the pK_a of acetic acid in water is 4.76 vs 9.63 in methanol while the pK_a of the triethlammonium ion is 10.75 in water and 10.78 in methanol.[30] At this point, we turned our attention to the nature of the base, hypothesizing that increasing either the pK_a of the conjugate acid or the steric bulk (which would increase the charge separation in the corresponding charged pair) could improve the yield. Change of base to the somewhat more basic and bulkier 2,4,6-collidine saw a modest improvement in yield to 51% (entry 5), while the significantly more basic *N*,*N*-diisopropylethylamine saw an increase in yield to 81% (entry 6). Although oxidizable amine bases are known to form aminium radical cations in similar photoredox systems,[30,31] their success in our system can be rationalized by noting that they likely predominately exist in solution as the ammonium salts which are insulated from oxidation. When broadening the scope of this method to include primary carboxylic acids however, the yield of ethylbenzene was greatly diminished to 14% (entry 9). A fortuitous solvent screen found that another polar alcohol, trifluoroethanol, gave dramatically improved yields for the primary substrate (entry 10) at 97%. In this system, the tertiary carboxylic acid only saw a modest reduction in yield compared to the methanol/water system (entry 8). Control experiments showed that base was necessary for the reaction (entry 7) as was phenyl disulfide (entry 11). It is also important to note that the change from **Mes-Acr-Me** (section 3.2.1) to the very similar **Mes-Acr-Ph** (9-mesityl-10-phenylacridinium) was undertaken as we considered more polar solvents and more strongly basic conditions. The **Mes-Acr-Ph** catalyst behaves very similarly, but is somewhat more robust under nucleophilic conditions.[32]

Table 3.1: Optimization of conditions for monoacid substrates

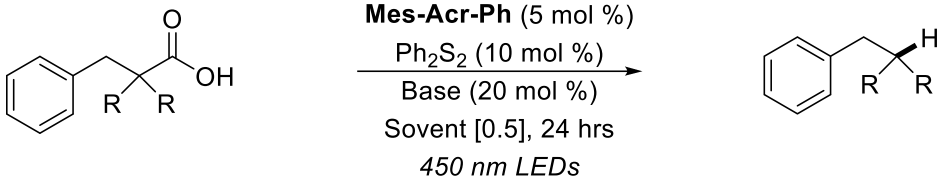

Entry	R	Solvent	Base	Yield (%)
1	Me	$CHCl_3$	2,6-Lutdine	<10
2	Me	MeCN	2,6-Lutidine	<10
3	Me	MeOH	2,6-Lutidine	<10
4	Me	MeOH/H_2O (9:1)	2,6-Lutidine	21
5	Me	MeOH/H_2O (9:1)	2,4,6-Collidine	51
6	Me	MeOH/H_2O (9:1)	*i*-Pr_2NEt	81
7	Me	MeOH/H_2O (9:1)	None	No Rxn
8	Me	TFE	*i*-Pr_2NEt	77
9	H	MeOH/H_2O (9:1) (72 hrs)	*i*-Pr_2NEt	14
10	H	TFE (72 hrs)	*i*-Pr_2NEt	97
11	H	TFE (no Ph_2S_2, 72 hrs)	*i*-Pr_2NEt	<10

With optimized conditions in hand, we then turned our attention to substrate scope (Figure 3.16). We were pleased to see that the primary hydrocinnamic acid derivatives ranging from moderately electron rich to moderately electron deficient worked quite well under this system, as we were able to form ethylbenzene, 4-chloroethylbenzene, and 4-methylethylbenzene in good yields over 24 hours. Longer reaction times could give somewhat improved yields. Di-

and tri- alkyl substituted carboxylic acids were also hydrodecarboxylated, producing propyl benzene and isobutylbenzene in good yields. Unsurprisingly, substituents bearing phenyl substitution or α-heteroatom substitution worked quite well, as seen by the good yields of diphenylmethane and 1,2-diphenylethane, as well as the strong reactivity of the Cbz protected proline. Benzyl substitution was not necessary for quality reactivity, as evidenced by the cyclohexyl and piperidinyl substrate, however decreased yields were observed. Additionally, in some cases where solubility seemed to be an issue, a solvent system modification of including a more dilute 20% ethyl acetate was used. The monoester malonate 2-benzyl-3-ethoxy-3-oxopropanoic acid also gave appreciable yields of hydrodecarboxylated product. Tridecanoic acid was a challenging substrate, however improved yields were found when employing a more appropriate solvent system and increased disulfide loadings. One explanation is that the addition of ethyl acetate may help to break up some intermolecular interactions between the greasy tridecanoic acid and the polar trifluoroethanol, helping to improve availability of the tridecanoic acid for oxidation. The complex steroid natural product enoxolone was effectively decarboxylated as well. The addition of ethyl acetate under more dilute than standard conditions allowed for improved reactivity, as the steroid is not appreciably soluble in trifluoroethanol alone.

Figure 3.16: Scope of monoacid hydrodecarboxylation

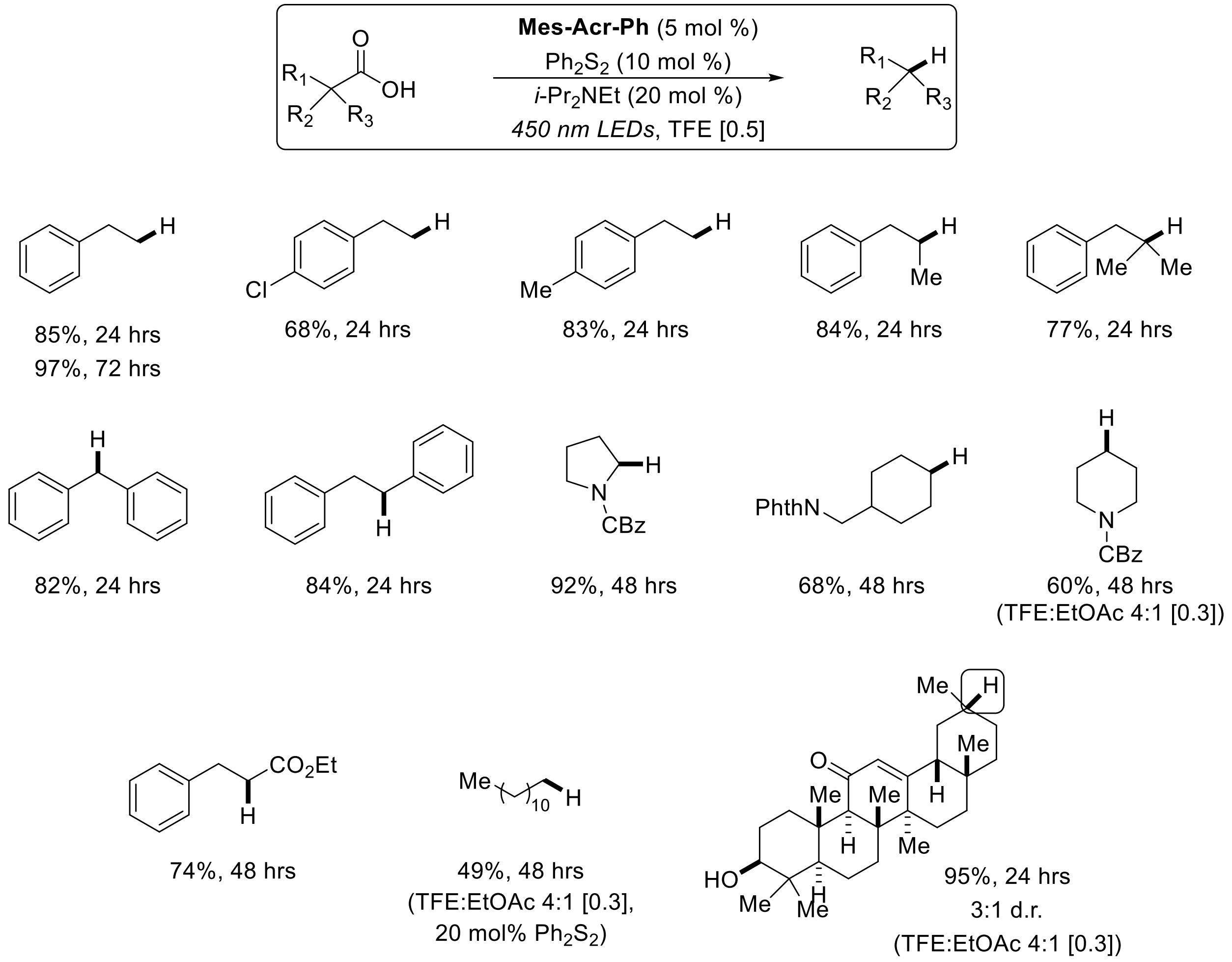
Mes-Acr-Ph (5 mol %)
Ph2S2 (10 mol %)
i-Pr2NEt (20 mol %)
450 nm LEDs, TFE [0.5]
85%, 24 hrs
97%, 72 hrs
68%, 24 hrs
83%, 24 hrs
84%, 24 hrs
77%, 24 hrs
82%, 24 hrs
84%, 24 hrs
92%, 48 hrs
68%, 48 hrs
60%, 48 hrs
(TFE:EtOAc 4:1 [0.3])
74%, 48 hrs
49%, 48 hrs
(TFE:EtOAc 4:1 [0.3],
20 mol% Ph2S2)
95%, 24 hrs
3:1 d.r.
(TFE:EtOAc 4:1 [0.3])

3.3.3 Unsuccessful substrates

Although the scope of competent substrates was large and broad, encompassing a variety of functional groups and substitution patterns, the scope of substrates that were either less reactive or unreactive was also fairly broad (Figure 3.17). For this reason, it can be difficult to make generalizations about which sort of substrates work and do not work in this system. The electron rich *p*-methoxyhydrocinnamic acid was not a compatible substrate for this transformation, even though oxidation would still occur on the carboxylate. Roth et al. had measured the reduction potential of anisole at 1.81 V vs. SCE[33], much higher than the reduction potential of the carboxylate, indicating competitive oxidation of the electron rich arene was probably not the reason for the lack of reactivity. Additionally, the electron deficient *p*-nitrohydrocinnamic acid was not reactive under these conditions. Some reactivity was observed with the primary carboxylic acid with the pendant protected amine, however this was a surprisingly lower yield then with the tridecanoic acid cousin. Substituting a pyridine for the phenyl group in hydrocinnamic acid gave minimal product, and no product was observed with a furyl substituent. Additionally, loss of acid starting material was not observed with acetic acid. Unfortunately, trifluoroacetic acid was also not a viable substrate for this reaction. It is unfortunate because formation of trifluoromethyl radical from cheap and readily available starting materials, of which trifluoroacetic acid is arguably the cheapest and most readily available, would be a very useful advance in organic chemistry. Our lab had previously reported an antimarkovnikov hydrotrifluoromethylation reaction whereby photochemical single electron oxidation of Langlois' reagent (CF_3SO_2Na) formed the desired triflouromethyl radical, which then underwent radical addition to various alkenes.[34] This reaction also employed the mesityl acridinium and phenyl disulfide catalyst system, which indicates that if trifuoroacetic acid could be appreciably decarboxylated, there would be potential for the utilization of it as a source of trifluoromethyl radical in similar hydrotrifluoromethylation transformations.

Figure 3.17: Less successful and unsuccessful substrates for monodecarboxylation

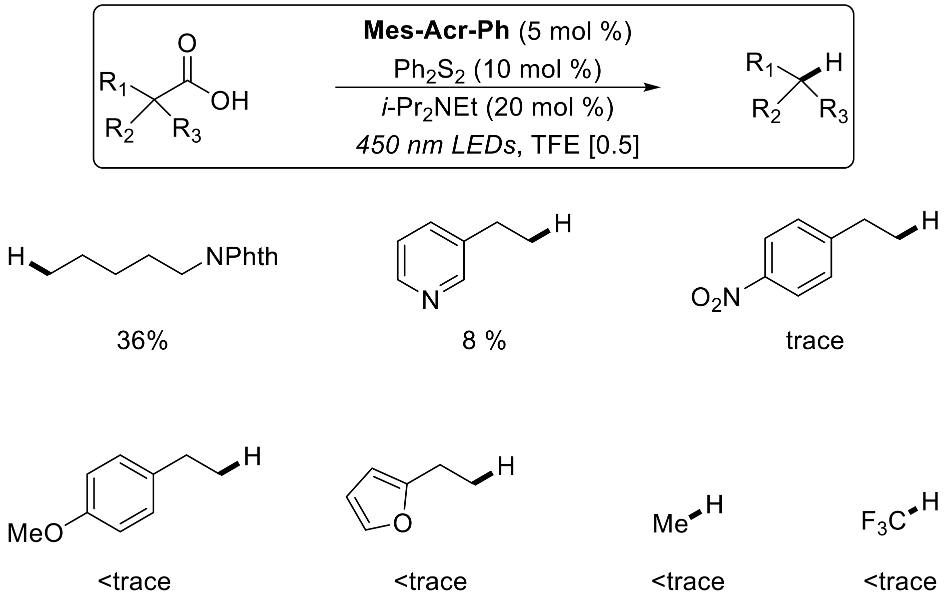

We were surprised by the lack of predictability we found in our successful and unsuccessful substrates when trifluoroethanol was solvent. This surprise, coupled with the highly specific functional group requirements in chlorinated solvents reported by Wallentin and demonstrated in our intial considerations, made us curious about the role of trifluoroethanol in this transformation.

3.3.4 Insights into the role of trifluoroethanol

In order to better elucidate the role of trifluoroethanol, and explain the dramatic gains in yield especially for primary alkyl carboxylic acids, several mechanistic studies were undertaken by Jeremy Griffin. Although the trends in yield associated with the strength of base indicate that a more polar solvent would help increase oxidation by increasing the nakedness of the anion, the polarity of trifluoroethanol alone does not explain the drastic increase in yield. In fact, trifluoroethanol is less polar than the 9:1 Methanol:Water system, which was nearly as effective for 2,2-dimethyl-3-propanoic acid. The dielectric constant measured for a 9:1 Methanol:Water system is 36.8[35], while TFE is 27.1.[36] Trifluoroethanol has been shown to act as a hydrogen atom donor[34], however as only trace product was observed when no other hydrogen atom donor was present (Table 3.1, entry 11), it did not appear that this was a major role of trifluoroethanol in this particular reaction. In considering the role of trifluoroethanol, we considered the proposed mechanism more carefully (Figure 3.18).

Figure 3.18: Proposed mechanism of hydrodecarboxylation

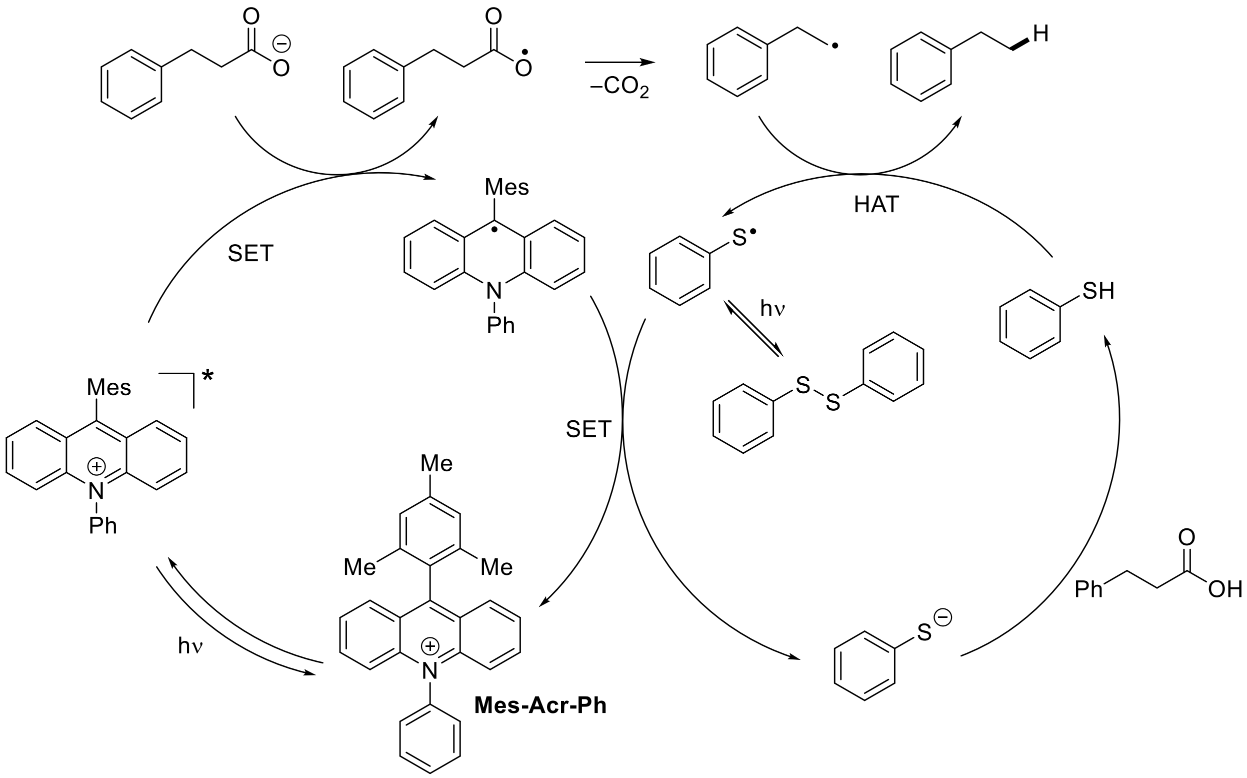

Jeremy Griffin conducted an experiment to determine the kinetic isotope effect, in order to elucidate whether hydrogen atom transfer (HAT) was the rate limiting step of this transformation. Reacting the tertiary carboxylic acid under standard conditions, and comparing the initial rates to the deuterated acid analog in ***d_1*-**TFE, Jeremy observed essentially no difference in rate. He calculated a KIE of 1.01. This indicates that hydrogen atom transfer, the product producing step, was not rate limiting. The Nicewicz lab had previously discovered that thiyl radical oxidation of the acridine radical to turn over the catalyst was essentially diffusion controlled.[37] Additionally, as previously mentioned, the rate of acyloxyl radical rearrangement to produce carbon dioxide is also very rapid (Section 3.2.2). From this information, including the lack of a kinetic isotope effect, we began to consider that carboxylate oxidation was rate limiting. In the course of optimizing this reaction, we had observed that in the 9:1 methanol water system, tertiary carboxylic acids reacted much better than primary (Table 3.1 entries 6 and 9). We had also observed that in switching to trifluoroethanol, better yields were observed for primary carboxylic acids over tertiary. In order to further study this facet, Jeremy Griffin conducted a competition experiment, whereby 0.33 equivalents of each acid (primary, secondary, and tertiary) in the same vial were reacted in both solvent systems, and the product distribution was analyzed (Figure 3.19). It was found that the product distribution in these two solvents were reversed. The 9:1 Methanol:Water system showed faster reactivity with the tertiary carboxylic acid and slower reactivity with the primary. The reaction time across the board was much slower than in trifuoroethanol, where the same conversion could be undertaken in 8 hours verses 24. In trifluoroethanol, the primary carboxylic acid reacted faster than the tertiary. The 24 hours to reach 30% conversion in the 9:1 methanol:water system came as a surprise, as the tertiary carboxylic acid, when reacted separately, could reach much greater conversions in that same amount of time (Table 3.1, entry 6). For this reason, we considered that catalyst decomposition could be one reason for poor reactivity of primary carboxylic acids in the 9:1 methanol:water system, as a primary carbon centered radical could add into the acridinium core and degrade the catalyst. In addition, a solution of only the catalyst in a 9:1 methanol:water solvent system turns dark brown after being irradiated by blue LEDs overnight, indicating that solvent decomposition in this nucleophilic solvent system could be an issue. Trifluoroethanol could be perhaps considered a goldilocks solvent in this context, as it is polar yet less nucleophilic.

Figure 3.19: Competition experiment in two solvent systems.

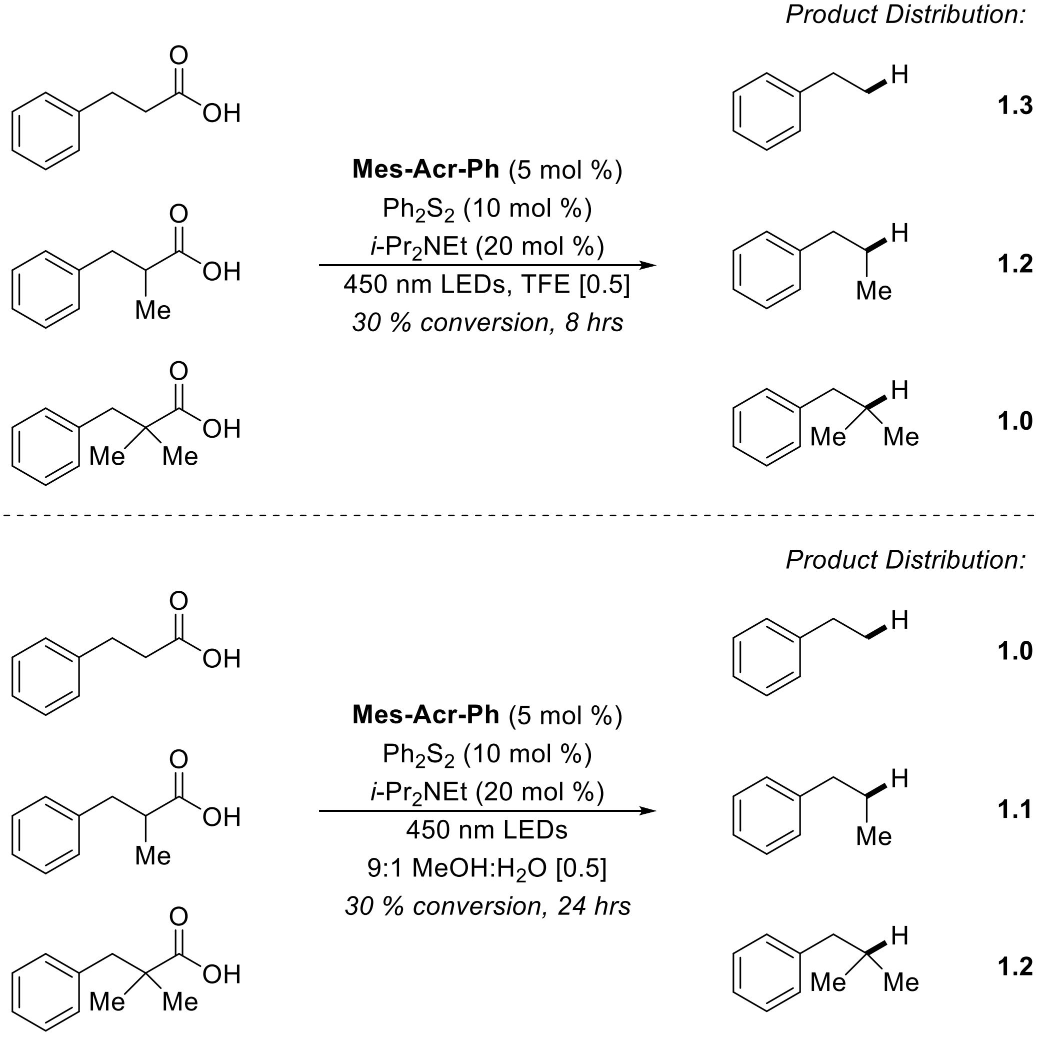
Product Distribution:
OH
Me
Mes-Acr-Ph (5 mol %)
Ph_2S_2 (10 mol %)
i-Pr_2NEt (20 mol %)
450 nm LEDs, TFE [0.5]
30 % conversion, 8 hrs
H
1.3
1.2
1.0
Product Distribution:
Mes-Acr-Ph (5 mol %)
Ph_2S_2 (10 mol %)
i-Pr_2NEt (20 mol %)
450 nm LEDs
9:1 MeOH:H_2O [0.5]
30 % conversion, 24 hrs
1.0
1.1
1.2

Jeremy Griffin, with the help of Nathan Romero, was able to measure the fluorescence lifetime of **Mes-Acr-Ph** in both methanol and trifluoroethanol via Time-Correlated Single Photon Counting, using a method described by Romero in his mechanistic studies of a similar system.[37] It was found that the catalyst displayed two fluorescence decay components in Methanol, having lifetimes of 0.49 and 5.5 ns. However, in trifluoroethanol the fluorescence lifetime was found to be 10.9 ns. The longer lifetime could contribute to the picture of why trifluoroethanol was the more competent solvent. We then considered the possibility that the differences in reactivity between the primary, secondary, and tertiary carboxylic acids could be explained by sterics, at least when trifluoroethanol was solvent. Jeremy Griffin measured the bimolecular quenching constants (k_q) for the potassium salts of three different carboxylic acids by Stern-Volmer analysis of fluorescence quenching of the excited catalyst in trlfluoroethanol (Figure 3.20)

Figure 3.20: Rate constants of oxidation

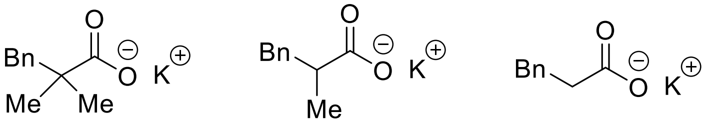

k_q ($M^{-1}s^{-1}$)	2.34×10^8	2.52×10^8	3.91×10^8

These results indicate that, although the primary carboxylate quenches the acridinium excited state the fastest, it is by a narrow margin. Each of these is a smaller quenching constant than the alkenes used in chapter two. For example, Romero measured the k_q for β-methylstyrene quenching **Mes-Acr-Me*** in DCE at 6.92×10^9 $M^{-1}s^{-1}$, which is more than an order of magnitude faster than the hydrocinnamate anion.[37] Taking into account that in these Stern-Volmer experiments the quenching efficiency was low (only 2% of **Mes-Acr-Ph*** was quenched for 5 mM hydrocinnamate) and the competitively fast decay of the **Mes-Acr-Ph*** back to the ground state **Mes-Acr-Ph** by fluorescence ($k_F = 9.3 \times 10^7$ s^{-1} in TFE), as well as the observation that reaction rates are increased by having more lamps, we began to think that oxidation was the slow step in this reaction. The slow rate of oxidation was determined less by the rate constants, which are fairly fast, but by the available concentration of excited state acridinium and the low quenching efficiency.

Jeremy Griffin was able to demonstrate a ground state preassociation complex of hydrocinnamate with **Mes-Acr-Ph** by both ^{1}H and ^{19}F NMR in CD_3OD. In the ^{1}H NMR, increasing amounts of tetrabutylammonium hydrocinnamate caused an upfield shift in the acridinum signals, as well as significant peak broadening. This potentially indicated an exchange of the BF_4^- counterion with the carboxylate. This was also observed in the ^{19}F NMR, whereby the BF_4^- counterion shifts upfield with increasing amounts of carboxylate, indicating that it is more electron rich and less associated with the acridinium. A preassociation complex could help certain less sterically hindered, or more associated, carboxylates oxidize, as it increases the local concentration of **Mes-Acr-Ph*** available to the carboxylate to quench.

Although these studies do not provide conclusive evidence to a specific reason why trifluoroethanol works for such a broader range of substrates as compared to dichloroethane, or the 9:1 methanol:water system, these results paint a picture of a number of factors that affect the efficiency of this reaction. Trifluoroethanol improves catalyst stability relative to the methanol:water system. It is polar enough to give efficient deprotonation of the carboxylic acid. It increases the catalyst lifetime relative to methanol. Trifluoroethanol could also aid in the development of preassociation complexes that improves the oxidation step. The complexity of what determines this preassociation complex could explain the lack of predictability of successful and unsuccessful substrates under these conditions (Sections 3.3.2 and 3.3.3)

3.3.5 Application towards malonic acid derivatives

When applying this methodology to the double decarboxylation of malonic acid derivatives, it quickly became apparent that some minor modifications would need to be undertaken to the system. For example, the mono-ester malonate undergoes hydrodecarboxylation quite well under standard conditions, however the free malonic acid gives drastically reduced yields of the single decarboxylation product (Figure 3.21). No double decarboxylation is observed under standard conditions.

Figure 3.21: Comparison of malonates and mono-ester malonates

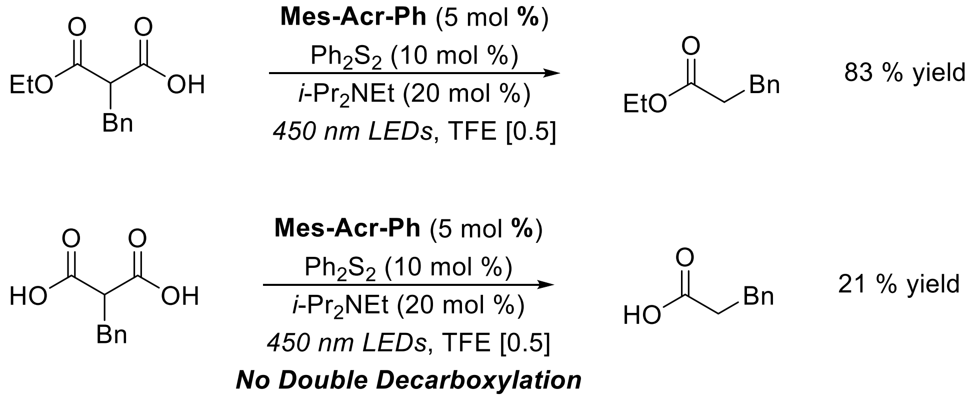
EtO
OH
Bn
Mes-Acr-Ph (5 mol %)
Ph2S2 (10 mol %)
i-Pr2NEt (20 mol %)
450 nm LEDs, TFE [0.5]
EtO
Bn
83 % yield
HO
OH
Bn
Mes-Acr-Ph (5 mol %)
Ph2S2 (10 mol %)
i-Pr2NEt (20 mol %)
450 nm LEDs, TFE [0.5]
No Double Decarboxylation
HO
Bn
21 % yield

With this in mind, we considered increasing the equivalents of base used. We posited that intramolecular hydrogen bonding could impede on the oxidation, and that oxidation would more favorably occur when the malonate was fully deprotonated. Using one full equivalent of DIPEA, we were pleased to see that phenyl malonic acid could be doubly hydrodecarboxylated to toluene in a 45 % yield (Table 3.2, entry 1). However, under these conditions, double hydrodecarboxylation of benzyl malonic acid was not observed (entry 2). Using 1.2 equivalents of DIPEA resulted in 61 % yield of toluene (entry 3), however only the mono hydrodecarboxylation product was observed for benzyl malonic acid (entry 4). Knowing that the second pK_a of malonic acids is much higher, we considered using a stronger base. The first pK_a

of diethylmalonic acid is 2.21, while the second is 7.29 in water.[38] Using KOH, a stronger base, resulted in an 8 % yield of ethyl benzene, the double hydrodecarboxylation product (entry 5). The more substituted 2-benzyl-2-methylmalonic acid gave a 40 % yield of the propyl benzene, the double hydrodecarboxylation product (entry 6). This could be improved to a 55 % yield by using increased catalyst and disulfide loading, indicating the harshness of these conditions (entry 7). In fact, reactions would often turn very dark over the course of the reaction, indicating catalyst degradation. It was found that using one equivalent of KO*t*Bu instead of KOH could improve this aspect, although yields were not greatly improved. However, due to ease of use in terms of weighing a powder vs small quantities of a pellet (KOH had been used in a bulk solution in trifluoroethanol, stored in a Nalgene container and refreshed often), potassium *tert*-butoxide became the standard base.

Table 3.2: Optimization of malonic acid double decarboxylation

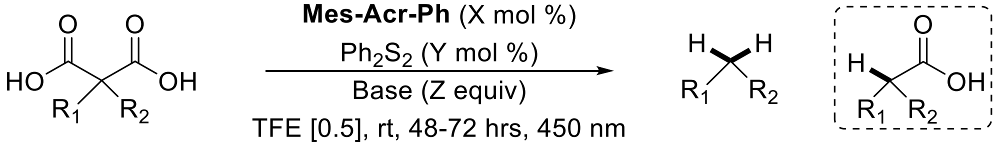

Entry	R_1	R_2	X	Y	Base	Z	Yield Di	Yield Mono
1	Ph	H	5	10	DIPEA	1.0	45	–
2	Bn	H	5	10	DIPEA	1.0	0	–
3	Ph	H	5	10	DIPEA	1.2	61	39
4	Bn	H	5	10	DIPEA	1.2	0	20
5	Bn	H	5	10	KOH	1.15	8	25
6	Bn	Me	5	10	KOH	1.15	40	60
7	Bn	Me	7.5	15	KOH	1.15	55	32

With standard conditions in hand, we then considered the substrate scope (Figure 3.22). It was found that the aryl substituted malonic acids phenyl malonic acid and 2(thiopheyn-3-

yl)malonic acid worked well, and comparatively quickly, under these conditions. Indan-2,2-dicarboxylic acid underwent double decarboxylation in good yields, albeit in 72 hours and under the 1.15 equiv KOH conditions. The di- alkyl substituted malonic acids 2-benzyl-2-methylmalonic acid and 2-benzyl-2-(3-oxobutyl)malonic acid underwent a double hydrodecarboxylation to moderate yield. Benzyl malonic acid was somewhat reactive under these conditions, giving the product ethyl benzene in a 23 % yield.

Figure 3.22: Substrate scope of the Malonic acid hydrodecarboxylation

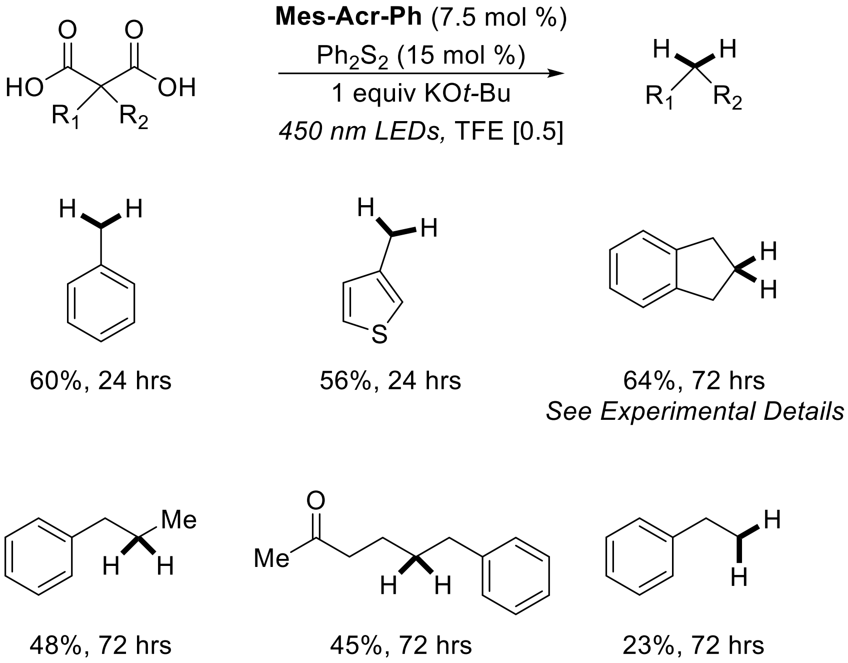
Mes-Acr-Ph (7.5 mol %)
Ph_2S_2 (15 mol %)
1 equiv KO*t*-Bu
450 nm LEDs, TFE [0.5]
60%, 24 hrs
56%, 24 hrs
64%, 72 hrs
See Experimental Details
48%, 72 hrs
45%, 72 hrs
23%, 72 hrs

3.4 Conclusion and Outlook

In summary, we have developed a direct organocatalytic protocol for the hydrodecarboxylation of carboxylic acids and malonic acids to alkanes. A prior report by Wallentin indicated that the **Mes-Acr-Me** and disulfide catalyst system would be limited to hydrodecarboxylation of α-heteroatom and α-phenyl carboxylic acids. However, buoyed by a consideration of carboxylate reduction potentials and acyloxyl radical decomposition rates, we strongly believed that this was not so much an inherent limitation but a limitation that represented unexplored space. We demonstrated that a change to a stronger base, as well as a change in solvent system from dichloroethane to trifluoroethanol could drastically expand the scope of carboxylates able to be hydrodecarboxylated by **Mes-Acr-Ph**.

Although the scope of this report was hydrodecarboxylation, the success of the hydrotrifluoromethylation reaction developed in the Nicewicz lab (Section 1.6, Figure 1.18) indicates the potential for the development of a carbon-carbon bond forming anti-Markovnikov hydrofunctionalization strategy. For example, this hydrotrifluoromethylation reaction relies on the oxidation of Langlois' reagent, subsequent expulsion of SO_2, and then radical addition into alkenes, instead of relying on the oxidation of alkenes to radical cations. Perhaps simple carboxylic acids could take the place of Langlois' reagent, expel CO_2, and add to alkenes in a similar manner (Figure 3.23).

Figure 3.23: Possible application of hydrodecarboxylation methodology to the hydrofunctionalization of alkenes

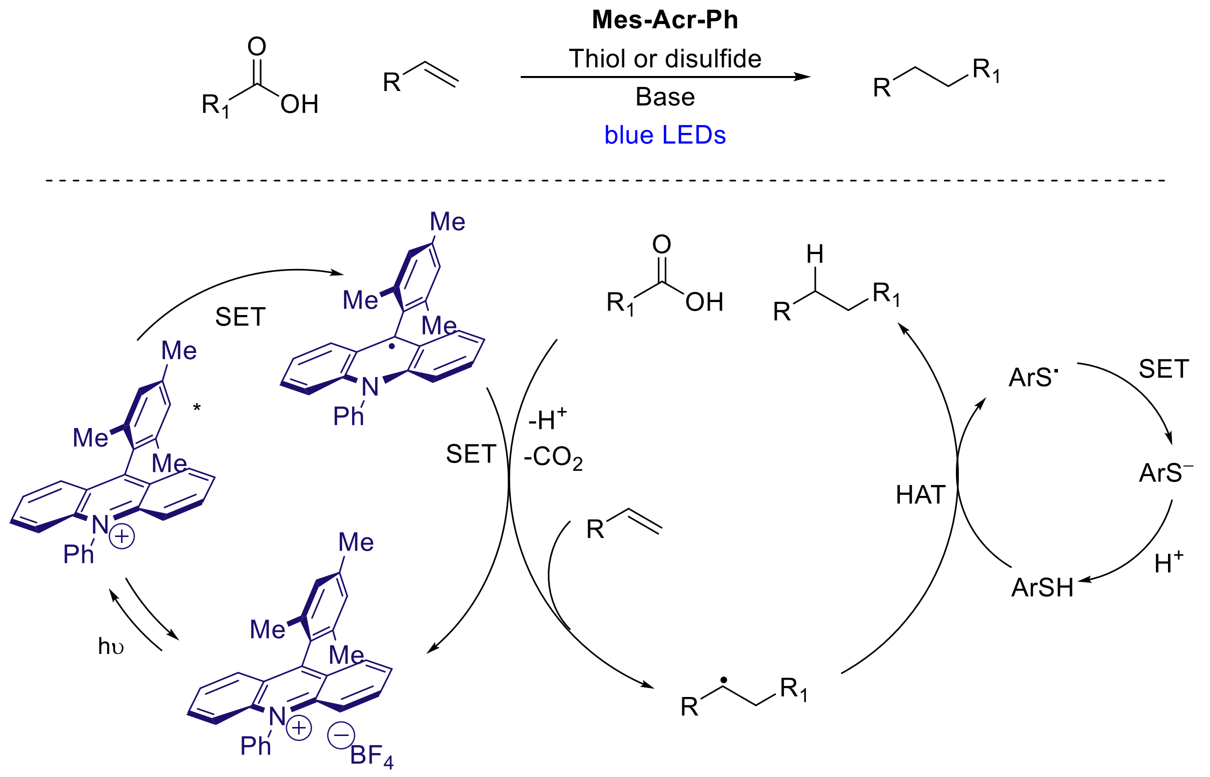
Mes-Acr-Ph
Thiol or disulfide
Base
blue LEDs
O
R_1
OH
R
R
R_1
Me
Me
Me
SET
*
N
Ph
BF$_4$
hυ
SET
-H$^+$
-CO$_2$
H
HAT
ArS$^\cdot$
SET
ArS$^-$
H$^+$
ArSH

However, development of this type of method would require careful consideration of solvent in order to achieve efficient oxidation of the carboxylate instead of the alkenes. As discussed in section 3.3.4, many alkenes typically employed in hydrofunctionalization reactions developed in the Nicewicz lab have quenching constants of the mesityl acridinium much larger than that of carboxylates. However, the trifluoromethylation methodology was able to access alkenes outside of the oxidizing power of the acridinium, and the use of these alkenes might allow for this type of reactivity to occur.

3.5 Experimental Details

General Methods

Infrared (IR) spectra were obtained using a Jasco 260 Plus Fourier transform infrared spectrometer. Proton and carbon magnetic resonance spectra (1H NMR and 13C NMR) were recorded on a Bruker model DRX 400 or a Bruker AVANCE III 600 CryoProbe (1H NMR at 400 MHz or 600 MHz and 13C NMR at 101 or 151 MHz) spectrometer with solvent resonance as the internal standard (^{1}H NMR: $CDCl_3$ at 7.26 ppm, and $(CD_3)_2O$ at 2.05 ppm; 13C NMR: $CDCl_3$ at 77.0 ppm and $(CD_3)_2O$ at 206.26 ppm). ^{1}H NMR data are reported as follows: chemical shift, multiplicity (s = singlet, d = doublet, t = triplet, dd = doublet of doublets, ddt = doublet of doublet of triplets, ddd = doublet of doublet of doublets, dddd = doublet of doublet of doublet of doublets m = multiplet, brs = broad singlet), coupling constants (Hz), and integration. Mass spectra were obtained using a Micromass (now Waters Corporation, 34 Maple Street, Milford, MA 01757) Quattro-II, Triple Quadrupole Mass Spectrometer, with a Z-spray nano-Electrospray source design, in combination with a NanoMate (Advion 19 Brown Road, Ithaca, NY 14850) chip based electrospray sample introduction system and nozzle. Thin layer chromatography (TLC) was performed on SiliaPlate 250 μm thick silica gel plates provided by Silicycle. Visualization was accomplished with short wave UV light (254 nm), aqueous basic potassium permanganate solution, cerium ammonium molybdate solution followed by heating. Flash chromatography was performed using SiliaFlash P60 silica gel (40-63 μm) purchased from Silicycle. Irradiation of photochemical reactions was carried out using 2 15W PAR38 Royal Blue Aquarium LED floodlamps Model# 6851 purchased from Ecoxotic with borosilicate glass vials purchased from Fisher Scientific. Gas chromatography (GC) was performed on an Agilent 6850 series instrument equipped with a split-mode capillary injection system accompanied by an Agilent 5973 network mass spec detector (MSD) or Agilent 6850 Series II with flame ionization detector. GC yields were determined by standardization against pure compounds purchased from Sigma-Aldrich along with an internal standard. NMR yields were determined using hexamethyldisiloxane as an internal standard.

Materials:

Commercially available reagents were purchased from Sigma-Aldrich, Acros, Alfa Aesar, or TCI-America, and used as received unless otherwise noted. Diethyl ether (Et_2O), dichloromethane (CH_2Cl_2), tetrahydrofuran (THF), toluene, and dimethylformamide (DMF) were dried by passing through activated alumina columns under nitrogen prior to use. 2,2,2-trifluoroethanol (TFE) was distilled from anhydrous potassium carbonate and sparged with nitrogen before use. Other common solvents and chemical reagents were purified by standard published methods. Diphenyl disulfide (Ph_2S_2), diisopropylethylamine (DIPEA), 2,6 Lutidine, 2,4,6 trimethylpryidine (Collidine), hydrocinnamic acid, 2-methyl-3-phenylpropanoic acid 3-(4-chlorophenyl)propanoic acid, 3-(*p*-tolyl)propanoic acid, ((benzyloxy)carbonyl)-*L*-proline, Enoxolone, 1,3-dihydro-2*H*-indene-2,2-dicarboxylic acid, benzylmalonic acid, and phenylmalonic acid were all purchased from Sigma-Aldrich and used without further purification.

Mechanistic data:

Mechanistic studies were undertaken by Jeremy Griffin, the details of which can be found in the published report.

Preparation of Carboxylic acid substrates

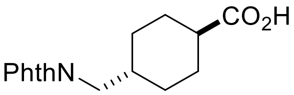

trans-4-((1,3-dioxoisoindolin-2-yl)methyl)cyclohexane-1-carboxylic acid: Prepared according to previously published literature procedure. Analytical data were in agreement with literature values[39]

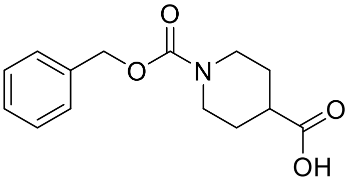

1-((benzyloxy)carbonyl)piperidine-4-carboxylic acid: Prepared according to previously published literature procedure. Analytical data were in agreement with literature values.[40]

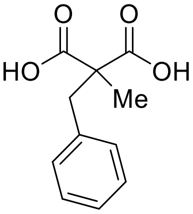

2-benzyl-2-methylmalonic acid: To a 250 mL round bottom flask was added 1.2 g (2.0 equivalents) of sodium hydride and 160 mg of potassium tertbutoxide (0.1 equivalents), followed by 75 mL of dry DMF. This was cooled to 0 ˚C before adding 3.4 mL of diethyl benzyl malonate slowly. This was allowed to react until Hydrogen evolution ceased, at which point 2.7 mL (3 equivalents) of methyl iodide was added to the solution. The solution was allowed to warm to room temperature, then heated to 70 ˚C for 24 hours while stirring. The reaction was then quenched with H_2O and extracted x3 with DCM. The combined organic layers were washed with H_2O x3 and with a 5% solution of LiCl twice to remove DMF. The solvent was then evaporated in vacuo, giving an orange oil. This crude material was placed intoa round bottom flask along with 5 equivalents of potassium hydroxide in 1:1 EtOH:H_2O and heated to reflux overnight. Ethanol was removed in vacuo, before diluting the reaction with H_2O and washing the aqueous layer with 10 mL diethyl ether. The pH of the aqueous layer was then brought to 2 and extracted with ethyl acetate x3. The organic layer was dried over sodium sulfate, and solvent removed in vacuo giving a brownish solid. The solid was then recrystallized from hexanes:EtOAc to give 1.9 grams of the product as a white solid (63%). Analytical data were in agreement with literature values.[41]

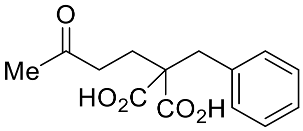

2-benzyl-2-(3-oxobutyl)malonic acid: Diethyl 2-benzyl-2-(3-oxobutyl)malonate was prepared according to literature procedure.[42] The ethyl ester was purified via column chromatography (3-5% acetone in hexanes). The ethyl ester was then hydrolyzed. A 100 mL round bottom equipped with a stir bar and reflux condenser was charged with potassium hydroxide 85% (5.0 equiv) in H_2O (0.75 M). A solution of diethyl 2-benzyl-2-(3-oxobutyl)malonate (1.0 equiv) in EtOH (0.75 M) was then added and the reaction mixture was heated at reflux for 20 hours. The mixture was then removed from heat, quenched to pH 3 with 3 M HCl, extracted with ethyl acetate and washed with brine. The organic layer was dried with Na_2SO_4, and the solvent was evaporated. The crude material was purified by recrystallization in Ethyl Acetate/Hexanes. **^{1}H NMR** (400 MHz, Acetone-*d*$_6$) δ 7.38 – 7.08 (m, 5H), 3.26 (s, 2H), 2.66 – 2.58 (m, 2H), 2.11 (s, 3H), 2.08 – 1.98 (m, 2H). **^{13}C NMR** (101 MHz, Acetone-*d*$_6$) δ 206.84, 172.74, 137.27, 130.84, 129.01, 127.66, 58.21, 39.55, 39.00, 27.03.

General Procedure for Decarboxylation of Monoacids:

To a flame-dried one dram vial equipped with a magnetic stir bar was added the acid (1 equiv.), **Mes-Acr-Ph** (5 mol%), and phenyl disulfide (10 mol%). The vial was transferred into a nitrogen filled glovebox and sparged trifluoroethanol was added to achieve a concentration of 0.5 M with respect to acid substrate. *N*,*N*-diisopropylethylamine (20 mol%), was added, and the vial sealed with a Teflon coated septum screwcap. The reaction were removed from the glovebox and irradiated with two 450 nm lamps and stirred at ambient temperature from 24-96 hours. Upon completion, lightweight products were treated differently than heavy products. Light products were not purified, but internal standard was added and the yield was determined by GC. In some cases, proton and carbon NMR could be obtained for the light products through purification on silica plug with pentanes as eluent, the pentanes was then removed in *vacuo*, carefully. For heavier products, the solvent was removed in *vacuo* and the product was further purified by flash chromatography. Those products not described herein were produced by Jeremy Griffin. Details of these products can be found in the supplementary information of that published report.

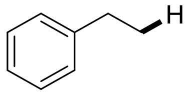

Ethylbenzene: The compound was prepared according to the general procedure using 105.1 mg 3-phenylpropanoic acid (0.7 mmol), 15.4 mg phenyl disulfide, 16.1 mg **Mes-Acr-Ph**, 24 µL *N*,*N*-diisopropylethylamine, and 1.4 mL trifluoroethanol. The mixture was allowed to react at ambient temperature under irradiation for 24 or 72 hours, at which time the reaction was washed with a solution of sodium hydroxide and extracted with DCM three times. The combined organic layer was dried over sodium sulfate. The reactions were then passed through a plug of silica into a vial containing internal standard before GC analysis.

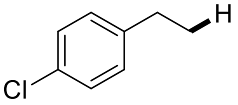

1-Chloro-4-ethylbenzene: The compound was prepared according to the general procedure using 129.2 mg 3-(4-chlorophenyl)propanoic acid (0.7 mmol), 15.4 mg phenyl disulfide, 16.1 mg **Mes-Acr-Ph**, 24 μL *N*,*N*-diisopropylethylamine, and 1.4 mL trifluoroethanol. The mixture was allowed to react at ambient temperature under irradiation for 24 hours, at which time the reaction was washed with a solution of sodium hydroxide and extracted with DCM three times. The combined organic layer was dried over sodium sulfate. The reactions were then passed through a plug of silica into a vial containing internal standard before GC analysis. NMR spectra were optained by running a sample through a silica plug with pentanes as eluent and carefully evaporating the solvent. **^{1}H NMR** (400 MHz, Chloroform-*d*) δ 7.29 – 7.21 (m, 2H), 7.16 – 7.09 (m, 2H), 2.62 (q, *J* = 7.6 Hz, 2H), 1.24 (t, *J* = 7.6 Hz, 3H). **^{13}C NMR** (101 MHz, Chloroform-*d*) δ142.60, 131.21, 129.18, 128.33, 28.24, 15.52.

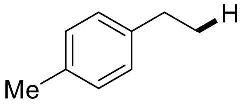

1-Ethyl-4-methylbenzene: The compound was prepared according to the general procedure using 114.9 mg 3(*p*-tolyl)propanoic acid (0.7 mmol), 15.4 mg phenyl disulfide, 16.1 mg **Mes-Acr-Ph**, 24 μL *N*,*N*-diisopropylethylamine, and 1.4 mL trifluoroethanol. The mixture was allowed to react at room temperature under irradiation for 24 hours, at which time the reaction was washed with a solution of sodium hydroxide and extracted with DCM three times. The combined organic layer was dried over sodium sulfate. The reactions were then passed through a plug of silica into a vial containing internal standard before GC analysis.

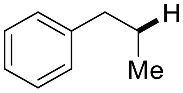

Propylbenzene: The compound was prepared according to the general procedure using , 114.9mg 2-methyl-3-phenylpropanoic acid (0.7 mmol), 15.3 mg phenyl disulfide, 16.1 mg **Mes-Acr-Ph**, 24 µL *N,N*-diisopropylethylamine, and 1.4 mL trifluoroethanol. The mixture was allowed to react at ambient temperature under irradiation for 24 hours, at which time the reaction was washed with a solution of sodium hydroxide and extracted with DCM three times. The combined organic layer was dried over sodium sulfate. The reactions were then passed through a plug of silica into a vial containing internal standard before GC analysis.

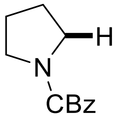

Benzyl pyrrolidine-1-carboxylate: The compound was prepared according to the general procedure using 124.6 mg Z-L-proline (0.5 mmol), 11 mg phenyl disulfide, 11.5 mg **Mes-Acr-Ph**, 17.2 µL *N,N*-diisopropylethylamine, and 1.0 mL trifluoroethanol. The mixture was allowed to react at room temperature under irradiation for 48 hours, at which time the reaction mixture was diluted with dichloromethane, washed with 10% NaOH (aq), extracted with dichloromethane and dried over Na_2SO_4. The solvent was evaporated under reduced pressure and the crude residue was purified via silica column chromatography (3% Acetone in Hexanes). The product was isolated as a white solid 88 mg (92%). Analytical data were in agreement with literature values.[43] **^{1}H NMR** (400 MHz, Chloroform-*d*) δ 7.40 – 7.25 (m, 5H), 5.13 (s, 2H), 3.39 (dt, *J* = 13.6, 6.3 Hz, 4H), 1.85 (pd, *J* = 7.6, 4.8 Hz, 4H). **^{13}C NMR** (101 MHz, $CDCl_3$) δ 154.78, 136.97, 128.21, 127.69, 127.67, 66.42, 46.09, 45.65, 25.59, 24.81.

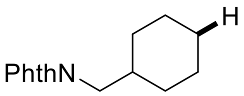

2-(cyclohexylmethyl)isoindoline-1,3-dione: The compound was prepared according to the general procedure using 143.7mg trans-4-((1,3-dioxoisoindolin-2-yl)methyl)cyclohexane-1-carboxylic acid (0.5 mmol), 11mg phenyl disulfide, 11.5mg **Mes-Acr-Ph**, 17.2µL *N*,*N*-diisopropylethylamine, and 1mL trifluoroethanol. The mixture was allowed to react at room temperature under irradiation for 48 hours, at which time the reaction was diluted with DCM and washed with 10% sodium hydroxide solution. The aqueous layer was washed with DCM three times. The combined organic layers were washed with brine and dried over sodium sulfate. The reaction was purified by column chromatography using Acetone/hexanes (3% Acetone) as eluent to give the product as a white solid (68%). Analytical data were in agreement with literature values[44]. **^{1}H NMR** (400 MHz, Chloroform-*d*) δ 7.80 (dp, *J* = 7.2, 4.3 Hz, 2H), 7.67 (dp, *J* = 6.9, 4.2 Hz, 2H), 3.49 (d, *J* = 7.3 Hz, 2H), 1.77 (dtt, *J* = 10.9, 7.3, 3.4 Hz, 1H), 1.71-1.54 (m, 5H), 1.27-1.07 (m, 4H), 0.98 (tt, *J* = 11.8, 8.4, 6.5 Hz, 2H). **^{13}C NMR** (101 MHz, Chloroform-*d*) δ168.52 , 133.71 , 131.98 , 123.03 , 44.00 , 36.89 , 30.66 , 26.15 , 25.56 .

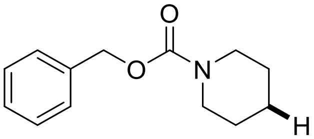

Benzylpiperidine-1-carboxylate: The compound was prepared according to the general procedure using 131.6 mg 1-((benzyloxy)carbonyl)piperidine-4-carboxylic acid, 11 mg diphenyl disulfide, 11.5 mg **Mes-Acr-Ph**, 17.2 µL *N*,*N*-diisopropylethylamine, and 1.6 mL 4:1 TFE:EtOAc [0.3]. The mixture was allowed to react at ambient temperature under irradiation for 48 hours, at which time the solvent was evaporated and the reaction was purified by column chromatography (3% Acetone in Hexanes). The yield was 65.7 mg (61%). CAS registry number: 3742-91-4. **^{1}H NMR** (400 MHz, $CDCl_3$) δ 7.33 (dd, J = 20,7, 4.4 Hz, 5H), 5.13 (s, 2H), 3.45 (t, J = 5.4 Hz, 4H), 1.68-1.44 (m, 6H). 13C NMR (101 MHz, CDCl3) δ 155.21, 136.91, 128.33, 127.76, 127.67, 66.77, 44.75, 25.58, 24.26.

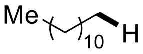

Dodecane: The compound was prepared according to the general procedure using 129 mg tridecanoic acid, 26.4 mg diphenyl disulfide, 13.8 mg Mes-Acr-Ph, 21 µL N,N-diisopropylethylamine, 2.0 mL 4:1 TFE:EtOAc [0.3M]. The mixture was allowed to react at ambient temperature under irradiation for 48 hours, at which time the reaction mixture was passed through a plug of silica into a vial containing internal standard before GC/MS analysis. The yield was 51%.

General Procedure for the double decarboxylation of Malonic acid derivatives:

Potassium *tert*-butoxide (1 equiv) and the malonic acid (1 equiv) were dissolved in N_2 sparged trifluoroethanol (0.5M), under an N_2 atmosphere. This solution was transferred to a 2 dram vial equipped with a stir bar, phenyl disulfide (15 mol%), and **Mes-Acr-Ph** (7.5 mol%). The vials were fitted with a Teflon screw cap and allowed to react under blue light irradiation for 24-72 hours at ambient temperature.

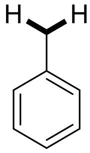

Toluene: The compound was prepared according to the general procedure using 126.1 mg phenylmalonic acid (0.7 mmol), 79 mg of KO*t*Bu, 23.1 mg phenyl disulfide, 24.2 mg **Mes-Acr-Ph,** and 1.4 mL TFE. The mixture was allowed to react at ambient temperature under irradiation for 24 hours, at which time the reaction was washed with a solution of sodium hydroxide and extracted with DCM three times. The organic layer was dried over sodium sulfate. The reactions were then passed through a plug of silica into a vial containing internal standard before GC analysis.

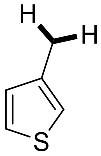

3-methylthiophene: The compound was prepared according to the general procedure using 130.3 mg 2-(thiophen-3-yl)malonic acid (0.7 mmol), 79 mg of KOtBu, 23.1 mg diphenyl disulfide, 24.2 mg **MesAcr-Ph**, and 1.4 mL TFE. The mixture was allowed to react at ambient temperature under irradiation for Me 3a S Me 3b S15 24 hours, at which time the reaction was washed with a solution of sodium hydroxide and extracted with DCM three times. The organic layer was dried over sodium sulfate. The reactions were then passed through a plug of silica into a vial containing internal standard before GC analysis.

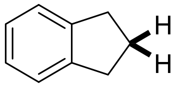

2,3-dihydro-1*H*-indene: The compound was prepared according to the general procedure using 144.3 mg 1,3-dihydro-2*H*-indene-2,2-dicarboxylic acid (0.7 mmol), 22.9 mg phenyl disulfide, 24.2 mg **Mes-Acr-Ph**, and 1.4 mL of 0.57M solution KOH in TFE. The mixture was allowed to react at ambient temperature under irradiation for 72 hours, at which time the reaction was washed with a solution of sodium hydroxide and extracted with DCM three times. The organic layer was dried over sodium sulfate. The reactions were then passed through a plug of silica into a vial containing internal standard before GC analysis.

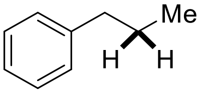

Propylbenzene: The compound was prepared according to the general procedure using 145.7 mg 2-benzyl-2-methylmalonic acid, 23.1 mg pheny disulfide, 24.2 mg **Mes-Acr-Ph**, 79 mg KO*t*Bu, and 1.4 mL trifluoroethanol. The mixture was allowed to react at ambient temperature under irradiation for 72 hours, at which time the reaction was washed with a 10% sodium hydroxide solution and extracted with dichloromethane. The organic layer was dried over sodium sulfate. The solution was then passed over a short plug of silica into a vial containing internal standard before GC analysis.

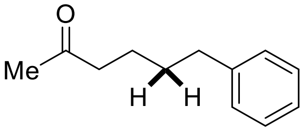

6-phenylhexan-2-one: The compound was prepared according to the general procedure using 185 mg 2-benzyl-2-(3-oxobutyl)malonic acid, 79 mg KO*t*Bu, 24.2 mg **Mes-Acr-Ph**, 23.1 mg phenyl disulfide, and 1.4 mL triflouroethanol. The reaction was allowed to react for 72 hours, upon which time the solvent was evaporated. The product was purified via column chromatography (3% acetone in hexanes). The yield was 57.7 mg (48%). Spectral data was in agreement with literature values.[45] **^{1}H NMR** (400 MHz, $CDCl_3$) δ 7.28 (dd, *J* = 8.5, 6.7 Hz, 2H), 7.18 (dd, *J* = 7.8, 5.6 Hz, 3H), 2.73 – 2.51 (m, 2H), 2.52 – 2.35 (m, 2H), 2.12 (s, 3H), 1.62 (p, *J* = 3.5 Hz, 4H). **^{13}C NMR** (101 MHz, $CDCl_3$) δ 208.88, 142.09, 128.29, 128.22, 125.67, 43.47, 35.64, 30.86, 29.81, 23.37.

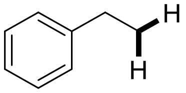

Ethylbenzene 3e: The compound was prepared according to the general procedure using 136.0 mg benzylmalonic acid (0.7 mmol), 79 mg of KO*t*Bu 23.1 mg phenyl disulfide, 24.2 mg **Mes-Acr-Ph,** and 1.4 mL TFE. The mixture was allowed to react at ambient temperature under irradiation for 72 hours, at which time the reaction was washed with a solution of sodium hydroxide and extracted with DCM three times. The organic layer was dried over sodium sulfate. The reactions were then passed through a plug of silica into a vial containing internal standard before GC analysis.

REFERENCES

(1) Rossiter,B. E.; Swingle, N. M. *Chem. Rev.* **1992**, *92*, 771.

(2) Alexakis, A.; Bäckvall, J. E.; Krause, N.; Pàmies, O.; Diéguez, M. *Chem. Rev.* **2008**, *108*, 2796.

(3) Kagan, H. B.; Riant, O. *Chem. Rev.* **1992**, *92*, 1007.

(4) Jung, M. E.; Piizzi, G. *Chem. Rev.* **2005**, *105*, 1735.

(5) Barton, D. H. R.; Dowlatshahi, H.; Motherwell, W. B.; Villemin, D. *J. Chem. Soc., Chem. Commun* **1980**, 732.

(6) Barton, D. H. R.; Zard, S. Z. *Pure Appl. Chem.* **1986**, *58*, 675.

(7) Fang, C.; Shanahan, C S.; Paull, D. H.; Martin, S. F. *Angew. Chem. Int. Ed.* **2012**, *51*, 10596.

(8) Yamaguchi, K.; Kazuta, Y.; Abe, H.; Matsuda, A.; Shuto, S. *J. Org. Chem.* **2003**, *68*, 9255.

(9) Ho, J.; Zheng, J.; Meana-Pañeda, R.; Truhlar, D. G.; Ko, E. J.; Savage, G. P.; Williams, C. M.; Coote, M. L.; Tsanaktsidis, J. *J. Org. Chem.* **2013**, *78*, 6677.

(10) Poigny, S.; Guyot, M.; Somadi, M. *J. Org. Chem.* **1998**, *63*, 1342.

(11) Kolbe, H. *Ann. Chem.* **1849**, *69*, 257.

(12) Vijh, A. K.; Conway, B. E. *Chem. Rev*. **1967**, *67*, 623.

(13) Hilborn, J. W.; Pincock, J. A. *J. Am. Chem. Soc.* **1991**, *113*, 2683.

(14) Fraind, A.; Turncliff, R.; Fox, T.; Sodano, J.; Ryzhkov, L. R. *J. Phys. Org. Chem.* **2011**, *24*, 809.

(15) Perkins, R. J.; Xu, H.-C.; Campbell, J. M.; Moeller, K. D. *Belstein J. Org. Chem.* **2013**, *9*, 1630.

(16) Anderson, J. M.; Kochi, J. K. *J. Am. Chem. Soc.* **1970**, *92*, 1651.

(17) Minisci, F.; Bernardi, R.; Bertini, F.; Galli, R.; Perchinummo, M. *Tetrahedron* **1971**, *27*, 3575.

(18) Davidson, R. S.; Steiner, P. R. *J. Chem. Soc. C* **1971**, 1682.

(19) Yoshimi, Y.; Itou, T.; Hatanaka, M. *Chem. Commun.* **2007**, 5244.

(20) Zuo, Z.; MacMillan, D. W. C. *J. Am. Chem. Soc.* **2014**, *136*, 5257.

(21) Chu, L.; Ohta, C.; Zuo, Z.; MacMillan, D. W. C. *J. Am. Chem. Soc.* **2014**, *136*, 10886.

(22) Ventre, S.; Petronijevic, F. R.; MacMillan, D. W. C. *J. Am. Chem. Soc.* **2015**, *137,* 5654.

(23) Zuo, Z.; Ahneman, D. T.; Chu, L.; Terrett, J. A.; Doyle, A. G.; MacMillan, D. W. C. *Science* **2014**, *345*, 437.

(24) Griffin, J. D.; Zeller, M. A.; Nicewicz, D. A. *J. Am. Chem. Soc.* **2015**, *137*, 11340.

(25) Braun, W.; Rajbenbach, L.; Elrich, F. R. *J. Phys. Chem.* **1962**, *66*, 1591.

(26) Falvey, D. E.; Schuster, G. B. *J. Am. Chem. Soc.* **1986**, *108*, 7419.

(27) Chateauneuf, J.; Lusztyk, J.; Ingold, K. U. *J. Am. Chem. Soc.* **1988**, *110*, 2877.

(28) Hilborn, J. W.; Pincock, J. A. *J. Am. Chem. Soc.* **1991**, 113, *2683.*

(29) Cassani, C.; Bergonzini, G.; Wallentin, C.-J. *Org. Lett.* **2014**, *16*, 4228.

(30) Miguel, E. L. M.; Silva, P. L.; Pliego, J. R. *J. Phys. Chem. B* **2014**, *118*, 5730.

(31) Prier, C. K.; Rankic, D. A.; MacMillan, D. W. C. *Chem. Rev.* **2013**, *113,* 5322.

(32) Wilger, D. J.; Grandjean, J.-M. M.; Lammert, T. R.; Nicewicz, D. A. *Nat. Chem.* **2014**, *6*, 720.

(33) Roth, H. G.; Romero, N. A.; Nicewicz, D. A. *Synlett*, **2016**, *27*, 714.

(34) Wilger, D. J.; Gesmundo, N. J.; Nicewicz, D. A. *Chem. Sci.* **2013**, *4,* 3160.

(35) Akerlof, G. *J. Am. Chem. Soc.* **1932**, *54*, 4125.

(36) Hong, D.-P.; Hoshino, M.; Kuboi, R.; Goto, Y. *J. Am. Chem. Soc.* **1999**, *121*, 8427.

(37) Romero, N. A.; Nicewicz, D. A. *J. Am. Chem. Soc.* **2014**, *136*, 17024.

(38) Brown, H. C. *Determination of Organic Structures by Physical Methods*; Braude, E. A.; Nachod, F. C., Eds.; Academic Press: New York, NY, 1955

(39) Singh, D.; Baraugh, J. B. *Cryst. Growth. Des.* **2012**,*12*, 210

(40) Maligres, P. E.; Houpis, I.; Rossen, K.; Molina, A.; Sager, J.; Upadhyay, V.; Wells, K. M.; Reamer, R. A.; Lynch, J. E.; Askin, D.; Volante, R. P.; Reider, P. J.; Houghton, P. Tetrahedron 1997, 53, 10983.

(41) Moriuchi-Kawakami, T.; Kawata, K.; Nakamura, S.; Koyama, Y.; Shibutani, Y. *Tetrahedron* **2014**, *70*, 9805.

(42) Brewer, J. T.; Parkin, S.; Grossman, R. B. *Cryst. Growth Des.* **2004***,* *4*, 591.

(43) Krivickas, S. J.; Tamanini, E.; Todd, M. H.; Watkinson, M. *J. Org. Chem.* **2007**, *72*, 8280.

(44) Khedkar, M. V.; Shinde, A. R.; Sasaki, T.; Bhanage, B. M. *J. Mol. Catal. Chem.* **2014**, *385*, 91.

(45) Shukla, P.; Hsu, Y.-C.; Cheng, C.-H. *J. Org. Chem.* **2006**, *71*, 655.

APPENDIX ONE: NMR SPECTRA FOR CHAPTER TWO

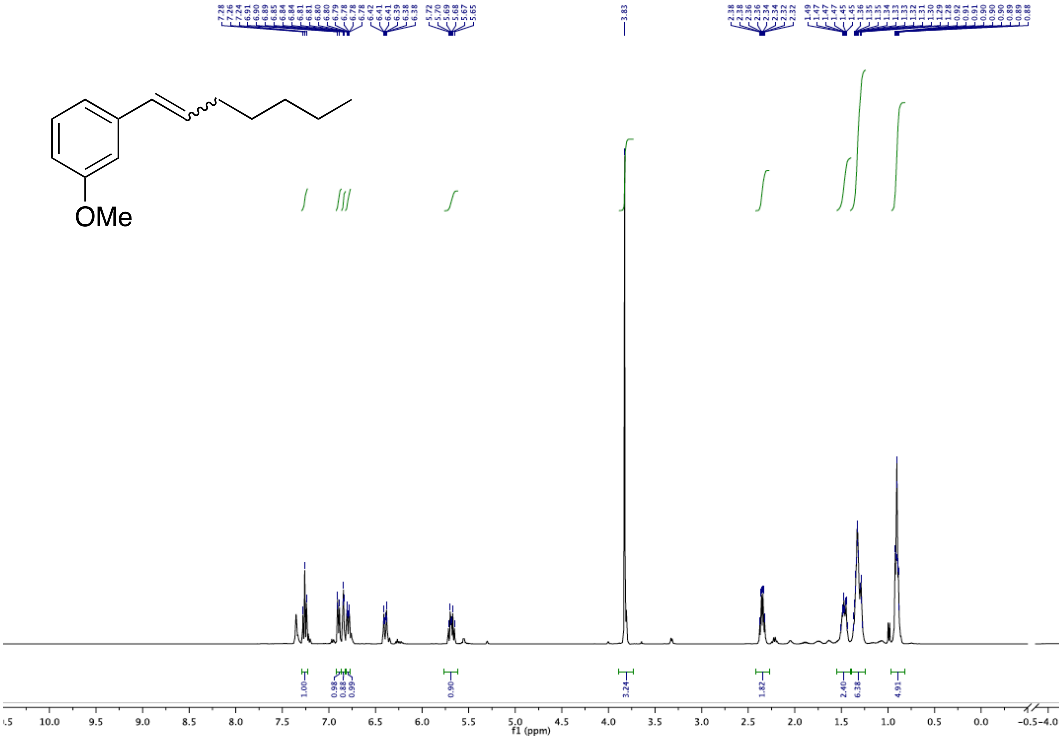

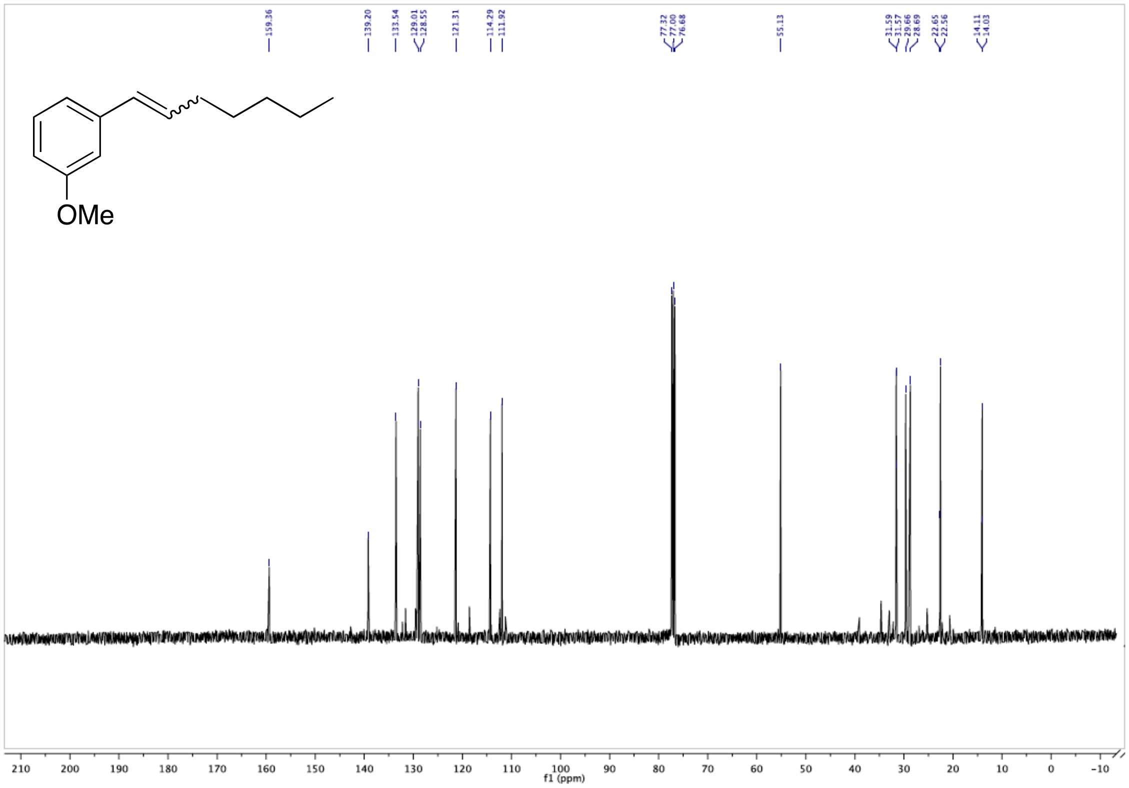

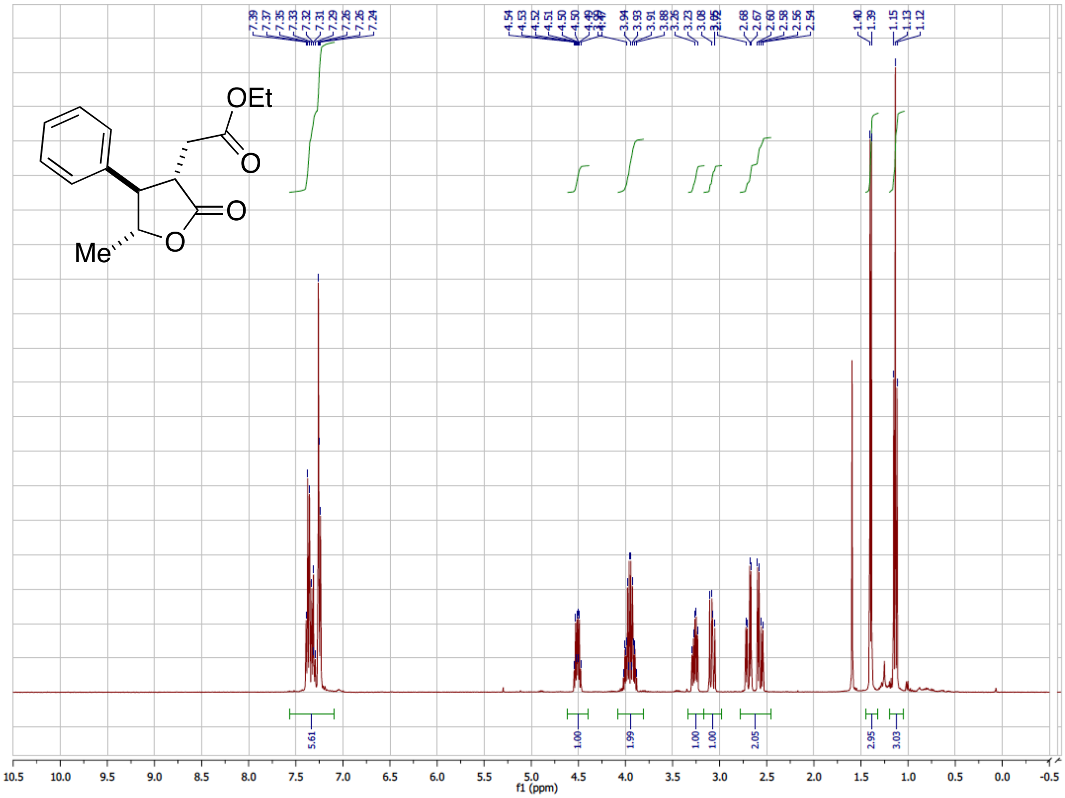
OEt
O
O
Me
O
7.39
7.37
7.35
7.33
7.32
7.31
7.29
7.26
7.26
7.24
4.54
4.53
4.52
4.51
4.50
4.50
4.49
4.47
3.94
3.93
3.91
3.88
3.26
3.23
3.08
3.05
3.02
2.68
2.67
2.60
2.58
2.56
2.54
1.40
1.39
1.15
1.13
1.12
5.61
1.00
1.99
1.00
1.00
2.05
2.95
3.03
10.5
10.0
9.5
9.0
8.5
8.0
7.5
7.0
6.5
6.0
5.5
5.0
4.5
4.0
3.5
3.0
2.5
2.0
1.5
1.0
0.5
0.0
-0.5
f1 (ppm)

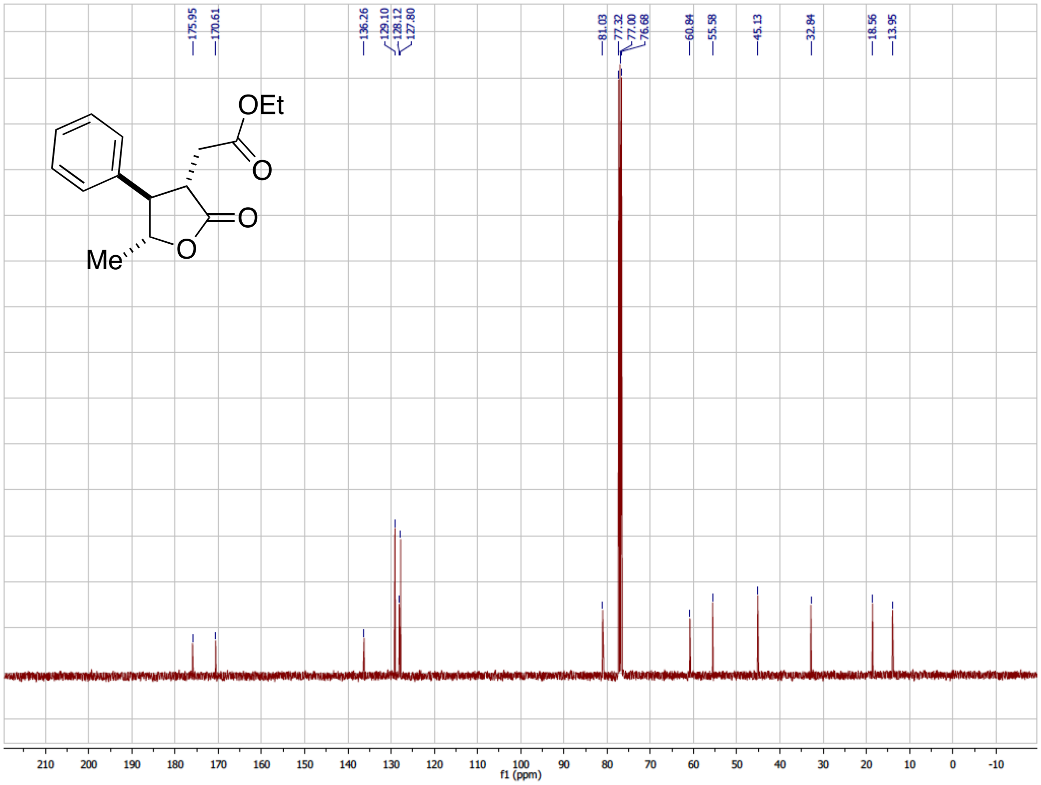
175.95
170.61
136.26
129.10
128.12
127.80
81.03
77.32
77.00
76.68
60.84
55.58
45.13
32.84
18.56
13.95
OEt
O
O
Me
O
210
200
190
180
170
160
150
140
130
120
110
100
90
80
70
60
50
40
30
20
10
0
-10
f1 (ppm)

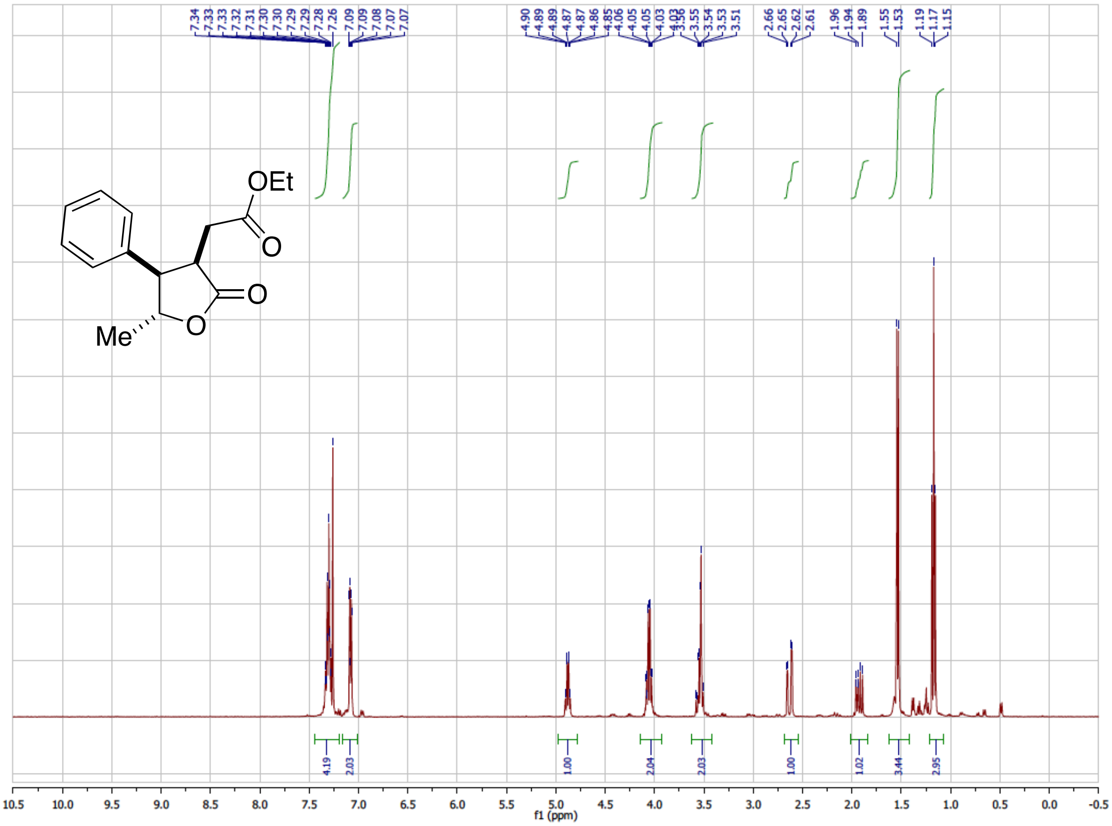
7.34
7.33
7.33
7.32
7.31
7.30
7.30
7.29
7.29
7.28
7.26
7.09
7.09
7.08
7.07
7.07
4.90
4.89
4.89
4.87
4.87
4.86
4.85
4.06
4.05
4.05
4.03
4.03
3.56
3.55
3.54
3.53
3.51
2.66
2.65
2.62
2.61
1.96
1.94
1.89
1.55
1.53
1.19
1.17
1.15
OEt
O
O
Me
O
4.19
2.03
1.00
2.04
2.03
1.00
1.02
3.44
2.95
10.5
10.0
9.5
9.0
8.5
8.0
7.5
7.0
6.5
6.0
5.5
5.0
4.5
4.0
3.5
3.0
2.5
2.0
1.5
1.0
0.5
0.0
-0.5
f1 (ppm)

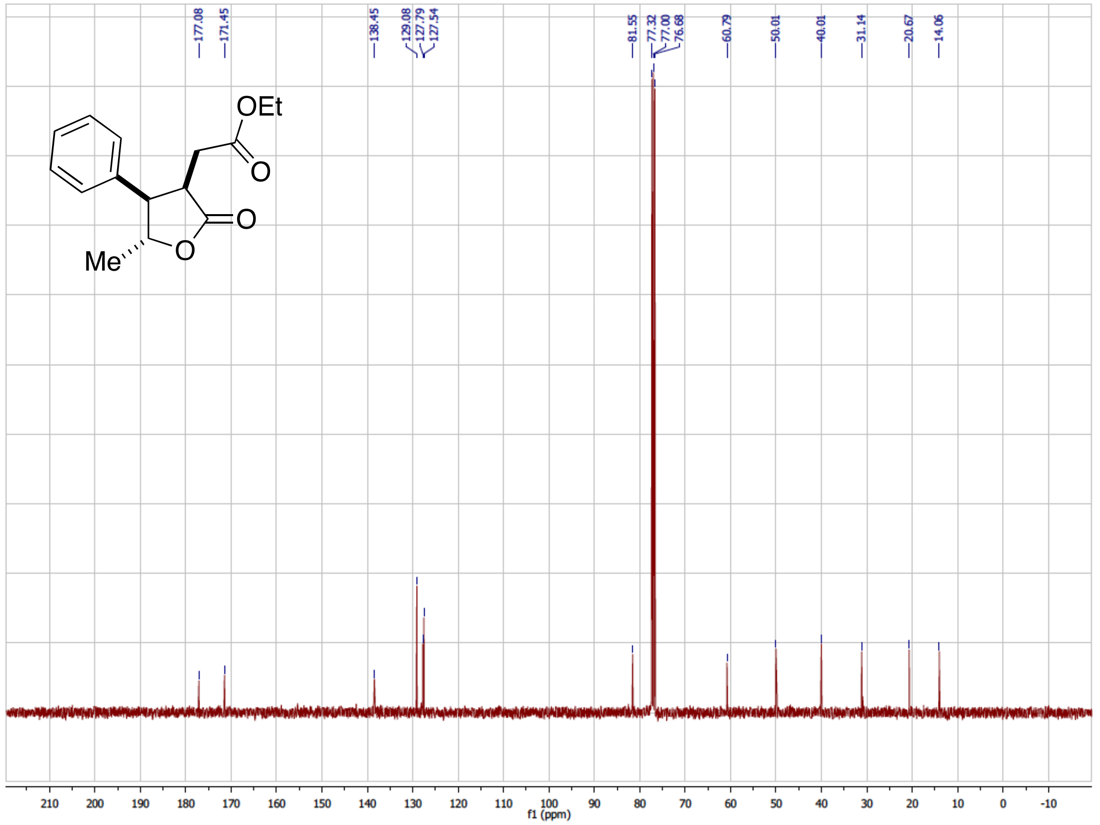
177.08
171.45
138.45
129.08
127.79
127.54
81.55
77.32
77.00
76.68
60.79
50.01
40.01
31.14
20.67
14.06
OEt
O
O
Me
O
210
200
190
180
170
160
150
140
130
120
110
100
90
80
70
60
50
40
30
20
10
0
-10
f1 (ppm)

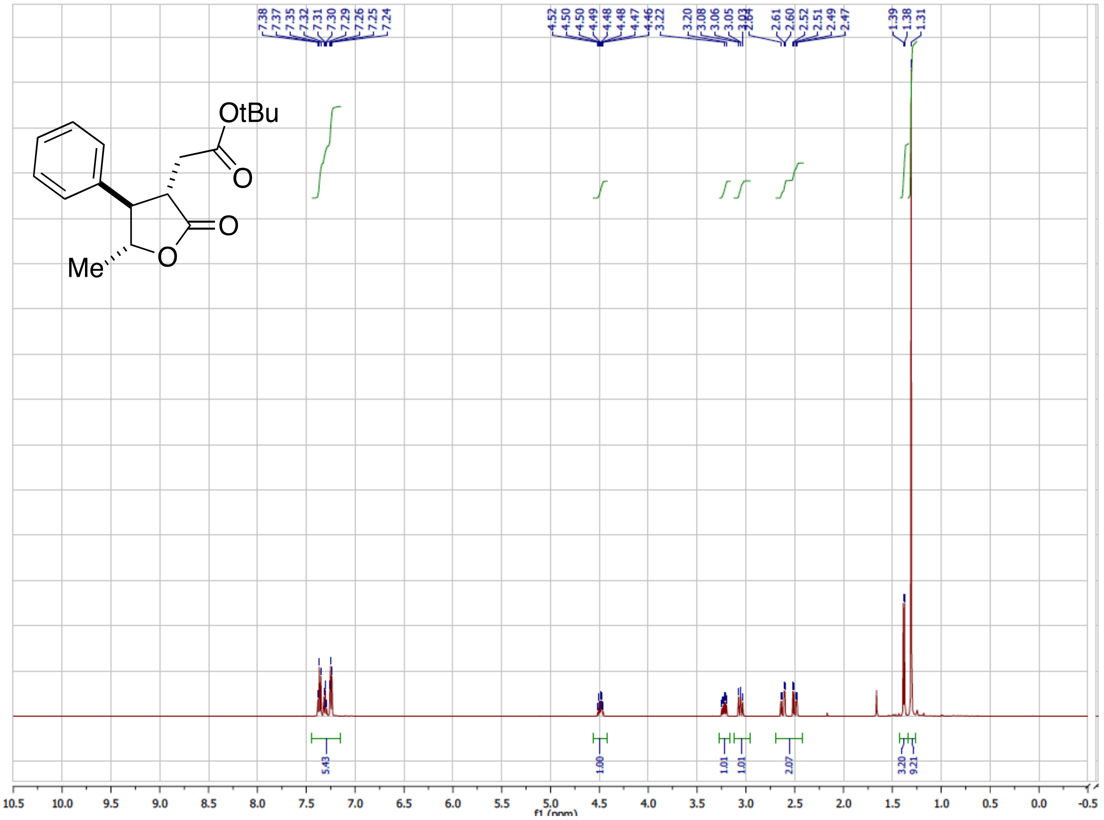
7.38
7.37
7.35
7.32
7.31
7.30
7.29
7.26
7.25
7.24
4.52
4.50
4.50
4.49
4.48
4.48
4.47
4.46
3.22
3.20
3.08
3.06
3.05
3.03
3.04
2.61
2.60
2.52
2.51
2.49
2.47
1.39
1.38
1.31
OtBu
O
O
O
Me
5.43
1.00
1.01
1.01
2.07
3.20
9.21
10.5
10.0
9.5
9.0
8.5
8.0
7.5
7.0
6.5
6.0
5.5
5.0
4.5
4.0
3.5
3.0
2.5
2.0
1.5
1.0
0.5
0.0
-0.5
f1 (ppm)

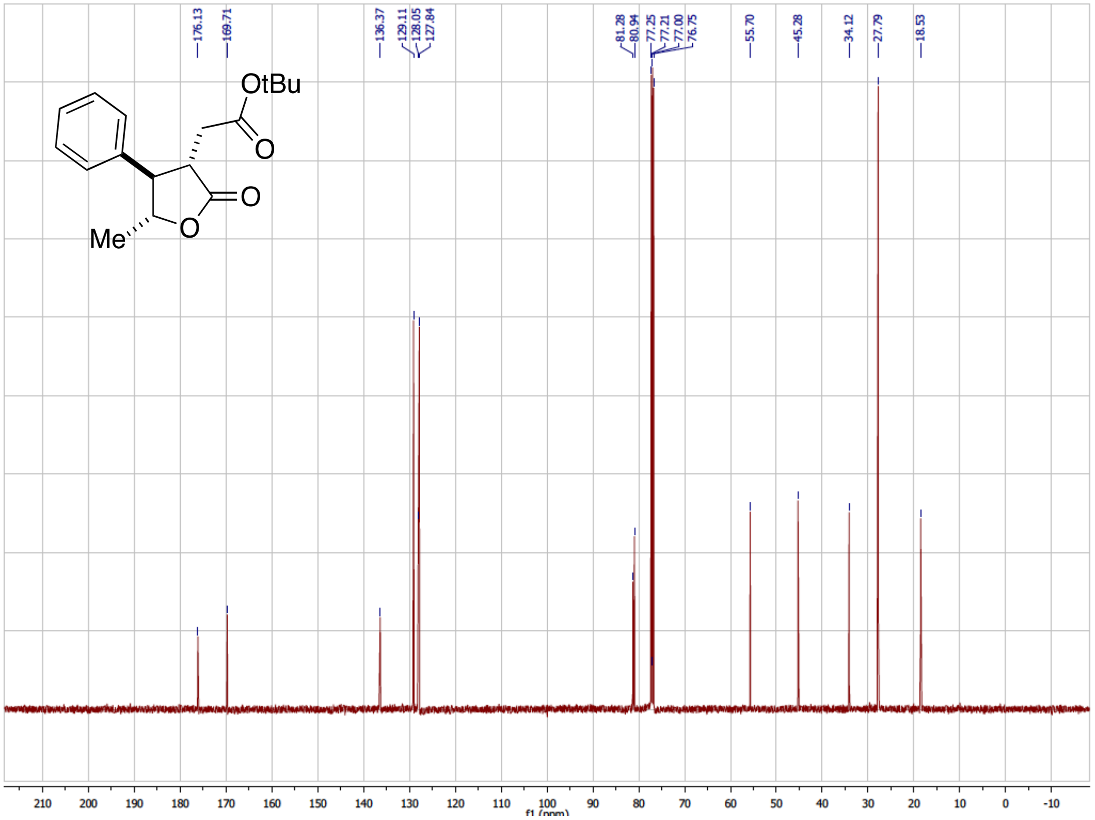
176.13
169.71
136.37
129.11
128.05
127.84
81.28
80.94
77.25
77.21
77.00
76.75
55.70
45.28
34.12
27.79
18.53
OtBu
O
O
O
Me
210
200
190
180
170
160
150
140
130
120
110
100
90
80
70
60
50
40
30
20
10
0
-10
f1 (ppm)

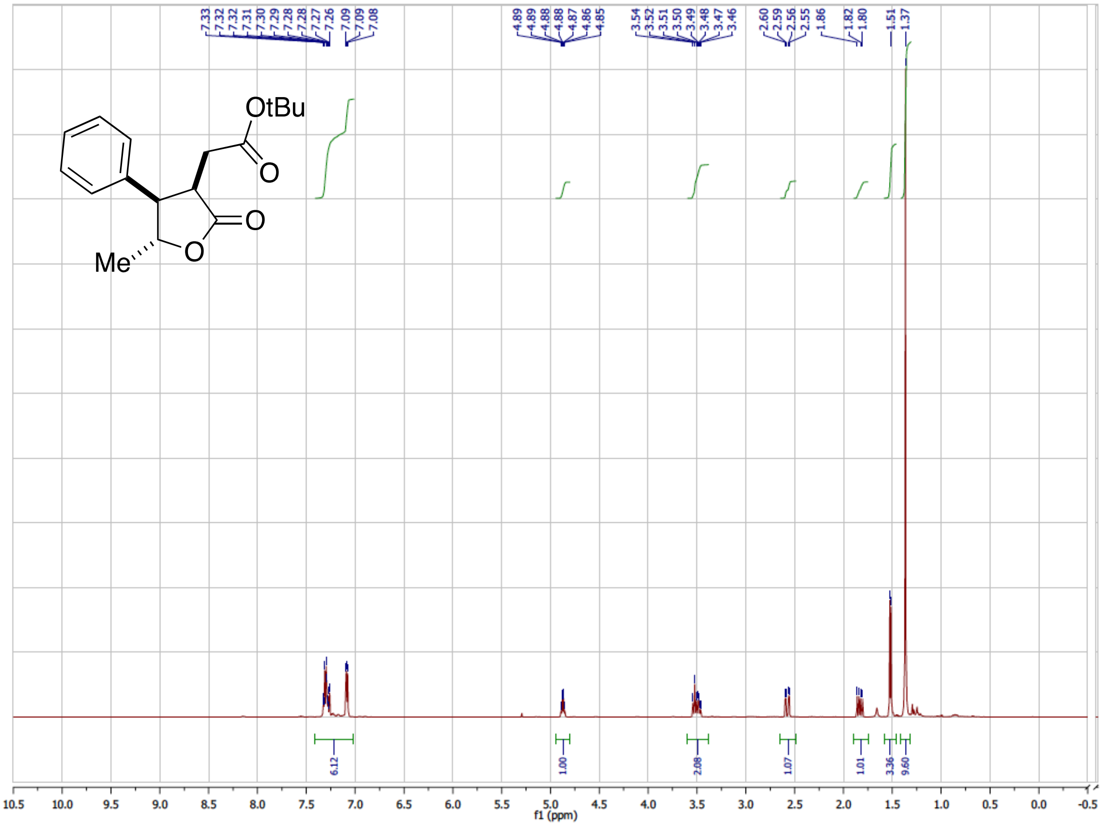
7.33
7.32
7.32
7.31
7.30
7.29
7.28
7.28
7.27
7.26
7.09
7.09
7.08
4.89
4.89
4.88
4.88
4.87
4.86
4.85
3.54
3.52
3.51
3.50
3.49
3.48
3.47
3.46
2.60
2.59
2.56
2.55
1.86
1.82
1.80
1.51
1.37
OtBu
O
O
Me
O
6.12
1.00
2.08
1.07
1.01
3.36
9.60
10.5
10.0
9.5
9.0
8.5
8.0
7.5
7.0
6.5
6.0
5.5
5.0
4.5
4.0
3.5
3.0
2.5
2.0
1.5
1.0
0.5
0.0
-0.5
f1 (ppm)

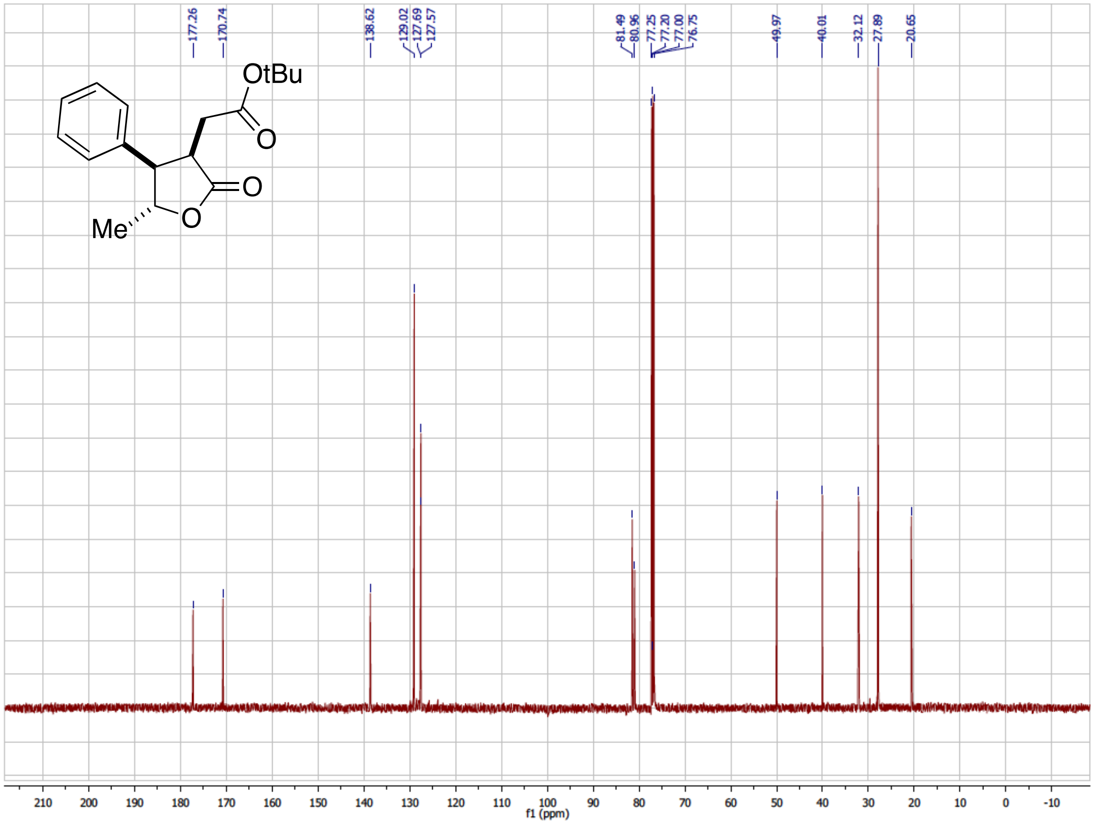
177.26
170.74
138.62
129.02
127.69
127.57
81.49
80.96
77.25
77.20
77.00
76.75
49.97
40.01
32.12
27.89
20.65
OtBu
O
O
Me
O
210
200
190
180
170
160
150
140
130
120
110
100
90
80
70
60
50
40
30
20
10
0
-10
f1 (ppm)

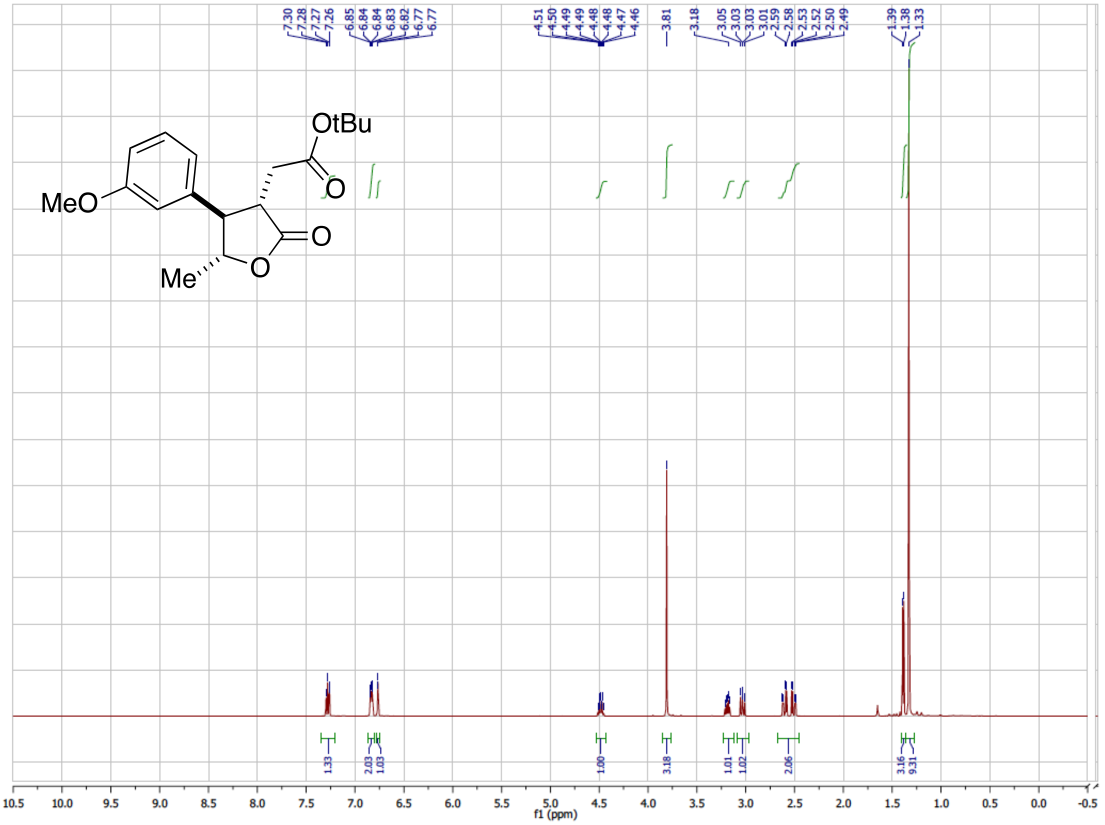
7.30
7.28
7.27
7.26
6.85
6.84
6.84
6.83
6.82
6.77
6.77
4.51
4.50
4.49
4.49
4.48
4.48
4.47
4.46
3.81
3.18
3.05
3.03
3.03
3.01
2.59
2.58
2.53
2.52
2.50
2.49
1.39
1.38
1.33
OtBu
MeO
O
O
Me
O
1.33
2.03
1.03
1.00
3.18
1.01
1.02
2.06
3.16
9.31
f1 (ppm)

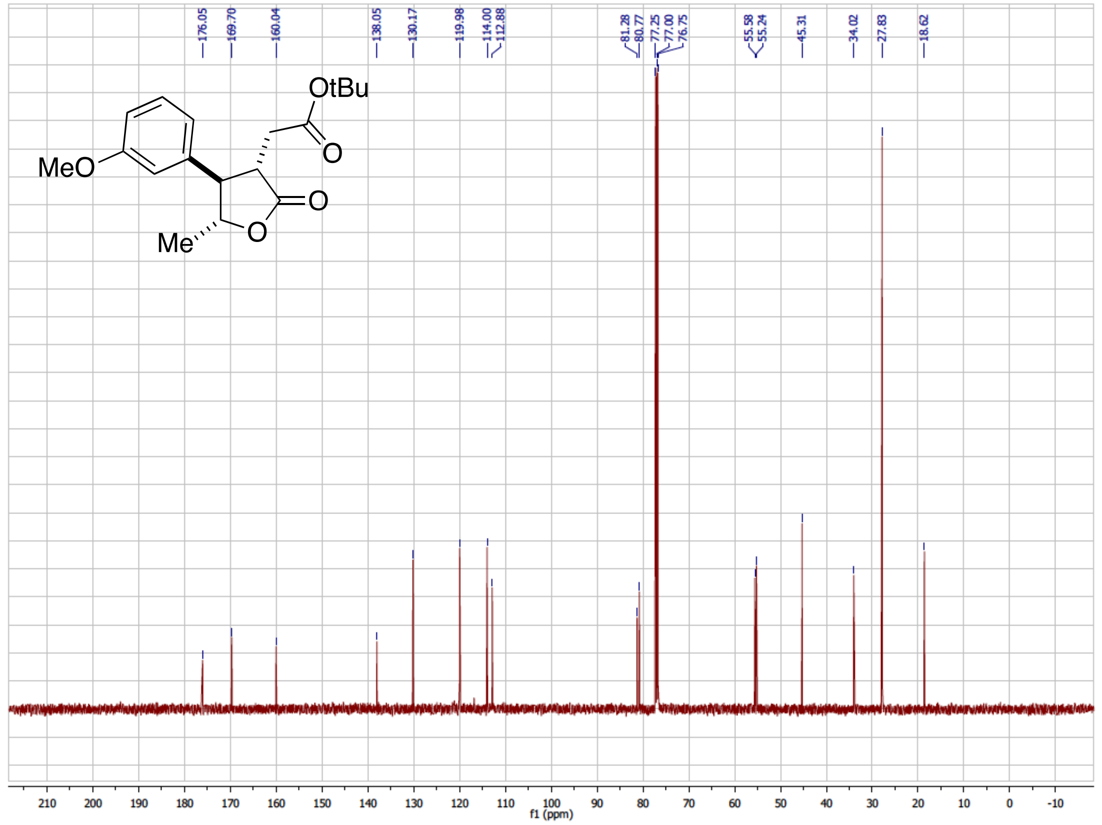
176.05
169.70
160.04
138.05
130.17
119.98
114.00
112.88
81.28
80.77
77.25
77.00
76.75
55.58
55.24
45.31
34.02
27.83
18.62
OtBu
MeO
O
O
Me
O
f1 (ppm)

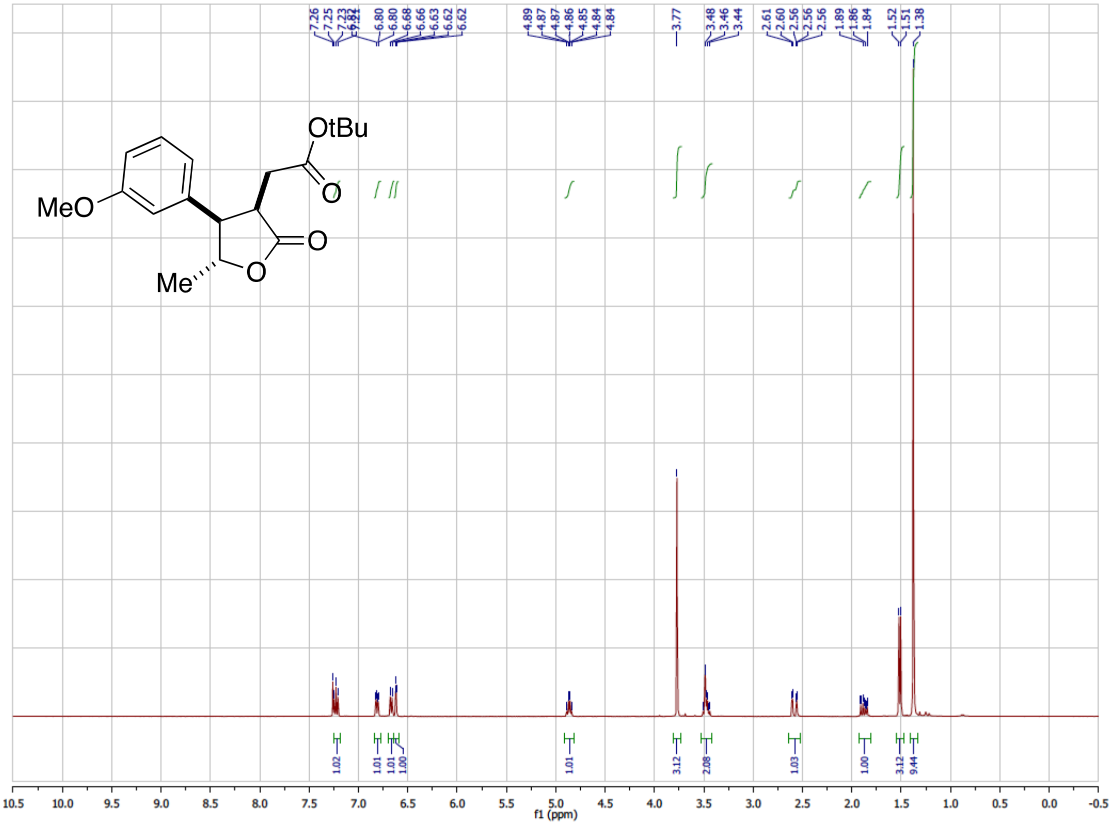
7.26
7.25
7.23
7.22
7.21
6.80
6.80
6.68
6.66
6.63
6.62
6.62
4.89
4.87
4.87
4.86
4.85
4.84
4.84
3.77
3.48
3.46
3.44
2.61
2.60
2.56
2.56
2.56
1.89
1.86
1.84
1.52
1.51
1.38
OtBu
O
MeO
O
Me
O
1.02
1.01
1.01
1.00
1.01
3.12
2.08
1.03
1.00
3.12
9.44
10.5
10.0
9.5
9.0
8.5
8.0
7.5
7.0
6.5
6.0
5.5
5.0
4.5
4.0
3.5
3.0
2.5
2.0
1.5
1.0
0.5
0.0
-0.5
f1 (ppm)

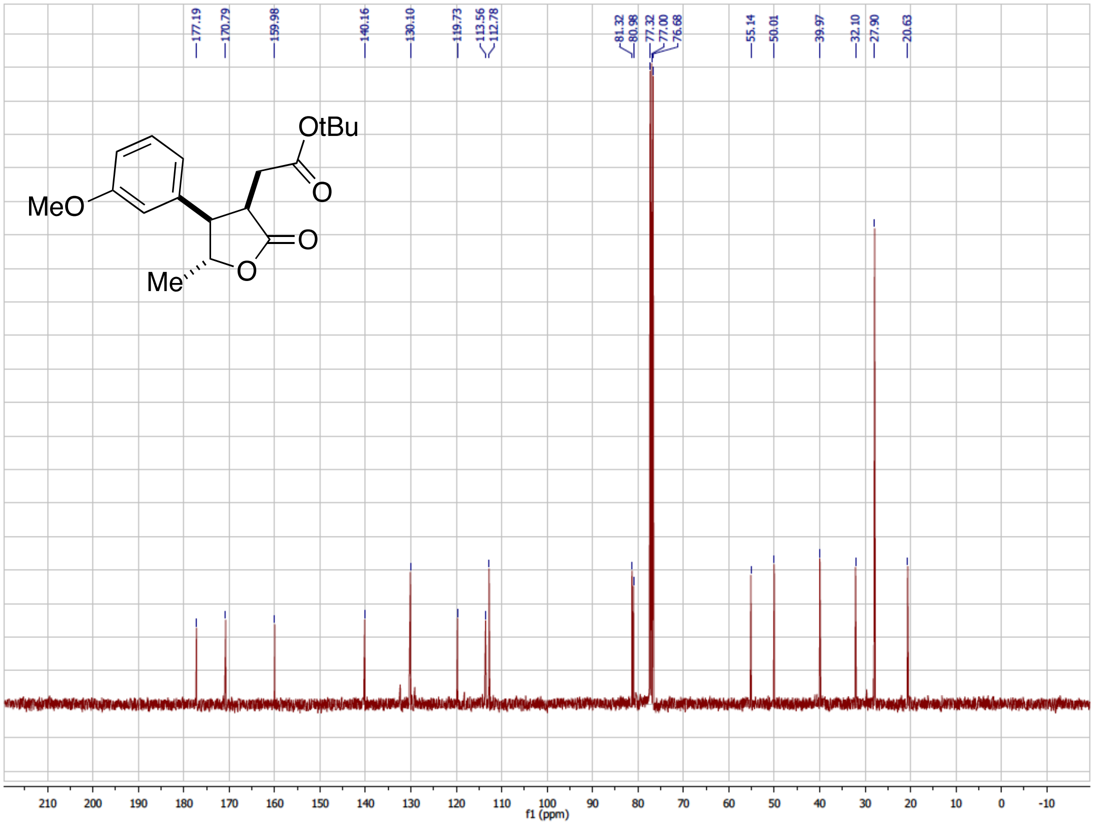
177.19
170.79
159.98
140.16
130.10
119.73
113.56
112.78
81.32
80.98
77.32
77.00
76.68
55.14
50.01
39.97
32.10
27.90
20.63
OtBu
O
MeO
O
Me
O
210
200
190
180
170
160
150
140
130
120
110
100
90
80
70
60
50
40
30
20
10
0
-10
f1 (ppm)

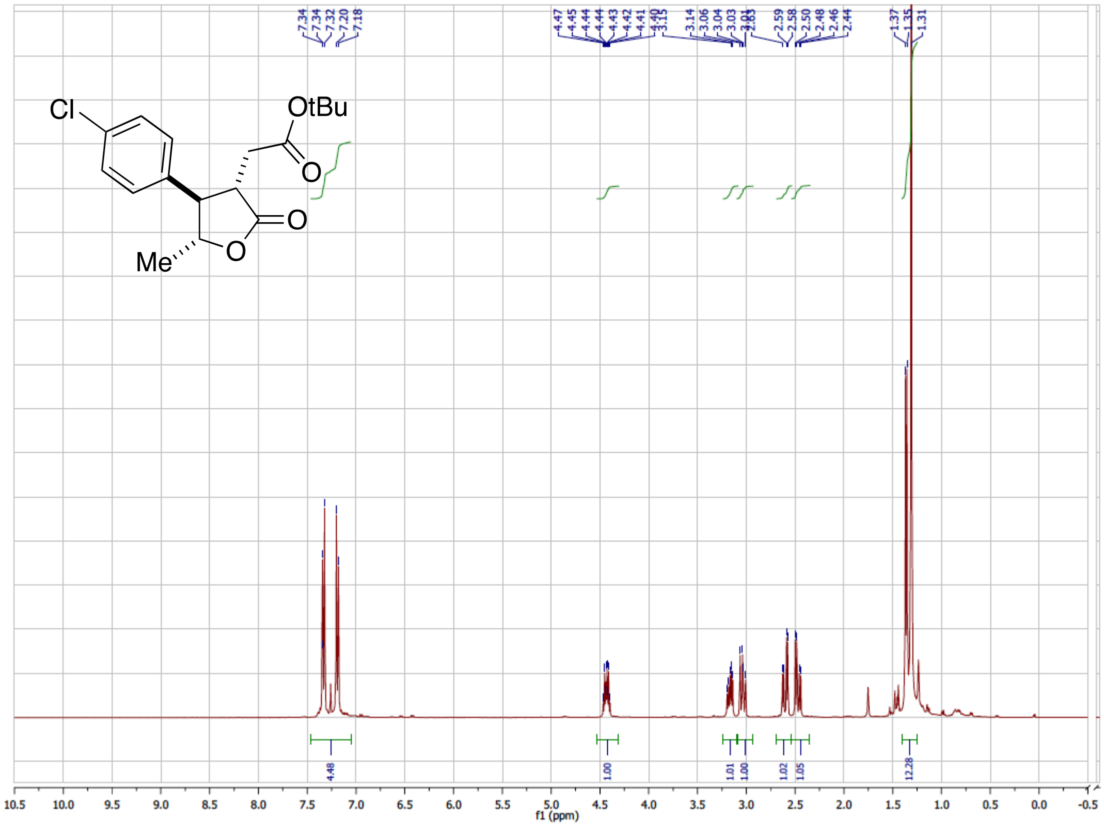
7.34
7.34
7.32
7.20
7.18
4.47
4.45
4.44
4.44
4.43
4.42
4.41
4.40
3.15
3.14
3.06
3.04
3.03
3.01
3.00
2.59
2.58
2.50
2.48
2.46
2.44
1.37
1.35
1.31
Cl
OtBu
O
O
Me
O
4.48
1.00
1.01
1.00
1.02
1.05
12.28
10.5
10.0
9.5
9.0
8.5
8.0
7.5
7.0
6.5
6.0
5.5
5.0
4.5
4.0
3.5
3.0
2.5
2.0
1.5
1.0
0.5
0.0
-0.5
f1 (ppm)

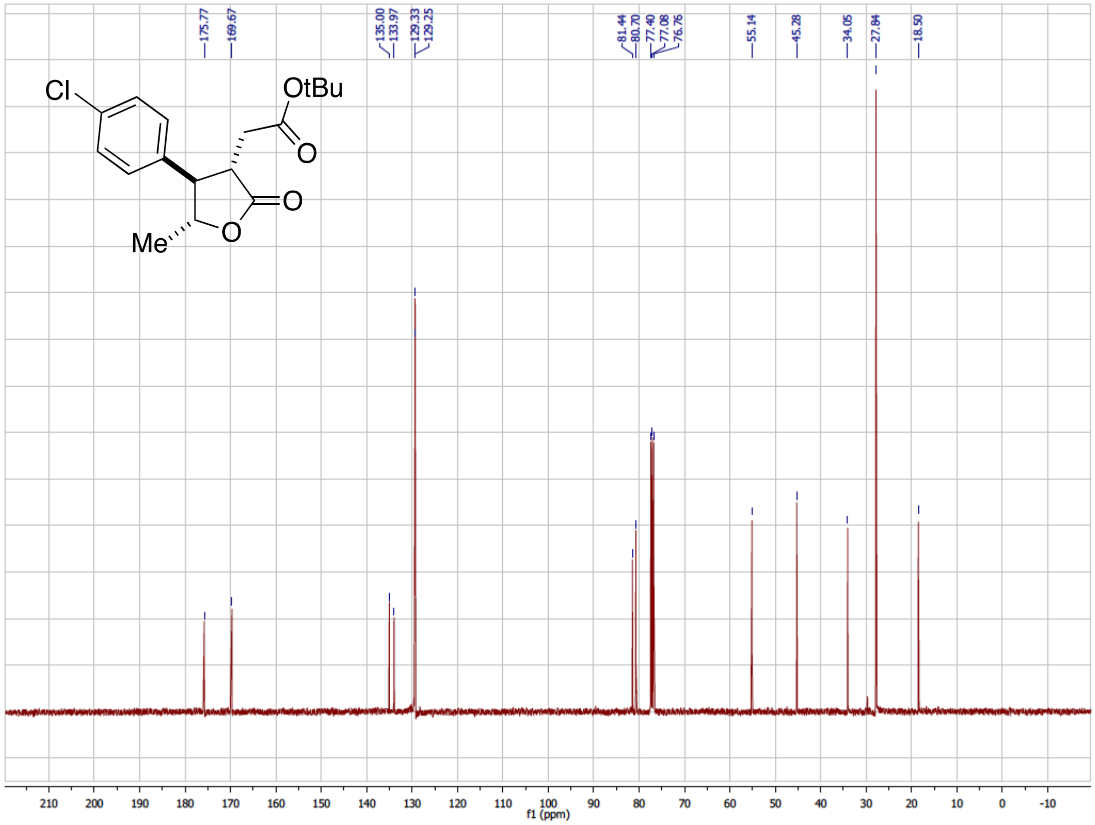
175.77
169.67
135.00
133.97
129.33
129.25
81.44
80.70
77.40
77.08
76.76
55.14
45.28
34.05
27.84
18.50
Cl
OtBu
O
O
Me
O
210
200
190
180
170
160
150
140
130
120
110
100
90
80
70
60
50
40
30
20
10
0
-10
f1 (ppm)

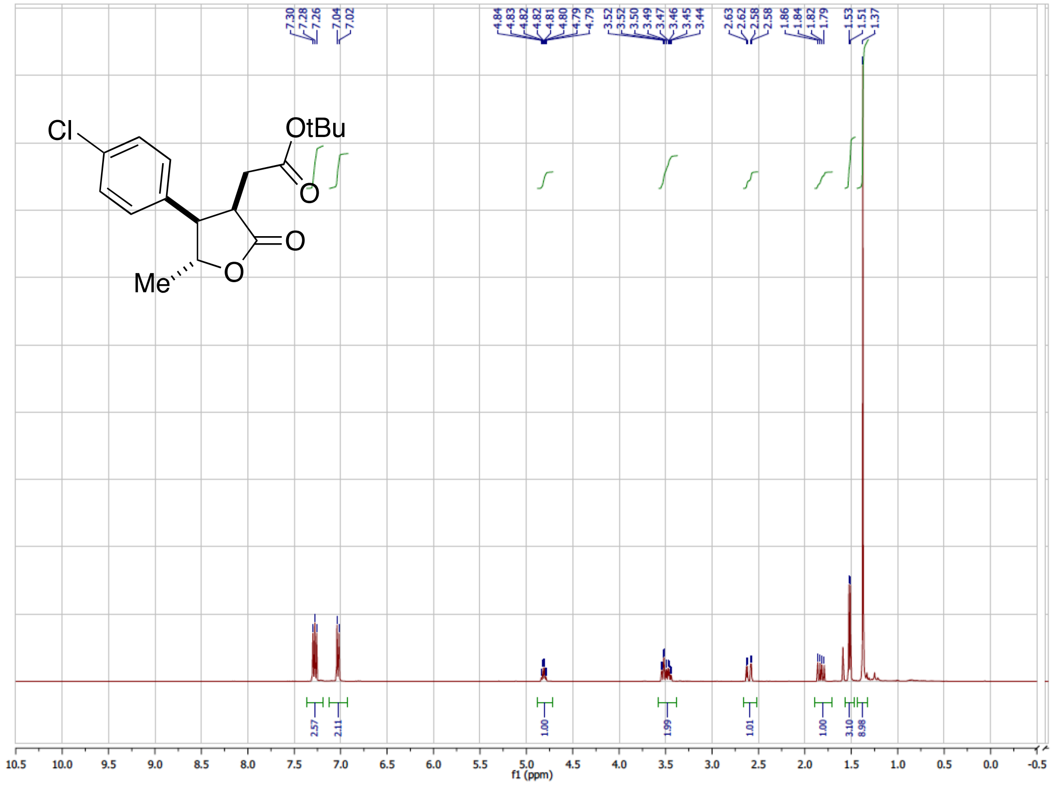
7.30
7.28
7.26
7.04
7.02
4.84
4.83
4.82
4.82
4.81
4.80
4.79
4.79
3.52
3.52
3.50
3.49
3.47
3.46
3.45
3.44
2.63
2.62
2.58
2.58
1.86
1.84
1.82
1.79
1.53
1.51
1.37
Cl
OtBu
O
O
Me
O
2.57
2.11
1.00
1.99
1.01
1.00
3.10
8.98
f1 (ppm)

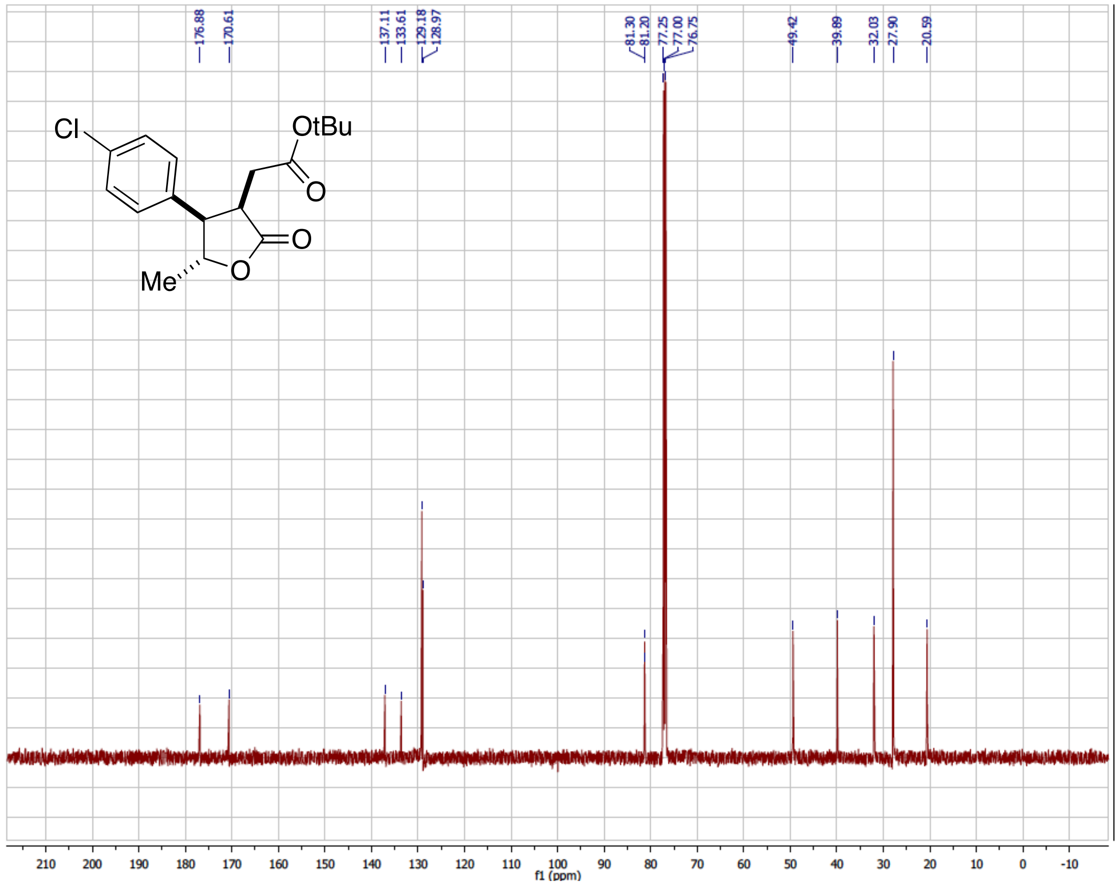
176.88
170.61
137.11
133.61
129.18
128.97
81.30
81.20
77.25
77.00
76.75
49.42
39.89
32.03
27.90
20.59
Cl
OtBu
O
O
Me
O
f1 (ppm)

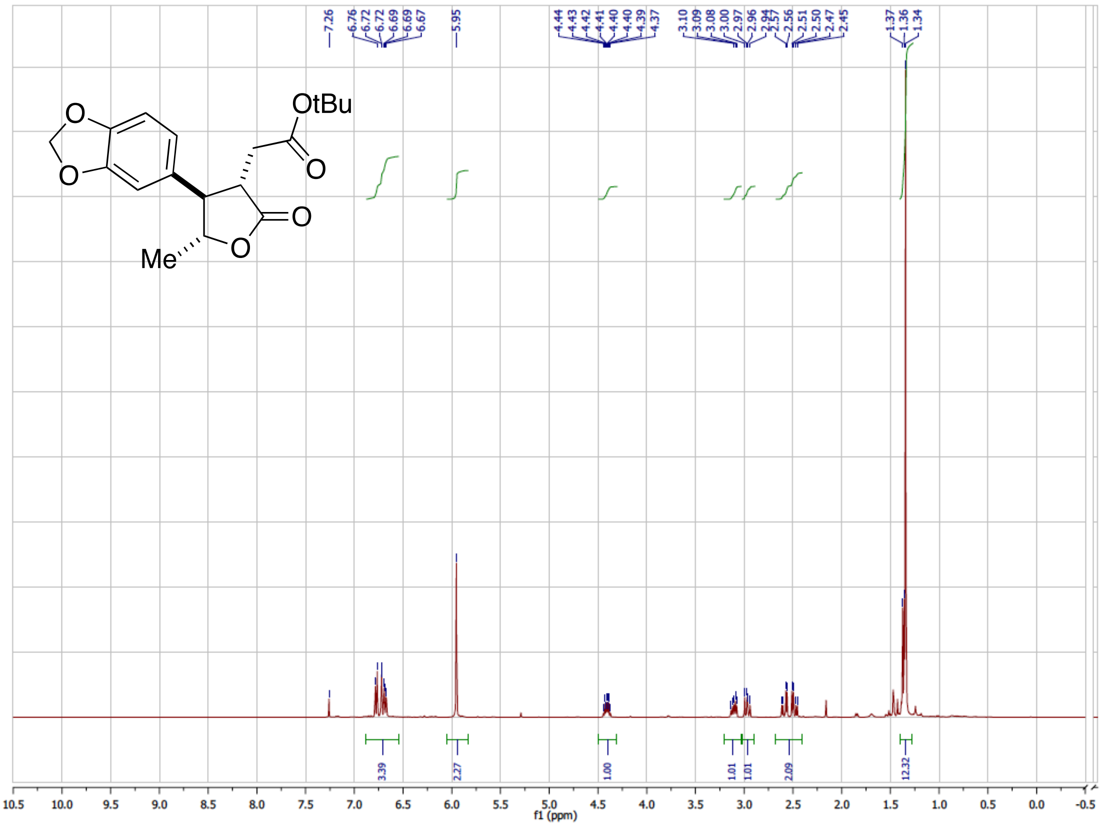
7.26
6.76
6.72
6.72
6.69
6.69
6.67
5.95
4.44
4.43
4.42
4.41
4.40
4.40
4.39
4.37
3.10
3.09
3.08
3.00
2.97
2.96
2.94
2.57
2.56
2.51
2.50
2.47
2.45
1.37
1.36
1.34
OtBu
O
O
O
O
O
Me
3.39
2.27
1.00
1.01
1.01
2.09
12.32
10.5
10.0
9.5
9.0
8.5
8.0
7.5
7.0
6.5
6.0
5.5
5.0
4.5
4.0
3.5
3.0
2.5
2.0
1.5
1.0
0.5
0.0
-0.5
f1 (ppm)

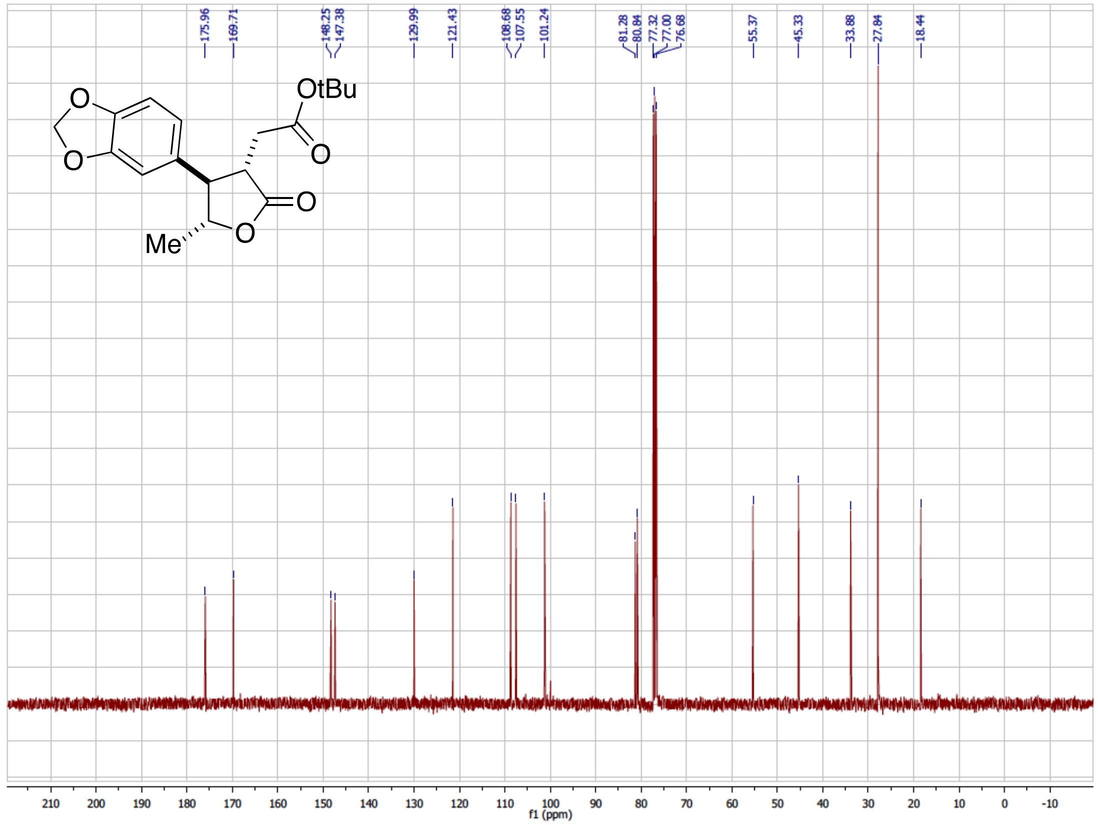
175.96
169.71
148.25
147.38
129.99
121.43
108.68
107.55
101.24
81.28
80.84
77.32
77.00
76.68
55.37
45.33
33.88
27.84
18.44
OtBu
O
O
O
O
O
Me
210
200
190
180
170
160
150
140
130
120
110
100
90
80
70
60
50
40
30
20
10
0
-10
f1 (ppm)

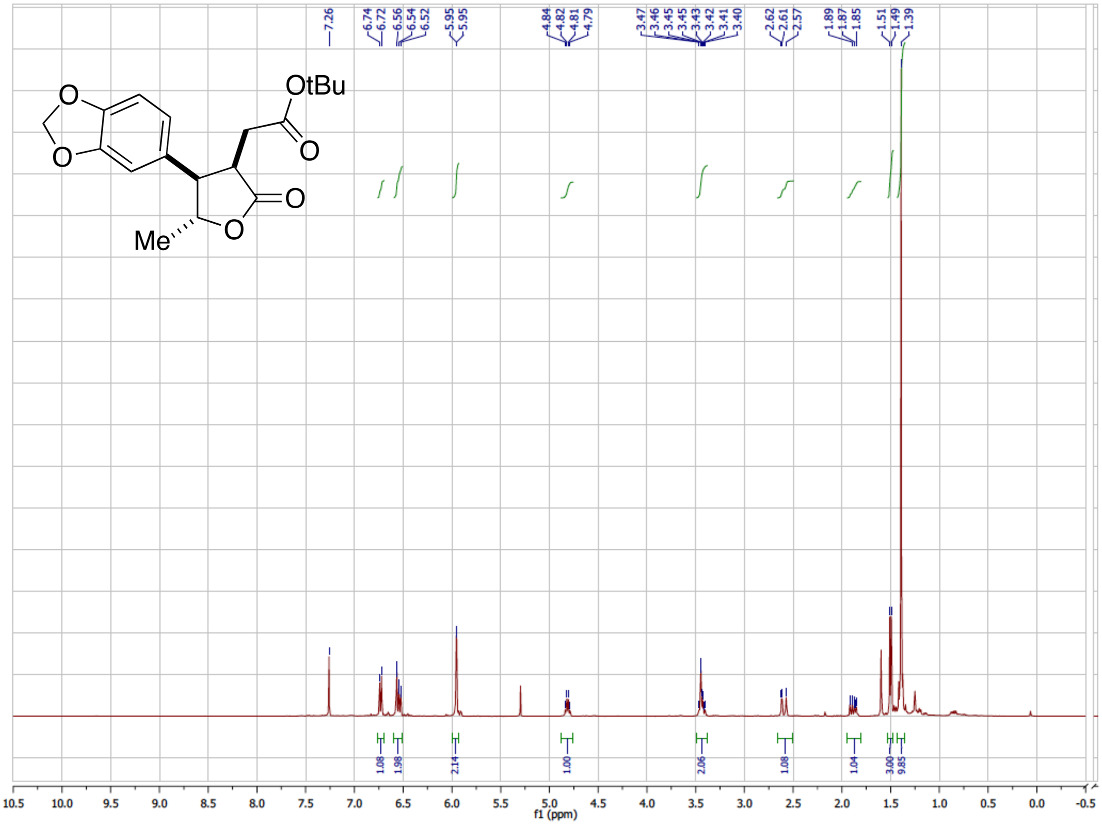
7.26
6.74
6.72
6.56
6.54
6.52
5.95
5.95
4.84
4.82
4.81
4.79
3.47
3.46
3.45
3.45
3.43
3.42
3.41
3.40
2.62
2.61
2.57
1.89
1.87
1.85
1.51
1.49
1.39
OtBu
O
O
O
O
O
Me
1.08
1.98
2.14
1.00
2.06
1.08
1.04
3.00
9.85
10.5
10.0
9.5
9.0
8.5
8.0
7.5
7.0
6.5
6.0
5.5
5.0
4.5
4.0
3.5
3.0
2.5
2.0
1.5
1.0
0.5
0.0
-0.5
f1 (ppm)

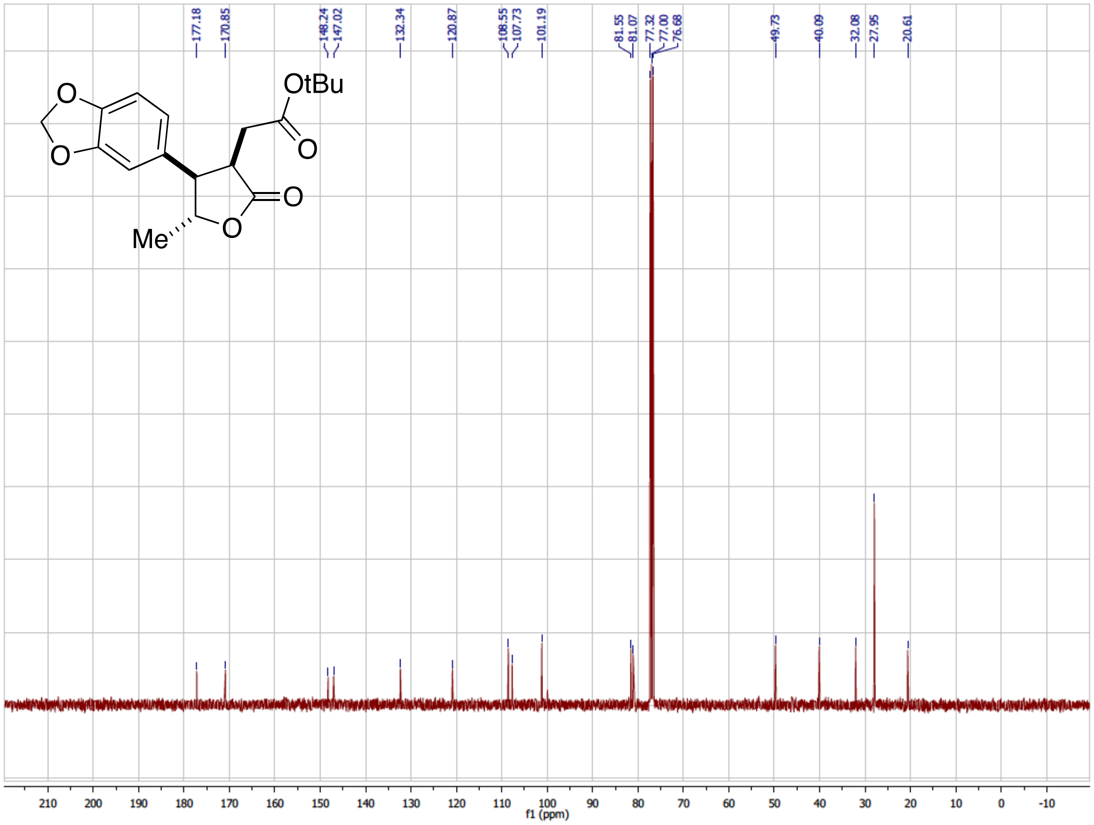
177.18
170.85
148.24
147.02
132.34
120.87
108.55
107.73
101.19
81.55
81.07
77.32
77.00
76.68
49.73
40.09
32.08
27.95
20.61
OtBu
O
O
O
O
O
Me
210
200
190
180
170
160
150
140
130
120
110
100
90
80
70
60
50
40
30
20
10
0
-10
f1 (ppm)

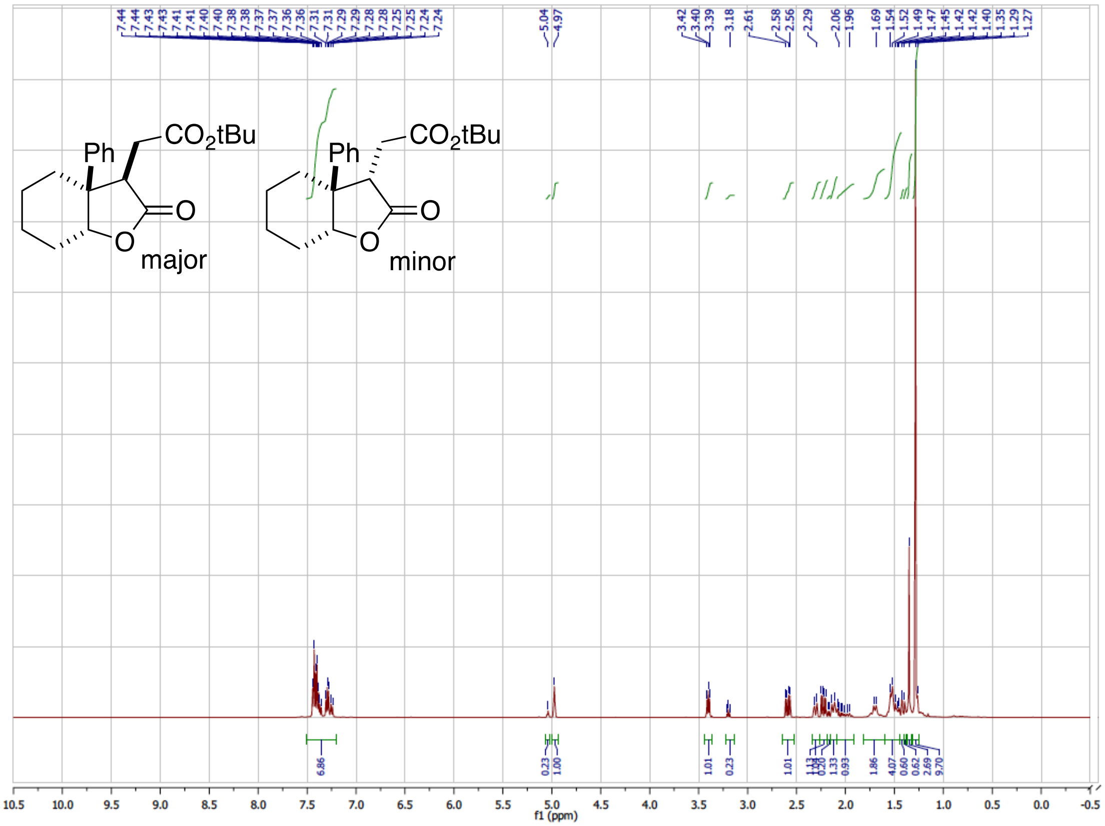
7.44
7.44
7.43
7.43
7.41
7.41
7.40
7.40
7.38
7.38
7.37
7.37
7.36
7.36
7.31
7.31
7.29
7.29
7.28
7.28
7.25
7.25
7.24
7.24
5.04
4.97
3.42
3.40
3.39
3.18
2.61
2.58
2.56
2.29
2.06
1.96
1.69
1.54
1.52
1.49
1.47
1.45
1.42
1.42
1.40
1.35
1.29
1.27
Ph
CO2tBu
O
O
major
Ph
CO2tBu
O
O
minor
6.86
0.23
1.00
1.01
0.23
1.01
1.13
1.04
0.20
1.33
0.93
1.86
4.07
0.60
0.62
2.69
9.70
10.5
10.0
9.5
9.0
8.5
8.0
7.5
7.0
6.5
6.0
5.5
5.0
4.5
4.0
3.5
3.0
2.5
2.0
1.5
1.0
0.5
0.0
-0.5
f1 (ppm)

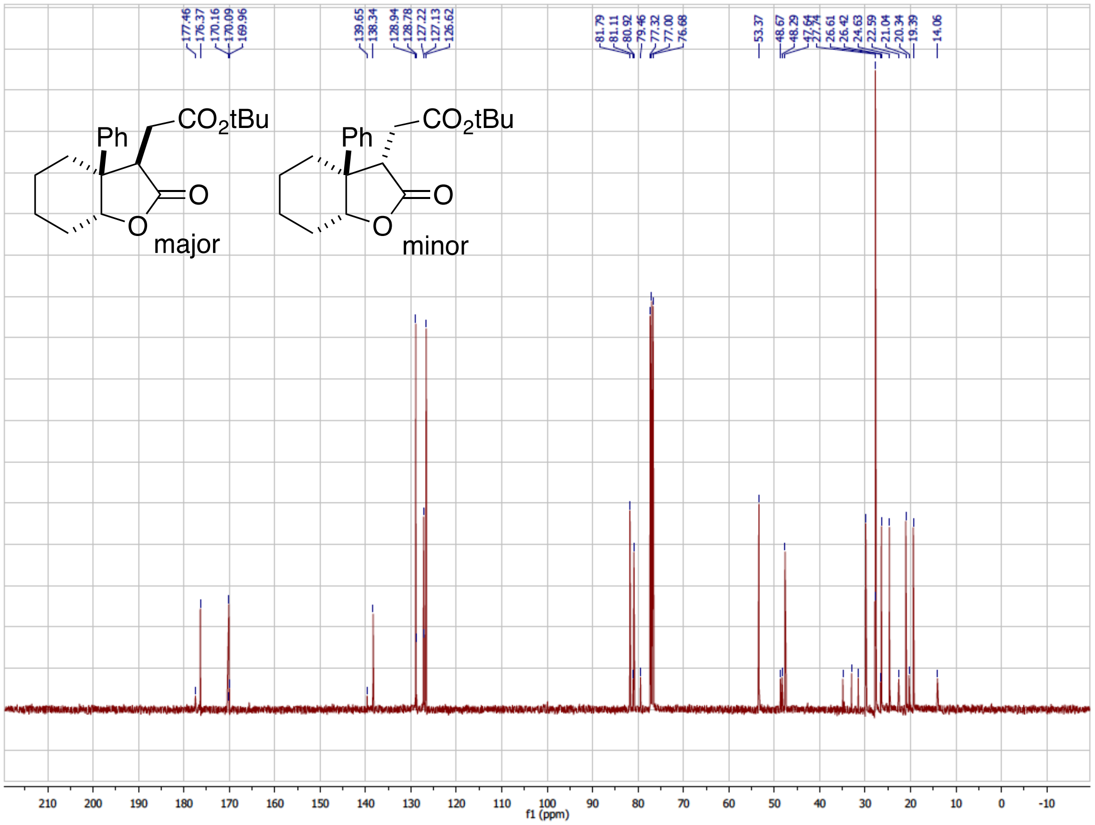
177.46
176.37
170.16
170.09
169.96
139.65
138.34
128.94
128.78
127.22
127.13
126.62
81.79
81.11
80.92
79.46
77.32
77.00
76.68
53.37
48.67
48.29
47.64
27.74
26.61
26.42
24.63
22.59
21.04
20.34
19.39
14.06
Ph
CO2tBu
O
O
major
Ph
CO2tBu
O
O
minor
210
200
190
180
170
160
150
140
130
120
110
100
90
80
70
60
50
40
30
20
10
0
-10
f1 (ppm)

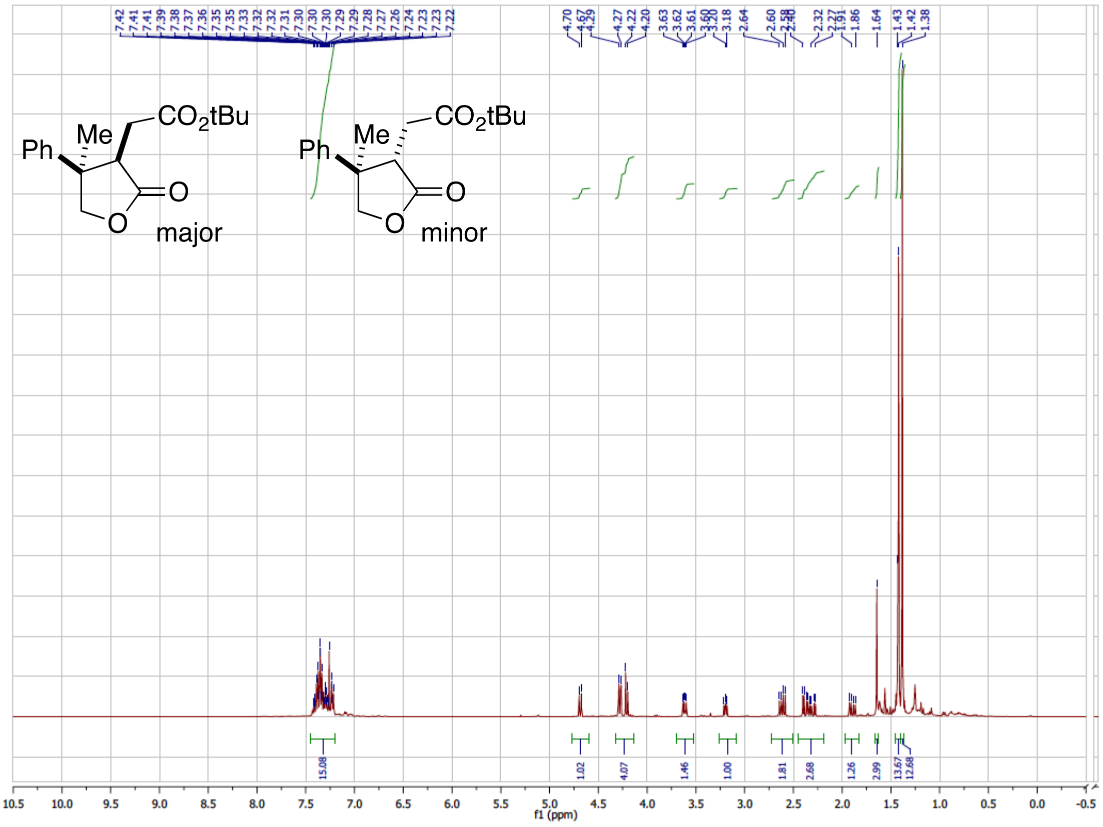
7.42
7.41
7.41
7.39
7.38
7.37
7.36
7.35
7.35
7.33
7.32
7.32
7.31
7.30
7.30
7.30
7.29
7.29
7.28
7.27
7.26
7.24
7.23
7.23
7.22
4.70
4.67
4.29
4.27
4.22
4.20
3.63
3.62
3.61
3.60
3.20
3.18
2.64
2.60
2.58
2.40
2.32
2.27
1.91
1.86
1.64
1.43
1.42
1.38
Ph
Me
CO2tBu
O
O
major
Ph
Me
CO2tBu
O
O
minor
15.08
1.02
4.07
1.46
1.00
1.81
2.68
1.26
2.99
13.67
12.68
10.5
10.0
9.5
9.0
8.5
8.0
7.5
7.0
6.5
6.0
5.5
5.0
4.5
4.0
3.5
3.0
2.5
2.0
1.5
1.0
0.5
0.0
-0.5
f1 (ppm)

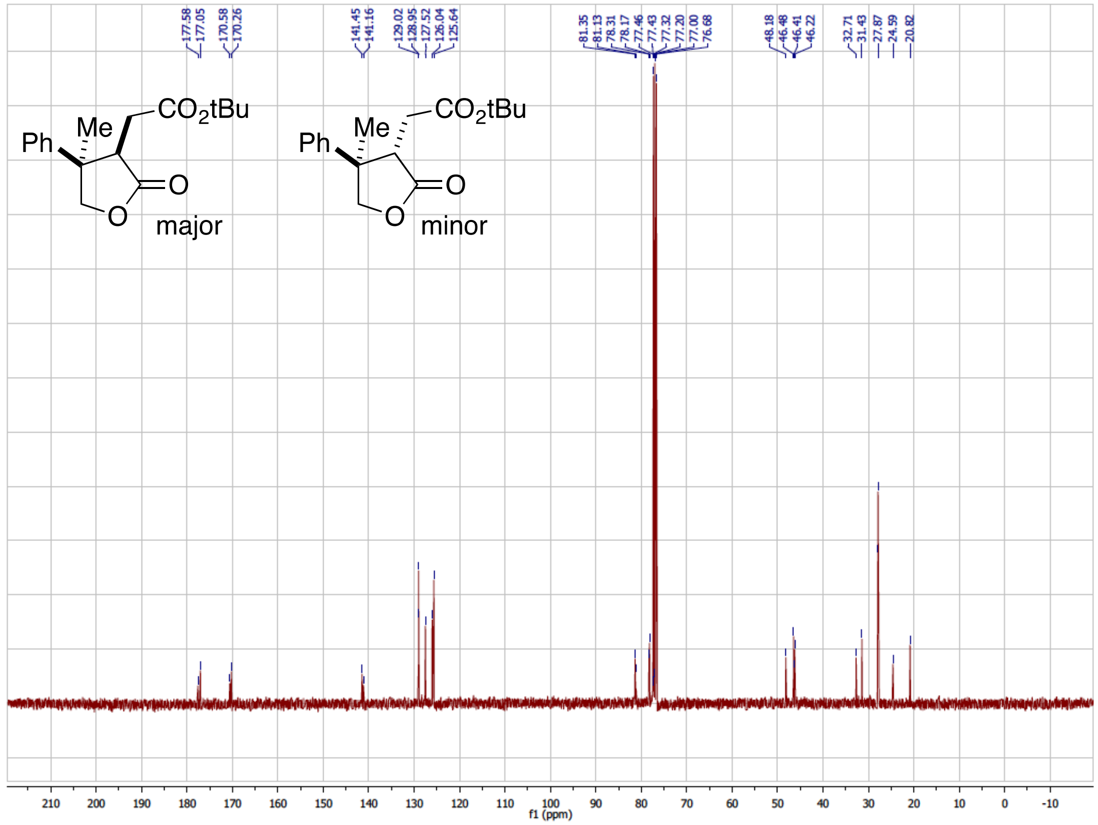
177.58
177.05
170.58
170.26
141.45
141.16
129.02
128.95
127.52
126.04
125.64
81.35
81.13
78.31
78.17
77.46
77.43
77.32
77.20
77.00
76.68
48.18
46.48
46.41
46.22
32.71
31.43
27.87
24.59
20.82
Ph
Me
CO2tBu
O
O
major
Ph
Me
CO2tBu
O
O
minor
210
200
190
180
170
160
150
140
130
120
110
100
90
80
70
60
50
40
30
20
10
0
-10
f1 (ppm)

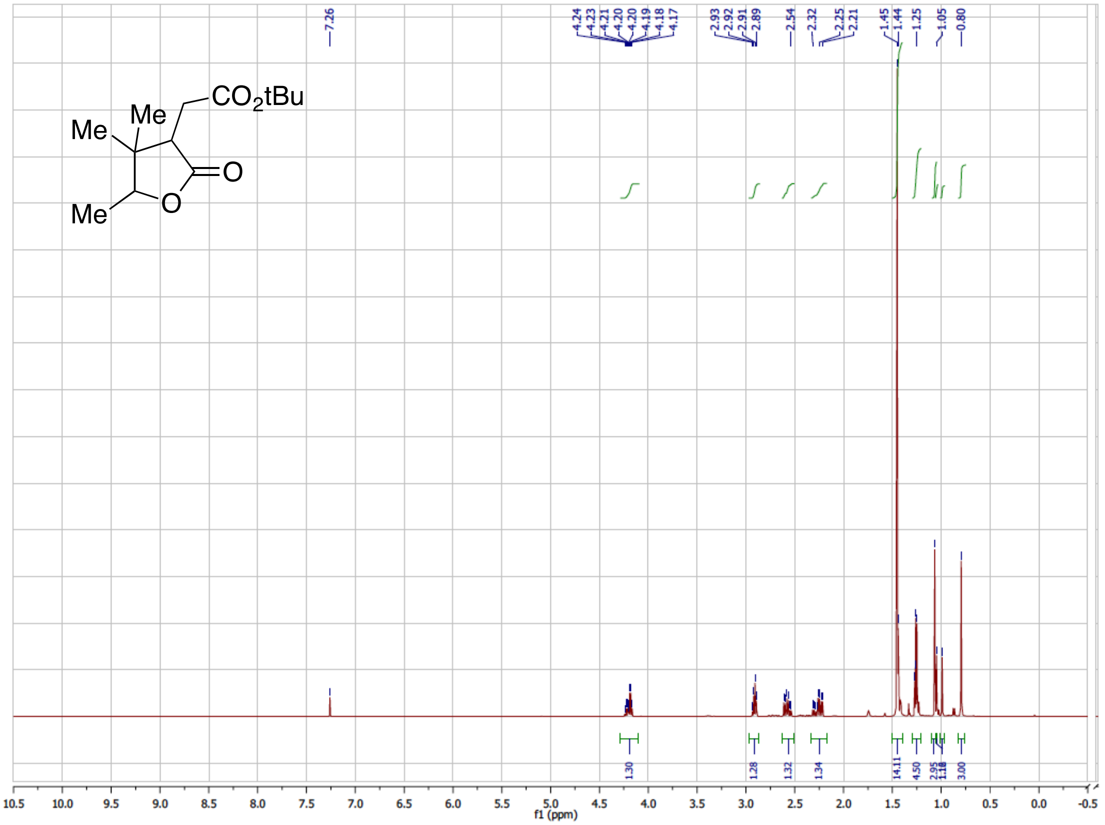
CO2tBu
Me
Me
O
Me
O
7.26
4.24
4.23
4.21
4.20
4.20
4.19
4.18
4.17
2.93
2.92
2.91
2.89
2.54
2.32
2.25
2.21
1.45
1.44
1.25
1.05
0.80
1.30
1.28
1.32
1.34
14.11
4.50
2.95
1.18
3.00
10.5
10.0
9.5
9.0
8.5
8.0
7.5
7.0
6.5
6.0
5.5
5.0
4.5
4.0
3.5
3.0
2.5
2.0
1.5
1.0
0.5
0.0
-0.5
f1 (ppm)

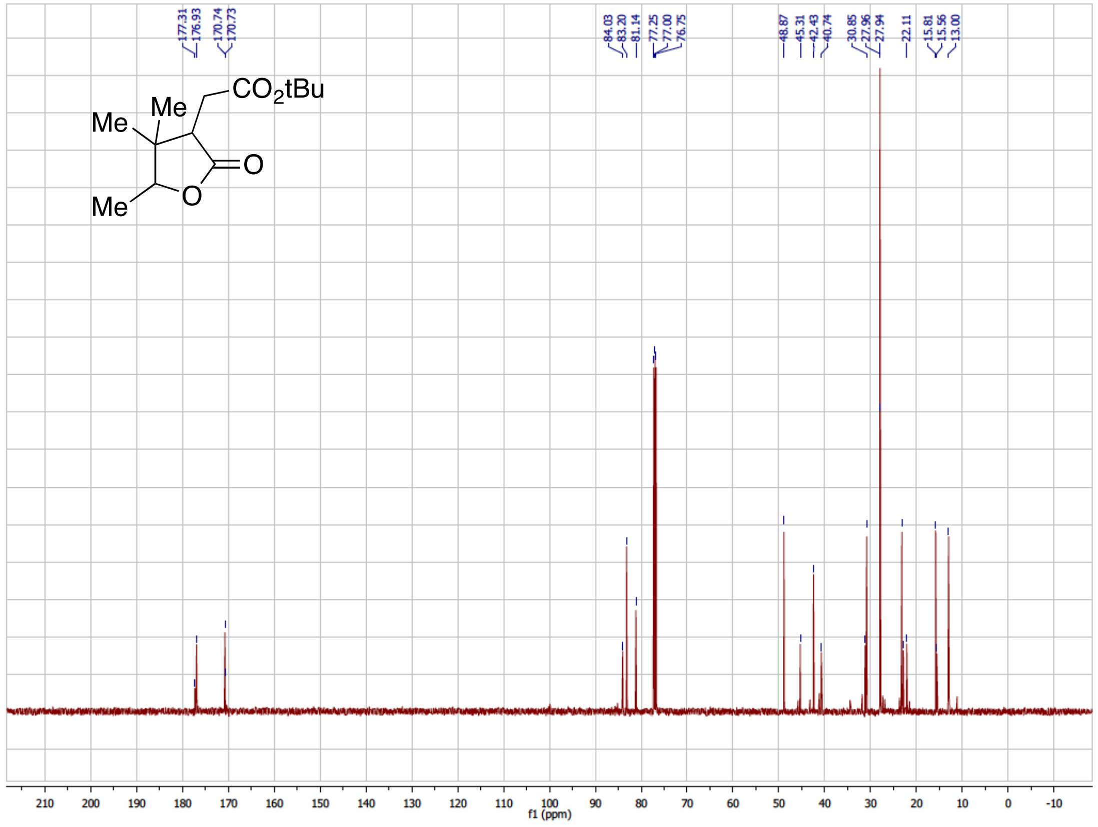
CO2tBu
Me
Me
O
Me
O
177.31
176.93
170.74
170.73
84.03
83.20
81.14
77.25
77.00
76.75
48.87
45.31
42.43
40.74
30.85
22.96
27.94
22.11
15.81
15.56
13.00
210
200
190
180
170
160
150
140
130
120
110
100
90
80
70
60
50
40
30
20
10
0
-10
f1 (ppm)

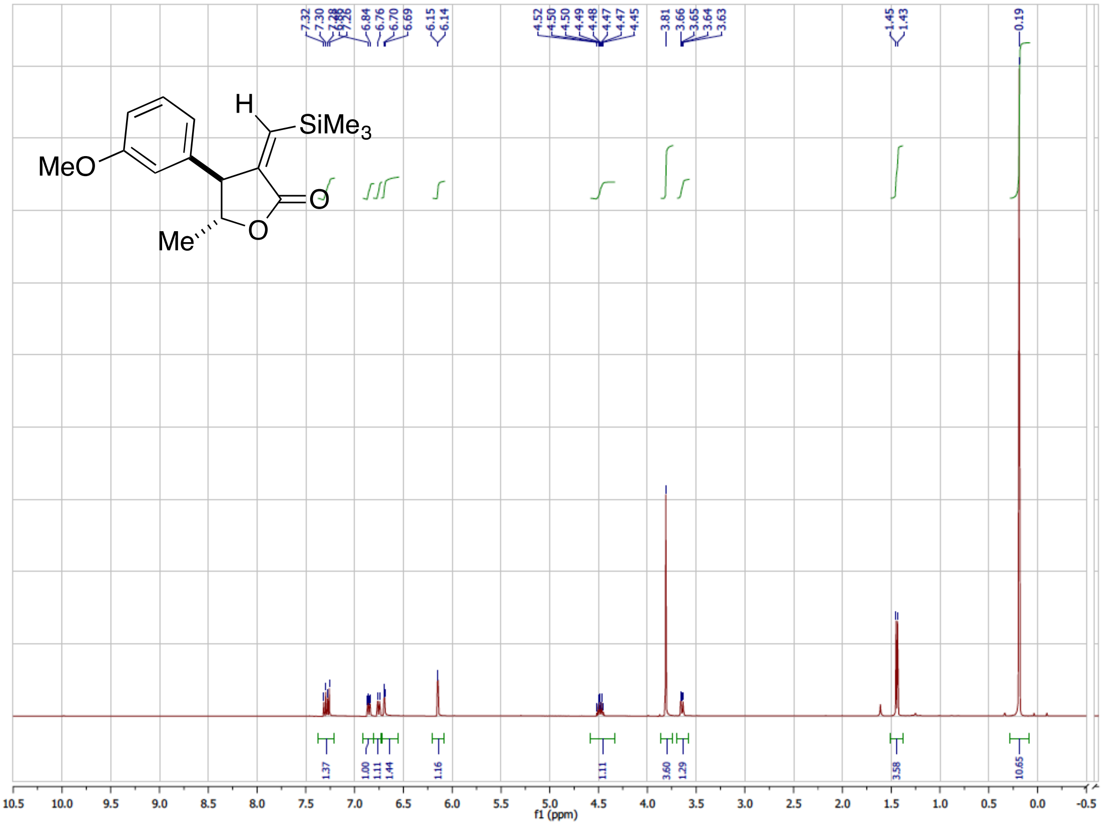
7.32
7.30
7.28
7.28
7.26
6.84
6.76
6.70
6.69
6.15
6.14
4.52
4.50
4.50
4.49
4.48
4.47
4.47
4.45
3.81
3.66
3.65
3.64
3.63
1.45
1.43
0.19
MeO
H
SiMe3
O
Me
O
1.37
1.00
1.11
1.44
1.16
1.11
3.60
1.29
3.58
10.65
10.5 10.0 9.5 9.0 8.5 8.0 7.5 7.0 6.5 6.0 5.5 5.0 4.5 4.0 3.5 3.0 2.5 2.0 1.5 1.0 0.5 0.0 -0.5
f1 (ppm)

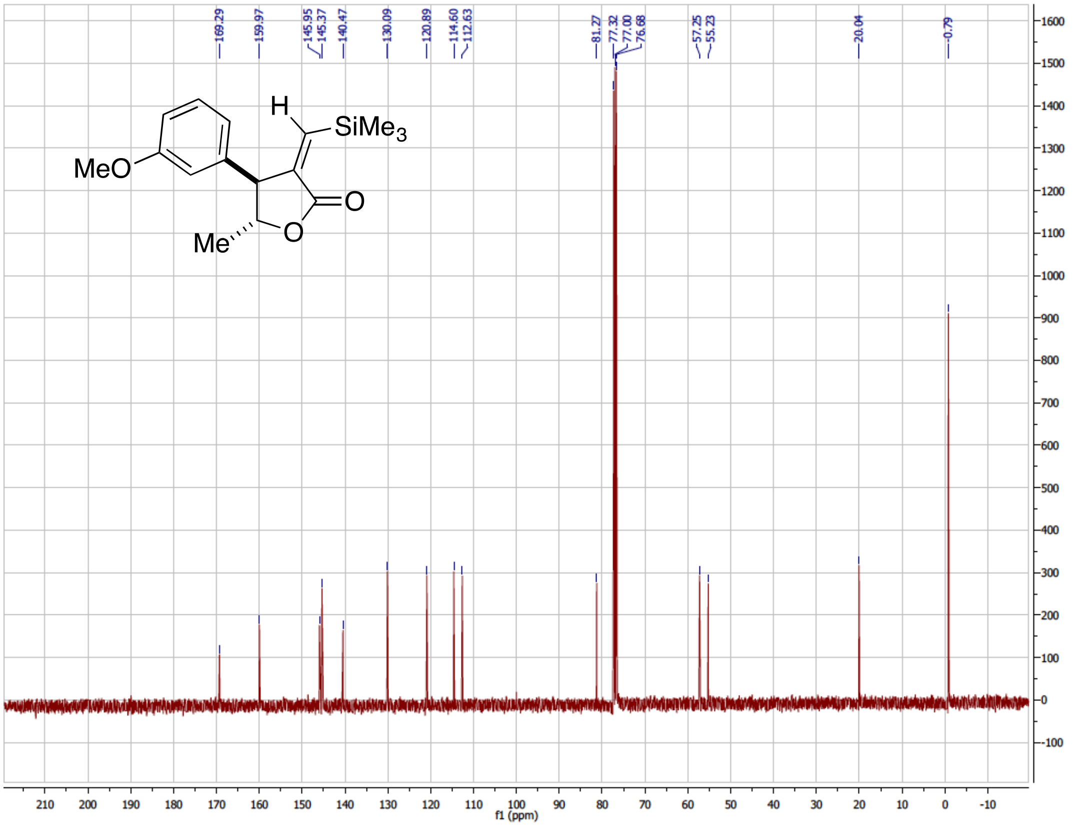
169.29
159.97
145.95
145.37
140.47
130.09
120.89
114.60
112.63
81.27
77.32
77.00
76.68
57.25
55.23
20.04
-0.79
MeO
H
SiMe3
O
Me
O
1600 1500 1400 1300 1200 1100 1000 900 800 700 600 500 400 300 200 100 0 -100
210 200 190 180 170 160 150 140 130 120 110 100 90 80 70 60 50 40 30 20 10 0 -10
f1 (ppm)

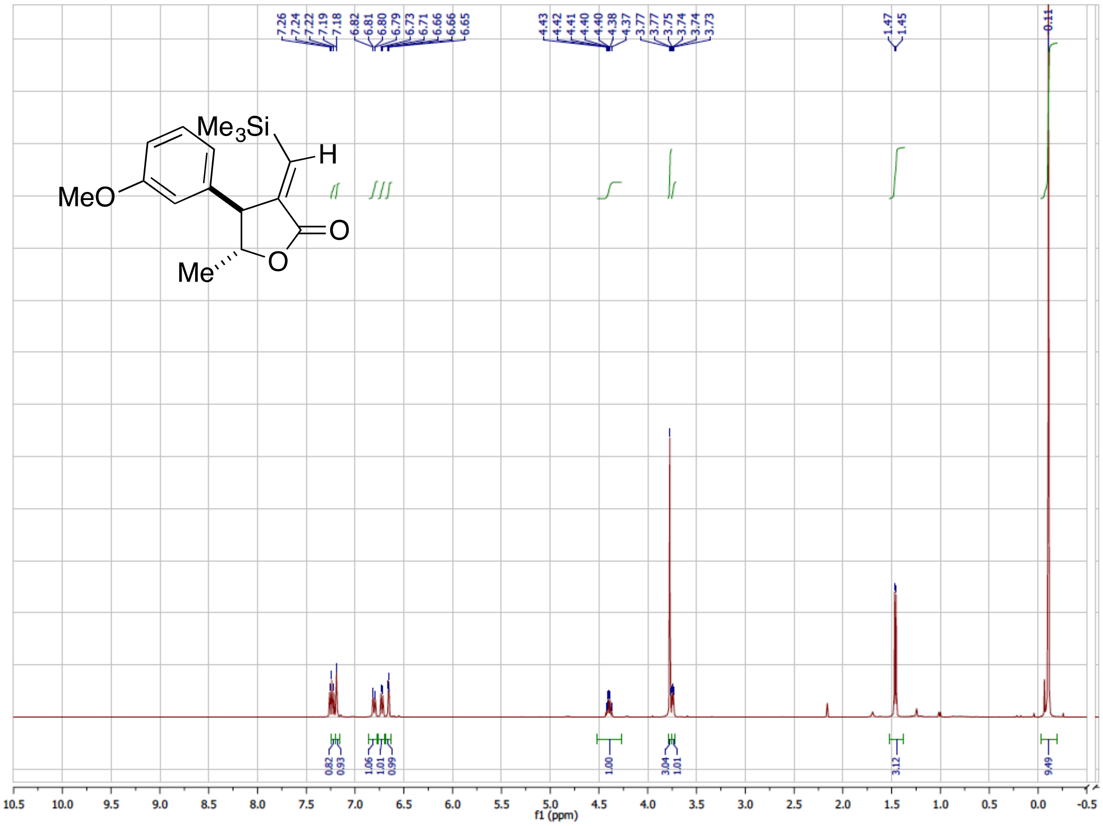
7.26
7.24
7.22
7.19
7.18
6.82
6.81
6.80
6.79
6.73
6.71
6.66
6.65
4.43
4.42
4.41
4.40
4.40
4.38
4.37
3.77
3.77
3.75
3.74
3.74
3.73
1.47
1.45
0.11
Me3Si
H
MeO
O
Me
O
0.82
0.93
1.06
1.01
0.99
1.00
3.04
1.01
3.12
9.49
10.5
10.0
9.5
9.0
8.5
8.0
7.5
7.0
6.5
6.0
5.5
5.0
4.5
4.0
3.5
3.0
2.5
2.0
1.5
1.0
0.5
0.0
-0.5
f1 (ppm)

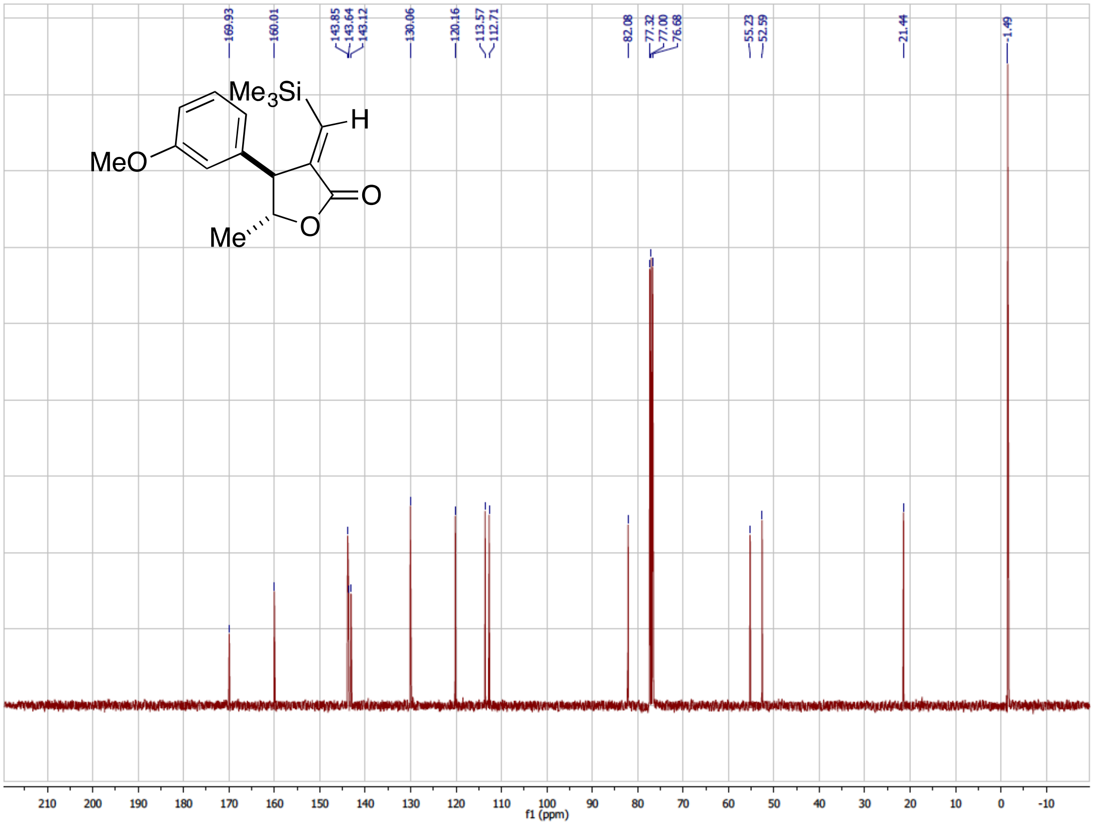
169.93
160.01
143.85
143.64
143.12
130.06
120.16
113.57
112.71
82.08
77.32
77.00
76.68
55.23
52.59
21.44
-1.49
Me3Si
H
MeO
O
Me
O
210
200
190
180
170
160
150
140
130
120
110
100
90
80
70
60
50
40
30
20
10
0
-10
f1 (ppm)

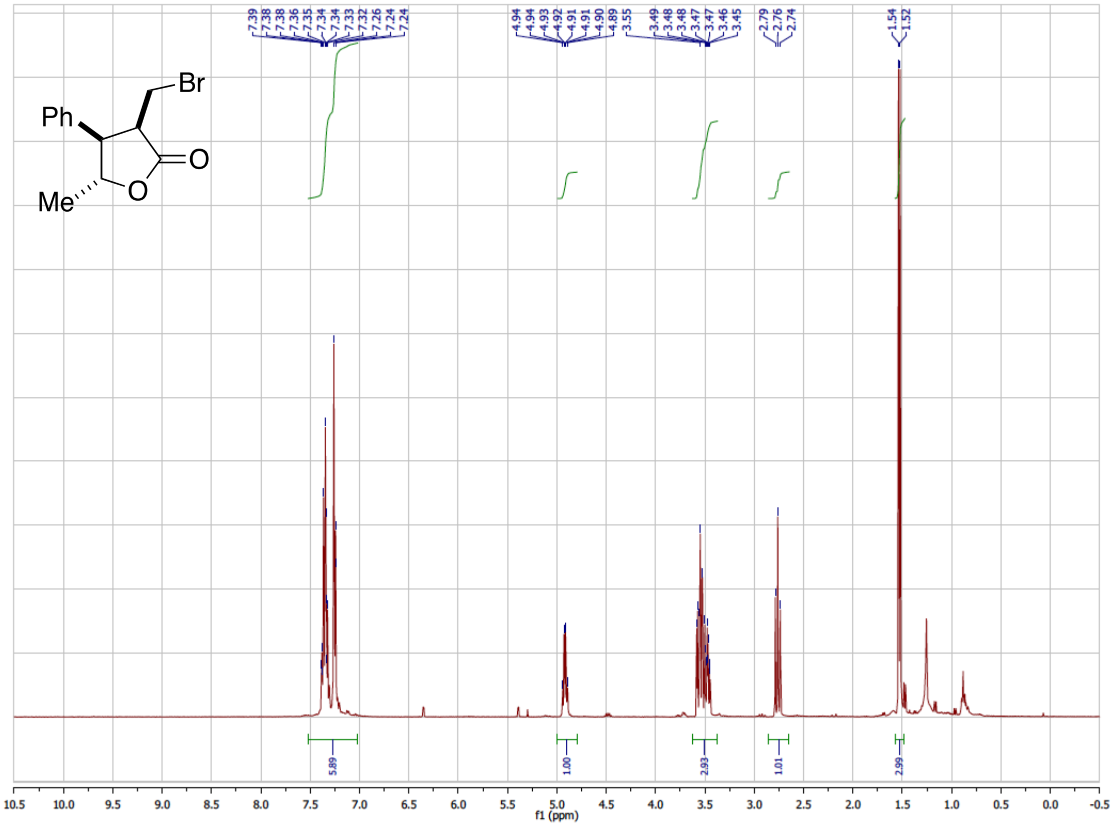
Ph
Br
O
Me
O
7.39
7.38
7.38
7.36
7.35
7.34
7.34
7.33
7.32
7.26
7.24
7.24
4.94
4.94
4.93
4.92
4.91
4.91
4.90
4.89
3.55
3.49
3.48
3.48
3.47
3.47
3.46
3.45
2.79
2.76
2.74
1.54
1.52
5.89
1.00
2.93
1.01
2.99
10.5
10.0
9.5
9.0
8.5
8.0
7.5
7.0
6.5
6.0
5.5
5.0
4.5
4.0
3.5
3.0
2.5
2.0
1.5
1.0
0.5
0.0
-0.5
f1 (ppm)

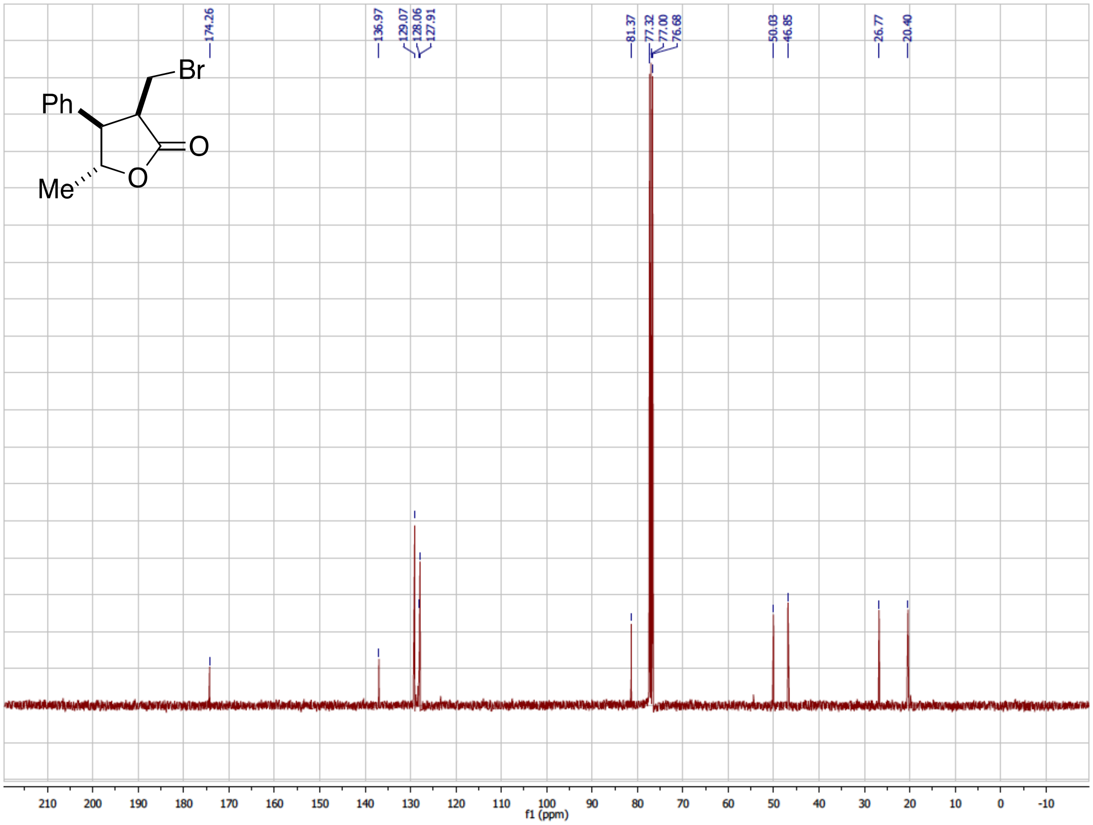
Ph
Br
O
Me
O
174.26
136.97
129.07
128.06
127.91
81.37
77.32
77.00
76.68
50.03
46.85
26.77
20.40
210
200
190
180
170
160
150
140
130
120
110
100
90
80
70
60
50
40
30
20
10
0
-10
f1 (ppm)

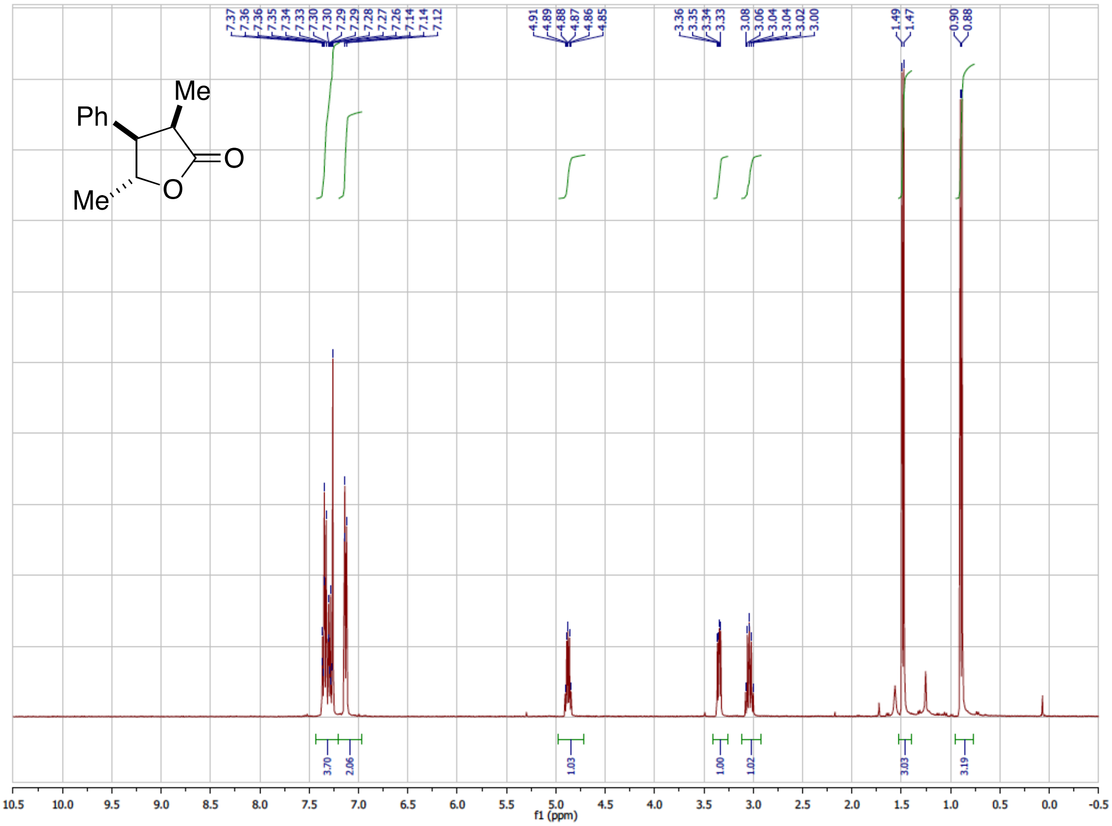
7.37
7.36
7.36
7.35
7.34
7.33
7.30
7.30
7.29
7.29
7.28
7.27
7.26
7.14
7.12
4.91
4.89
4.88
4.87
4.86
4.85
3.36
3.35
3.34
3.33
3.08
3.06
3.04
3.04
3.02
3.00
1.49
1.47
0.90
0.88
Ph
Me
O
Me
O
3.70
2.06
1.03
1.00
1.02
3.03
3.19
10.5
10.0
9.5
9.0
8.5
8.0
7.5
7.0
6.5
6.0
5.5
5.0
4.5
4.0
3.5
3.0
2.5
2.0
1.5
1.0
0.5
0.0
-0.5
f1 (ppm)

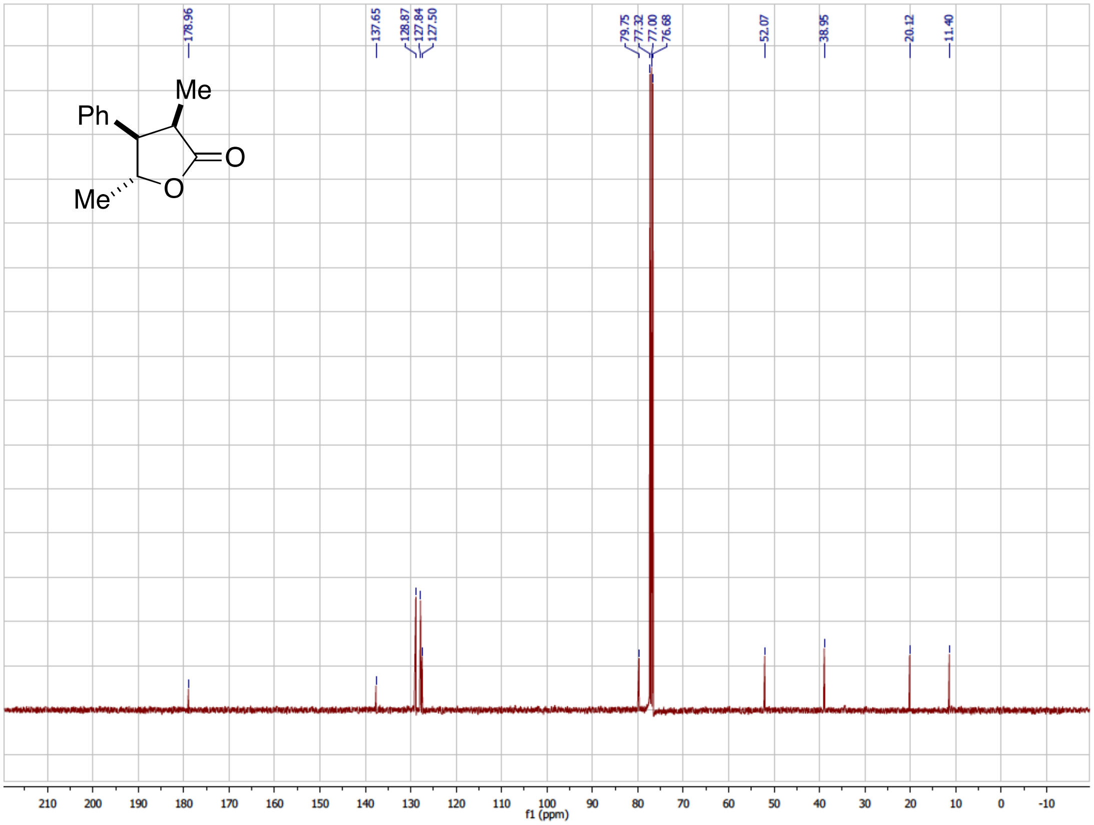
178.96
137.65
128.87
127.84
127.50
79.75
77.32
77.00
76.68
52.07
38.95
20.12
11.40
Ph
Me
O
Me
O
210
200
190
180
170
160
150
140
130
120
110
100
90
80
70
60
50
40
30
20
10
0
-10
f1 (ppm)

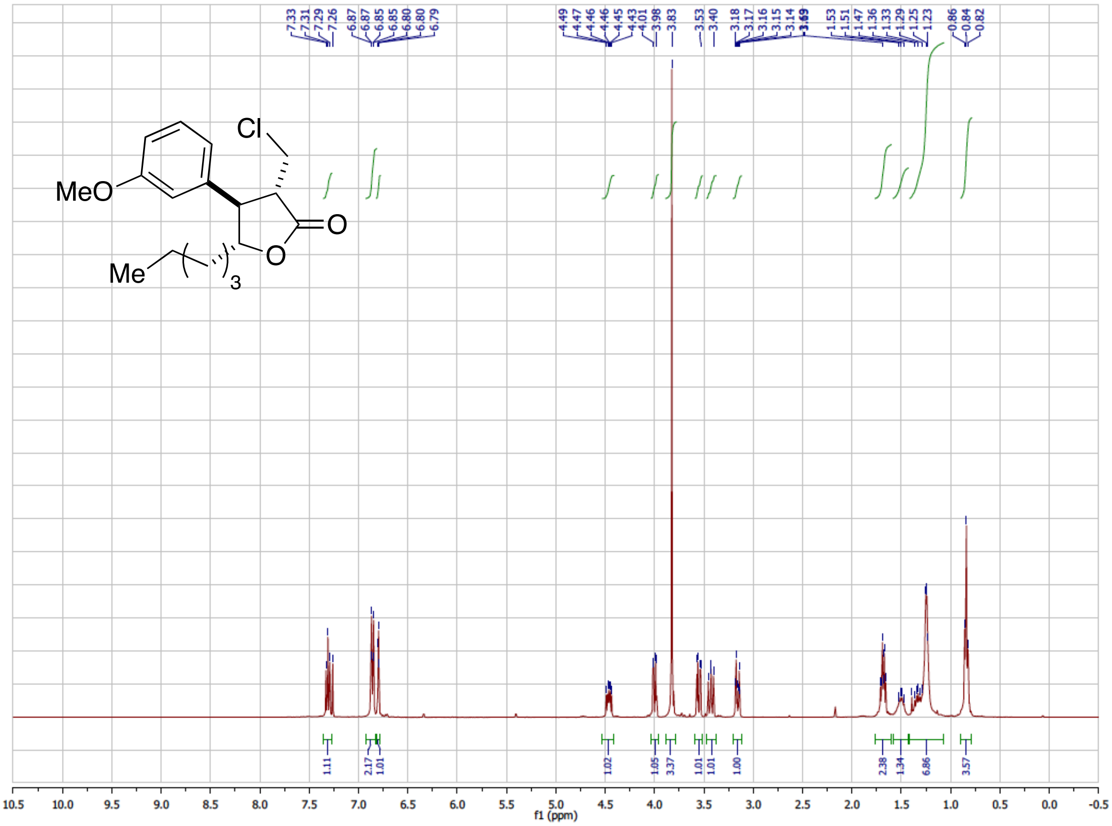
7.33 7.31 7.29 7.26 6.87 6.87 6.85 6.85 6.80 6.80 6.79
4.49 4.47 4.46 4.46 4.45 4.43 4.01 3.98 3.83 3.53 3.40 3.18 3.17 3.16 3.15 3.14 3.69 1.53 1.51 1.47 1.36 1.33 1.29 1.25 1.23 0.86 0.84 0.82
Cl
MeO
O
O
Me
3
1.11 2.17 1.01 1.02 1.05 3.37 1.01 1.01 1.00 2.38 1.34 6.86 3.57
10.5 10.0 9.5 9.0 8.5 8.0 7.5 7.0 6.5 6.0 5.5 5.0 4.5 4.0 3.5 3.0 2.5 2.0 1.5 1.0 0.5 0.0 -0.5
f1 (ppm)

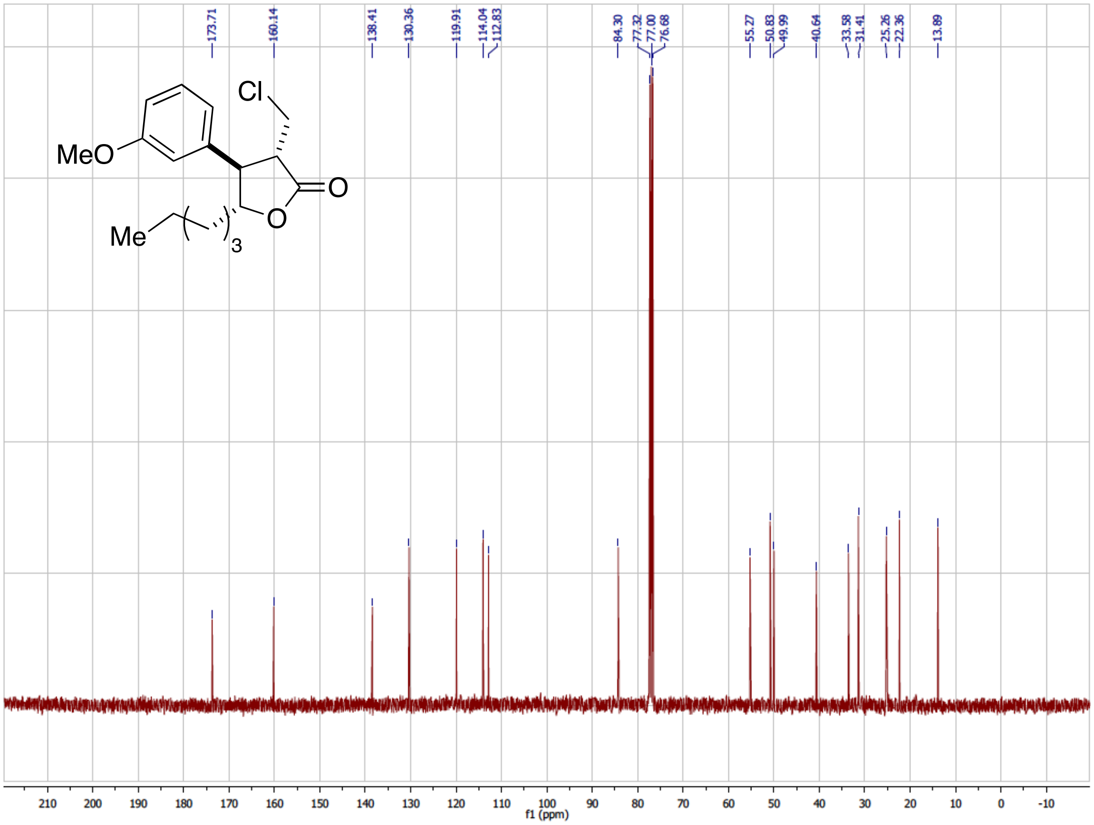
173.71 160.14 138.41 130.36 119.91 114.04 112.83 84.30 77.32 77.00 76.68 55.27 50.83 49.99 40.64 33.58 31.41 25.26 22.36 13.89
Cl
MeO
O
O
Me
3
210 200 190 180 170 160 150 140 130 120 110 100 90 80 70 60 50 40 30 20 10 0 -10
f1 (ppm)

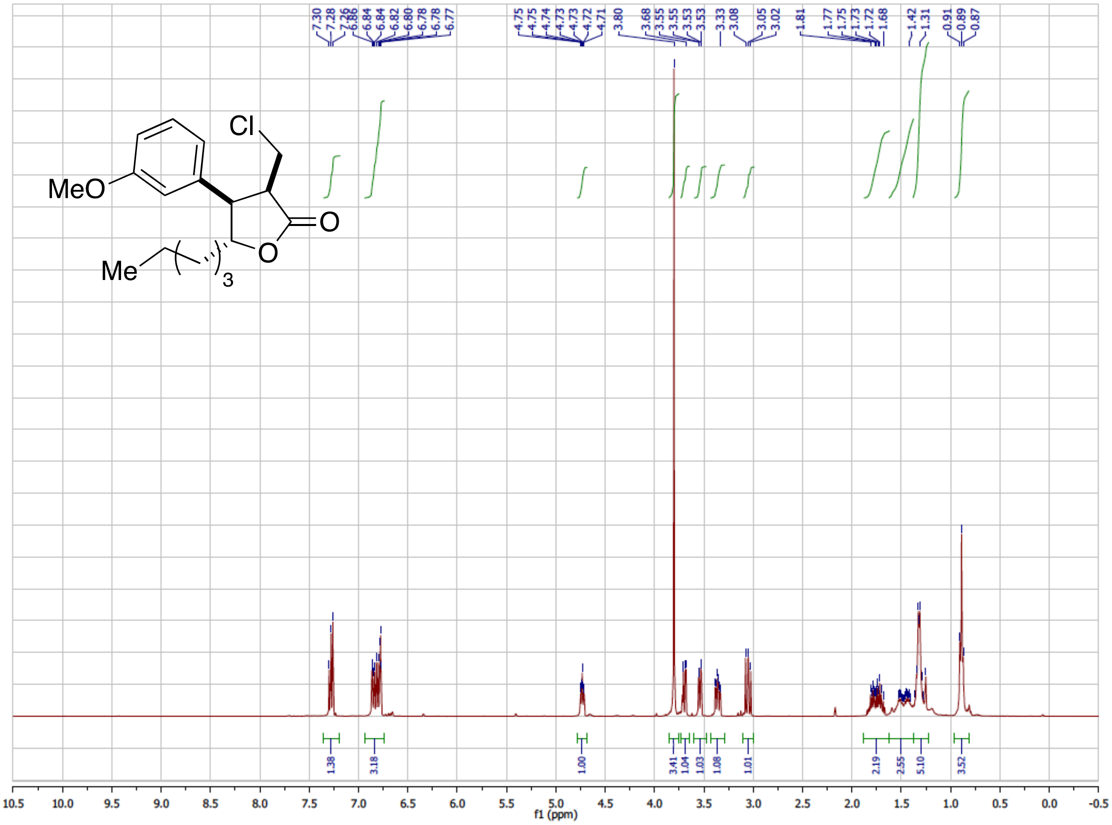
Cl
MeO
O
O
Me
3
7.30
7.28
7.26
6.86
6.84
6.84
6.82
6.80
6.78
6.78
6.77
4.75
4.75
4.74
4.73
4.73
4.72
4.71
3.80
3.68
3.55
3.55
3.53
3.53
3.33
3.08
3.05
3.02
1.81
1.77
1.75
1.73
1.72
1.68
1.42
1.31
0.91
0.89
0.87
1.38
3.18
1.00
3.41
1.04
1.03
1.08
1.01
2.19
2.55
5.10
3.52
10.5
10.0
9.5
9.0
8.5
8.0
7.5
7.0
6.5
6.0
5.5
5.0
4.5
4.0
3.5
3.0
2.5
2.0
1.5
1.0
0.5
0.0
-0.5
f1 (ppm)

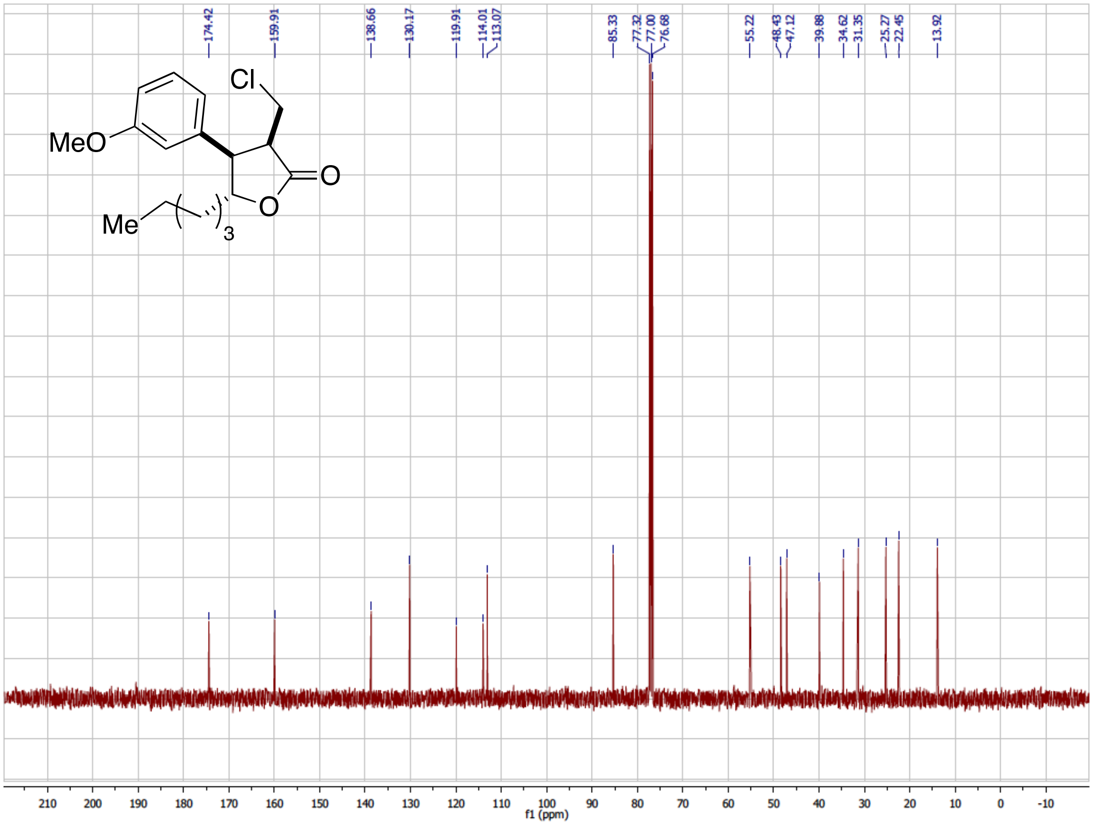
Cl
MeO
O
O
Me
3
174.42
159.91
138.66
130.17
119.91
114.01
113.07
85.33
77.32
77.00
76.68
55.22
48.43
47.12
39.88
34.62
31.35
25.27
22.45
13.92
210
200
190
180
170
160
150
140
130
120
110
100
90
80
70
60
50
40
30
20
10
0
-10
f1 (ppm)

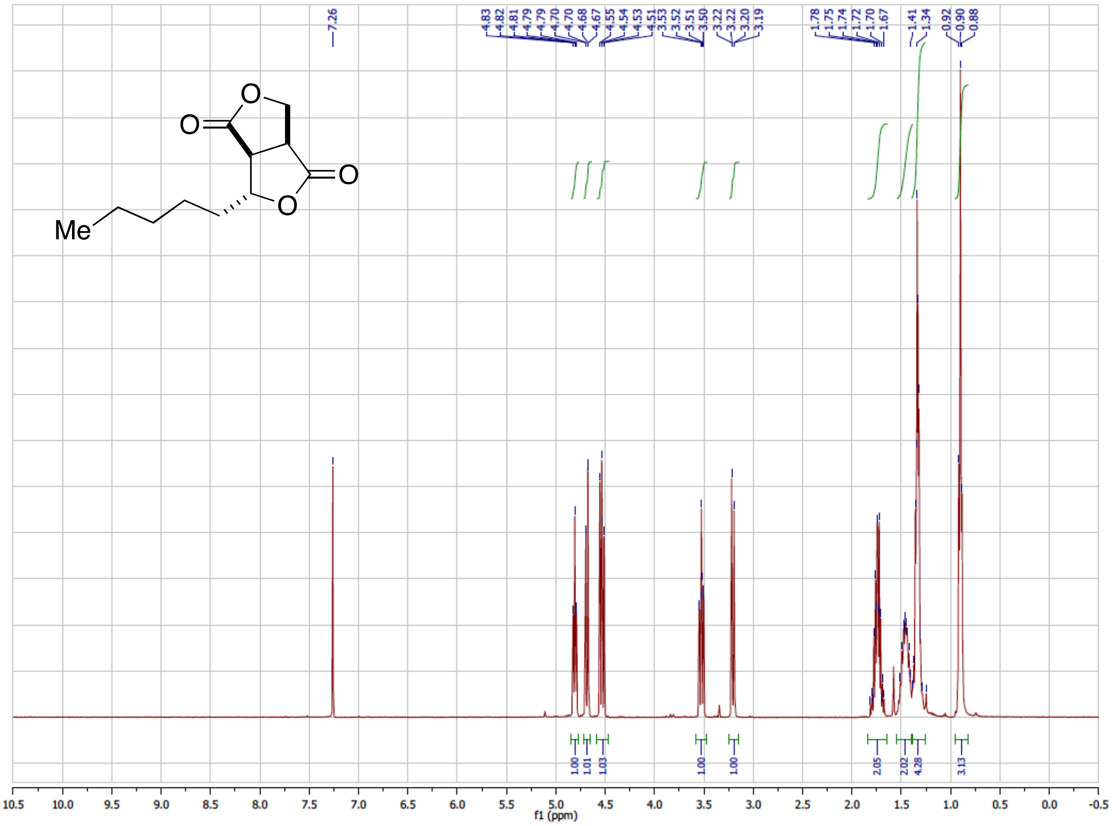

7.26
4.83
4.82
4.81
4.79
4.79
4.70
4.70
4.68
4.67
4.55
4.54
4.53
4.51
3.53
3.52
3.51
3.50
3.22
3.22
3.20
3.19
1.78
1.75
1.74
1.72
1.70
1.67
1.41
1.34
0.92
0.90
0.88
O
O
O
O
Me
1.00
1.01
1.03
1.00
1.00
2.05
2.02
4.28
3.13
10.5
10.0
9.5
9.0
8.5
8.0
7.5
7.0
6.5
6.0
5.5
5.0
4.5
4.0
3.5
3.0
2.5
2.0
1.5
1.0
0.5
0.0
-0.5
f1 (ppm)

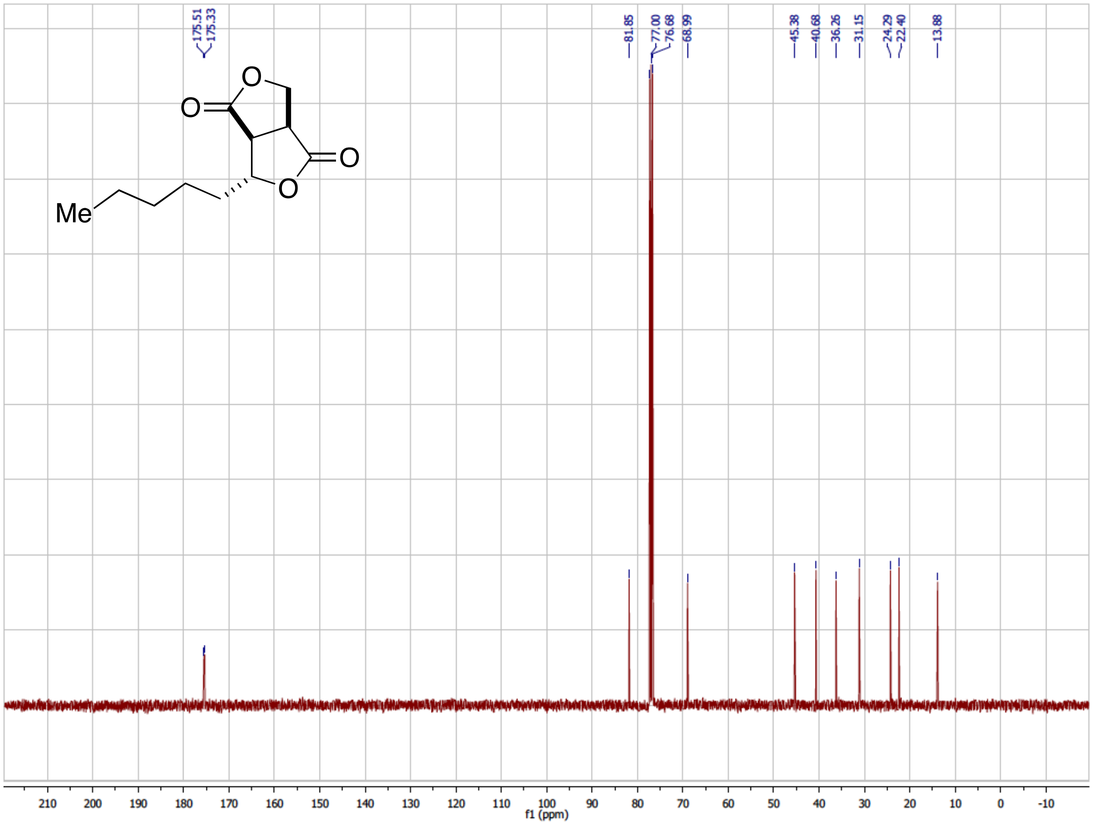

175.51
175.33
81.85
77.00
76.68
68.99
45.38
40.68
36.26
31.15
24.29
22.40
13.88
O
O
O
O
Me
210
200
190
180
170
160
150
140
130
120
110
100
90
80
70
60
50
40
30
20
10
0
-10
f1 (ppm)

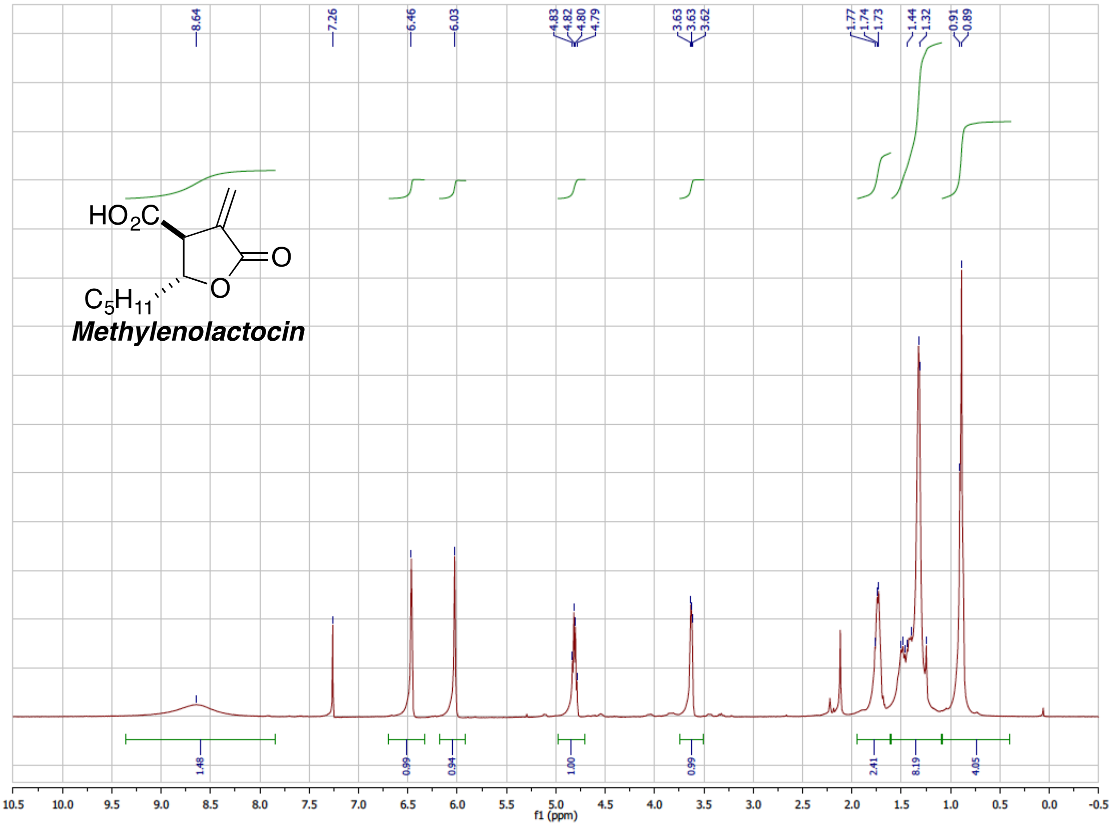
8.64
7.26
6.46
6.03
4.83
4.82
4.80
4.79
3.63
3.63
3.62
1.77
1.74
1.73
1.44
1.32
0.91
0.89
HO_2C
O
O
C_5H_{11}
Methylenolactocin
1.48
0.99
0.94
1.00
0.99
2.41
8.19
4.05
10.5
10.0
9.5
9.0
8.5
8.0
7.5
7.0
6.5
6.0
5.5
5.0
4.5
4.0
3.5
3.0
2.5
2.0
1.5
1.0
0.5
0.0
-0.5
f1 (ppm)

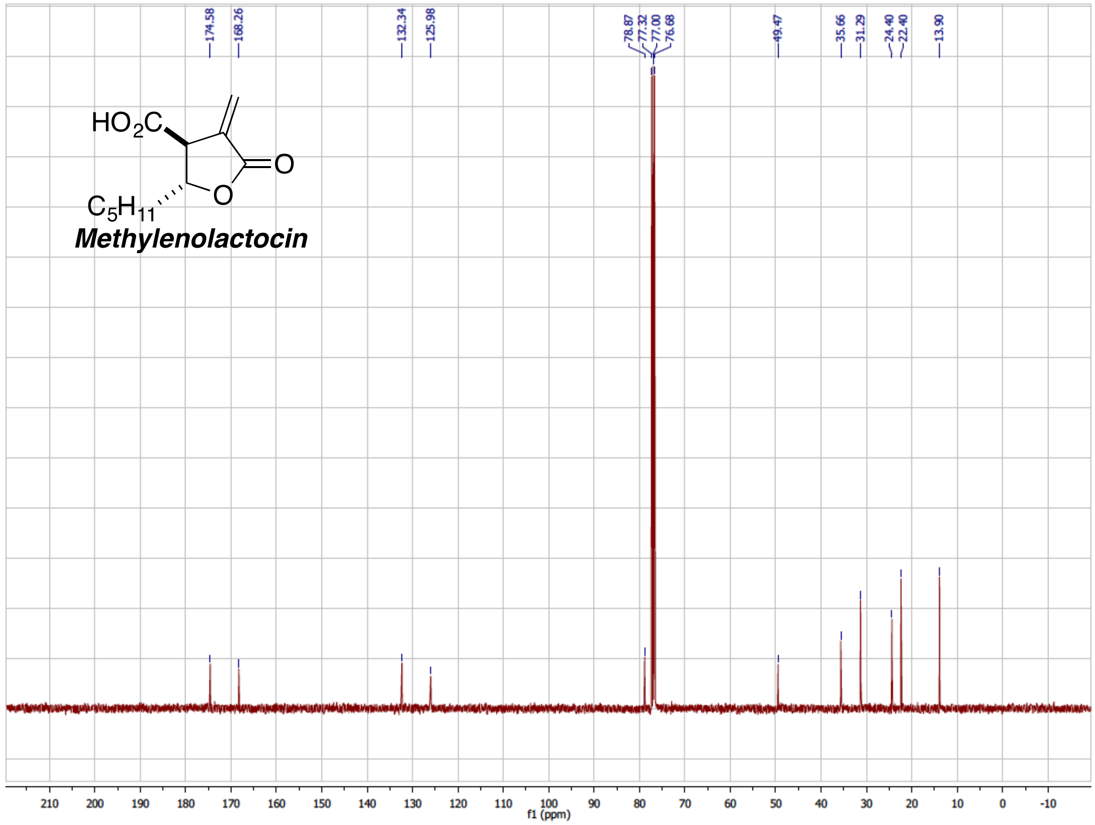
174.58
168.26
132.34
125.98
78.87
77.32
77.00
76.68
49.47
35.66
31.29
24.40
22.40
13.90
HO_2C
O
O
C_5H_{11}
Methylenolactocin
210
200
190
180
170
160
150
140
130
120
110
100
90
80
70
60
50
40
30
20
10
0
-10
f1 (ppm)

APPENDIX TWO: NMR SPECTRA FOR CHAPTER THREE

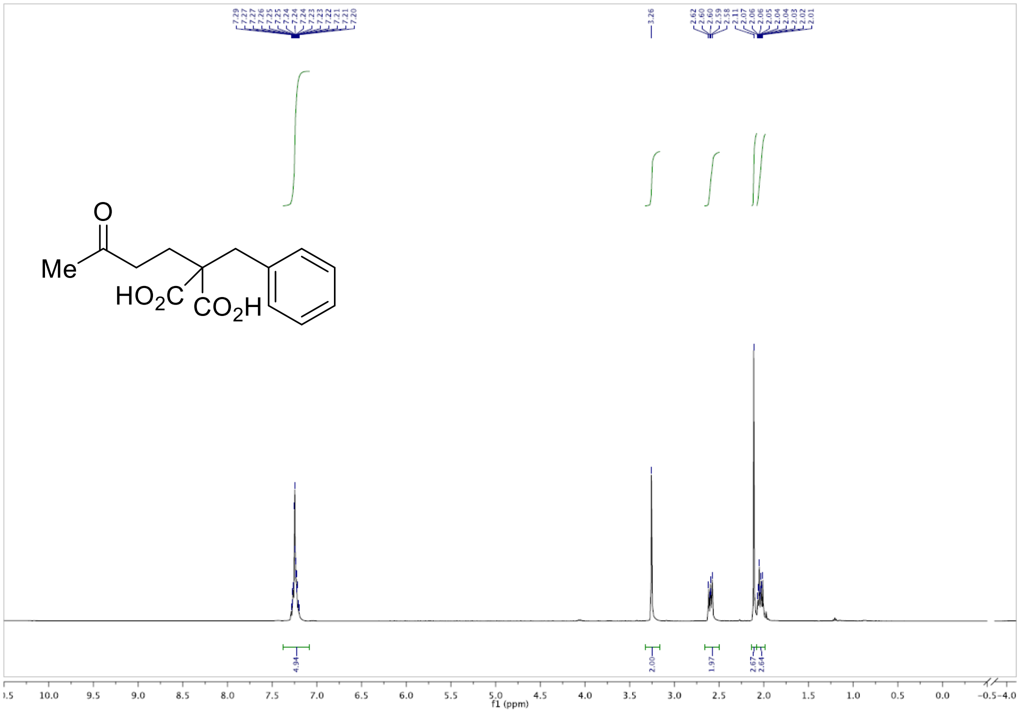

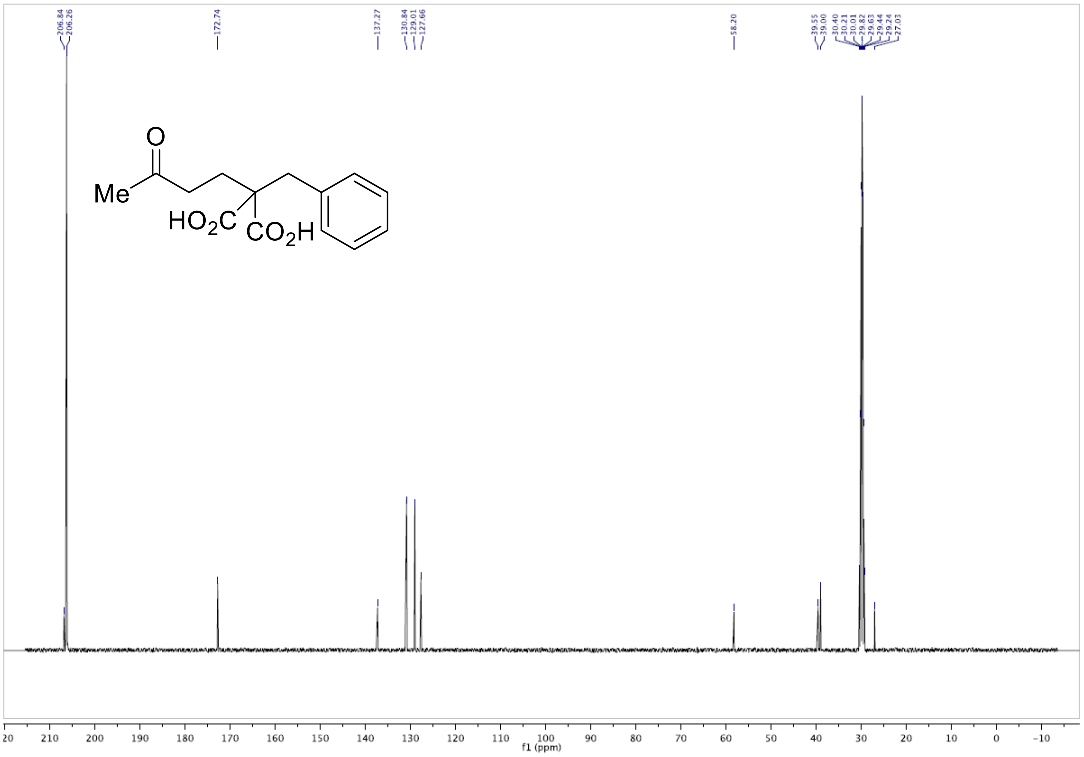

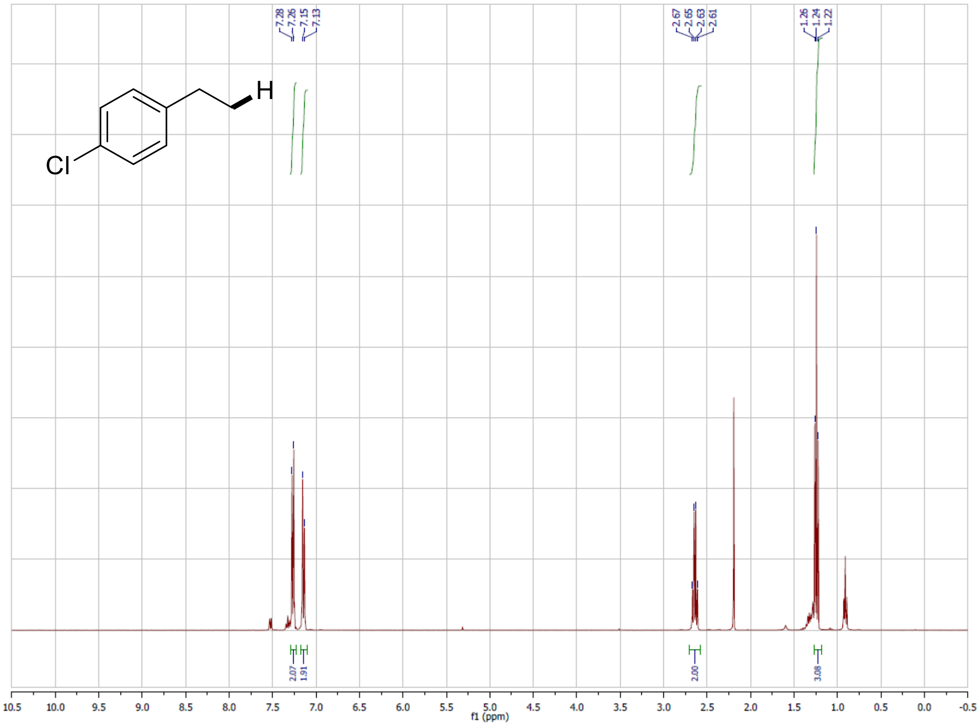

7.28
7.26
7.15
7.13
2.67
2.65
2.63
2.61
1.26
1.24
1.22
Cl
H
2.07
1.91
2.00
3.08
10.5 10.0 9.5 9.0 8.5 8.0 7.5 7.0 6.5 6.0 5.5 5.0 4.5 4.0 3.5 3.0 2.5 2.0 1.5 1.0 0.5 0.0 -0.5
f1 (ppm)

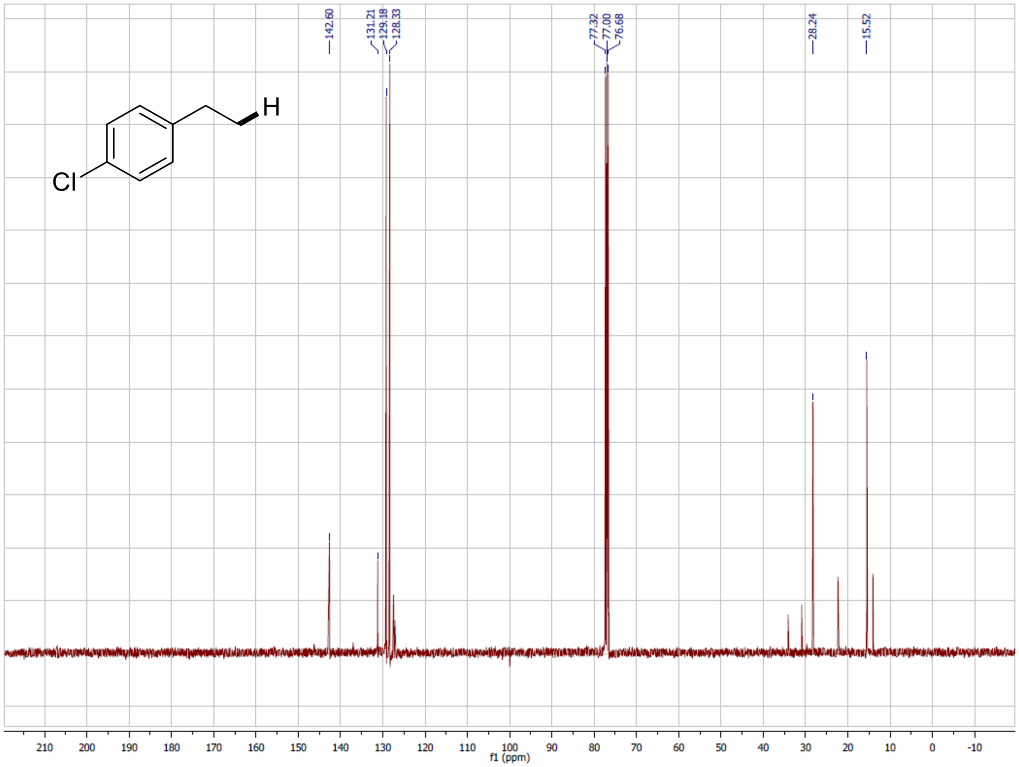

142.60
131.21
129.18
128.33
77.32
77.00
76.68
28.24
15.52
Cl
H
210 200 190 180 170 160 150 140 130 120 110 100 90 80 70 60 50 40 30 20 10 0 -10
f1 (ppm)

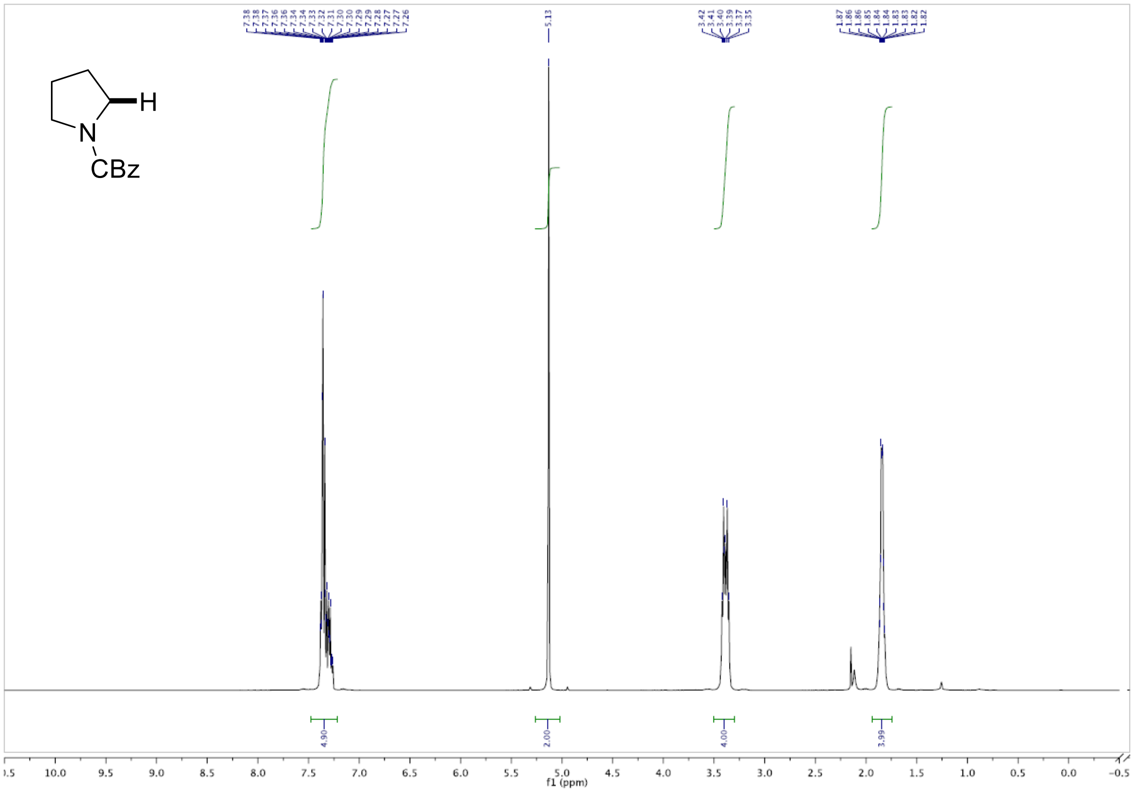
H
N
CBz
7.38
7.38
7.37
7.36
7.36
7.34
7.34
7.33
7.32
7.31
7.30
7.30
7.29
7.29
7.28
7.27
7.27
7.26
5.13
3.42
3.41
3.40
3.39
3.37
3.35
1.87
1.86
1.86
1.85
1.84
1.84
1.83
1.83
1.82
1.82
4.90
2.00
4.00
3.99
10.0
9.5
9.0
8.5
8.0
7.5
7.0
6.5
6.0
5.5
5.0
4.5
4.0
3.5
3.0
2.5
2.0
1.5
1.0
0.5
0.0
-0.5
f1 (ppm)

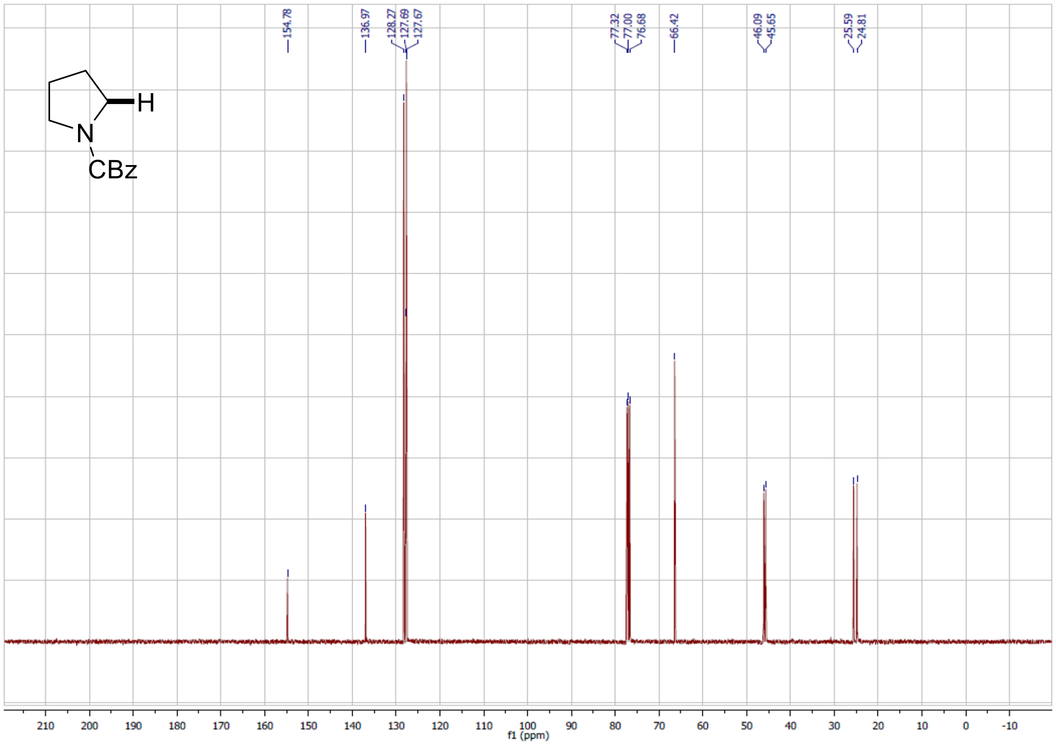
H
N
CBz
154.78
136.97
128.27
127.69
127.67
77.32
77.00
76.68
66.42
46.09
45.65
25.59
24.81
210
200
190
180
170
160
150
140
130
120
110
100
90
80
70
60
50
40
30
20
10
0
-10
f1 (ppm)

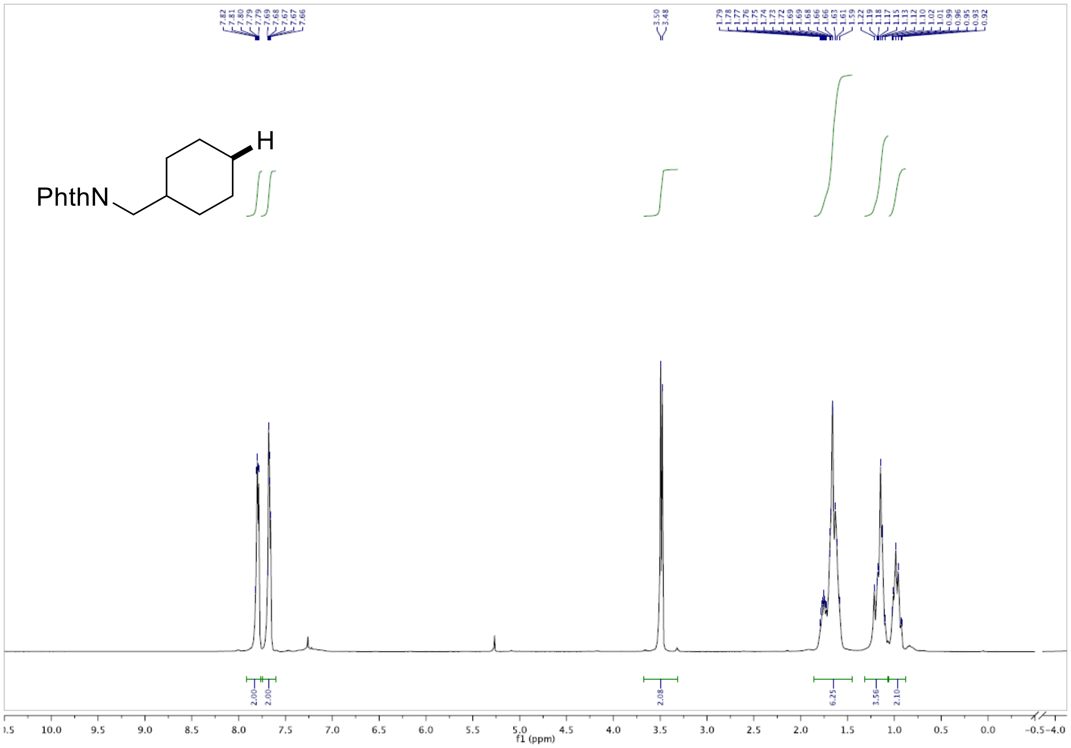
7.82
7.81
7.80
7.79
7.79
7.69
7.68
7.67
7.67
7.66
3.50
3.48
1.79
1.78
1.77
1.76
1.75
1.74
1.73
1.72
1.69
1.69
1.68
1.66
1.66
1.63
1.61
1.59
1.22
1.19
1.18
1.17
1.15
1.13
1.12
1.10
1.02
1.01
0.99
0.96
0.95
0.93
0.92
H
PhthN
2.00
2.00
2.08
6.25
3.56
2.10
10.0
9.5
9.0
8.5
8.0
7.5
7.0
6.5
6.0
5.5
5.0
4.5
4.0
3.5
3.0
2.5
2.0
1.5
1.0
0.5
0.0
-0.5
-4.0
f1 (ppm)

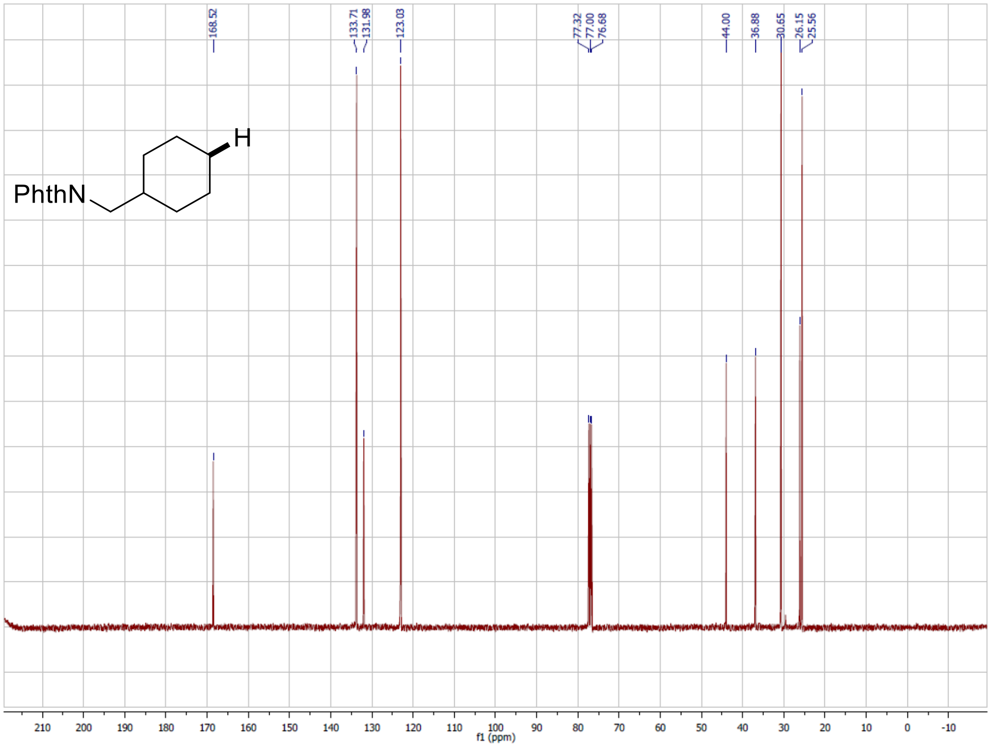
168.52
133.71
131.98
123.03
77.32
77.00
76.68
44.00
36.88
30.65
26.15
25.56
H
PhthN
210
200
190
180
170
160
150
140
130
120
110
100
90
80
70
60
50
40
30
20
10
0
-10
f1 (ppm)

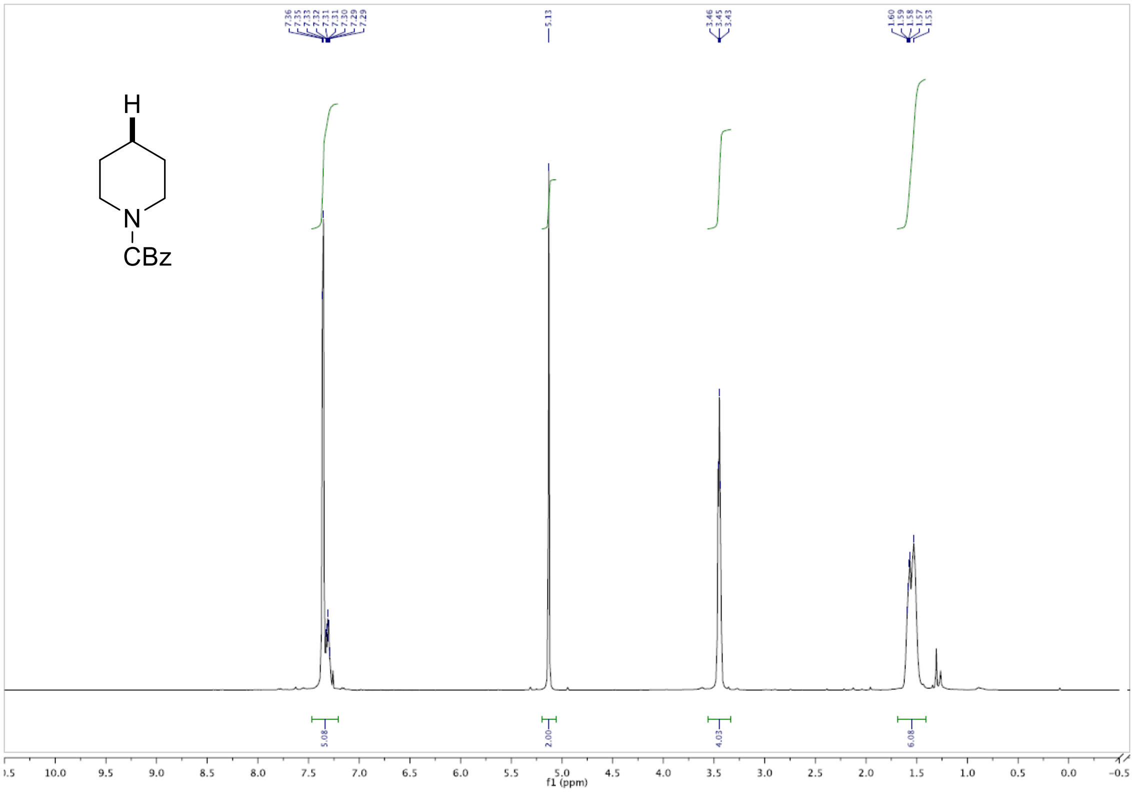

H
N
CBz
7.36
7.35
7.33
7.32
7.31
7.31
7.30
7.29
7.29
5.13
3.46
3.45
3.43
1.60
1.59
1.58
1.57
1.53
5.08
2.00
4.03
6.08
10.0
9.5
9.0
8.5
8.0
7.5
7.0
6.5
6.0
5.5
5.0
4.5
4.0
3.5
3.0
2.5
2.0
1.5
1.0
0.5
0.0
-0.5
f1 (ppm)

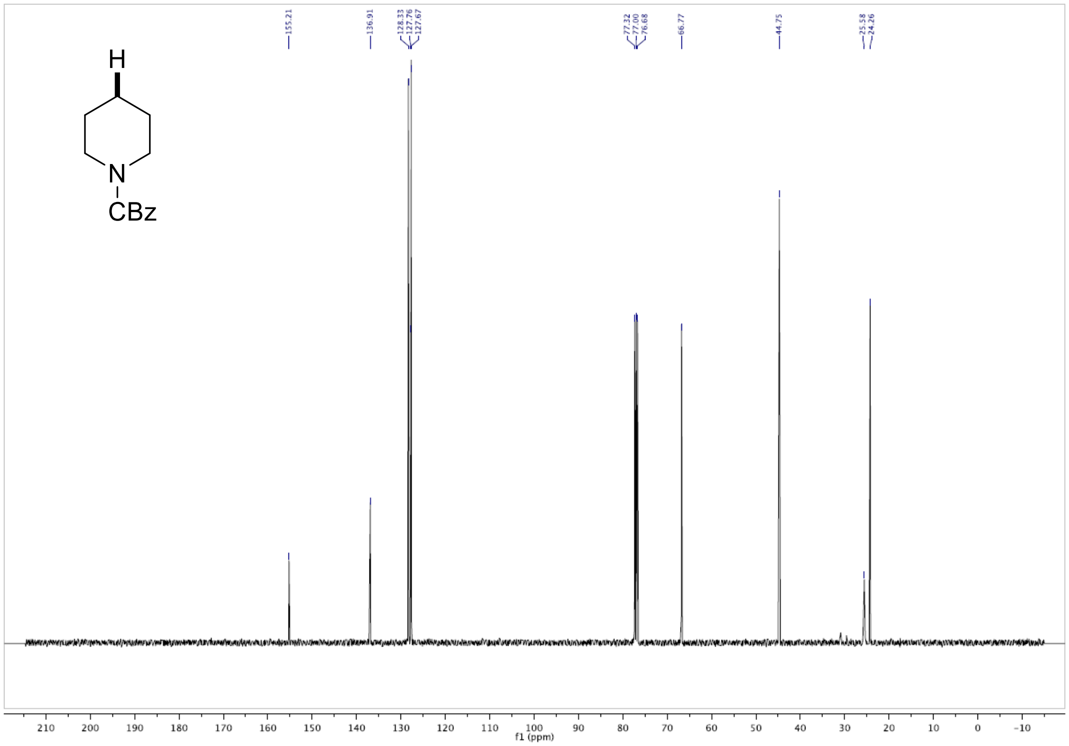

H
N
CBz
155.21
136.91
128.33
127.76
127.67
77.32
77.00
76.68
66.77
44.75
25.58
24.26
210
200
190
180
170
160
150
140
130
120
110
100
90
80
70
60
50
40
30
20
10
0
-10
f1 (ppm)

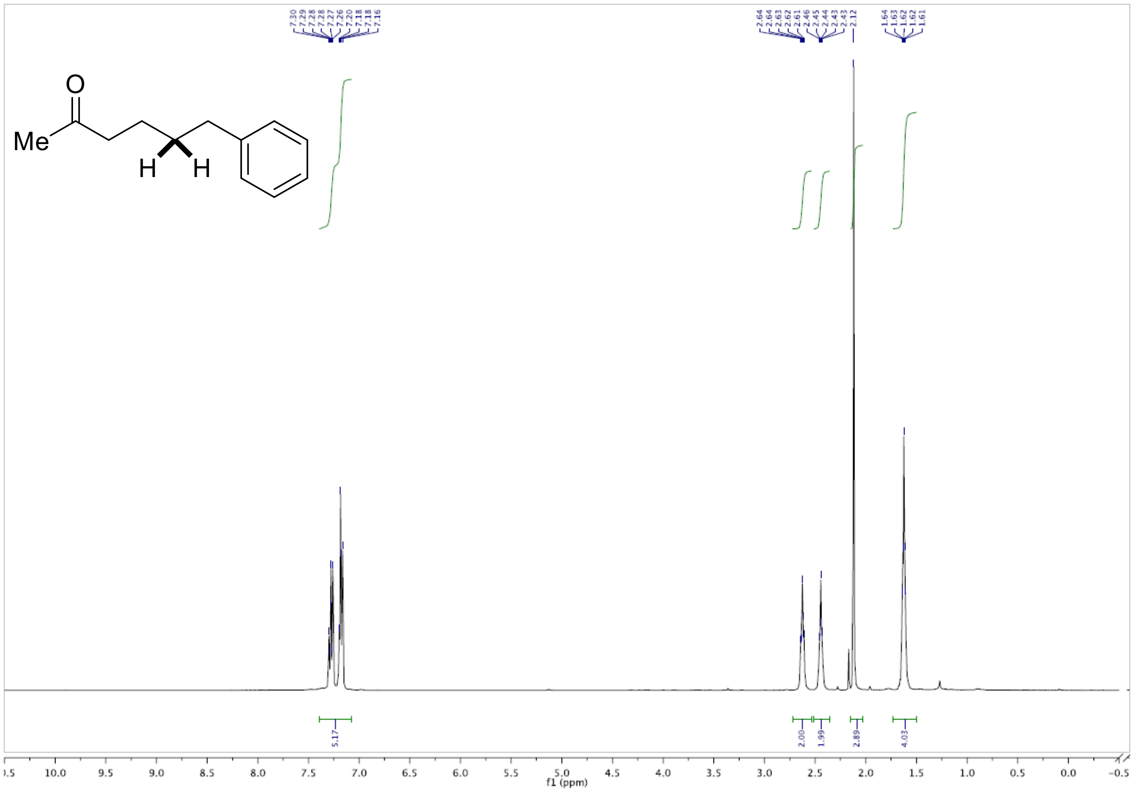
7.30
7.29
7.28
7.28
7.27
7.26
7.20
7.18
7.18
7.16
2.64
2.64
2.63
2.62
2.61
2.46
2.45
2.44
2.43
2.43
2.12
1.64
1.63
1.62
1.62
1.61
O
Me
H
H
5.17
2.00
1.99
2.89
4.03
10.5
10.0
9.5
9.0
8.5
8.0
7.5
7.0
6.5
6.0
5.5
5.0
4.5
4.0
3.5
3.0
2.5
2.0
1.5
1.0
0.5
0.0
-0.5
f1 (ppm)

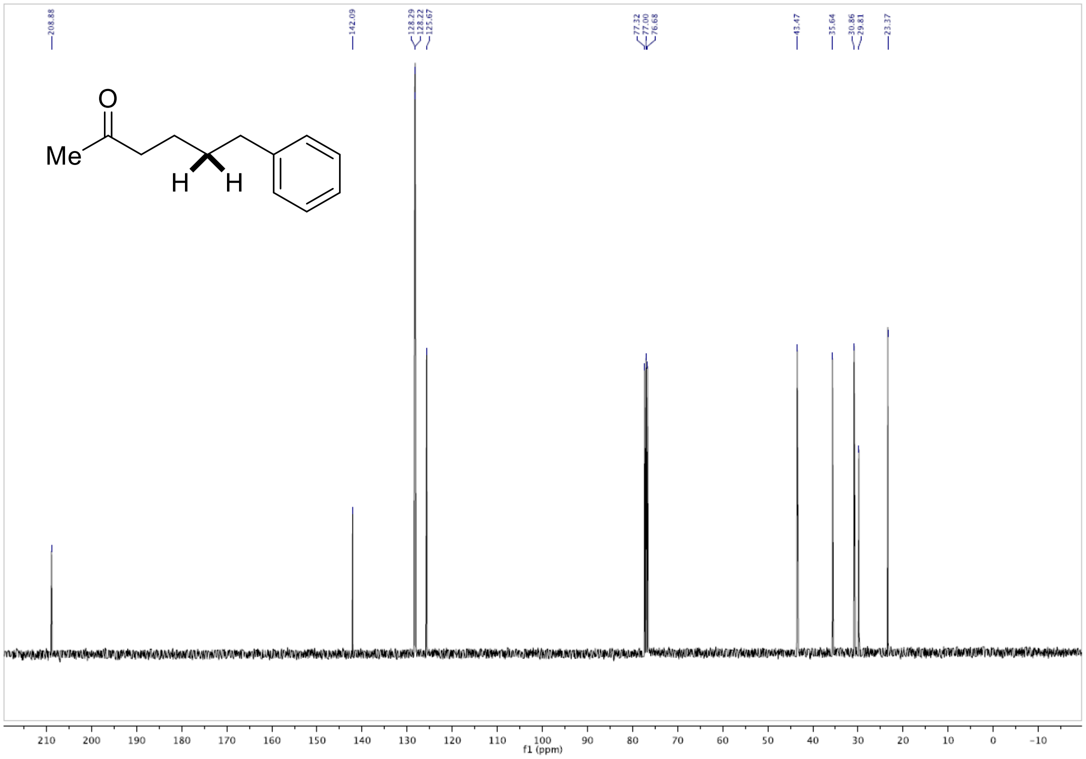
208.88
142.09
128.29
128.22
125.67
77.32
77.00
76.68
43.47
35.64
30.86
29.81
23.37
O
Me
H
H
210
200
190
180
170
160
150
140
130
120
110
100
90
80
70
60
50
40
30
20
10
0
-10
f1 (ppm)